NTNU – Trondheim
Norwegian University of
Science and Technology

Dynamic Analysis and Verification of the Universal Buoyancy System

Anna Kristine Hertzenberg
Fæhn

Marine Technology
Submission date: June 2014
Supervisor: Bernt Johan Leira, IMT

Norwegian University of Science and Technology
Department of Marine Technology

DYNAMIC ANALYSIS AND VERIFICATION OF THE UNIVERSAL BUOYANCY SYSTEM

Master thesis
Norwegian University of Science and Technology
03.06.2014

Anna Kristine Hertzenberg Fæhn
Marine Structures and Hydrodynamics
Department of Marine Technology

Supervisor: Bernt J. Leira

MASTER THESIS IN MARINE TECHNOLOGY

Spring 2014
For
Anna Kristine Hertzenberg Fæhn

Dynamic Analysis and Verification of the Universal Buoyancy System

The background for this thesis is related to a new concept for LNG import and export. The concept eliminates the need for quays/piers and includes an onshore reel and a floating flexible pipeline connecting the terminal to an off-loading buoy. The buoy is positioned in the near-shore area to avoid full exposure to environmental loads. The overall aim of the thesis is to study the hydrodynamic behaviour of the buoy and pipeline that comprises the UBS system.

This thesis includes the following elements:

- A literature study, concerning the techniques used to perform response analysis for floating flexible pipelines including non-linear finite element methods and non-linear time-domain analysis techniques. Focus should be on the methods which are employed by in computer programs such as RIFLEX/SIMA.
- Define relevant pipeline design scenarios in terms of water depth, offset requirements, wave and current conditions, buoy RAO, pipe properties, hydrodynamic coefficients etc.
- Given the defined scenario, establish a static FE model and perform dynamic analyses in order to investigate the maximum response of the loading-buoy. Study the effect of the presence of the pipeline and the ship on the behaviour of the buoy.
- Plan and carry out a model test corresponding to the relevant design scenario.
- Analyse and present model test results in terms of behaviour of the platform under different conditions
- Compare the results from the calculations and model test. Based on the results, give recommendations regarding the hydrodynamic aspects of the design and give recommendations for further work.

In the thesis the candidate shall present his personal contribution to the resolution of problems within the scope of the thesis work. Theories and conclusions should be based on mathematical derivations and/or logic reasoning identifying the various steps in the deduction.

The candidate should utilise the existing possibilities for obtaining relevant literature.

The thesis should be organized in a rational manner to give a clear exposition of results, assessments and conclusions. The text should be brief and to the point, with a clear language. Telegraphic language should be avoided.

The thesis shall contain the following elements: A text defining the scope, preface, list of contents, summary, main body of thesis, conclusions with recommendations for further work, list of symbols and acronyms, reference and (optional) appendices. All figures, tables and equations shall be numerated.

The supervisor may require that the candidate, in an early stage of the work, present a written plan for the completion of the work. The plan should include a budget for the use of computer and laboratory resources that will be charged to the department. Overruns shall be reported to the supervisor.

The original contribution of the candidate and material taken from other sources shall be clearly defined. Work from other sources shall be properly referenced using an acknowledged referencing system.

The thesis shall be submitted in two copies:

Signed by the candidate

The text defining the scope included

In bound volume(s)

Drawings and/or computer prints that cannot be bound should be organized in a separate folder

A CD or DVD containing the written thesis in Word of PDF format shall accompany the bound volume. In case computer programmes have been made as part of the thesis work, the source code shall be included. In case of experimental work, the experimental results shall be included in a suitable electronic format.

Supervisor: Professor Bernt J. Leira
Start: 14.01.2014
Deadline: 10.06.2014

ABSTRACT

Liquefied Natural Gas (LNG) is becoming an increasingly popular alternative to traditional marine fuels, as it is a cost-effective solution so comply with the new Emission Control Area (ECA) sulphur emission regulations that take effect on 1st January 2015. Connect LNG has developed The Universal Buoyancy System (UBS), a cost-effective and simple concept for offloading LNG for small-scale ships. The system consists of a flexible cryogenic pipeline, a reel on land and a floating semisubmersible platform. The platform is designed to support the external forces acting on the floating cryogenic pipeline and hence protect the vessel's manifold. The platform is attached to the ship side by vacuum technology, and the LNG hose may then safely be connected to the ship's manifold.

This thesis investigates the behaviour of the platform in three different configurations by using two different methods; simulations in MARINTEK's finite element programme SIMA, and model tests performed in the Marine Cybernetics laboratory at MARINTEK, Trondheim.

The platform was exposed to one extreme sea state for three hours, under different configurations and wave headings. The platform was tested alone, connected to the ship side, and connected to both the ship side and the pipeline. As far as possible, the same conditions are used in both model test and in SIMA. In addition, parameters used in the SIMA simulations such as computed transfer functions added mass and damping will be validated in the model test.

The results from the model test to some extent validated the input parameters in SIMA, but were not accurate enough to confirm them. The extreme sea states and setups tested showed that the complete system, with platform, pipeline and ship side was the most vulnerable configuration. The computer simulations and the model test results disagree on whether it is the 315 degree or 90 degree wave heading that is the most severe for the complete system, but the differences between the different wave headings are small in both methods, so this might be due to the modelling differences as well as statistical randomness.

SAMMENDRAG

Liquefied Natural Gas (LNG), eller flytende naturgass, har de senere år blitt et populært alternativ til tradisjonelle marine drivstoff, fordi det er en økonomisk måte å etterfølge de nye restriksjonene på sulfurutslipp i ECA-sonen (Emission Control Area) som trer i kraft 1. januar 2015. Connect LNG har utviklet "Universal Buoyancy System", som er et billig og enkelt konsept for lasting av LNG fra småskala skip til terminaler på land. Systemet består av en fleksibel kryogenisk rørledning som i den ene enden er festet i rørnettet på land, og i den andre enden er festet på en liten flytende plattform. Denne plattformen kan festes til skipssiden med vakuumteknologi, slik at en rørledning trygt kan festes på skipets manifold.

Denne oppgaven undersøker plattformens oppførsel i tre forskjellige konfigurasjoner ved å bruke to forskjellige metoder; simuleringer i MARINTEKs elementmetodeprogram SIMA, samt modelltesting i Marin Kybernetikk-laboratoriet på MARINTEK, Trondheim.

Plattformen ble testet i en ekstrem-sjøtilstand med en varighet på tre timer, i forskjellige konfigurasjoner og bølgeretninger. Plattformen er testet alene, festet til skipssiden, samt festet til både rørledning og skipsside. Så langt det er mulig, ble de samme omgivelsene brukt i både modelltesten og i simuleringene. I tillegg ble parameterne som ble brukt til simuleringene i SIMA, slik som tilleggsmasse, demping og transferfunksjoner, validert i modelltesten.

Resultatene fra modelltestingen validerte til en viss grad parameterne brukt i SIMA-simuleringene, men de var ikke nøyaktige nok til å bekrefte dem. Testene og simuleringene i ekstremsjøtilstandene med forskjellige konfigurasjoner viste at det komplette systemet, inkludert både rørledning, plattform og skipsside, var den mest utsatte. Data-simuleringene viste at, for det komplette systemet, var det 315 grader som var den verste bølgeretningen, mens modelltestene viste at det var 90 graders bølgeretnings som var mest alvorlig. Forskjellene mellom de forskjellige retningene var imidlertid ikke så store at de ikke like godt kan ha sin opprinnelse i modelleringsfeil eller statistisk tilfeldighet.

PREFACE

This thesis concludes the Master's Degree programme in Marine Technology at the Norwegian University of Science and Technology, written during the spring semester of 2014.

The background for this thesis is a project on the UBS carried out in autumn 2013. The project provided and introduction to the concept and the company behind it, Connect LNG. The prospective of being able to cooperate with young entrepreneurs on developing a new concept was very intriguing, and a huge motivator for choosing this topic for my dissertation.

The thesis is split into two main parts. The first weeks of the semester was spent planning the model test together with fellow student Odd Staalesen. As neither of us had any experience with model testing, we spent quite a lot of time reading, researching and planning the model test.

We agreed to do the post processing individually, because of practical as well as learning reasons. We did, however, confer with each other, and compared results along the way, which proved useful. Some of the material in out theses will therefore be similar, but each has written their own reports. After completing the post processing the model tests, I started with the SIMA simulations, as well as the writing of this report.

The work has been very challenging at times, in particular the model test, but good assistance as well as motivation to learn has been of good help. In particular, I would like to thank PhD candidate Lin Li, Engineers Pål Levold and Andreas Amundsen at MARINTEK for help and tips with SIMA modelling. Torgeir Wahl at MARINTEK and Professor Sverre Steen were of great assistance in the planning and execution of the model test.

I sincerely thank my supervisor Prof. Bernt Leira as well as Stian Magnusson and David Knutsen at Connect LNG for help, guidance, and in general answering any question I may possibly have had during the semester.

Lastly, I would like to thank Connect LNG for giving me the opportunity to work with them on this exciting project, I wish them all the best for the future.

TABLE OF CONTENTS

Dynamic analysis and verification of the Universal Buoyancy system i
Abstract iii
Sammendrag iv
Preface v
Table of contents vi
List of tables xi
List of figures xii
List of equations xiv
Abbreviations xvii
Nomenclature xvii
List of appendix tables xxi
List of appendix figures xxi

Part 1: The Universal Buoyancy System 1
1 LNG as an alternative fuel 1
2 The UBS concept 1
3 Problem statement 3
4 Thesis overview 3

Part 2: Modelling in SIMA 5
1 Introduction 5
2 Analysis theory 5
2.1 SIMA 5
2.2 Riflex 5
2.2.1 Introduction 5
2.2.2 Finite element modelling 6
2.2.3 Implementation of the finite element method 7
2.2.4 Elements 7

2.2.5 Mass, stiffness and damping matrices 9
2.3 SIMO 10
2.3.1 Introduction 10
2.3.2 Environment 10
2.3.3 Equilibrium equations 11
2.3.4 Coupling and station keeping 12
3 System description 15
3.1 General 15
3.2 Ship 15
3.3 Platform 16
3.4 Vacuum pads 17
3.5 Pipeline 19
3.6 Supernodes 19
3.7 Lines and cross-section 20
3.8 Bodies 22
3.8.1 Hydrodynamic data 24
3.9 Ship to pipeline connection system 27
3.10 Environment and Location 28
3.11 Calculation parameters 29
3.11.1 Static and dynamic calculation parameters 29
3.12 Simulation runs 30
3.13 Post-processing 31
4 Results 32
4.1 Configuration 1: Platform only 32
4.1.1 Run 1: Wave heading 0 degrees 33
4.1.2 Run 2: Wave heading 90 degrees 33
4.1.3 Transfer functions for configuration 1 34
4.2 Configuration 2: Platform and ship, coupled condition 37
4.2.1 Run 3: Wave heading 0 degrees 38

4.2.2 Run 4: Wave heading 315 degrees 39
4.2.3 Run 5: Wave heading 90 degrees 40
4.2.4 Transfer functions for configuration 2 41
4.3 Configuration 3: Complete system 45
4.3.1 Run 6: Wave heading 0 degrees 45
4.3.2 Run 7: Wave heading 315 degrees 46
4.3.3 Run 8: Wave heading 90 degrees 47
4.3.4 Transfer functions for Configuration 3 48

Part 3: Model test 52
1 Introduction 52
1.1 Introduction 52
1.2 motivation 52
1.3 Previous testing 52
1.4 objectives of model test 52
2 Test set-up 53
2.1 Test facilities 53
2.2 Model scale and parameters 53
2.3 Model description 54
2.3.1 Overview of test arrangement 54
2.3.2 Platform 55
2.3.3 Mooring 56
2.3.4 Connection system 56
2.3.5 Ship 57
2.3.6 Additional model equipment 57
2.4 Units and coordinate systems. 58
2.5 Calibration and verification 58
2.5.1 Weight and waterline 58

2.5.2 Strain transducers 59
2.5.3 Oqus cameras 60
2.6 Data acquisition 60
2.6.1 Strain transducers 61
2.6.2 Wave probe 61
2.6.3 Control check and routines 61
2.7 Test Conditions 61
2.7.1 Environmental conditions 61
2.7.2 Test arrangement 62
2.7.3 Test programme 62
2.7.4 Duration of tests 63
3 Data analysis and post-processing 65
3.1 Scaling 65
3.2 Bias 67
3.3 Wave probe 67
3.4 Filters 68
3.5 Regular tests 70
3.6 Irregular tests 71
3.6.1 Spectral analysis 72
3.6.2 Extreme value analysis 74
3.7 Decay tests 74
4 Results 77
4.1 Regular runs 78
4.1.1 Setup 1: Uncoupled condition, wave heading 90 degrees. 78
4.1.2 Setup 2: Uncoupled condition, wave heading 0 degrees 80
4.1.3 Setup 3: Coupled condition, wave heading 0 degrees 83
4.1.4 Setup 4: coupled condition, wave heading 315 degrees 87
4.1.5 Setup 5: Coupled condition, wave heading 90 degrees 91

4.2 Irregular runs. 95
4.2.1 Maximum values 95
4.2.2 Transfer functions 97
4.3 Special case – setup 6. 101
4.4 Decay tests 103
5 Uncertainties and errors 106
5.1 Scaling errors 106
5.2 Structural errors 106
5.3 Environmental modelling 107
5.4 Measurements and calculations 108

Part 4: Comparison 109
1 Regular waves – validate input RAO 109
1.1 Wave heading 0 degrees 109
1.2 Wave heading 90 degrees 111
2 Decay tests 115
3 Irregular runs 116
3.1 Uncoupled condition 116
3.2 Coupled condition 116
3.3 Full model 117
3.4 Worst case scenario for complete system 118

Part 5: conclusion 119
1 Summary 119
2 Recommendations for further research 121

References 122
Appendix A: SIMA modelling results 123
Appendix B: Model test results, regular and irregular runs 144
Appendix C: Decay test time series 160

LIST OF TABLES

Table 1: Force characteristic of fenders 17
Table 2: Body points overview 18
Table 3: Supernode positions 20
Table 4: Cryoline data 21
Table 5: Lines overview 22
Table 6: Drag and added mass coefficients for Cryoline 27
Table 7: Wave parameters 28
Table 8: SIMA runs 30
Table 9: Statistics, SIMA run 1 33
Table 10: Statistics, SIMA run 2 34
Table 11: Statistics, SIMA run 3 38
Table 12: Statistics, SIMA run 4 39
Table 13: Statistics, SIMA run 5 40
Table 14: Statistics, SIMA run 6 46
Table 15: Statistics, SIMA run 7 47
Table 16: Statistics, SIMA run 8 48
Table 17: Wavemaker capacity 53
Table 18: Main parameters, model and full scale 54
Table 19: Transducers overview 59
Table 20: Acquired data overview 60
Table 21: Irregular sea state parameters 62
Table 22: Condensed test programme 63
Table 23: Maximum statistics for setup 1 79
Table 24: Maximum values, setup 2 82
Table 25: Statistics for setup 3 86
Table 26: Statistics for setup 4 90
Table 27: Statistics model test setup 5 94
Table 28: Maximum measured values, irregular runs 95
Table 29: Tension from pipeline representation 101
Table 30: Statistical values, special case run 101

Table 31: Decay tests..... 103
Table 32: Accuracy of instrumentation..... 108
Table 33: Comparison of calculated and measured damping and added mass..... 115
Table 34: Comparison of max.values for wave heading 0 degrees, uncoupled condition..... 116
Table 35: Comparison of max. values for wave heading 90 degrees, coupled condition..... 117
Table 36: Full model comparison, SIMA vs. model test..... 117
Table 37: Summary of runs in SIMA, setup 3..... 118
Table 38: Summary of SIMA simulations..... 119
Table 39: Summary of model test results..... 120

LIST OF FIGURES

Figure 1: Sketch of LNG offloading system. Image courtesy of Connect LNG..... 2
Figure 2: Translations and rotations in RIFLEX [4]..... 7
Figure 3: Beam element in RIFLEX [4]..... 8
Figure 4: Complete SIMA model..... 15
Figure 5: WAMIT platform sketch..... 16
Figure 6: Simple wire coupling force characteristic..... 18
Figure 7: Tension-elongation relation for Cryoline. [28]..... 21
Figure 8: Initial configuration SIMA..... 23
Figure 9: Prescribed configuration SIMA..... 23
Figure 10: Added mass and damping coefficient for a cylinder in the free surface [28]..... 24
Figure 11: Depth-dependent added mass coefficient [7]..... 25
Figure 12: Drag coefficient for rough circular cylinders in cross flow. Comparison with results of Fage & Warsap (1930). See [9]..... 26
Figure 13: Depth-dependent drag coefficient [7]..... 26
Figure 14: Wave spectrum..... 29
Figure 15: SIMA configuration 1 overview..... 32
Figure 16: Wave spectrum, configuration 1..... 35
Figure 17: Heave transfer functions, configuration 1..... 36
Figure 18: Roll transfer functions, configuration 1..... 36

Figure 19: Pitch transfer functions, configuration 1 37
Figure 20: Configuration 2 SIMA overview 37
Figure 21: Heave transfer functions, configuration 2 42
Figure 22: Roll transfer functions, configuration 2 42
Figure 23: X-force transfer functions, configuration 3 43
Figure 24: Y-force transfer functions, configuration 3 44
Figure 25: Z-force transfer funtions, configuration 3 44
Figure 26: Configuration 3 SIMA overview 45
Figure 27: Heave transfer functions, SIMA configuration 3 49
Figure 28: Roll transfer functions, SIMA configuration 3 49
Figure 29: X-force transfer functions, SIMA configuration 3 50
Figure 30: Y-force transfer functions, SIMA configuration 3 50
Figure 31: Z-force transfer functions, SIMA configuration 3 51
Figure 32: Independent condition 54
Figure 33: Coupled condition 55
Figure 34: Connection system 56
Figure 35: Frame used in coupled condition 57
Figure 36: Laboratory coordinate system 58
Figure 37: Illustration of wave headings and strain transducers. 63
Figure 38: Example Butterworth filter 69
Figure 39: Spike removal 72
Figure 40: Overview of model test configurations 77
Figure 41: Model test setup 1 78
Figure 42: Motion transfer function, setup 1 79
Figure 43: Setup 2 80
Figure 44: Motion transfer function, setup 2 81
Figure 45: Model test setup 3 83
Figure 46: Motion transfer function, model test setup 3 84
Figure 47: Force transfer function, setup 3 85
Figure 48: Model test setup 4 87
Figure 49: Motion transfer function, setup 4 88
Figure 50: Force transfer function, setup 4 89

Figure 51: Model test setup 5 91
Figure 52: Motion transfer function, setup 5 92
Figure 53: Force transfer function, setup 5 93
Figure 54: Wave spectra from irregular runs, model test 97
Figure 55: Roll transfer functions, irregular runs 98
Figure 56: Pitch transfer functions for irregular runs 99
Figure 57: Y force transfer functions, irregular runs 100
Figure 58: Z-force transfer functions, irregular runs 100
Figure 59: Roll and pitch transfer functions, setup 6 102
Figure 60: Coupled heave decay test 103
Figure 61: WAMIT transfer functions 110
Figure 62: Motion transfer functions, model test 110
Figure 63: WAMIT transfer functions, wave heading 90 degrees 113
Figure 64: Motion transfer functions from model test, wave heading 90 degrees 114
Figure 65: Fitted curve, decay test uncoupled heave 115

LIST OF EQUATIONS

Equation (1) 6
Equation (2) 9
Equation (3) 9
Equation (4) 9
Equation (5) 9
Equation (6) 10
Equation (7) 11
Equation (8) 11
Equation (9) 11
Equation (10) 11
Equation (11) 12
Equation (12) 13
Equation (13) 14

Equation (14) 14
Equation (15) 14
Equation (16) 24
Equation (17) 25
Equation (18) 28
Equation (19) 59
Equation (20) 59
Equation (21) 60
Equation (22) 61
Equation (23) 66
Equation (24) 66
Equation (25) 66
Equation (26) 67
Equation (27) 67
Equation (28) 67
Equation (29) 67
Equation (30) 67
Equation (31) 68
Equation (32) 70
Equation (33) 70
Equation (34) 70
Equation (35) 72
Equation (36) 72
Equation (37) 73
Equation (38) 73
Equation (39) 73
Equation (40) 73
Equation (41) 74
Equation (42) 74
Equation (43) 74
Equation (44) 75
Equation (45) 75

Equation (46) 75
Equation (47) 75
Equation (48) 75
Equation (49) 75
Equation (50) 76
Equation (51) 76
Equation (52) 76

ABBREVIATIONS

AR	Arbitrary riser
CLNG	Connect LNG
ECA	Emission control areas
JIP	Joint Industry Project
LNG	Liquefied natural gas
MARINTEK	Norwegian Marin Technology Research Institute
MARPOL	International Convention for the prevention of pollution from ships
MC	Marine Cybernetics
RAO	Response amplitude operator

NOMENCLATURE

A	-	Added mass matrix
A	-	Cross-sectional area
A_0, A_1	-	Wave amplitudes
A_{33}^{2D}	-	Two-dimensional added mass in heave
A_{WL}	-	Water line area
a	-	Acceleration
C	-	Potential damping matrix
C_D	-	Drag coefficient
C_{ij}	-	Damping in direction ij
c	-	Damping constant
D_1	-	Linear damping matrix
D_2	-	Quadratic damping matrix
d	-	Water depth
F_T	-	Tension force
F_N	-	Normal force
F_F	-	Friction force
F_D	-	Drag force

F_i	-	Inertia force
F_g	-	Gravitational force
f	-	Vector function
f	-	Frequency
f(x)	-	Probability density function
$\overline{GM}_i$	-	Distance from centre of gravity to metacentre in direction i
g	-	Acceleration of gravity
H	-	Transfer function
H_s	-	Significant wave height
h	-	Wave steepness
K	-	Stiffness matrix
KG	-	Distance keel-to-centre of gravity
k	-	Wave number
k_s	-	Shear stiffness
L	-	Element length
L_0	-	Undeformed element length
M	-	Mass
M	-	Mass matrix
m	-	Body mass matrix
$\overline{m}_s$	-	Mass per unit length
m_s	-	Mass
N, N_x	-	Interpolation function
N_w	-	Expected number of waves in a three hour period
$\vec{n}$	-	Normal vector
p_1	-	Linear damping
p_2	-	Quadratic damping
p_x	-	Distributed external load
p_{EQ}	-	Equivalent damping
q	-	Excitation force vector
R	-	Response function
$\dot{R}$	-	Deformation velocity of fender
r	-	Radius
S_i	-	Internal reaction forces

S_e	-	External nodal loads
S, S(ω), S(f)	-	Wave spectrum
$\vec{s}$	-	Sliding motion along the plane
T	-	Wave period, Eigen period
T_0	-	Undamped Eigen period
T_d	-	Damped Eigen period
t	-	Time
U_∞, U	-	Incoming flow velocity
u	-	Particle velocity in X-direction
V_P	-	Phase velocity
V_D	-	Displaced volume
v	-	Particle velocity in Y-direction
X_{LM}	-	Largest maximum of X
X_0	-	Most probable largest maximum of X
x	-	Position vector
x	-	Position coordinate, elongation
x_i	-	Amplitude
w	-	Particle velocity in Z-direction

Greek letters:

β	-	Direction of wave propagation
γ	-	Peak shape parameter
ε_G	-	Engineering strain
ζ_a	-	Wave amplitude
Λ	-	Logarithmic decrement
λ	-	Scale ratio
μ_x	-	Mean
ν	-	Viscosity of water
ξ	-	Non-dimensional length coordinate, damping ratio
ρ	-	Mass density
σ	-	Spectral width parameter
σ_x	-	Standard deviation

ϕ_0	-	Velocity potential
ϕ_ζ	-	Phase angle
ω	-	Angular frequency
ω_P	-	Peak period

LIST OF APPENDIX TABLES

Table A - 1: Statistical values SIMA run 1, platform only, wave heading 0 degrees 124
Table A - 2: Statistical values SIMA run 2, platform only, wave heading 90 degrees 124
Table A - 3: Statistical values, SIMA run 3, coupled condition, wave heading 0 degrees 128
Table A - 4: Statistical values, SIMA run 4, coupled condition, wave heading 315 degrees .. 129
Table A - 5: Statistical values SIMA run 5, coupled condition, wave heading 90 degrees 130
Table A - 6: Statistical values SIMA run 6, total system, wave heading 0 degrees 136
Table A - 7: Statistical values SIMA run 7, total system, wave heading 315 degrees 137
Table A - 8: Statistical values SIMA run 8, total system, wave heading 90 degrees 138

Table B - 1: Statistical values, uncoupled regular runs, wave heading 90 degrees 145
Table B - 2: Statistical values, uncoupled regular runs, wave heading 0 degrees 146
Table B - 3: Statistical values, coupled regular runs, wave heading 0 degrees 147
Table B - 4: Statistical values, coupled regular runs, wave heading 315 degrees 148
Table B - 5: Statistical values, coupled regular runs, wave heading 90 degrees 149
Table B - 6: Spectral analysis, coupled irregular runs, wave heading 90 degrees 150
Table B - 7: Spectral analysis, coupled irregular runs, wave heading 0 degrees 150
Table B - 8: Spectral analysis, coupled irregular runs, wave heading 0 degrees 151
Table B - 9: Spectral analysis, coupled irregular runs, wave heading 315 degrees 152
Table B - 10: Spectral analysis, coupled irregular runs, wave heading 90 degrees 153
Table B - 11: Spectral analysis, irregular runs, total system, wave heading 315 degrees 154

LIST OF APPENDIX FIGURES

Figure A - 1: Surge transfer functions, SIMA runs 1 and 2: Uncoupled condition 125
Figure A - 2: Sway transfer functions, SIMA runs 1 and 2: Uncoupled condition 125
Figure A - 3: Heave transfer functions, SIMA runs 1 and 2: Uncoupled condition 126
Figure A - 4: Roll transfer functions, SIMA runs 1 and 2: Uncoupled condition 126
Figure A - 5: Yaw transfer functions, SIMA runs 1 and 2: Uncoupled condition 127
Figure A - 6: Pitch transfer functions, SIMA runs 1 and 2: Uncoupled condition 127
Figure A - 7: Surge transfer functions, SIMA runs 3-5, coupled condition 131

Figure A - 8: Sway transfer functions, SIMA runs 3-5, coupled condition 131
Figure A - 9: Heave transfer functions, SIMA runs 3-5, coupled condition..... 132
Figure A - 10: Roll transfer functions, SIMA runs 3-5, coupled condition..... 132
Figure A - 11: Pitch transfer functions, SIMA runs 3-5, coupled condition..... 133
Figure A - 12: Yaw transfer functions, SIMA runs 3-5, coupled condition 133
Figure A - 13: Y-force transfer functions, SIMA runs 3-5, coupled condition 134
Figure A - 14: X-force transfer functions, SIMA runs 3-5, coupled condition 134
Figure A - 15: Z-force transfer functions, SIMA runs 3-5, coupled condition 135
Figure A - 16: Sway transfer functions, SIMA, complete system 139
Figure A - 17: Surge transfer functions, SIMA, complete system 139
Figure A - 18: Roll transfer functions, SIMA, complete system 140
Figure A - 19: Heave transfer functions, SIMA, complete system 140
Figure A - 20: Yaw transfer functions, SIMA, complete system 141
Figure A - 21: Pitch transfer functions, SIMA, complete system 141
Figure A - 22: Y-force transfer functions, SIMA, complete system 142
Figure A - 23: X-force transfer functions, SIMA, complete system 142
Figure A - 24: Z-force transfer functions, SIMA, complete system 143

Figure B - 1: Surge transfer functions, irregular model test runs 155
Figure B - 2: Sway transfer functions, irregular model test runs 155
Figure B - 3: Surge transfer functions, irregular model test runs 155
Figure B - 4: Heave transfer functions, irregular model test runs 156
Figure B - 5: Roll transfer functions, irregular model test runs 156
Figure B - 6: Yaw transfer functions, irregular model test runs 157
Figure B - 7: Pitch transfer functions, irregular model test runs 157
Figure B - 8: X-force transfer functions, irregular model test runs 158
Figure B - 9: Y-force transfer functions, irregular model test runs 158
Figure B - 10: Z-force transfer functions, irregular model test runs 159

Figure C - 1: Decay test, uncoupled condition, roll 161
Figure C - 2: Decay test, uncoupled condition, heave 161

Figure C - 3: Decay test, uncoupled condition, pitch 162
Figure C - 4: Decay test, coupled condition, heave 162
Figure C - 5: Decay test, coupled condition, roll 163
Figure C - 6: Decay test, coupled condition, pitch 163

PART 1: THE UNIVERSAL BUOYANCY SYSTEM

1 LNG AS AN ALTERNATIVE FUEL

Liquefied Natural Gas (LNG) is becoming an increasingly popular alternative to traditional marine fuels. A large contributor to the increasing popularity is the new ECA regulations. ECAs, or emission control areas are areas where there are stricter rules with respect to emissions of sulphur. In some areas restrictions are also placed on nitrogen oxide and particle emission. The areas included in ECA are the North Sea, the Baltic Sea, most of the North American coastline and parts of the Caribbean and were established in the MARPOL 73/78 Annex VI. The ECAs include approximately 70% of the world fleet [1].

On the 1st of January 2015, new emission limits on sulphur will take effect in the ECAs. The new limit for fuel sulphur content will be 0.1% (of total weight) as opposed to 1% as it is per January 2014. Also outside the maximum emission will be reduced from 3.5% to 0.5% of total weight in 2020.

The introduction of these new emission rules means that the ship owners will have to either introduce scrubbers, use a cleaner type of marine oil (like low sulphur heavy fuel oil), or invest in new engines that can run on LNG. Cost estimates by for example Kolwan & Narewski or Bech (see [1], [2]) conclude that converting into LNG is the most economical solution for most ships.

This new development in the marine industry means that the market for LNG distribution will increase. Today, there are about 50 LNG powered vessels worldwide, but various estimates predicts that in 2020 the number will be in the range 6000 -10000 [3]. Another example is China; their current 5 year-plan includes the construction of 1500 new LNG terminals along the Yangtze River within 2015.

Connect LNG has come up with a new concept for LNG offloading called Universal Buoyancy System, UBS. It is intended for small-scale vessels, and is a cheap and simple alternative compared to other concepts. This thesis will concern the hydrodynamic and structural properties of the system.

2 THE UBS CONCEPT

An initial sketch of the UBS LNG offloading system is shown in figure 1. At the left side is the harbour. The LNG storage tanks will be placed here, together with the reel that stores the LNG hose when not in use. When the system is needed for offloading, it will be pulled out by a service vessel or some other method.

Clamps will be placed at the edge of the pier to keep the floating hose extended at the desired length. The hose it attached to the semisubmersible at the other end, which in turn will be attached to the ship. The buoy is placed 100 m from shore. The pipeline is 110 m long, so the initial configuration will be a C- or S-like shape (not shown in the figure).

Figure 1: Sketch of LNG offloading system. Image courtesy of Connect LNG

The LNG hose is the Cryoline pipe from Trelleborg. Cryoline is a bonded flexible pipe that uses vacuum to insulate the inner fluid. I received pipe specifications from Trelleborg on the type of hose that Connect LNG will use. As mentioned earlier, the hose is kept in place at shore by clamps at the pier. A pipe shoot will also be needed to guide the hose into the water smoothly without risking damage to the outer sheath.

The platform will be the link between the hose and the ship. The flexible hose is connected to a rigid end termination hose on the platform, which is connected to the ship's manifold. A bellmouth or bend stiffener is needed at the connection between the stiff and the flexible pipe to ensure a smooth connection. The platform itself is not equipped with a station-keeping system, as the connection system to the ship is enough to restrain the platform. Station keeping of the LNG Carrier is maintained using a multi buoy mooring system.

Connect LNG has, in collaboration with several master students (some of which are the founders of CLNG), evaluated several different concepts for the platform and the connection system. Examples include spar boys, mooring the platform to the sea floor or the ship, the use of pre-tension in the pipeline and so on. For further reading, see for example the master's theses by Syvertsen (2013), Knutsen (2012) and Magnusson (2013). The conclusion from these investigations were that a tripod semisubmersible is best suited with respect to hydrodynamic properties. Its size is about 12 m x 11 m, and it weighs about 38 tonnes. The platform is connected to the ship via four vacuum pads, two at each corner of the tripod. Connect LNG has now decided on this design, and are now proceeding with the

development and implementation of the system. The next milestone in the development is to receive certification from DNV, scheduled to take place this year.

3 PROBLEM STATEMENT

One part of the development of the UBS is to ensure structural integrity. It is important to have thorough knowledge about the hydrodynamic properties of the structure, both to be approved for the market by authorities and for credibility with respect to potential customers. This thesis will look at the motions of the UBS system in different configurations and sea states in order to determine the most suitable configuration and to uncover any especially unfavourable conditions. Two different methods will be used, namely computer simulations in MARINTEKs finite element programme SIMA, as well as model tests in the Marine Cybernetics (MC) laboratory at MARINTEK, Tyholt. The use of two different methods enables confirmation of the results by providing a source of comparison. In addition, input parameters to the computer simulations like transfer functions, added mass and so on, may be validated.

4 THESIS OVERVIEW

This report follows the problem text quite closely, and is for convenience divided into five main parts. The first part covers the introductions and the basics of the UBS system and ends with this overview of the thesis.

Part two covers the simulations in SIMA. The first two chapters gives a very brief summary of the analytical theory behind RIFLEX and SIMO. The third chapter covers the modelling and simulations in SIMA. In addition, any simplifications and assumptions made along the way will be laid out. The calculation parameters and description of the different configurations are also included here. The results from the different simulations are presented in chapter 4.

Part three considers the model testing. The first chapter covers some background information and motivation for the testing, before the actual model test set-up is described in detail in chapter two. This includes the test arrangement, data acquisition, and the different runs and setups. The post-processing of the model test data is performed in MATLAB. The data analysis performed for each kind of run is described in detail in chapter three. The main results are presented in chapter four. Lastly, a chapter on uncertainties and errors are included.

The fourth and last part concludes this thesis by comparing the results from the SIMA simulations with the model tests. A brief summary of the main results, as well as some recommendations for further work are included in part five.

PART 2: MODELLING IN SIMA

1 INTRODUCTION

Computer analysis is an established way of performing investigations on hydrodynamic bodies. For coupled systems such as the UBS, one would use a finite element method-based programme, like for example Flexcom 3D, Orcaflex or SIMA. As this thesis is written at NTNU, SIMA, which is created by MARINTEK, is the preferred analysis tool. In the following sections, the underlying theory behind the computer programme will be outlined, followed by the modelling of the Universal Buoyancy System.

2 ANALYSIS THEORY

2.1 SIMA

SIMA is developed as a JIP (joint industry project) by MARINTEK and Statoil. SIMA is a graphical user interface for the programmes SIMO and RIFLEX. According to SIMA's user manual, the main goals of the programme are:

- Creating a tool for beginners that shorten the time it takes to become proficient in modelling and analysis
- Creating a tool for experts that shorten the time from project initiation to conclusion.

Without SIMA, the user has to create input files by manually, that is, by text editing. Seeing as SIMA has a graphical user interface, it is both easier to learn and to validate one's work. Within SIMA it is possible to create models that are based on only one of the programmes, or combine them in a coupled task. As SIMAs main function is to provide a graphical user interface, the underlying theory is that of SIMO and RIFLEX, which will be described in further detail in the subsequent paragraphs. Also included in SIMA is a simple post-processor, which can perform simple arithmetic operations, apply some filters, and present plots for chosen parameters.

2.2 RIFLEX

2.2.1 INTRODUCTION

RIFLEX is a finite element programme. It was developed by MARINTEK and can be used for analysing slender submerged structures like risers, pipeline and mooring lines.

RIFLEX can model the following [4]:

- All translations and rotations in 3D space
- Small strain theory
- Beam and bar elements
- Nonlinear material properties
- Stiffness contribution from both material and geometry
- A number of system configurations and boundary conditions.

The following sections will give a brief explanation of how RIFLEX uses the finite element method to model elements, forces, displacements and so on. The focus is to explain the most important topics in a fairly colloquial manner, and not dive into the mathematical theory. A more complete and thorough description may be found in the RIFLEX Theory manual.

2.2.2 FINITE ELEMENT MODELLING

RIFLEX uses the total Lagrangian model to describe de motion of particles. It uses a fixed rectangular Cartesian coordinate system. This indicates that all configurations and motions are described relative to the initial configuration. When using the Lagrangian formulations, the strains are measured in terms of the Green's strain tensor. The Green strain, which is given by equation (1):

$$\varepsilon_G = \frac{1}{2}\left(\frac{L^2 - L_0^2}{L_0^2}\right) \quad (1)$$

When using the Green strain, the corresponding stress is the Piola-Kirchhoff stress. More specifically, RIFLEX uses the symmetric (or 2nd) Piola-Kirchhoff stress.

In order to express equilibrium for each finite body, RIFLEX makes use of the principle of virtual work. The principle of virtual work states that "The total virtual work done by a system in equilibrium when exposed to virtual compatible displacements are equal to zero". By setting up this as an equilibrium equation (*internal virtual work* = *external virtual work)*, it is possible to calculate the geometrical and material stiffness matrix.

RIFLEX uses the principle of virtual work in order to formulate the dynamic equilibrium equations. The equations are written on the so-called incremental form, and when solved gives the mass and damping matrices.

2.2.3 IMPLEMENTATION OF THE FINITE ELEMENT METHOD

All nodal points in RIFLEX can have up to six degrees of freedom. This means that RIFLEX is able to analyse all movements in 3D space. In order to describe translations and rotations, RIFLEX uses a local coordinate system that is parallel to the global coordinate system, together with a rotation matrix. This means that we have three coordinate points that define the displacement of a node, plus a three-by-three rotation matrix that describes the rotations. The concept is shown in figure 2 below.

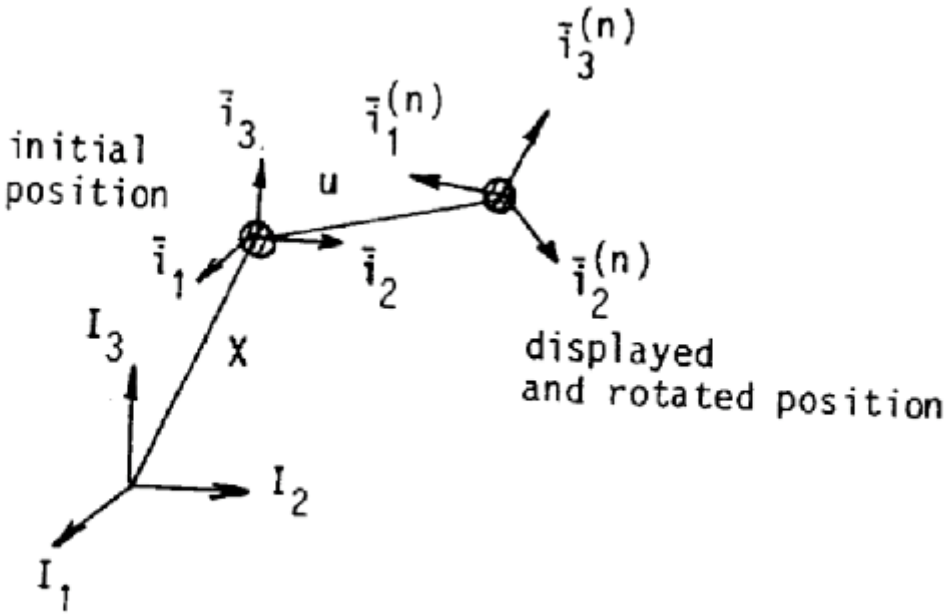

Figure 2: Translations and rotations in RIFLEX [4].

2.2.4 ELEMENTS

In RIFLEX, the user can specify which type of element RIFLEX should use. The options are bar and beam elements. Bar elements are similar to beam elements, but are simpler. They cannot model bending moments, only axial force. The model employed in the numerical analysis will use only beam elements, and so the focus will be on this type. The beam type element has one node in each end, both with (up to) six degrees of freedom, as shown in figure 3 on the following page.

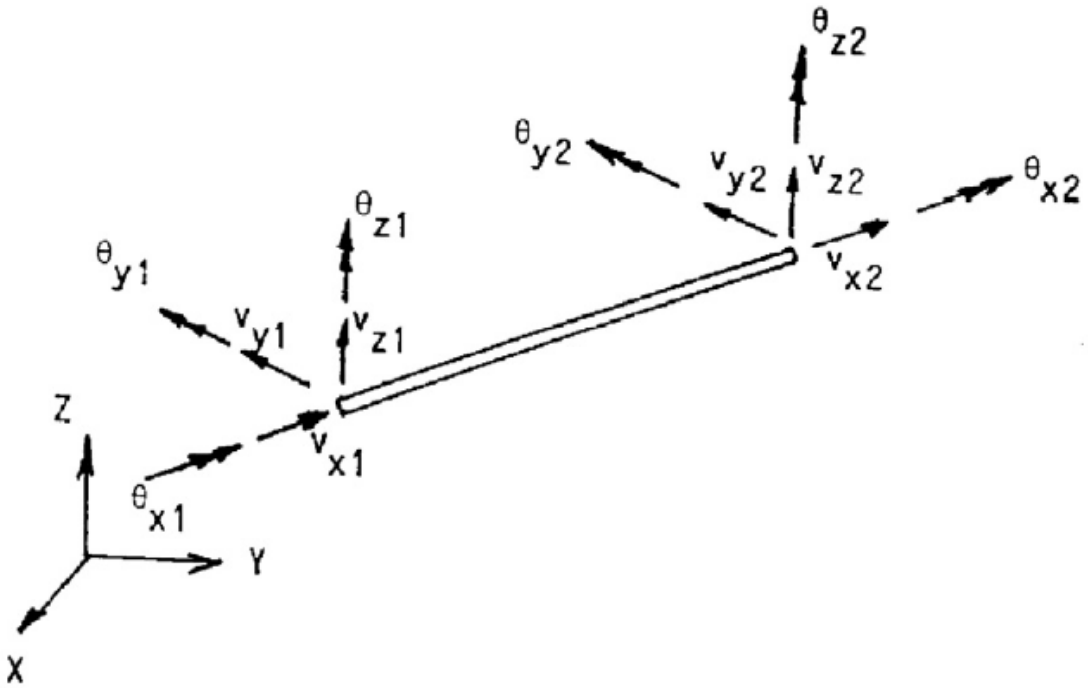

Figure 3: Beam element in RIFLEX [4].

Beams are initially straight and have a constant initial cross-sectional area. RIFLEX is based on beam theory that assumes the following:

- A plane section initially normal to the x-axis remains plane and normal to the x-axis during deformations (Navier's hypothesis).
- Lateral contraction caused by axial elongation is neglected, that is the cross-sectional area is constant
- The strains are small
- Shear deformations due to lateral loads are neglected, but St. Venant torsion is accounted for.
- Coupling effects between torsion and bending are neglected. This means we do not have to consider warping resistance and torsional stability.

In order to calculate the strain, the elongation of the beam must be known. Working with beams, we have to find displacements in each direction u, v, w, separately. Knowing the elongation, RIFLEX can find the strain and stress.

The equations mentioned up to this point only give information about stress conditions at the nodes. In order to find stresses within the element, we have to introduce interpolation functions. These assume

how stresses are distributed along the element length, allowing the user to obtain more detailed information about where on the element the largest stresses occur, and how large they are. An example of a linear interpolation function is shown in equation (2).

$$N = [1 - \xi, \xi] \quad (2)$$

Where ξ is the normalised length coordinate of the element, that is: $\xi = \frac{x}{L}$. For beam elements, a combination of linear and cubic interpolation functions are used. Using these interpolation functions mean that we can now express the internal reaction forces as shown in equation (3).

$$S_i = \int_L N_{u,x}^T N_{xx} dx \quad (3)$$

Similarly, the consistent external nodal loads are found by integrating the transposed interpolation function multiplied by p_x, which is the distributed external load per unit length (in the u-direction), shown in equation (4).

$$S_e = \int_L N_u^T N dx * p_x \quad (4)$$

The expressions given for S_i and S_e are for the u-direction only, the rest can be found in the RIFLEX theory manual.

2.2.5 MASS, STIFFNESS AND DAMPING MATRICES

The mass matrix has two contributing components; the structural mass and the added or hydrodynamic mass. The structural mass is the actual, physical mass of the object. We need to know the mass in terms of the nodes and element of the structure, and again we use the interpolation function, displayed in equation (5).

$$m_s = \bar{m}_s \int_L N^T N dx \quad (5)$$

$\bar{m}_s$ is the structural mass per unit length. Hydrodynamic mass is not a mass at all, but a force that makes the structure act as if its mass were larger, and so we call it added (or hydrodynamic) mass. The mass actually arises from the fact that when a structure is surrounded by water, and it starts to move, it also has to move a lot of water. It requires more power to move an object though water than through air, and this difference is manifested in the added mass. We find the added mass by using the interpolation functions.

The damping matrix also has two contributions; the structural damping and the hydrodynamic damping. Structural damping arises from the internal friction in the structure. This means that it is a property of the material in itself. The hydrodynamic damping is also called viscous damping, and arises from the viscosity, or friction, of water.

As mentioned previously, the stiffness matrix also has two contributions; the geometrical and the material stiffness. The geometric stiffness is found by use of the internal virtual work. The material stiffness is a property of the structure, meaning that it is dependent on the material properties in itself, in addition to shape and boundary conditions.

2.3 SIMO

2.3.1 INTRODUCTION

SIMO is another MARINTEK computer programme. Its purpose is to simulate motions and station-keeping of floating objects such as ships, platform and buoys. Some essential features are [5]:

- Flexible modelling of multi-body systems
- Nonlinear time-domain simulation of wave-frequency as well as low-frequency forces
- Environmental forces due to wind, waves and current
- Passive and active control forces

The SIMO programme uses the same global Cartesian coordinate system as RIFLEX does. It is usually earth-fixed for convenience. Do describe local motions of bodies one can use either a local coordinate system, or a so-called body-related coordinate system that follows the body's motions.

2.3.2 ENVIRONMENT

SIMO makes use of stochastic theory to describe environment. SIMO can model wind, current and waves. The current can either be defined explicitly by a current profile, or by using DNVs current velocity profile. Waves and wind is defined by means of a spectrum. For wind there are several spectra to choose from, examples include Davenport Harris type wind spectrum. SIMO also applies a wind profile, to take into account the fact that the velocity of the wind varies with height above sea surface.

For the waves, linear wave theory is used. This means we can model the incoming waves by a velocity potential function ϕ_0 , given by equation (6).

$$\phi_0 = \frac{\zeta_a g}{\omega} \frac{coshk(z+d)}{\cosh(kd)} \cos(\omega t - kxcos\beta - kysin\beta + \phi_\zeta) \quad (6)$$

Where:

ζ_a is wave amplitude

g is the acceleration of gravity

k is the wave number, $k = \frac{\omega^2}{g}$

β is the direction of wave propagation

ϕ_ζ is the phase angle

The surface elevation is now given by equation (7), and the linearized pressure is given by equation (8).

$$\zeta = \zeta_a sin\theta \tag{7}$$

$$p_d = -\rho g \zeta_a \frac{coshk(z+d)}{\cosh(kd)} sin\theta \tag{8}$$

For deep waters, the fraction simplifies: $\frac{coshk(z+d)}{\cosh(kd)} \approx e^{kz}$.

SIMO uses wave spectra to model waves. Some examples of commonly used wave spectra are the JONSWAP spectrum, the Pierson-Moskowitz spectrum and the Torsethaugen (two-peaked) spectrum. The relevant spectra for this thesis will be given in a later section.

When we use spectra to define wind and waves, we may use the transfer function to find the response of our object of interest. The transfer function is then the relation between a harmonic excitation and the response of the object. This can be for example a ship's heave response to an incoming wave. For example, if we know the wave spectrum S(ω) and the transfer function H, we can then find the response function R as displayed in equation (9).

$$R = H^2 S(\omega) \tag{9}$$

2.3.3 EQUILIBRIUM EQUATIONS

The equation of motion is given by equation (10).

$$\boldsymbol{M\ddot{x} + C\dot{x} + D_1\dot{x} + D_2 f(\dot{x}) + K(x)x = q(t, x, \dot{x})} \tag{10}$$

Where:

$$\boldsymbol{M = m + A(\omega)}$$

$$\boldsymbol{A(\omega) = A_\infty + a(\omega) = A(\omega = \infty) + a(\omega)}$$

$$\boldsymbol{C(\omega) = C_{\infty} + c(\omega) = C(\omega = \infty) + c(\omega) = c(\omega)}$$

Where:

M = Frequency-dependent mass matrix

m = Body mass matrix

A = Frequency-dependent added mass

C = Frequency-dependent potential damping matrix

D_1= Linear damping matrix

D_2= Quadratic damping matrix

f = Vector function where each element is given by $f_i = \dot{x}_i|\dot{x}_i|$

K = Hydrostatic stiffness matrix

x = Position vector

q = Excitation force vector

The excitation forces on the right-hand side are given by equation (11).

$$\boldsymbol{q(t, x, \dot{x}) = q_{WI} + q_{WA}^{(1)} + q_{WA}^{(2)} + q_{CU} + q_{ext}} \quad (11)$$

Here, $\boldsymbol{q_{WI}}$ is the wind drag force, $\boldsymbol{q_{WA}}$ are the first and second order wave excitation forces, $\boldsymbol{q_{CU}}$ is the current drag force and $\boldsymbol{q_{ext}}$ are any other forces, like wave drift damping, forces from station keeping and so on.

This is a rather complicated differential equation. If can be solved in the frequency domain by use of the convolution integral, which is an analytical solution method described in detail in for example the SIMO theory manual. Alternatively, the equilibrium equation can be solved in the time domain. To do this, we need to separate high-frequency motions and low-frequency motions.

The high-frequency-motions are solved in the frequency domain, assuming the motions to be linearly related to the incoming waves. Next the low-frequency motions are solved in the time domain. For a more in-depth explanation of the solution procedure, see the SIMO theory manual chapter 4.

2.3.4 COUPLING AND STATION KEEPING

Coupling forces

There are three types of coupling models included in SIMO; Simple wire coupling, multiple wire coupling and lift line coupling. The common denominator is that the user may specify stiffness and damping. The

simple wire coupling, which will be used later in this thesis, is modelled as a linear spring. The force-elongation relationship is given by Hooks' law, shown in equation (12).

$$F_T = kx \quad (12)$$

Where:

F_T = Tension

k = spring stiffness

x = elongation

SIMO calculates the position of the nodes at each end of the line first, giving the elongation. As the user has already given the spring stiffness, the tension in the wire may be found. The damping included is the material damping. The properties are defined by the user in a similar way, with a fixed, linear relationship between the elongation and the damping. For information on the multiple wire coupling and lift line coupling, a reference is made to the SIMO theory manual.

Station keeping forces

SIMO can model conventional station keeping forces like anchor lines, thrusters including conventional and ducted propellers, and rudders. In addition, fixed force-elongation type models can be specified as a station-keeping force. These can be linear or non-linear, with and without hysteresis. Again the used is able to specify the parameters in such a way that reflects the physical system most accurately.

There are two different versions of the fixed force-elongation type. These are "fixed contact points", where the distance is measured between a fixed point on the body and a globally fixed point, and a "docking device" which consists of a funnel and a docking post. This model is used when the body needs guiding towards a specific point, for example in offshore operations.

Fenders are a special case of the "fixed contact points" type, and the one that will be used later in this thesis. They can be used either as a positioning element or as a coupling element, providing the contact forces, both compressive (normal) force and friction force between two objects. The objects can be two ships, for example in an offshore operation, or a ship and a quay.

The fender consists of a fender point on the body, as well as an attachment point. The attachment point can be either a globally fixed plane or a globally fixed point. The fender point on the body is specified in terms of local coordinates, while the globally fixed plane or point is specified in global coordinates. Size and orientation, in terms of normal and parallel vector, must also be specified.

The normal force is found by interpolation of the distance between the two previously specified points. First the distance is calculated by means of geometry considerations, and the normal vector is found by vector algorithms. The normal force is then found by equation (13).

$$F_N = -\left\{ f(R) + c\left|\dot{R}\right|^e * \frac{\dot{R}}{\left|\dot{R}\right|} \right\} \vec{n} \quad (13)$$

Where:

$f(R)$ is the fender characteristics

c is the damping constant

$\dot{R}$ is the deformation velocity

$\vec{n}$ is the normal vector

e is the specified exponent

The friction coefficient μ can be either unidirectional, or it can be defined as a so-called roller, meaning that the friction is zero in the direction perpendicular to the fender plane. For a point symmetric fender, the friction force is given by equation (14).

$$F_F = -\mu|F_N| * \frac{\vec{s}}{|\vec{s}|} \quad (14)$$

Where $\vec{s}$ is the sliding motion along the plane. The in-plane fender force is found using the shear stiffness k_s, as shown in equation (15).

$$F_{F,inplane} = k_s * \vec{s} \quad (15)$$

The programme calculates the in-plane force and the static friction for each step, so that the fender point sticks to the fender plane as long as the in-plane force does not exceed the static friction.

3 SYSTEM DESCRIPTION

3.1 GENERAL

A rough sketch of the complete model for use in SIMA is shown in figure 4 below. The pier will be modelled as a fixed point. This is done by giving the supernode at shore a fixed prescribed position, and fixing it in all translations and rotations. The platform is modelled by a WAMIT-type body, whereas the ship will be a SIMO body. The pipeline will be modelled both as a RIFLEX-line and as a number of SIMO-bodies. The modelling of these will be explained in further detail later.

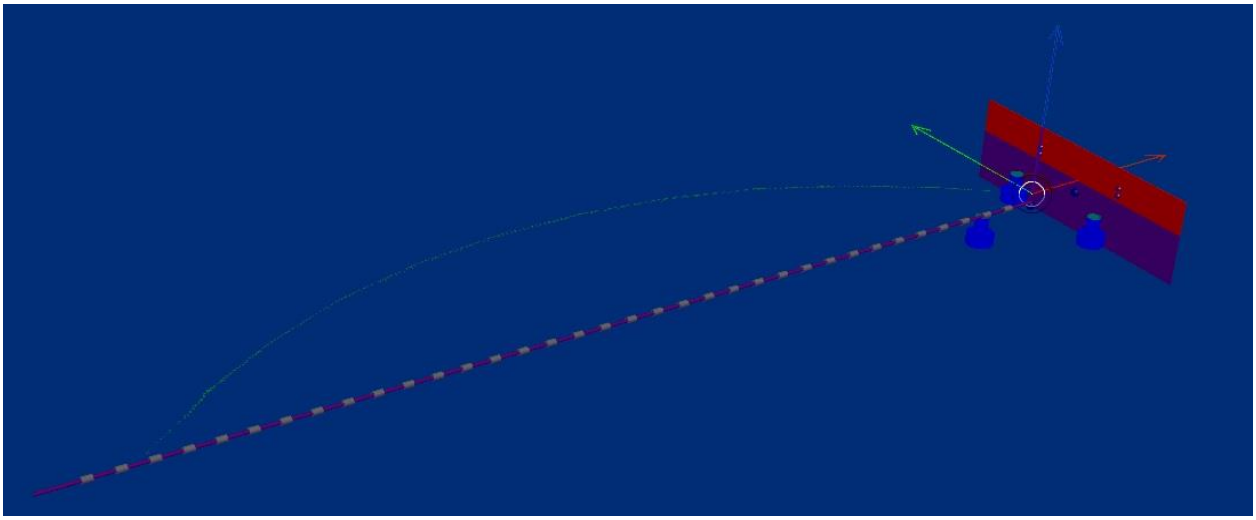

Figure 4: Complete SIMA model

The regular Cartesian coordinate system, with z being the out-of-plane direction (blue in the figure), x is parallel to the initial configuration of the pipeline (red in the figure) and y is perpendicular to the initial configuration of the pipeline (green in the figure), will be used. The origin is located where the pipeline meets the floater, such that the last supernode on the LNG hose is located at x = 0.

When considering the motion of the platform, the conventional names will be used. Translations in the x, y and z directions are referred to as surge, sway and heave, while rotations about x, y, and z axis are called roll, pitch and yaw. The coordinate system used for each setup will be indicated.

3.2 SHIP

The ship is modelled as a fixed wall. This is because the ships that will use the UBS system are physically very large in comparison with the platform. In addition, the sea state is so small that it is assumed that any motions of the ship are negligible. One important simplification is that the interaction between the waves and the ship is not taken into account. It is possible to model this in SIMA, but wave radiation data for the ship in question is not available. The waves therefore act as though the ship is not there, making the extreme values obtained conservative.

3.3 PLATFORM

The platform is, as previously mentioned, a semisubmersible tripod. David Knutsen with Connect LNG has previously executed an analysis in WAMIT that determined that hydrodynamic properties of the platform. The files are then simply imported into SIMA, and appears as a regular body in the model. The imported body features all necessary hydrodynamic data:

- Structural mass, including total mass, centre of gravity and moments of inertia
- Linear damping coefficients in six degrees of freedom
- Hydrostatic stiffness in six degrees of freedom
- Frequency dependent added mass and damping coefficients
- Linear motion and wave force transfer function
- Geometry

A picture of the platform with its local coordinate system is shown in figure 5. The z-axis is upwards, the x-axis is in the plane (left-right) and the y-axis points out of the plane. The dimensions are exactly equal to the planned, real life platform. The distance between the two front columns is, as shown, 12 m, but the distance from the front columns to the back column is 10.4 m. The three columns are identical.

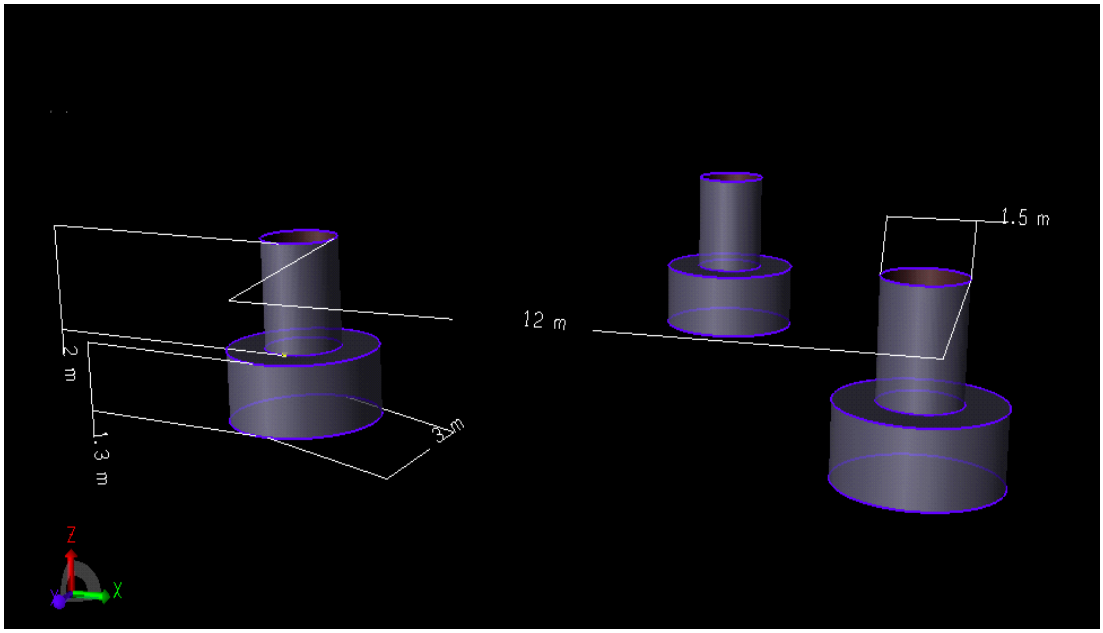

Figure 5: WAMIT platform sketch

The transfer functions cover all directions at 15 degrees intervals, in all 6 degrees of freedom. The transfer functions are included in the SIMA input files in the electronic appendices.

3.4 VACUUM PADS

There are four vacuum pads on the platform, two at each corner. The distances are such that the spacing between the centres of the pads is 12 m in the Y- (transverse) direction, and 850mm in the vertical direction. The size of the pads is 750x2000mm. Naturally, modelling these in SIMA posed a challenge as there is no such function included. After conferring with PhD candidate Lin Li as well as engineer Pål Levold at Marintek, the decision fell on using a combination of point berthing fenders and hawsers modelled as simple wire couplings.

Some trial and error was required in order to find a suitable configuration. For example, how many fenders and how many simple wire couplings should be used, and how should they be placed? It soon became evident that four simple wire couplings and four fenders was the best choice. Fewer would make the platform heel and/or pitch, and more gave convergence problems.

The four point berthing fenders are configured on the platform body. The coordinates and sizes of the fender planes correspond to that of the full-scale model. The fender points are placed in the centre of each respective fender plane. This analysis does not consider the operation of attaching the platform to the ship side, so it is assumed that the distance between the vacuum pads and ship side at the beginning of the simulation is zero. Thus the distance between the fender points and the fender planes in the x-direction is also zero. The normal and parallel vector of each fender plane is specified such that they coincide with the ship side.

The constant values of the force characteristic like friction and shear stiffness are left at their default values. The stiffness and damping was specified using linear interpolation. The values are shown in table 1.

Table 1: Force characteristic of fenders

Distance [m]	Force [kN]	Damping [kNs/m]
0.5	0	100
0	3	100
-0.5	7	100
-1	11	100

The required values for stiffness and damping was found through iteration. The initial values was borrowed from an example fender in the SIMA help section, and then adjusted according to what gave a reasonable response and minimum motions. As the values or stiffness and damping were adjusted, the response amplitude decreased further and further until the model did not converge. The built-in

postprocessor was very helpful in this process, as it provides simple results like minimum, maximum and average response instantly.

The simple wire couplings are of the type “fixed elongation couplings”. The name indicates that there is a fixed relation between the force and elongation in the coupling, which the user may specify. Each coupling must start and end in body points. This means that body points must be created on each body and the coordinates adjusted such that the distance between two corresponding body points is appropriate with respect to the specified force-elongation relationship. Four body points were created on each body. The coordinates are given in table 2. All values are in the global coordinate system.

The force characteristics are specified by interpolation. This can be either linear or parabolic, and linear was chosen. As with the fenders, some iteration was needed in order to find the most suitable solution. The initial values were copied from one of the examples included in the programme, where there was a similar stiff connection. The values were further adjusted by use of the post processor. The relationship used in the later analysis is given in figure 6.

Table 2: Body points overview

Body	Body point	X-coordinate	Y- coordinate	Z-coordinate
Platform	FP1_low	6.57	6	1.8
	FP1_up	6.57	6	2.65
	FP2_low	6.57	-6	1.8
	FP2_up	6.57	-6	2.65
Ship	SP1_low	6.57	6	1.8
	SP2_up	6.57	6	2.65
	SP1_low	6.57	-6	1.8
	SP2_up	6.57	-6	2.65

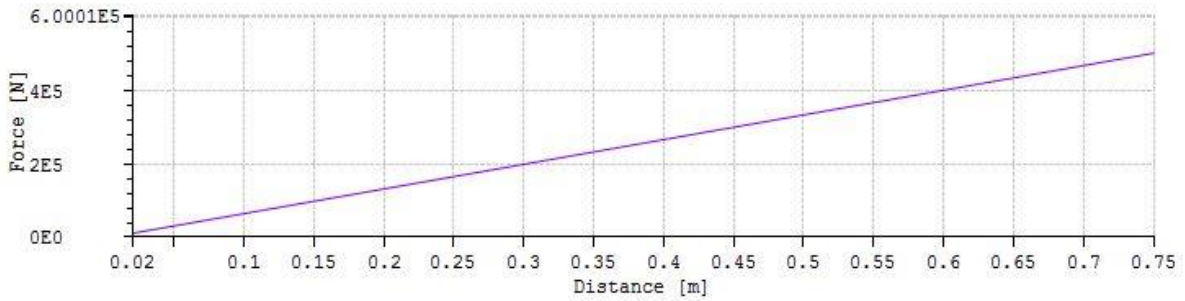

Figure 6: Simple wire coupling force characteristic

3.5 PIPELINE

To model the flexible pipeline, an arbitrary riser (AR) system is needed. The system consists of a number of supernodes, as well as lines that connects the nodes. In addition, SIMO bodies are added to capture the hydrodynamic effects of the hose. The AR system is explained further in the paragraphs that follow.

The distance between the platform and the pier is 110 meters. The Cryoline hose is produced and delivered in segments of 12 meters. This does not add up to 110 meters, but this will be neglected for now. The diameter of the hose varies along its length, being larger at the flanges and slimmer at the midpoint between two flanges. This is simplified by averaging the diameter over the length of each pipe section, so that the pipe only has one diameter for the whole length. Simple calculations in excel gives the necessary equivalent diameter and weight distribution.

3.6 SUPERNODES

SIMA requires that all lines start in one super node and end in another. Many flexible pipeline cases would only require two supernodes, one at each end. However, the prescribed configuration must be bent like a C, and to achieve this several supernodes are needed. The advice from S. Magnusson with Connect LNG was to use 12 nodes. It took some trial and error to find the correct coordinates, because both the length requirement (equal length of all line segments) and the shape requirement must be fulfilled. In addition, a supernode is needed at the ship location, in order to fulfil the “AR connection”-requirement as mentioned previously. Table 3 gives an overview of the supernodes and their coordinates.

The supernodes are defined as prescribed throughout the static calculation, as this must be in order to achieve the desired “C-shape”. However, the nodes must be released before the dynamic calculation starts, otherwise the pipeline behaves as though clamped by the nodes. The solution is to include an extra calculation step in the static calculation called “boundary change”. The boundary change step lets the user specify change of boundary condition at all the nodes, and so for this case modes M1-M10 was set to “free” in all degrees of freedom. This way, in the dynamic calculation the initial condition is the C-shape described earlier, but the pipeline is now only attached at the pier and at the platform.

Table 3: Supernode positions

	Constraint	Initial position		Prescribed configuration		Segment length [m]
		x	y	x	y	
Shore	Prescribed	-110	0	-100	0	10.0
M1	Prescribed	-100	0	-92.1	6.13	10.0
M2	Prescribed	-90	0	-83.6	11.4	10.0
M3	Prescribed	-80	0	-74.52	15.6	10.0
M4	Prescribed	-70	0	-64.9	18.3	10.0
M5	Prescribed	-60	0	-55	19.7	10.0
M6	Prescribed	-50	0	-45	19.7	10.0
M7	Prescribed	-40	0	-35.1	18.3	10.0
M8	Prescribed	-30	0	-25.48	15.6	10.0
M9	Prescribed	-20	0	-16.4	11.4	10.0
M10	Prescribed	-10	0	-7.9	6.13	10.0
Buoy	Prescribed	0	0	0	0	6.57
Ship	Free	6.57	0	6.57	0	

3.7 LINES AND CROSS-SECTION

The mass and geometry properties of a pipeline is specified by first creating a cross-section, and then creating a line type using that cross section. The cross section type “crs_cryoline” includes the mass properties for the LNG hose, and is of type CRS1. The cross section type indicates that the pipe is axi-symmetric with respect to the specified properties. The geometry and material properties of the pipeline was found in Trelleborg’s fact sheet, shown in table 4. The cross-section must be set to either bar or beam, depending on whether the pipe can transmit moments or not. The Cryoline can transmit moments, so the beam type was chose.

The bending and torsion stiffness values are constants, whereas the axial stiffness was specified according to a tension-elongation curve, which is shown in figure 7.

Table 4: Cryoline data

Mass	203.8	$\frac{kg}{m}$
Gyration radius	0.365	m
Cross-section type	Beam	
Bending stiffness	120	kNm^2
Torsion stiffness	800	$\frac{kNm^2}{rad}$

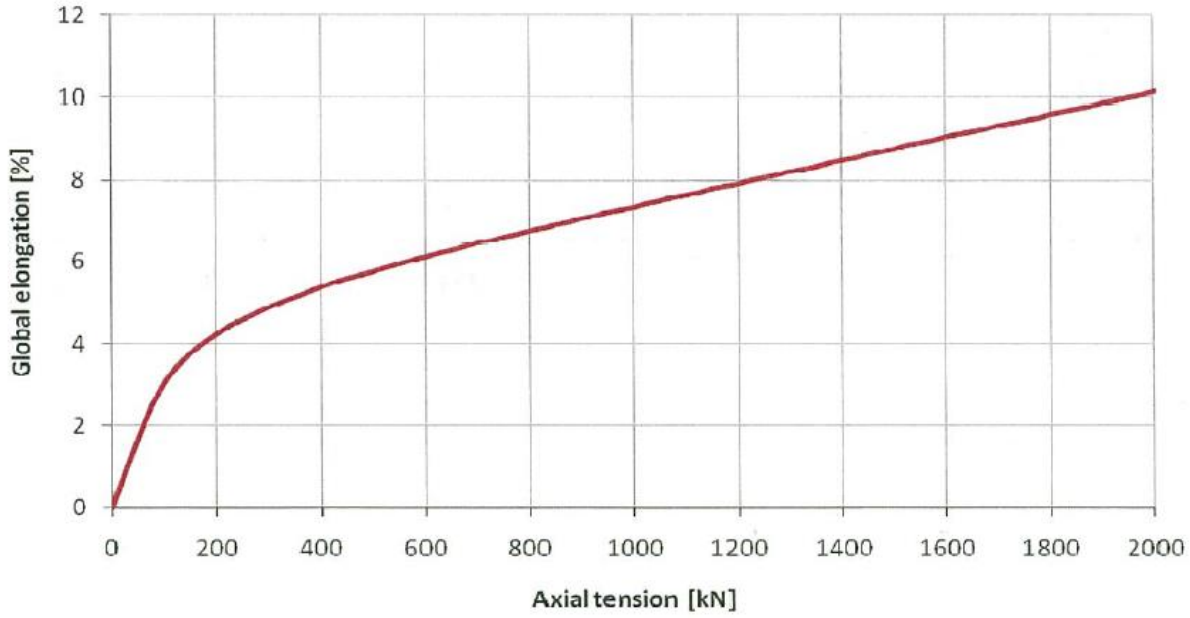

Figure 7: Tension-elongation relation for Cryoline. [28]

Next, two line types are created, one for the LNG pipeline and one for the connection line that would run from the platform to the ship side. Cryoline, the line type for the LNG hose, has one segment of 10 meters, corresponding to the distance between each supernode. The “flex” line type is the connection line, and have also got one segment of 6.57 meters. Both line types have 100 elements per segment, so that the element length becomes 0.1 m for the Cryoline.

To model the LNG hose 11 lines was used, so that all supernodes are connected to one or two line ends. Lines are defined through specifying a line type and a start-node and an end-node. An overview of the lines is shown in table 5.

Table 5: Lines overview

Name	Line type	End 1	End 2	Length [m]	Distance [m]
L1	Cryoline	Shore	M1	10	10
L2	Cryoline	M1	M2	10	10
L3	Cryoline	M2	M3	10	10
L4	Cryoline	M3	M4	10	10
L5	Cryoline	M4	M5	10	10
L6	Cryoline	M5	M6	10	10
L7	Cryoline	M6	M7	10	10
L8	Cryoline	M7	M8	10	10
L9	Cryoline	M8	M9	10	10
L10	Cryoline	M9	M10	10	10
L11	Cryoline	M10	Buoy	10	10
C	Flex	Buoy	Ship	6.57	6.57

3.8 BODIES

In order to include the hydrodynamic properties of the pipeline, SIMO-bodies must be included. S. Magnusson concluded in his Master thesis of spring 2013 that 100-120 bodies provided accurate solutions while keeping computation power on an attainable level. The number was therefore set to 110 bodies. The bodies are all identical in shape, size and hydrodynamic properties. SIMO has a feature that calculates the position of each body based on a so-called AR connection, in which the user specifies which element number the body is attached to. The programme then calculated the exact coordinates automatically. The bodies are classified as so-called “large bodies” which means that they each have six degrees of freedom (three rotations, three translations) and can simulate all motion in time domain.

The resulting model is shown in the following figures. Figure 8 displays the initial configuration, while figure 9 shows the prescribed configuration. All the bodies are the same size, but approximately every third body is yellow to visualize the varying diameter of the cryogenic hose. This is only a visual effect that makes no difference for the calculations.

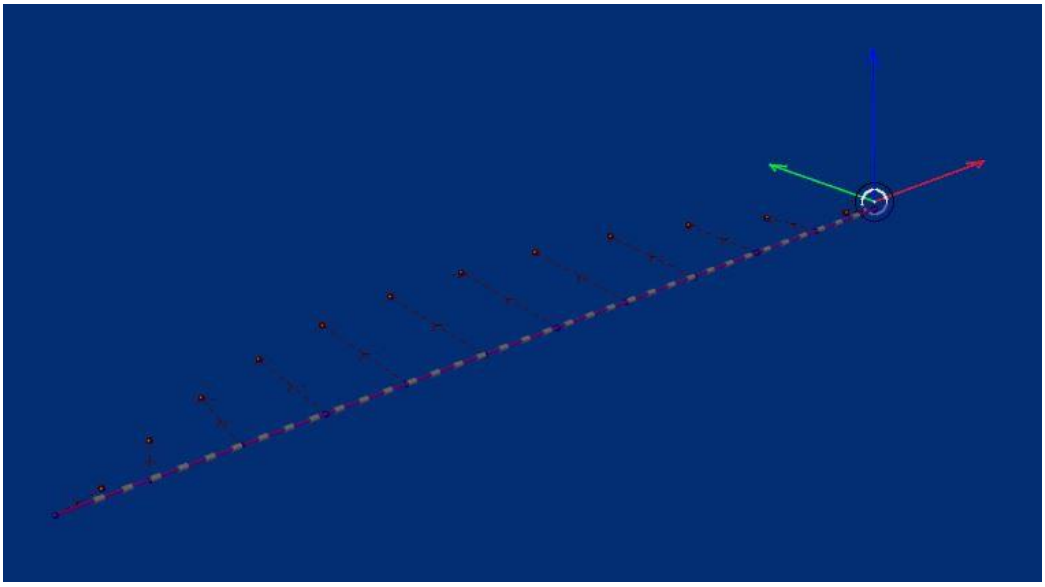

Figure 8: Initial configuration SIMA

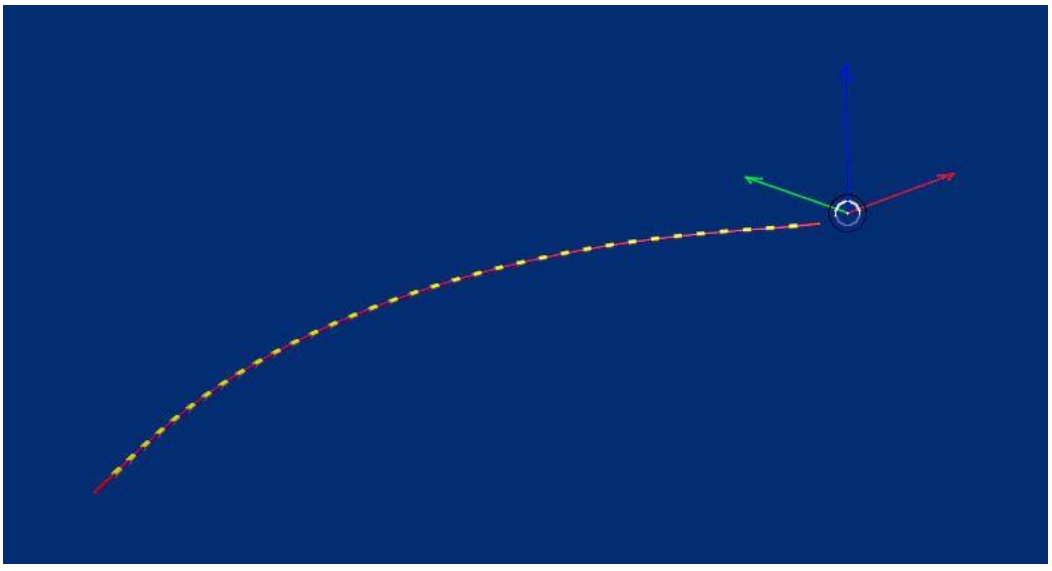

Figure 9: Prescribed configuration SIMA

3.8.1 HYDRODYNAMIC DATA

Hydrodynamic coefficients and data need to be specified for the SIMO bodies. The volume used is calculated from the averaged diameter described earlier. This way, all bodies have the same bodies, because they are of equal length.

Added mass

Added mass is not a physical mass, but a force that is in phase with the acceleration of the body and arises from the fact that water has a non-negligible density. In order to find the added mass coefficient, it is necessary to make some simplification, because there is no definite way of determining it. One common way of calculating the added mass coefficient is to use strip theory. Strip theory means that we divide the cylindrical pipeline into thin slices (usually of unit width), calculate the coefficient for the 2D strip and then multiply by the length to get the total result.

For a submerged cylinder the added mass in heave of a 2D strip is calculated according to equation (16), where r is the radius of the cylinder.

$$A_{33}^{2D} = \rho \pi r^2 \tag{16}$$

However, the LNG hose is not fully submerged. This means that 2D strip theory is not accurate enough to use. When the body of interest is in the vicinity of the free surface, or any other surface, the added

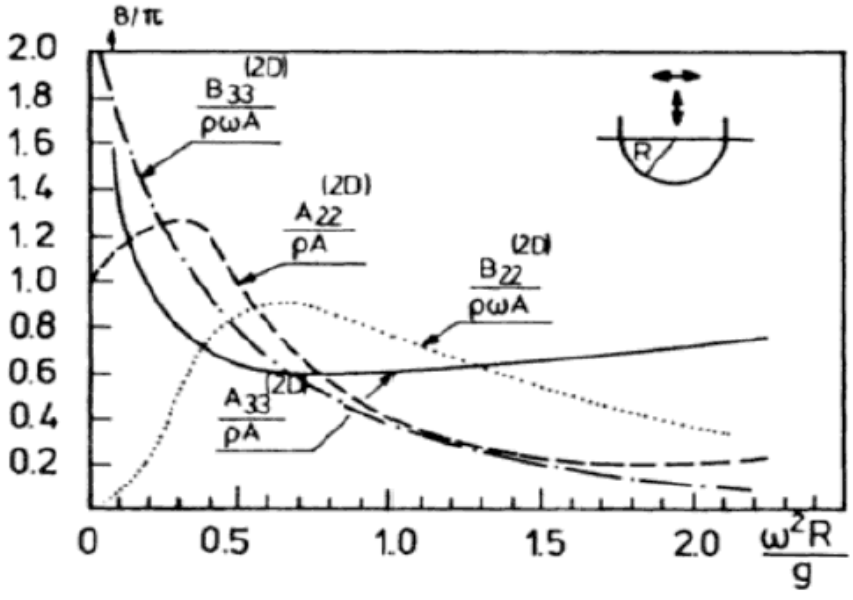

Figure 10: Added mass and damping coefficient for a cylinder in the free surface [28]

mass and damping are highly frequency-dependent. Faltinsen (see [6]) illustrates this in figure 10. In order to get as accurate results as possible, the depth-dependency graph found by Greenhow and Ahn as presented in [7] is applied in the calculations, shown in figure 11.

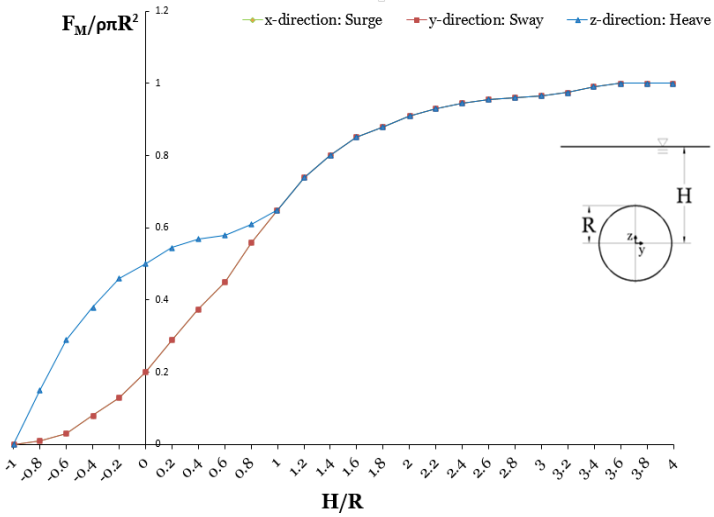

Figure 11: Depth-dependent added mass coefficient [7].

Damping

Damping has many similar properties to added mass, in the way that it is difficult to estimate and it is highly influenced by the presence of the free surface (or, again, other surfaces). This means we also have to estimate damping.

Drag damping, or viscous damping, is the most commonly implemented damping model and is fairly easy to apply [8]. One easy way to estimate the drag force is to use the drag term (the other is the inertia term) of Morison's equation, displayed in equation (17).

$$F_D = \frac{1}{2}\rho C_D A u|u| \qquad (17)$$

Here, A is the so-called characteristic area, or reference area (the cross-sectional area of the body perpendicular to the flow direction). For a fully submerged unit strip, the characteristic area is D*1=D. U is the flow velocity and ρ is the density of water. The only unknown is C_D, often denoted the drag coefficient. It is not possible to calculate C_D, but it is possible to make an estimation from empirical tests.

In this model values from experiments conducted by Achenbach (1971) and Fage & Warsap (1930), are applied. Achenbach has assembled results from Fage & Warsap and presented them in figure 13. The figure shows drag coefficient C_D for different surface roughness values k/D, where k is the average height of surface roughness and D is the cylinder diameter. Rn is Reynolds number, given by $Rn = {U_\infty D}/{\nu}$ where U_∞ is the incident flow velocity and ν is the viscosity of the water. The different curves

are: Δ → $\frac{k}{D} = 110 * 10^{-5}$, O → $\frac{\mathrm{k}}{\mathrm{D}} = 450 * 10^{-5}$, □ → $\frac{\mathrm{k}}{\mathrm{D}} = 900 * 10^{-5}$. The Cryoline has a surface roughness of $k = 1.5 * 10^{-6}$, a diameter of 0.516 and the incoming current has a velocity of 1m/s, so the drag coefficient becomes $C_D \approx 0.4$

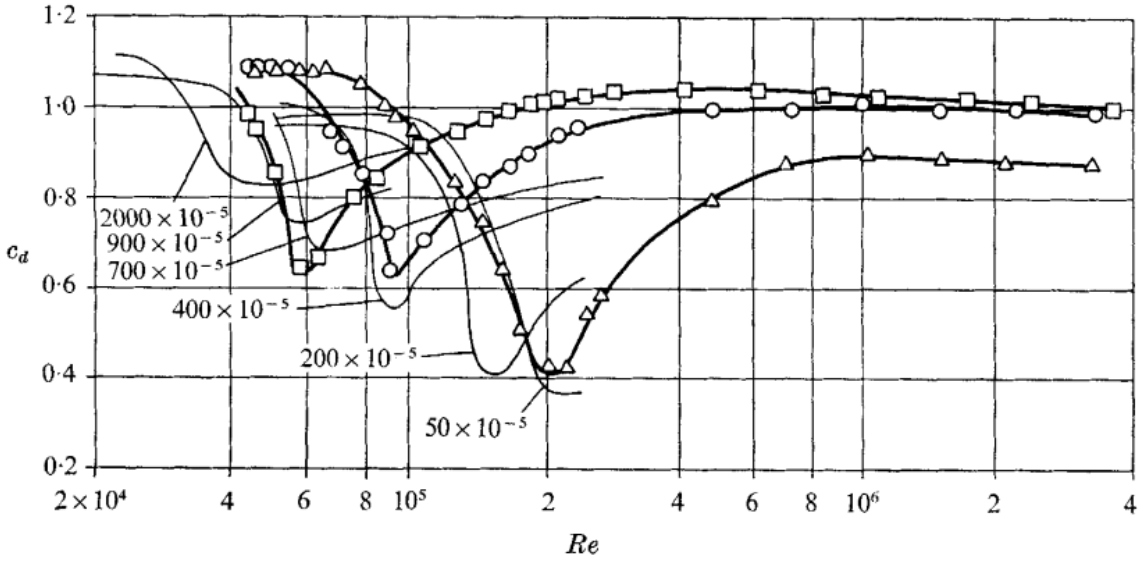

Figure 13: Drag coefficient for rough circular cylinders in cross flow. Comparison with results of Fage & Warsap (1930). See [9]

In addition to incoming current velocity and surface roughness, the drag coefficient will also vary with water depth like added mass does. To account for this effect, another depth-dependency graph will be used, developed by S. Magnusson in his master thesis. The graph is shown in figure 12 below.

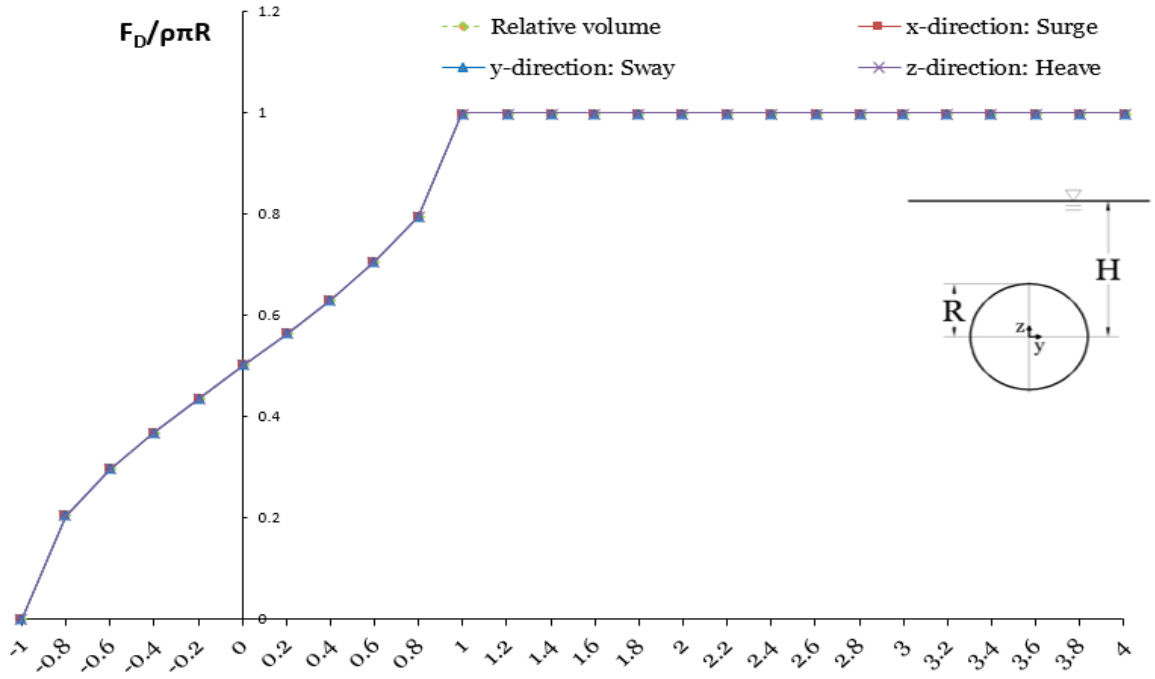

Figure 12: Depth-dependent drag coefficient [7].

Added mass and damping – summary

Added mass is estimated by means of 2D strip theory. The depth-dependency effect is included through weight factors found in figure 12 in previous section. Damping by drag forces is found through the use of Morison's equation. The drag coefficient is found from experimental data, and then the drag force is calculated using Morison's equation. The coefficients included in the analysis are shown in Table 6.

Table 6: Drag and added mass coefficients for Cryoline

Drag in x-direction	21.166	Ns^2/m^2
Drag in y-direction	105.830	Ns^2/m^2
Drag in x-direction	105.831	Ns^2/m^2
Added mass in x-direction	0	kg
Added mass in y-direction	214.552	kg
Added mass in z-direction	214.552	kg

3.9 SHIP TO PIPELINE CONNECTION SYSTEM

In the project thesis leading up to this master thesis, the platform was defined as a support vessel, such that attaching the last super node on the hose onto the platform was very simple. This may be done simply by choosing a prescribed position and choosing which support vessel the super node should be attached to. The support vessel is thusly directly connected to the arbitrary riser (AR) system as required by SIMA through the supernode.

The problem with using a support vessel for this system is that for a body type "support vessel", it is not possible to specify mass, body points, fenders and so on, only a motion transfer function. In other words, the body type is not sufficient for this analysis. Instead, regular bodies must be used, and so both ship and platform is defined as such.

In SIMA, all bodies except for support vessels need an AR connection, a connection to the supernode/pipeline system. But the ship is not, in reality, connected to the pipeline, so a work-around was needed. After conferring with Pål Levold at MARINTEK, the decision fell upon making a connection line that runs between the platform and the ship, but creating a cross-section (the previously mentioned "Flex") that has no mass, volume or stiffness. In this way, SIMA is satisfied, because both bodies are connected, but at the same time this "dummy" line has no mass or volume, so it does not interfere with the motion of the bodies. The connection line is not shown in the figures, for the previously mentioned reasons.

3.10 Environment and Location

Waves

The JONWAP-spectrum describes the waves in equation (18).

$$S(\omega) = \frac{5}{16} H_s^2 \omega_p^4 exp\left\{-\frac{5}{4}\left(\frac{\omega}{\omega_p}\right)^{-4}\right\} \times (1 - 0.287 \ln(\gamma)) \times \gamma^{exp\left\{-\frac{1}{2}\left(\frac{\omega-\omega_p}{\sigma\omega_p}\right)^2\right\}} \quad (18)$$

H_S is the significant wave height. ω_p is the peak period. γ is the peak shape parameter and σ is the spectral width parameter, which is defined as:

$$\sigma = \sigma_a \; for \; \omega \leq \omega_p$$

$$\sigma = \sigma_b \; for \; \omega > \omega_p$$

For this simple analysis, the values in table 7 will be used. The reason why the chosen sea state is so small, is that the UBS system is designed for use in calm waters like sheltered harbours. Unfortunately, the peak shape parameter cannot be changed from the default value of 3.3, although it should have been 1.65, as was specified for the design extreme state.

Table 7: Wave parameters

H_S	1.2	m
T_P	5	s
γ	3.3	

It is assumed that the wave spectrum is a sum of a large number of regular waves at different frequencies. The resulting spectrum is shown in figure 14.

Current and wind

Neither current nor wind is represented in this analysis.

Seabed and water depth

The water depth in the area is 10 meters. In the small sea state that is considered here, the system will have very low to no influence from the seabed, so this is not considered further.

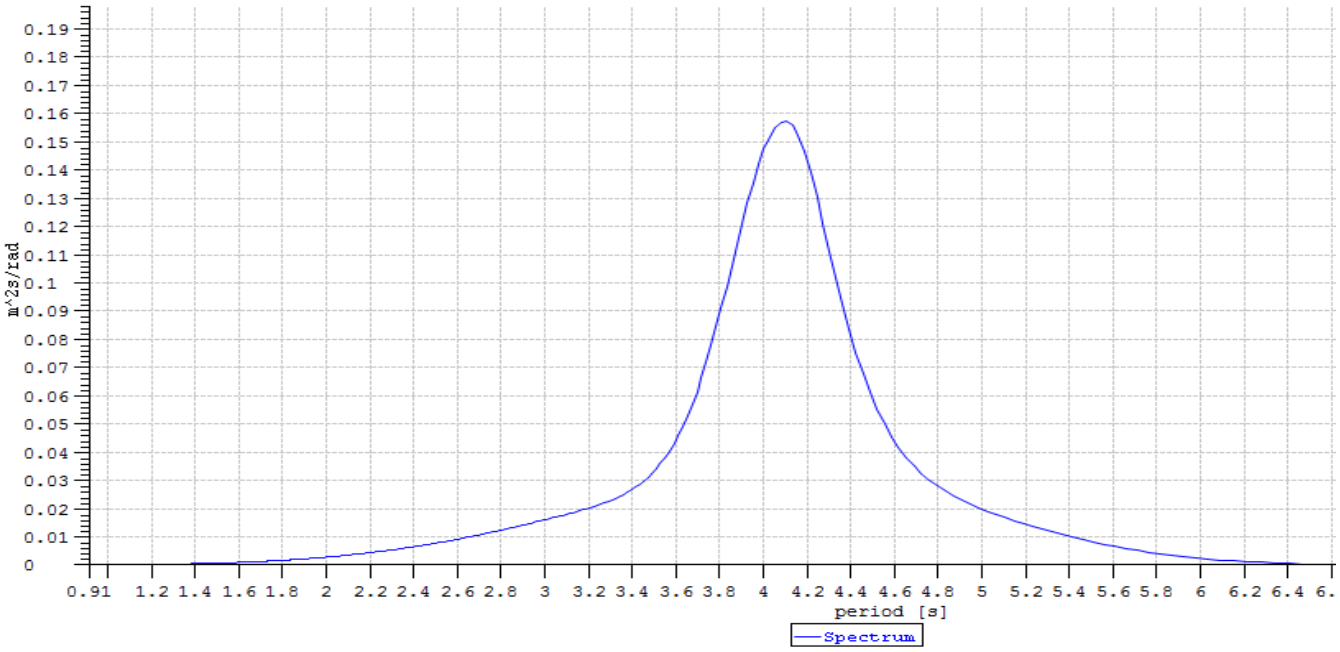

Figure 14: Wave spectrum

3.11 CALCULATION PARAMETERS

3.11.1 STATIC AND DYNAMIC CALCULATION PARAMETERS

SIMA requires that the user specifies the parameters, integration methods and so on. For the static calculation, the skyline method is used for matrix storage. The alternative would be to use sparse matrix storage. The load and mass formulation can be either lumped or consistent. Here, the consisted formulation is chosen, because it is more accurate – although it requires more computation time.

The loading steps must also be calculated. First, the volume and forces are calculated, followed by the specified displacements. For the volume and body forces the default values of 10 steps of 10 iterations were enough, whereas the specified displacements required as many as 60 steps to achieve convergence. Last follows the boundary change load sequence as described earlier, to free the pipeline from the restraint of the supernodes.

In the dynamic calculation parameters, the simulation length was set to 10800 seconds, which is equal to 3 hours. This is because a 3 hour sea state can be approximated as stationary, meaning it is fair to assume that the statistical properties of the sea state are constant during this time. The time step was set to 0.5 seconds for the two simplest configurations of the system with only SIMO bodies, whereas for setup 3 (complete system including the pipeline) the time step was reduced to 0.1 to achieve convergence. The user also has to specify the integration procedures. In these analyses, Newmark's β-family method is used, because it is an accurate and stable method. Lastly, the user must specify what

data SIMA should store from the calculations, so displacements of all bodies and nodes, waves, and connection forces were chosen.

3.12 SIMULATION RUNS

Different setups and directions will be considered. The conditions are designed with the model test in mind, to facilitate comparison and verification. Three different setups will be considered: the platform alone, platform and ship, and the total system including the flexible pipeline. In addition, several wave headings will be tested. Table 8 shows an overview of the runs.

The first two runs includes only the platform. However, a station keeping system is required to keep the platform from just drifting away. A simple mooring system consisting of three simple wire couplings, one attached at each column, was used. The force characteristics of each of the three simple wire couplings were specified such that they were as low as possible while still restraining the platform.

Runs 3 through 5 considers the platform and the ship. As the ship is modelled as a fixed structure, no mooring is needed for this setup.

Table 8: SIMA runs

No.	Condition	Wave heading (deg)
1	Platform only	0
2	Platform only	90
3	Platform and ship	0
4	Platform and ship	315
5	Platform and ship	90
6	Complete system (Pipeline, ship, platform)	0
7	Complete system (Pipeline, ship, platform)	315
8	Complete system (Pipeline, ship, platform)	90

The final configuration used in conditions 6 through 8 is the complete system, including the ship, the platform and the pipeline. The ship is fixed as in the previous setup, so no mooring is used in this condition either. The platform and pipeline is connected to the ship as described in the previous paragraphs, and the far end of the pipeline ends in a node which is fixed in all rotations and translations, representing the pier.

3.13 POST-PROCESSING

There is a simple post-processor in SIMA, however, with many different conditions and runs it is preferable to perform the post processing in MATLAB. There are some differences between the different runs, so three different scripts was needed, one for each setup, although they perform the same procedures.

According to whatever the user specifies, SIMA can write time series to file containing forces, motions, wave elevation and so on. The channels under consideration are the same as the ones in the model test – forces in x, y and z directions at the connection points, as well as the motions of the platform.

The time series are opened in MATLAB before the post-processing begins. The calculations that follows are similar to those performed in the post processing of the model test, as will be described in detail in section 3.6 of part 3. For this reason, only a brief outline of the process will be given here.

The results from SIMA does not need to be scaled, as they are already in full scale. However, the results show some bias, and this is removed. The built-in MATLAB function “buttord” is used to create an individual filter for each run. The limits of the filter are set at fractions of the wave period, as shown in equations (32) and (33). It should be noted that the same filter is applied for all channels of a single run, it is only for each new run that a new filter is created. The absolute value of the Fourier transform of each channel is plotted for visual inspection.

Spectra of the wave and responses are found using the “pwelch”-function. Once the spectra are found, the transfer function is found as the square root of the response spectrum divided by the wave spectrum. The transfer function for each channel is stored in a MATLAB-“struct” for later plotting.

The spectral moments and statistics are found using simple built-in functions. The three first spectral moments are found by numerical integration. In order to estimate the extreme values, the “findpeaks” function is applied to find all positive maxima and their locations. Assuming that the instantaneous wave elevation is stationary, ergodic and normally distributed, the local maxima follow the Rayleigh distribution. Knowing the distribution of the local maxima, it is possible to find the expected value of the largest maximum, as well as the most probably largest max. Finally, the statistics are printed to file.

4 RESULTS

The following sections present the results from the analysis. SIMA provides a well of results, and it would be too much to present in this report. The full statistical values from each run is attached in appendix A, while some selected values are displayed here. Each run is presented individually, with the maximum registered value as well as the expected value of the largest max and the standard deviation. These three values were chosen because they provide simple information about the response spectrum that is easily comparable. The transfer functions are displayed in groups for better comparison.

4.1 CONFIGURATION 1: PLATFORM ONLY

The first setup considers only the platform, shown in figure 15 . The results are only shown for heave, roll and pitch, as the transfer functions in surge, sway and yaw are heavily influenced by the mooring system. Furthermore, as the mooring system used in the model test was different there is no point in comparing them.

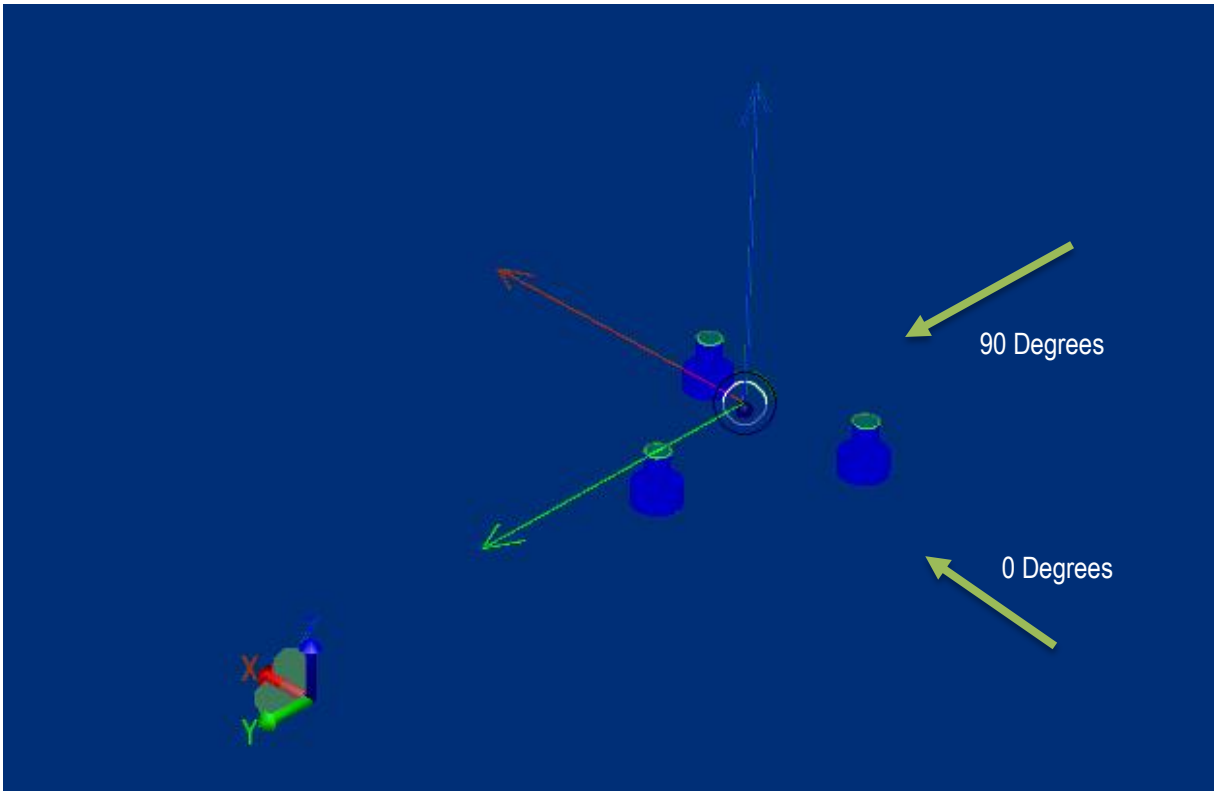

Figure 15: SIMA configuration 1 overview

4.1.1 RUN 1: WAVE HEADING 0 DEGREES

Some statistics for the first run is shown in table 9. Motions are in general small except for heave, which peaks at 2.7 m. The largest rotation is roll, with a maximum angle of 1.10 degrees. The translations in the horizontal plane are very small, with amplitudes of only 0.072 m in sway and 0.187 m in surge. The reason why surge is so much larger than sway is simply the direction of the incoming waves. The pitch angle is significant, with a maximum of 5.22 degrees. The reason pitch motion is so much larger than roll is, as with the translations, because of the direction of the incoming waves. As there is little or no coupling effect between the modes of motion most of the response will be in the form of pitching.

Table 9: Statistics, SIMA run 1

Degree of freedom	Maximum value
Surge (m)	0.187
Sway (m)	0.072
Heave (m)	2.737
Roll (deg)	1.095
Pitch (deg)	5.216
Yaw (deg)	0.996

4.1.2 RUN 2: WAVE HEADING 90 DEGREES

In the second run, platform is subjected to waves from a 90-degree angle, meaning that the ship that the platform would be connected to experiences beam sea. As seen in the previous run, this sea state will give the ship roll motions, which translates to pitch motion for the platform. This is shown in table 10 , where the maximum pitch angle is 2.8 degrees, whereas the maximum roll angle is only 0.001 degrees. The heave amplitudes are much smaller than for the first run, with a maximum amplitude of about 0.2 cm.

The results from the two runs indicate that in terms of translations, there is a very small difference between the two wave directions. The large difference in heave amplitudes are not easily explained, as the first run gave a maximum of 2.7m while the second gave a maximum of only 0.2 cm. The real values should lie somewhere in between.

The platform exhibits some coupling between roll and pitch in the first run, whereas in the second run there is practically no roll motion while pitch reaches 2.8 degrees. This happens because the platform is not symmetrical about its x-axis, which leads to the coupling shown in run 1.

Table 10: Statistics, SIMA run 2

Degree of freedom	Maximum value
Surge (m)	0.598
Sway (m)	0.059
Heave (m)	0.002
Roll (deg)	2.808
Pitch (deg)	0.002
Yaw (deg)	0.000

4.1.3 TRANSFER FUNCTIONS FOR CONFIGURATION 1

The wave spectrum for the runs is shown in figure 16, and the corresponding transfer functions from both runs are shown in figure 17, figure 18 and figure 19. The wave spectrum is very similar to the ones seen in textbooks, which is one of the positive aspects of computer analysis. The wave spectra for the two runs are so similar that they are completely overlapping. The peak at f=0.2 Hz is consistent with the input peak period of 5 seconds. The same frequency range is applied to all the transfer functions, based on the wave spectrum. Limits of 0 Hz to 1 Hz was chosen, as there is no contribution to the wave spectrum outside this frequency range.

The transfer functions for the beam sea condition are all very small, with heave and pitch being practically zero. The heave values are consistent with the values displayed in table 10. The pitch values are not really consistent with the maximum values. However, further investigation shows that there is actually a peak at a frequency around 0.05 Hz, where the maximum amplitude ratio is 1.8 (too small to see in the figure). This must be where the maximum value of 2.8 degrees occur. The exact opposite is seen in the roll transfer functions, which peaks with a maximum of 700 deg/m around 0.05 Hz, whereas the maximum absolute value is 0.001 degrees. As the maximum values are coherent with the time series displayed in SIMA, the difference in the transfer functions must be due to coincidences.

The conclusion from this setup is that the platform has very good sea keeping capabilities in the independent condition. All transfer functions show very small amplitude ratios in the wave frequency range. Some responses occur at around 0.05 Hz, indicating a possible Eigen frequency. This could, however, also be due to the mooring system and would require further investigation.

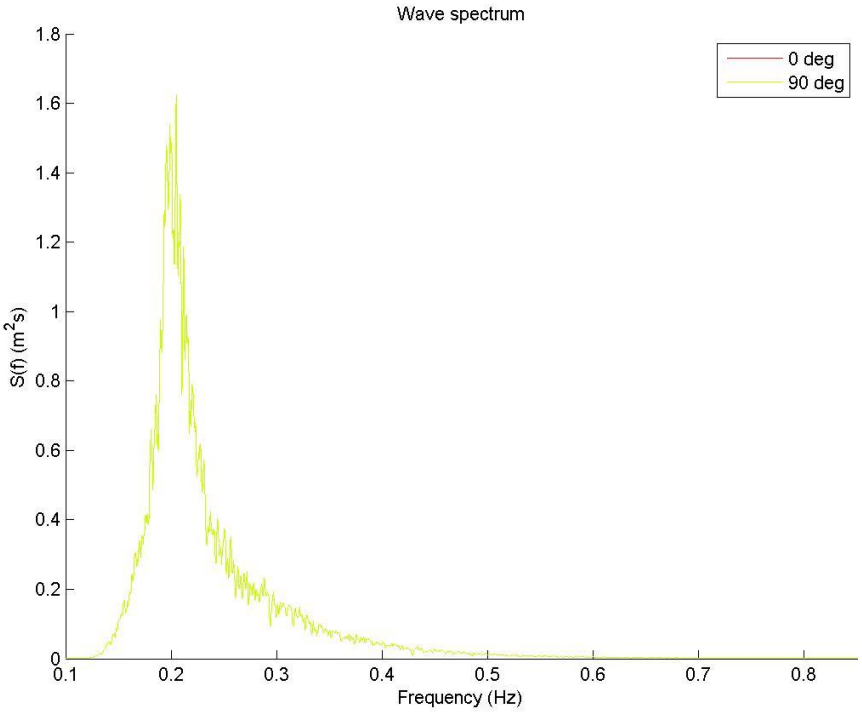

Figure 16: Wave spectrum, configuration 1

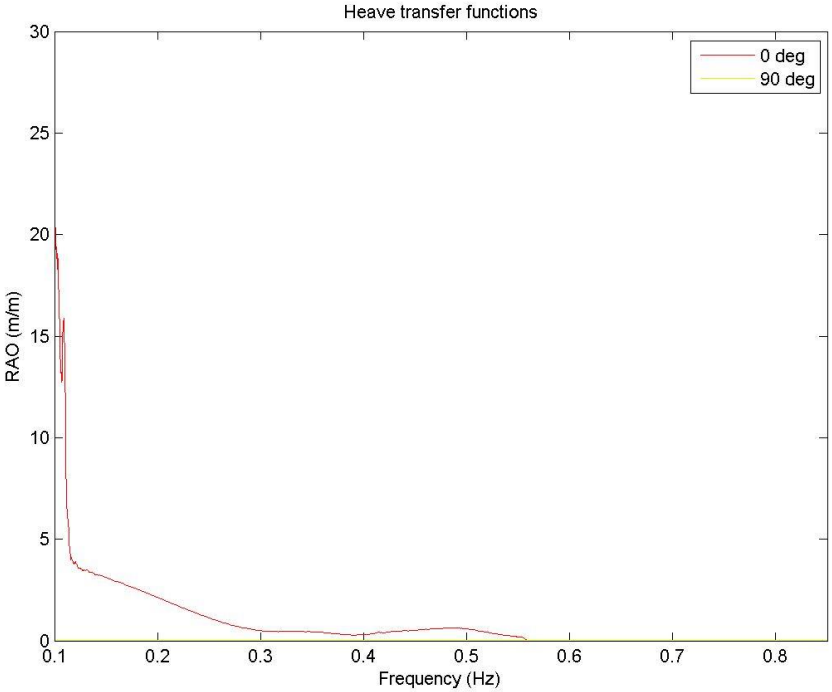

Figure 17: Heave transfer functions, configuration 1

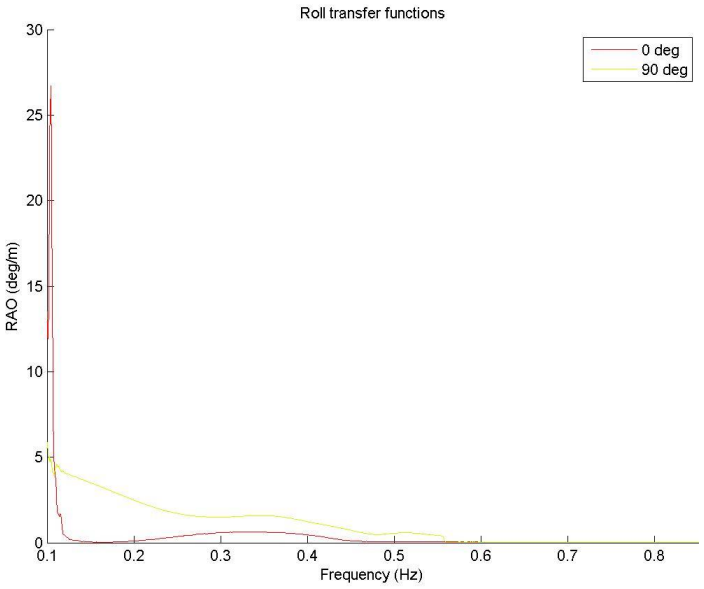

Figure 18: Roll transfer functions, configuration 1

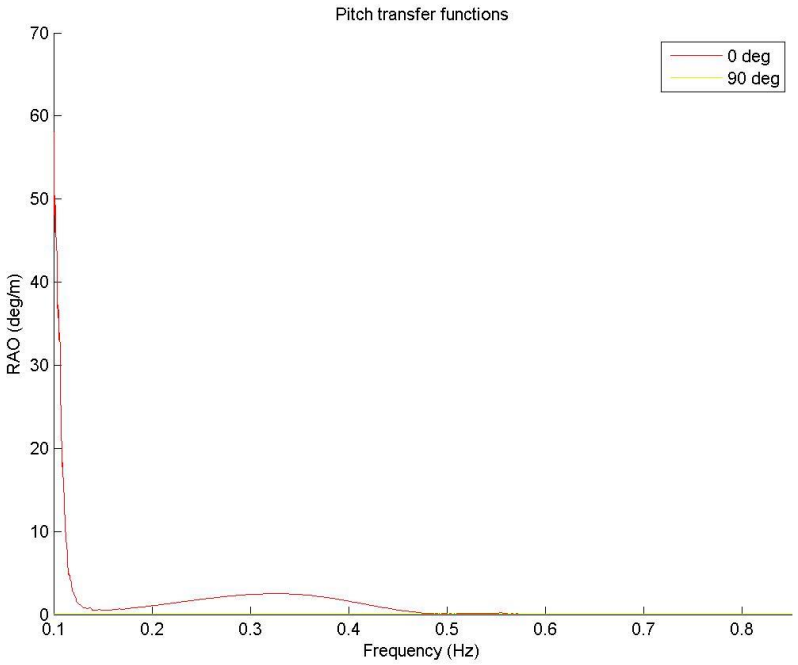

Figure 19: Pitch transfer functions, configuration 1

4.2 CONFIGURATION 2: PLATFORM AND SHIP, COUPLED CONDITION

The second setup modelled in SIMA includes the ship as well as the platform. For this setup, three wave headings are investigated; 0, 315 and 90 degrees. The maximum values are presented first, and the transfer functions are displayed in the last section for comparison.

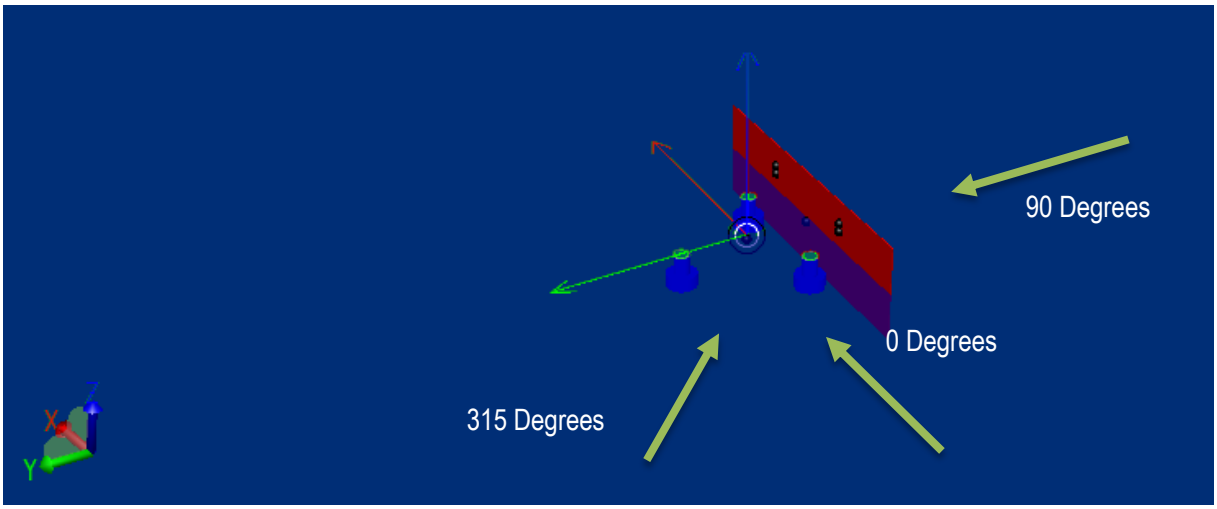

Figure 20: Configuration 2 SIMA overview

Figure 20 displays the setup with the coordinate system. In run 3 the wave heading is 0 degrees, with waves propagating along the positive x-axis. For run 2, the waves propagate along an axis midway

between the positive x-axis and the negative y-axis. In the third and final run, the waves propagate along the positive y-axis.

4.2.1 RUN 3: WAVE HEADING 0 DEGREES

Some statistical values from run 3 are shown in table 11. The translations in the water plane directions are small, although the response in sway is not insignificant at almost 0.2 m. Given the very rigid connection system, this should perhaps be smaller, in particular considering the fact that while the forces in x- and y-directions are of the same order of magnitude, the motions in sway are about three times as large as the motions in surge. That said, the coupling with the rotations (mainly roll) may increase the recorded sway magnitudes. Heave motions are somewhat larger than sway with a maximum of 0.241 m.

For this wave heading there are some displacements in roll and pitch. Considering the wave direction, the rotations about the y-axis (pitch) should intuitively be larger than the rotations about the x-axis (roll). However, the results show that the opposite is true. Inspecting the simulated video recording shows that there is in fact some visible roll motion (larger than pitch), so the values are assumed to be correct. From the simulation it looks like the platform is in fact excited in heave, but is restrained at one end (at the ship side) so that only one column is excited, which results in pitch motion.

Table 11: Statistics, SIMA run 3

	Maximum value
X-force (kN)	209.4
Y-force (kN)	194.0
Z-force (kN)	1428.9
Surge (m)	0.077
Sway (m)	0.198
Heave (m)	0.241
Roll (deg)	1.730
Pitch (deg)	0.406
Yaw (deg)	3.894

The yaw angle is the largest of the rotations, which is perhaps not what one would expect. Considering the rigid connection system, roll should be larger than yaw. One possible theory why the yaw angle is large, is that there is only limited stiffness in the connection system with respect to yaw motions, and when the platform is subjected to waves incoming from an angle of 0 degrees, a moment about the z-axis will arise, “pushing” the platform around its own axis. When the connection system fails to provide restraint, the movement will be executed. In a real life situation, this movement will probably be smaller,

as the connection system will have a larger spatial extent and have more stiffness than the one modelled in SIMA.

The forces in the water plane directions are, like the motions, small. Considering the small motions in surge, the forces are as expected. The Z-forces are, however, very large. From studying the video recording it is evident from the behaviour of the "free" column (the one that is not next to the ship side) that there is a lot of excitation in heave. Although the modelling of the vacuum pads has attempted to simulate that the platform is free to move in the vertical reaction, these results show that there is still a significant amount of restraint, probably in the fixed elongation couplings.

4.2.2 RUN 4: WAVE HEADING 315 DEGREES

The statistical values for the fourth run are shown in table 12. Surge motion has now increased significantly compared to the previous run, and the sway motion is also almost doubled. This increase in translations in the water plane directions is due to the change in wave heading, and the lack of restraint in surge and sway. Still, there is some restraint in the x- and y- directions, but as the wave is incident from a 315 degree angle, the movements cannot be fully avoided. Heave motion is, however, almost the same as before, as is expected due to the symmetric geometry of the platform.

Table 12: Statistics, SIMA run 4

	Maximum value
X-force (kN)	214.7
Y-force (kN)	192.5
Z-force (kN)	1211.2
Surge (m)	0.15
Sway (m)	0.40
Heave (m)	0.23
Roll (deg)	3.44
Pitch (deg)	0.25
Yaw (deg)	3.95

Pitch motions are very small for this run, even smaller than for the previous run. This result is as expected, as the waves are no longer propagating along the x-axis, but at an angle with the x-axis. A reduction in rotation about the y-axis is therefore anticipated. Roll, on the other hand, is much larger with a maximum angle of 3.44 degrees. Again, the angle of the incoming waves is the reason for this increase. In addition to the reason for the unexpectedly large roll motion explained in the previous section, the waves are now propagating with a 45 degree angle to the y-axis, as opposed to 90 degrees in the previous case. Yaw angles are again large. The reason must be, as mentioned in the previous

section, the moment created by the platform pulling and pushing on the hinges, resulting in a rotation about its own axis.

The forces in x- and y-direction are of the same order of magnitude as seen in the previous run. Even though the surge motion increases significantly, the corresponding force does not. This must be because the sway motion has also increased significantly, and that the two modes are out of phase, creating a cancellation effect. The z-forces are again very large with a maximum value of 1.2 MN, but not as large as in the previous wave heading, which recorded 1.4MN. As the heave motion is of the same order of magnitude, and roll is larger, one would expect the Z-forces to be larger. Instead, the forces are smaller. A possible theory is that the motions in the remaining degrees of freedom is such that there are some cancellation effects reducing the Z-forces.

4.2.3 RUN 5: WAVE HEADING 90 DEGREES

The results from the final run of this setup are shown in table 13. The translations of the platform are larger for this wave heading, with an increase of about 50%. With the waves now propagating along the positive y-axis, this is only as expected for translations along the y-axis. For surge, however, this result is peculiar, as the waves are incident from a 90 degree angle, so that the platform "should" not be excited in surge at all. Similarly, there is no clear reason as to why the heave motion is larger for this case.

The roll motions in this run are very large with a maximum of 5.12 degrees. On the other hand, almost all rotation is in the form of roll, as the pitch angle peaks at 0.15 degrees. Both these results are as expected considering the direction of the incoming waves. Yaw angles are again large with a maximum of 4.01.

Table 13: Statistics, SIMA run 5

	Maximum value
X-force (kN)	201.3
Y-force (kN)	248.0
Z-force (kN)	1042.7
Surge (m)	0.23
Sway (m)	0.59
Heave (m)	0.20
Roll (deg)	5.12
Pitch (deg)	0.15
Yaw (deg)	4.01

The x- forces are of the same order of magnitude as seen in the other runs, and is in coherence with the similar surge magnitudes. However, there is a larger relative increase in surge motion than in x-force. This is likely because the fender has some extent in the x-direction. Y-forces in run 5 are larger than in runs 3 and 4, which must be because the platform is now being pulled straight away from the ship side, inducing large forces perpendicular to the ship side.

Forces in the vertical direction are again the largest forces of all the components, but it is still smaller than for the previous runs. It could be that the pulling away of the platform from the ship side lets the platform move more freely in roll and heave, decreasing the reaction forces in the connection.

4.2.4 TRANSFER FUNCTIONS FOR CONFIGURATION 2

The wave spectrum for configuration 2 is so similar to the one from configuration 1 that there is no practical purpose of printing it again. The reader is therefore referred to figure 16. Some of the more interesting transfer functions are displayed in the figures to follow, while the rest is found in appendix A.

The motion transfer functions display some of the same behaviour as seen in the first configuration, with very large amplification factors in the 0-0.12 Hz frequency range, making it difficult to study the behaviour in the wave frequency range. A shorter frequency range is therefore chosen here, so the reader should keep in this in mind when comparing the transfer functions to the wave spectrum. The transfer functions in heave are displayed in figure 22. The general trends of runs 3 (0 degrees) and 4 (45 degrees) is the same, with a steady increase in amplification factor with the exception of a dip around 0.32 Hz. Run 5 displays a similar trend although the amplification factors are all over lower. The transfer function displays a steady increase in response except for a dip at around 0.2 Hz, the peak frequency of the spectrum. The system does not appear to have any natural frequencies in the wave frequency range.

Figure 21 shows the transfer functions in roll for setup 2. The magnitudes are small, with amplification factors mostly below 1.5 deg/m. The exceptions are the fourth and fifth runs for the smallest frequencies, where both start at large amplification factors at the lower limit of the plot, but this is a “false” peak due to the very low values of the wave spectrum in this frequency range.

In run 3, the response at least partially resembles the wave spectrum, with a “top” around 0.2 Hz. As the frequency increases, the response decreases, like the wave spectrum. Both transfer functions have a dip at about 0.3 Hz, with run 5 dipping significantly more than run 4.

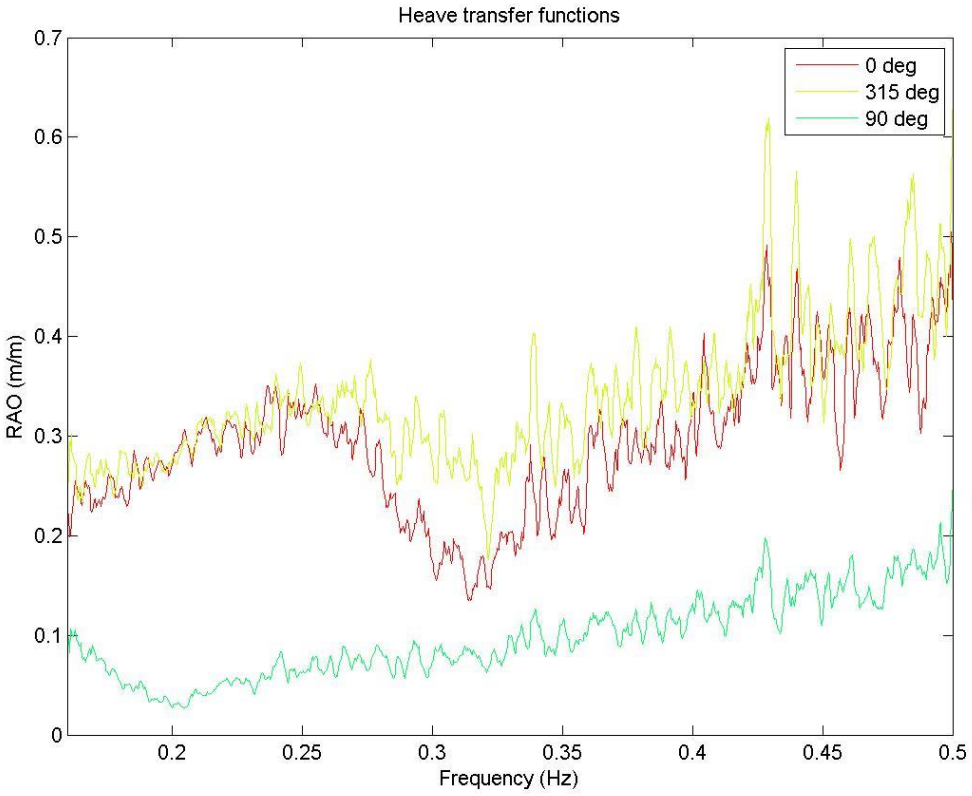

Figure 22: Heave transfer functions, configuration 2

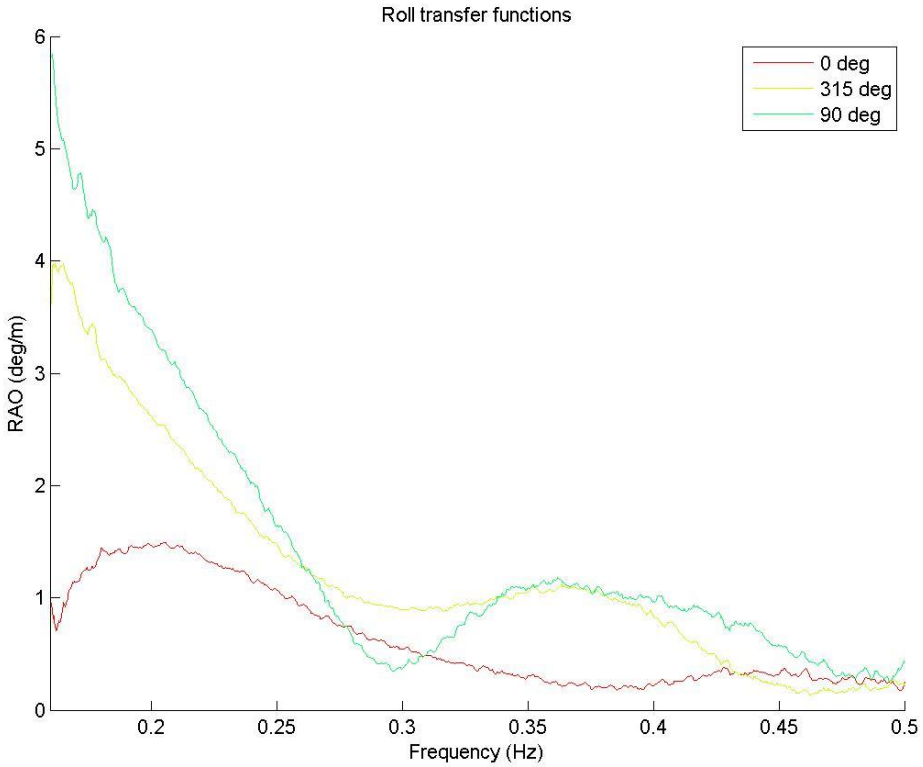

Figure 21: Roll transfer functions, configuration 2

The force transfer functions are displayed in figure 23, figure 24 and figure 25. The force transfer functions all follow a general trend of declining steadily as for the smallest wave frequencies until it reaches a minimum at about 0.2 Hz, and then increases almost linearly. The minimum at 0.2 Hz is probably due to the fact that the wave spectrum has a large spike here (making the relative force small), rather than actual cancellation effects.

In the x- and z-directions, the 90-degree case has the smallest RAOs, while in the y-force has the largest responses for beam sea condition. As the 90-degree case has waves that propagate along the y-axis, it is expected that the largest relative forces would occur here. The 0- and 315-degree runs both have a spike at about 0.43 Hz in the x-force transfer function, which indicates a possible Eigen frequency. There is also a small spike in the 90 degree transfer function for the same force, but this could also be coincidence. The z-force also has some peaks in the 0.35-0.5 Hz frequency range for the 0 and 315 degree runs, however, Eigen frequencies would result in larger spikes.

It is interesting that the transfer functions are so similar to one another, both in terms of force component and wave heading. This indicates that the platform is not very sensitive to changes in wave heading. There are also no indicators of Eigen frequencies in the wave frequency range, another indicator of good sea keeping capabilities.

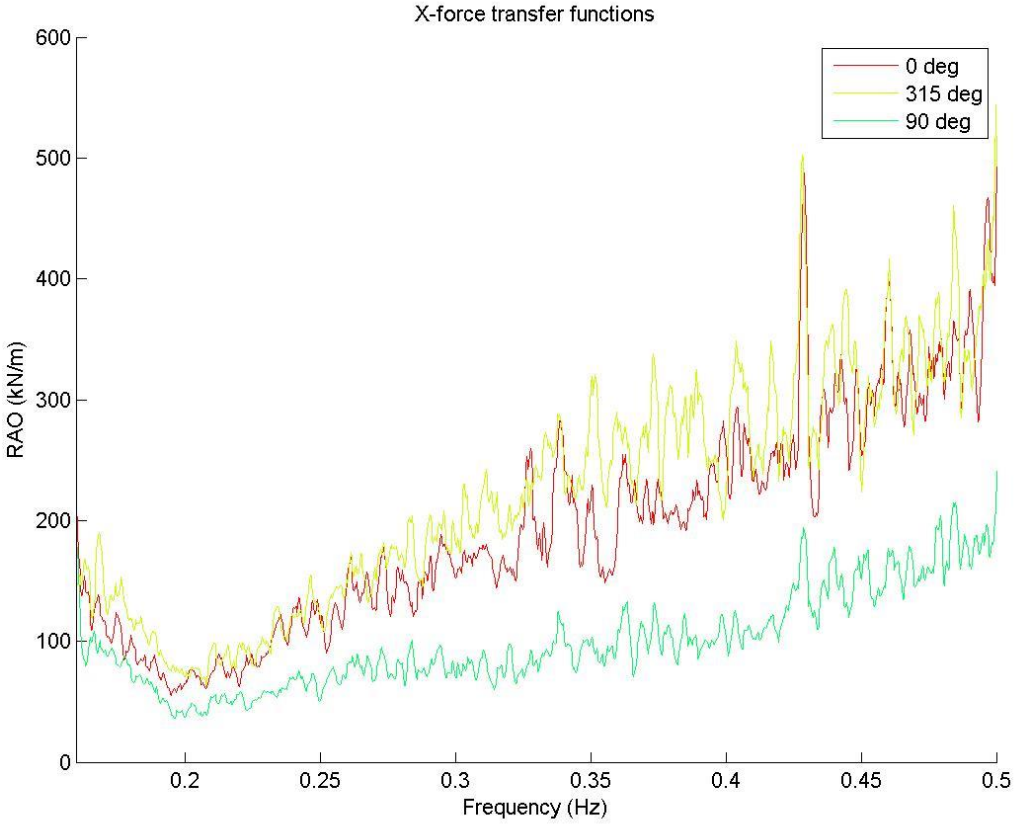

Figure 23: X-force transfer functions, configuration 3

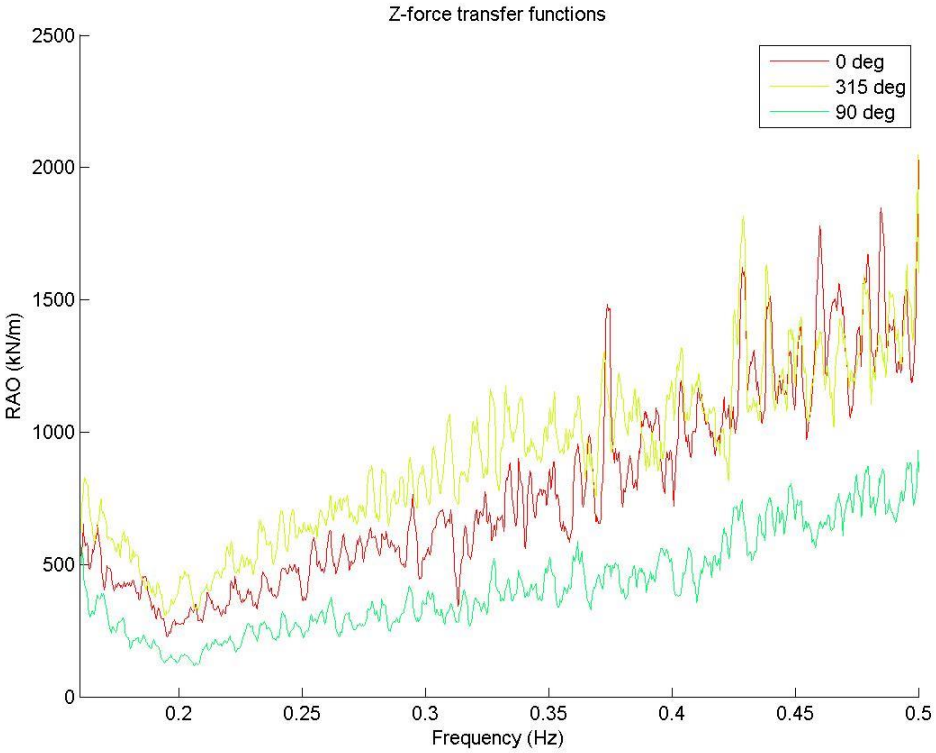

Figure 25: Z-force transfer funtions, configuration 3

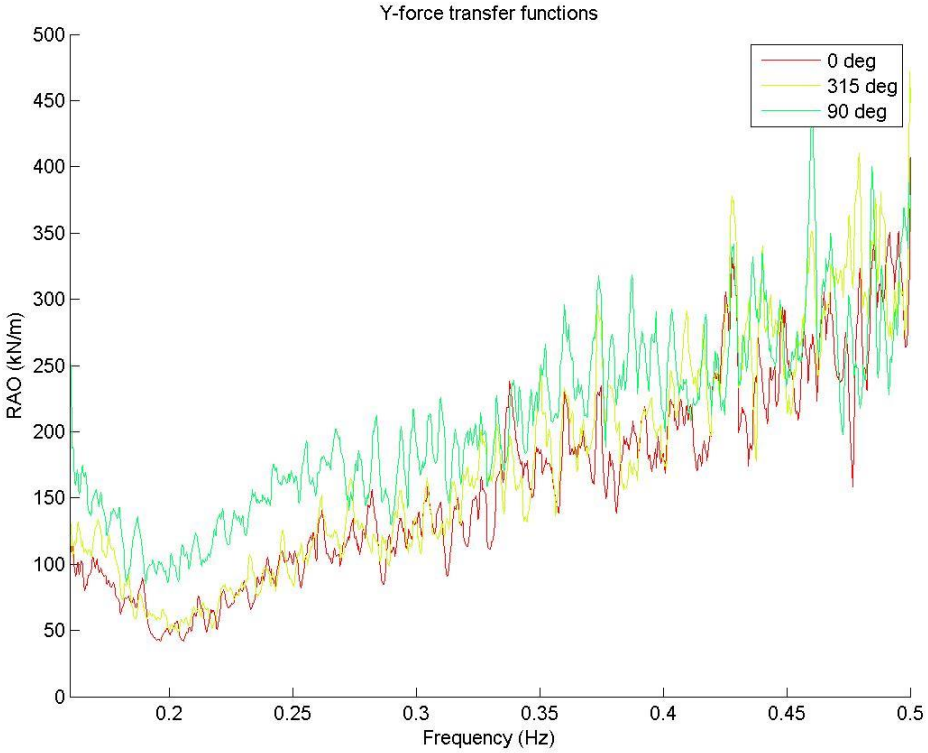

Figure 24: Y-force transfer functions, configuration 3

4.3 CONFIGURATION 3: COMPLETE SYSTEM

The third and final setup comprises the complete UBS system, with the flexible pipeline, platform and

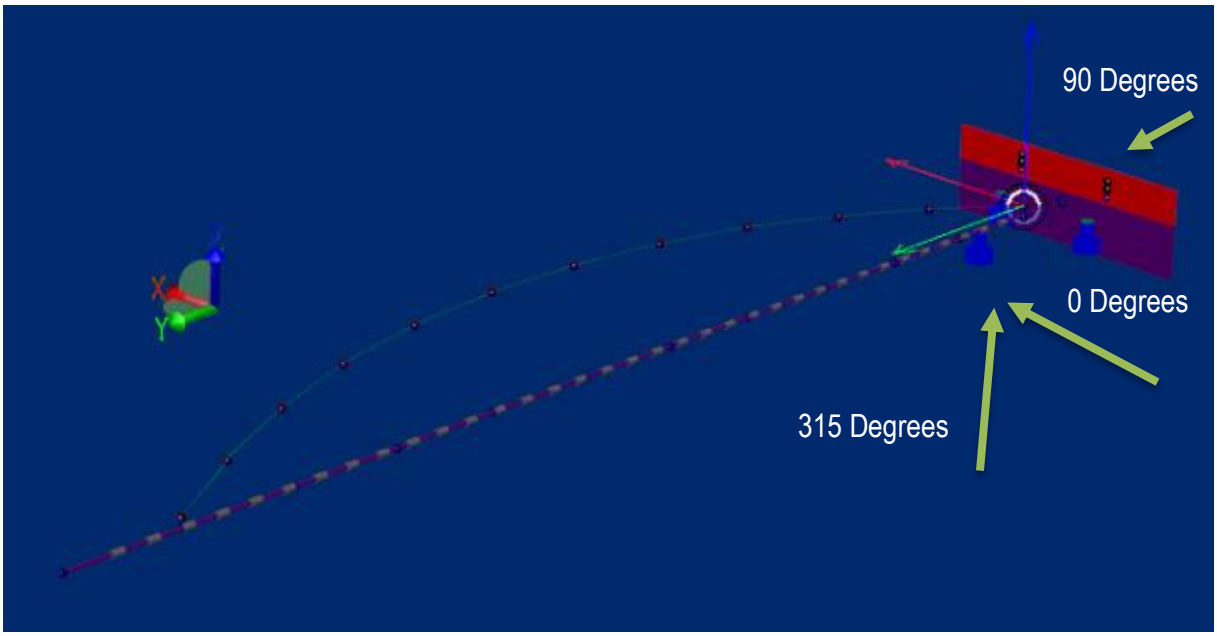

Figure 26: Configuration 3 SIMA overview

ship side. The setup, with static and initial configuration of the pipeline is shown in figure 26. As for setup 2, three wave headings will be tested, namely 0, 315 and 90 degrees, as indicated in the figure.

4.3.1 RUN 6: WAVE HEADING 0 DEGREES

The maximum recorded values for each channel is displayed in table 14. Of the translational motions, surge is the dominating degree of freedom with a maximum recorded displacement of 0.389 m. In comparison, the sway motion is small, with only about a quarter of the magnitude. Considering the wave direction, this result is as expected. It should also be noted that all three translations have larger peak magnitudes than the corresponding run in setup 2 (without the pipeline, wave heading 0 degrees).

Rotations are also larger in this configuration than in the previous. Roll peaks at 2.34 degrees, while pitch has a maximum of 1.1 degrees. The large roll and small pitch is not in coherence with the wave heading, which has been seen earlier in the SIMA analysis as well. As before, a distinct roll motion can be seen in the simulation video, even though the waves are incoming from a 0 degree angle. In this setup there are several possible sources, for example the asymmetry of the system about the x-axis, as well as inaccuracies in the modelling of the vacuum pads.

Rotations about the z-axis are again the largest rotations of all. This phenomenon is also the same as in the coupled condition. However, the rotations are now smaller than when the pipeline is not connected, indicating that the pipeline does help dampen some of the motions of the platform.

Table 14: Statistics, SIMA run 6

	Maximum value
X-force (kN)	561.5
Y-force (kN)	318.8
Z-force (kN)	482.9
Surge (m)	0.389
Sway (m)	0.090
Heave (m)	0.232
Roll (deg)	2.345
Pitch (deg)	1.111
Yaw (deg)	3.250

The total force resultants show some interesting effects of adding the pipeline to the system. Forces in the horizontal plane increase with percentages ranging from 50-100%, while the vertical force decreases by a threefold. The maximum Z-force value is, for example, 1430 kN in setup 2, but only 483 kN in setup 3. The vertical force has decreased by about 1000 kN, while the vertical motion has not. Motions like pitch and roll that also contribute to vertical displacement of the platform are also larger for the total system than for the coupled condition. One possible explanation is that the pitch and roll motions are large contributors to the total vertical displacement, and these motions yield forces in the horizontal plane as well as in the vertical directions. Thus, there will be additional contributions to the x- and y-forces from pitch and roll motions.

4.3.2 RUN 7: WAVE HEADING 315 DEGREES

The results from run 7 are presented in table 15. As in the previous run, surge motion is significantly larger than sway. In this case, this makes sense considering the wave heading, as the platform is excited in both x- and y-directions by the wave by an amount that should be equal in both directions. However, the ship side limits the movement in the y-direction, resulting in larger surge motions than sway motions. Note also that the expected value of maximum surge is even larger than the recorded value. Heave motions are large for this run, with a maximum of 0.43 m and an expected maximum of 0.36 m. These are the largest heave magnitudes that has occurred so far in the analysis.

Not unexpectedly, the roll is also large for this case, which could also be a contributing factor to the large heave motions. It is interesting that in this setup, roll and heave are both large, whereas in the same wave heading in the coupled condition, the roll motions are of the same order of magnitude, while heave is only about half the magnitude that it is now. The pipeline must therefore introduce an excitation mechanism to the system as the waves are pushing the pipeline towards the platform. Rotations about

the z-axis smaller than the corresponding run in the coupled condition, with about 3 degrees maximum compared to almost 4 degrees in run 4.

Table 15: Statistics, SIMA run 7

	Maximum value
X-force (kN)	576.6
Y-force (kN)	348.4
Z-force (kN)	474.9
Surge (m)	0.392
Sway (m)	0.141
Heave (m)	0.434
Roll (deg)	3.472
Pitch (deg)	1.063
Yaw (deg)	3.113

Some of the trends in the forces seen in run 6 are present also in run 7, large increases in the x- and y-forces, and a significant decrease in the z-force. Considering that the platform is restrained more in sway than in surge, the force results make sense. Vertical forces are about the same in this run as in the previous, although both roll, pitch and heave motions are larger in this run. The amount of restraint in the connection is therefore about the same in the two runs, while the excitation is much larger in run 7.

4.3.3 RUN 8: WAVE HEADING 90 DEGREES

The results from the final run are displayed in table 16. The waves are now propagating towards the positive y-axis (see figure 26), and so significant sway motions would be anticipated. However, the results show that surge is still larger than sway. Although the values are close to each other, the expected values differs more and must be taken into account. This is, however, the same trend as has occurred in all of the runs for setup 3. The answer as to why surge is larger than sway for all of the runs is that both the pipeline and the connection system provides a lot of restraint along the y-axis, limiting sway motions. There is, on the other hand, very little restraint in surge, as the connection system is omnidirectional, with equal restraint in all directions. This results in a total larger restraint in sway than in surge, and so the surge motions are larger than the sway motions.

Heave motions are even larger for this run than the previous two runs. Considering the platform alone, the heave amplitudes should be the same no matter the direction of the waves. However the pipeline seems to have an excitation effect on the platform, because both heave and roll motions are larger than in any of the other runs. One contributing factor to the heave motion is of course the large roll motion, which is expected for this wave heading.

Table 16: Statistics, SIMA run 8

	Maximum absolute value
X-force (kN)	528.9
Y-force (kN)	330.0
Z-force (kN)	497.5
Surge (m)	0.173
Sway (m)	0.175
Heave (m)	0.504
Roll (deg)	4.251
Pitch (deg)	0.991
Yaw (deg)	1.501

The forces are still of the same order of magnitude as seen in the two other runs for this configurations. It is an interesting feature that the system is so stable with respect to wave headings. Compared with the corresponding wave heading in the coupled condition, the trend seen in the two previous runs applies also here; increases in X- and Y- direction and a decrease in the Z-force. The vertical force, however, now only reduces by about 50%, but this might be because the Z-force in run 5 is comparatively small, with a maximum of 1043 kN.

4.3.4 TRANSFER FUNCTIONS FOR CONFIGURATION 3

The transfer functions for this final setup are presented on the following pages. Only a few transfer functions are displayed due to the large number of plots, and the complete list of plots is attached in appendix A. The wave spectrum is, to the naked eye, the same as seen in figure 16. The transfer functions in heave and roll are displayed in figure 27 and figure 28.

The general trends of the two degrees of freedom are very similar to one another, although the magnitudes are different, with heave maxing at 0.8 m/m and roll maxing at almost 7 deg/m. Both modes start with large responses for the lowest frequencies, peaking at about 0.12 and then decreasing. The 90 degree wave heading has the largest response for both modes. This wave heading has a very sharp dip to a minimum at 0.3 Hz. The other two wave headings also decrease, but does not have the sharp dip as the aforementioned. In heave, none of the response is larger than the wave, as the response amplitude operators never exceed 1 m/m. For roll, the responses are more significant, where there are responses of approximately 2 deg/m, 5 deg/m and 6.5 deg/m at the peak frequency of the wave spectrum, 0.2 Hz.

The force transfer functions are displayed in figure 29, figure 30 and figure 31. The transfer functions all follow the same general trend that has also been seen previously, with a small dip at or close to the peak wave frequency, and then a steady increase as the frequency increases. The tendency that all the

transfer functions are the “inverse” of the wave spectrum, and with no large peaks or other irregularities except for the expected statistical randomness is an indicator that the system is not very sensitive to changes in the environment. It does not react particularly to any specific frequency, neither are there any direction in which the contact forces are significantly larger than in the others.

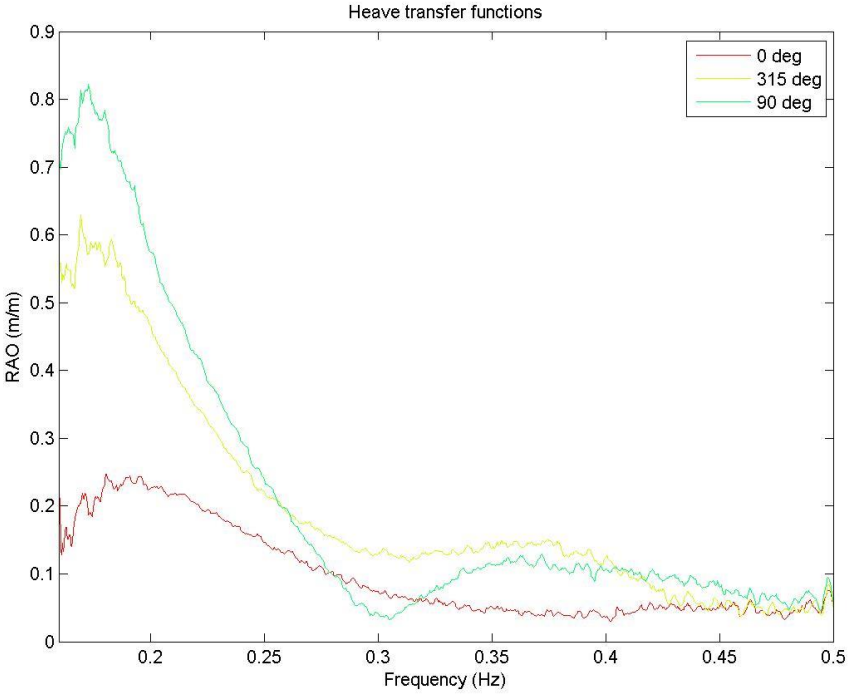

Figure 27: Heave transfer functions, SIMA configuration 3

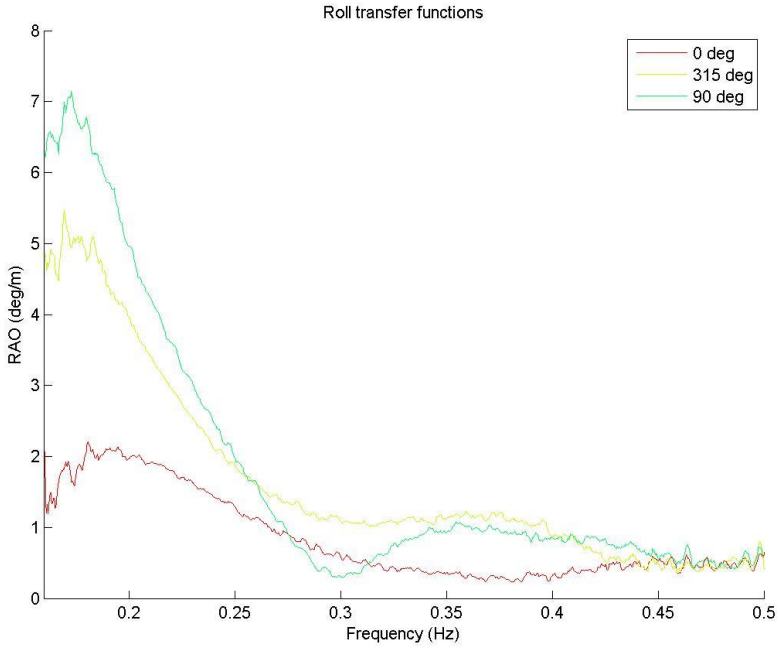

Figure 28: Roll transfer functions, SIMA configuration 3

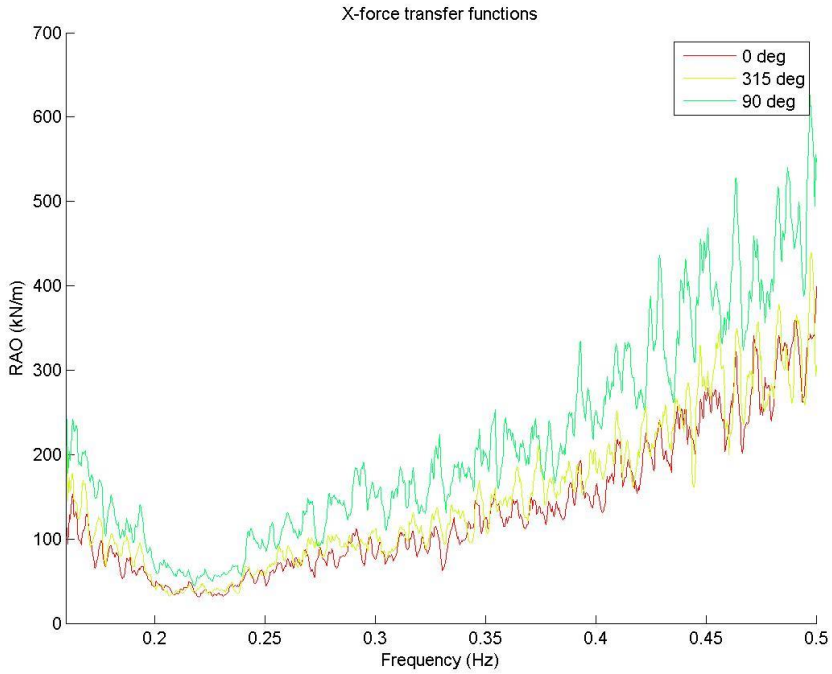

Figure 29: X-force transfer functions, SIMA configuration 3

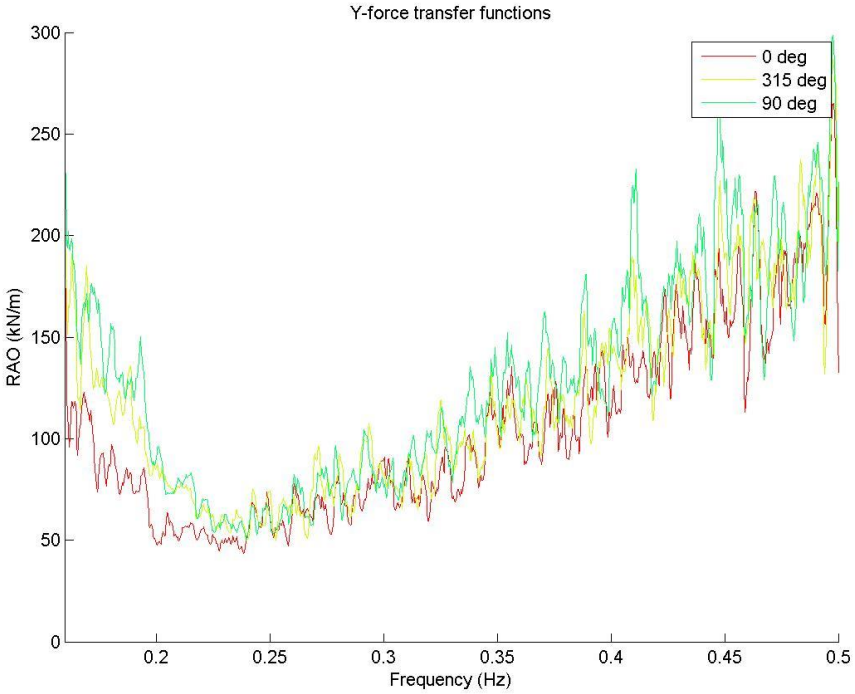

Figure 30: Y-force transfer functions, SIMA configuration 3

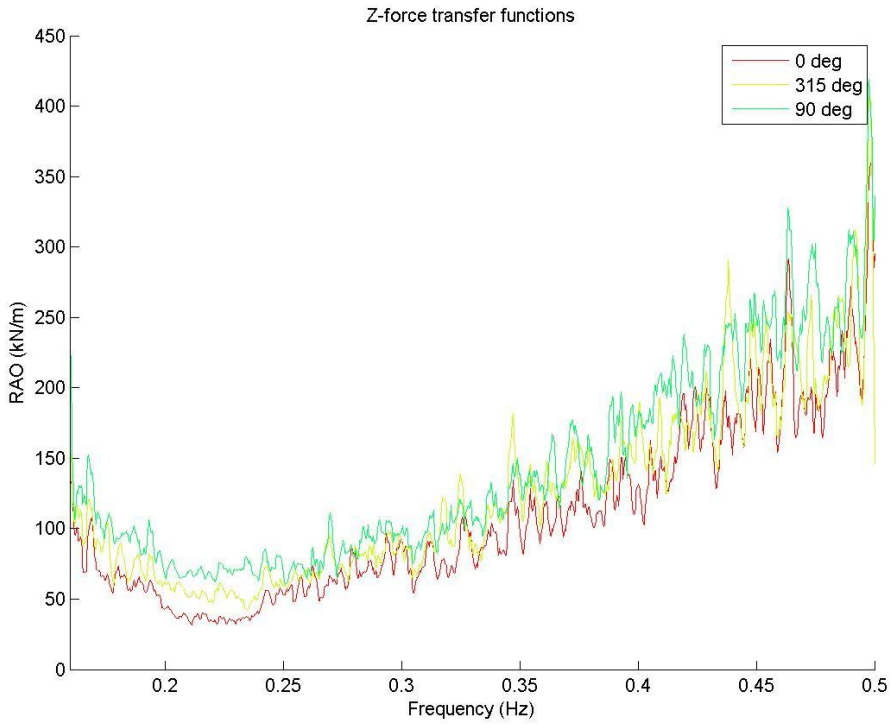

Figure 31: Z-force transfer functions, SIMA configuration 3

PART 3: MODEL TEST

1 INTRODUCTION

1.1 INTRODUCTION

This model test of the UBS system was performed in week 9 of 2014 in the Marine Cybernetics laboratory at Tyholt. The test was planned and performed by the author and fellow M.Sc. student Odd E. Staalesen with help from supervisors at NTNU, staff at MARINTEK and advisors at CLNG. The post-processing was done individually, because each's thesis require different results.

1.2 MOTIVATION

Model testing is a tool used by engineers in order to verify performance and numerical calculations, as well as to achieve a better understand of the physical concepts and challenges involved in the design tested [10]. A physical model can give a better understanding of the whole hydrodynamic picture than calculations can, because nothing is excluded. In numerical calculations, it is necessary to make some simplifications to be able to do any calculations (for example the assumption that water is inviscid). Even though one takes care to correct for the simplifications and assumptions made, the answer will not be absolutely correct. Because of this, model testing is very important because the engineer can compare results and get an understanding of how the calculations deviate from the correct answer, and in this way be able to reach a proper conclusion. In addition, a model test may reveal problems not previously considered, or phenomena that has not been revealed by numerical calculations.

1.3 PREVIOUS TESTING

The Universal Buoyancy System has been under development for the past five years and significant changes to the design has occurred throughout the different stages. The floating platform was previously designed as a spar buoy, and some tests has been performed on this concept. See for example the master theses by Knutsen (2012) and Nilsen (2013). The present design with a semisubmersible tripod has not yet been tested in a laboratory.

1.4 OBJECTIVES OF MODEL TEST

The objectives of this model test are as follows:

- Determine transfer platform motions independently and in coupled condition
- Determine coupling forces
- Calibrate numerical models of the coupled system
- Observe or measure and unexpected phenomena

2 TEST SET-UP

2.1 TEST FACILITIES

The Marine Cybernetics laboratory is one of the smaller wave basins at MARINTEK. It was constructed especially for tests of marine control systems, but other experiments are also conducted here. It has an advanced instrumentation package and towing carriage, making it suitable for specialized hydrodynamic tests. The basin is 40m long and 6.45m wide, and its depth is 1.5m.

To generate waves, a wave maker in installed at one end of the basin. Such a wave maker can be either flap type (horizontal driven) or wedge type (vertical driven). The MC lab has a flap type wave maker, which has a single flap and is electrically driven. In addition, a wave absorption system is installed. This is important with respect to reducing wave reflections, which gives better accuracy. The wave maker system can produce both regular and irregular waves with different spectrums like JONSWAP, Pierson-Moskowitz et cetera. The capacity is summarized in table 17.

Table 17: Wavemaker capacity

Type	Maximum wave height	Minimum period	Maximum period
Regular	H=0.25m	T=0.3s	T=3s
Irregular	H_s=0.15	T_P=0.6	T_P=1.5s

Current is generated by pumping water into the basin at one end and out at the other end. External pipes enables circulation of the water through the basin, out, and back in at the opposite end. The MC lab current generator can make currents up to 0.15 m/s.

The laboratory is equipped with a tracking system produced by Qualisys, consisting of Oqus cameras as well as Track Manager Software. The positions are measured in real time and is later exported for analysis.

2.2 MODEL SCALE AND PARAMETERS

The model scale was set to 1:15. This is slightly smaller than what is normally used in the MC laboratory, but necessary in this case in order to incorporate both the connection system and the platform, and still avoid too many reflections from the tank walls. This gives the parameters shown in table 18.

Table 18: Main parameters, model and full scale

Parameter	Model scale	Full scale	Unit
Scale	1	15	-
Volume displacement	11.31	38170	dm^3
Draft	220	3300	mm
Freeboard	120	1800	mm
Column separating distance	800	120000	mm
Column diameter	100	1500	mm
Column height below MSL	133.3	2000	mm
Step diameter	200	3000	mm
Step height	86.7	1300	mm
KG	189.4	2841	mm

2.3 MODEL DESCRIPTION

2.3.1 OVERVIEW OF TEST ARRANGEMENT

Two different test arrangements were used. For the independent condition, the platform was floating relatively freely in the basin, see figure 32. The platform is only kept in place by a very simple mooring system consisting of strings, whose objective is to prevent that the platform drifts out of the area of focus of the position measurement system. For the coupled condition, shown in figure 33, the semisubmersible in connected to a “ship”, here modelled by a steel frame. As the connection system, keeps the platform in place and visible to the cameras, no other mooring system is needed.

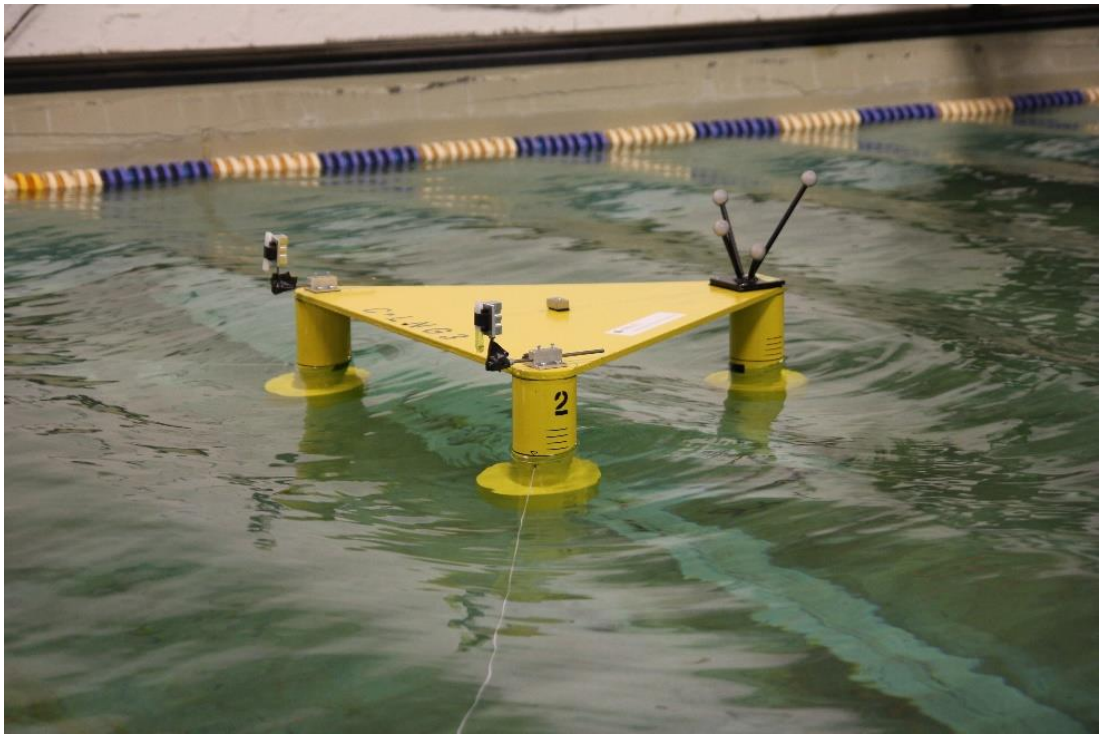

Figure 32: Independent condition

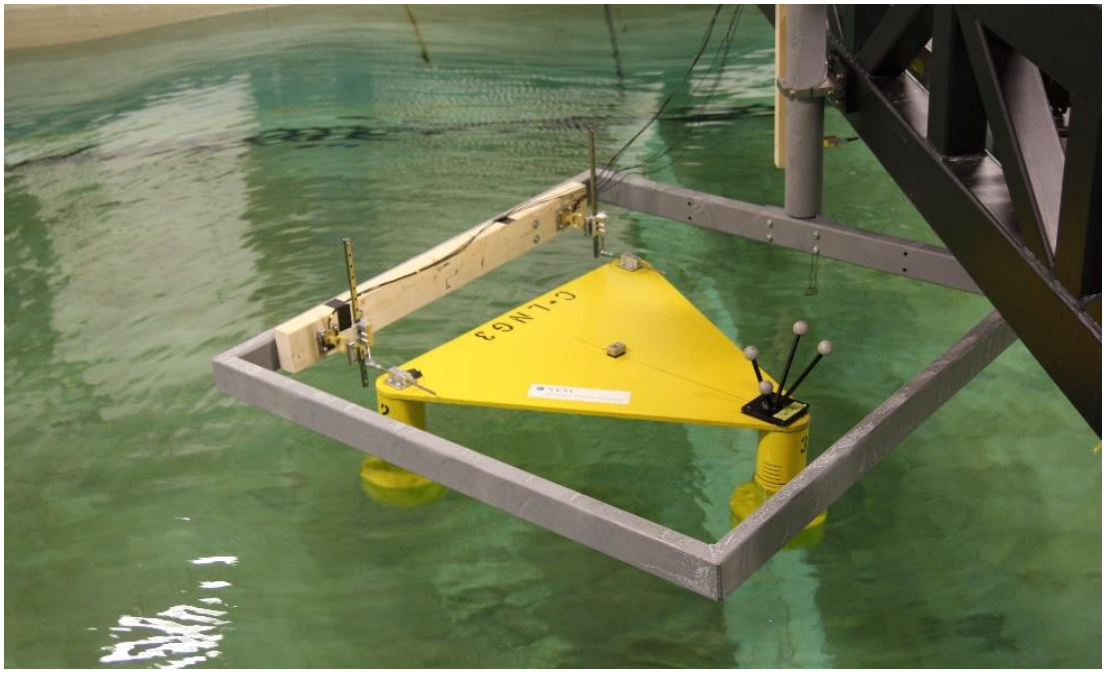

Figure 33: Coupled condition

2.3.2 PLATFORM

The semisubmersible consists of mainly two parts; the columns and the platform deck. The columns where cut out by the workshop at MARINTEK and is made from Divinycell, a light but strong material that is usually applied in ship testing at MARINTEK because of its beneficial properties. Its structure is reminiscent of sponge, making it suitable for all shapes. It does not, however, absorb water. The material has a “sandwich”-type composite structure, which makes it strong and durable. The columns were painted with polyester to make it fully water resistance and to create a smooth surface.

As mentioned previously, Divinycell is a very light material. Therefore, in order to get the correct weight and centre of gravity, holes were milled out at the bottom of each column, and brass disks were inserted. The calculations necessary to find the dimensions and properties of the platform were done in excel and are attached in the electronic appendices.

The platform deck is made from common plywood, cut out in the student’s workshop adjacent to the laboratories with rounded corners to match the diameter of the columns. The deck was fastened to the columns using epoxy glue. Stiffeners along the plate and/or at the intersection between the columns and the plate was considered, but the plywood plate provided enough stiffness by itself.

Lastly the whole semisubmersible was painted at the MARINTEK workshop. In addition, the calculated waterline was drawn on the columns together with “guidance lines” at intervals of one centimetre above and below the waterline, to facilitate observation. The columns were also numbered from one to three, for the same reason.

2.3.3 MOORING

For the uncoupled condition, a mooring system is needed to keep the platform from drifting away. The reason why this is a problem is because the model needs to be positioned within the focal area of the measurement system. Thin polyester strings were tied around each of the columns, and taped in place. The other end of the string was attached to the edges of the basin. A small nut was attached 1.5 meters from the column on each string so that the string would sink slightly, such that the strings only had to be tied very loosely, so as to not provide more station-keeping than what was necessary.

2.3.4 CONNECTION SYSTEM

One of the objectives of the test is to find motion transfer functions in heave, roll and pitch. Thus there is a need for a connection system that provides resistance in in the lateral and transverse directions as well as in yaw, while at the same time providing freedom to move in heave, pitch and roll. After some iterations, the system shown in figure 34 was decided upon. The connection consists of a rain, a “wagon”, and a two-legged cylindrical bar with a joint in the middle. One end of the cylindrical bar is attached to the platform by means of nuts and bolts. The other end is connected to a “wagon” on a rail. The wagon/rail has very low friction, allowing for free motion in heave. The joint provides freedom to rotate. With two of these connections (one at each column) the platform is also restricted in yaw.

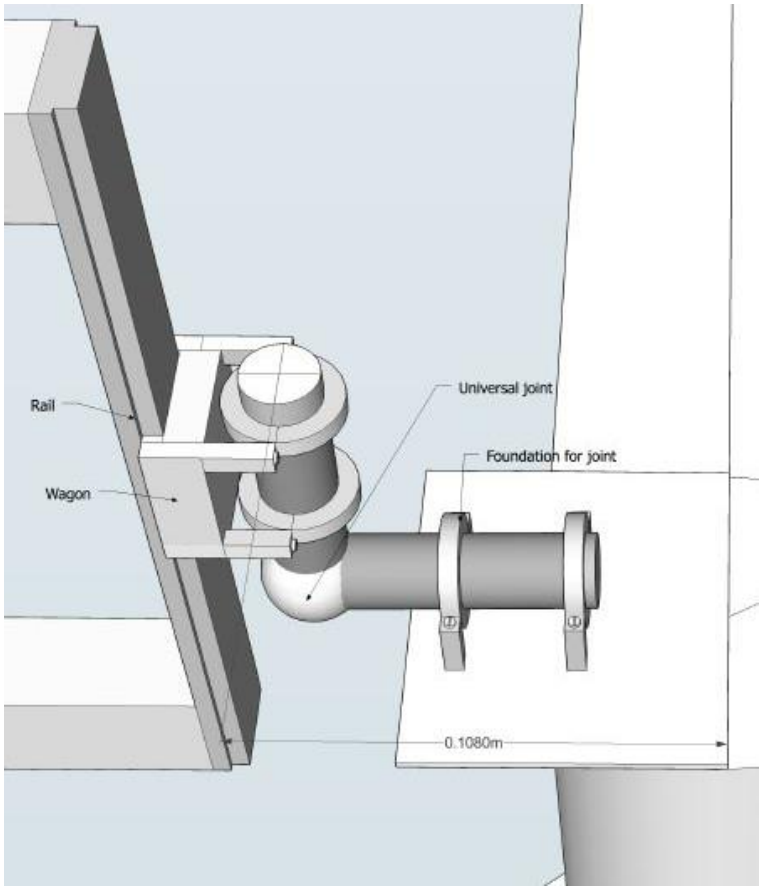

Figure 34: Connection system

2.3.5 SHIP

The UBS will operate along a ship side. This implies that there will be a lot of wave interaction in the small space between the platform and the ship. However, for one thing SIMA cannot model this, and it would be very difficult to get good results in a small basin like the MC laboratory, because of its limited size. It was therefore decided that the best solution is not to model the ship in the water, but keep the ship as a stationary object just above the water line, such that the connectors can be placed where they should according to the specification, but no other part of the ship would be included.

The initial solution was to use a bar, but after visiting the MC laboratory prior to the test, it was discovered that a bar alone would make it difficult to rotate the model, as would be necessary to test the model in waves of different heading. Instead, a steel frame that surrounded the platform was welded for this purpose. It is attached to a pipe for easy attachment to the wagon. This solution, which is shown in figure 35 made it easy to change the orientation of the platform, while at the same time making sure that the platform stayed within the focal area of the measurement equipment.

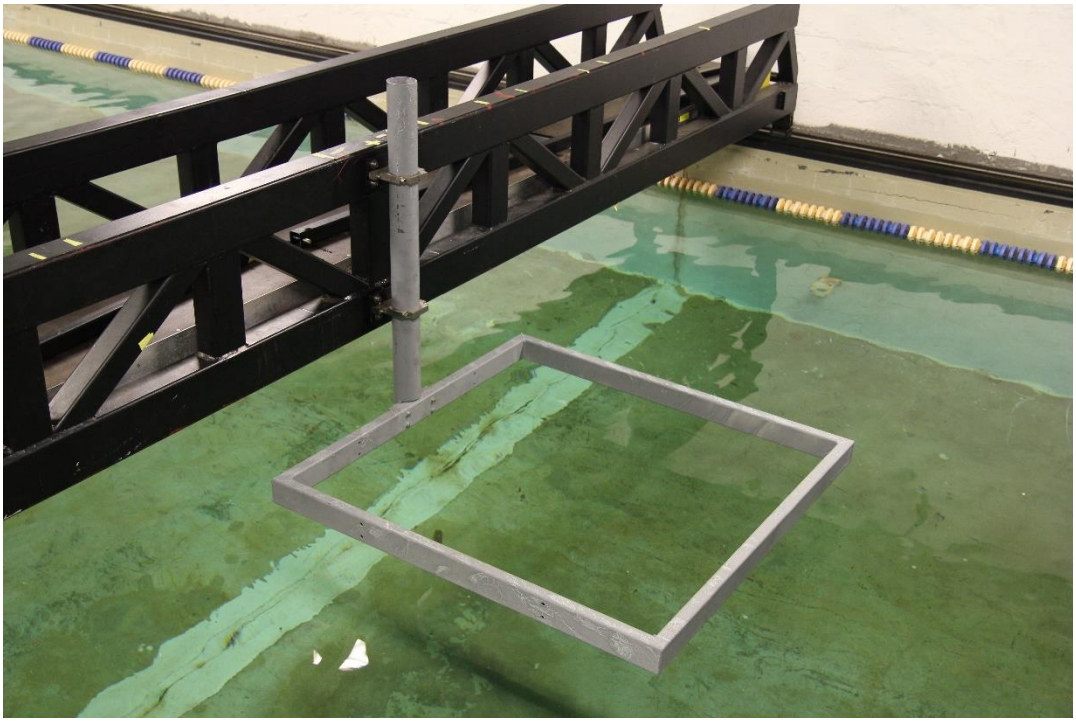

Figure 35: Frame used in coupled condition

2.3.6 ADDITIONAL MODEL EQUIPMENT

A second plywood plate was used to model the shipside. As with the platform deck, the plate was cut out in the student's workshop and painted. To investigate the effect of the pipeline, a simple tensioning system was set up. This was improvised on the day of the test and consisted of a nylon string running through a hook, as well as a weight attached at the end of the string.

2.4 UNITS AND COORDINATE SYSTEMS.

The coordinate system of the platform can be seen in figure 36. This is in accordance with what is used in SIMA. The measurement systems in the MC lab operates with two different coordinate systems. The Oqus cameras use the global coordinate system shown in the figure.

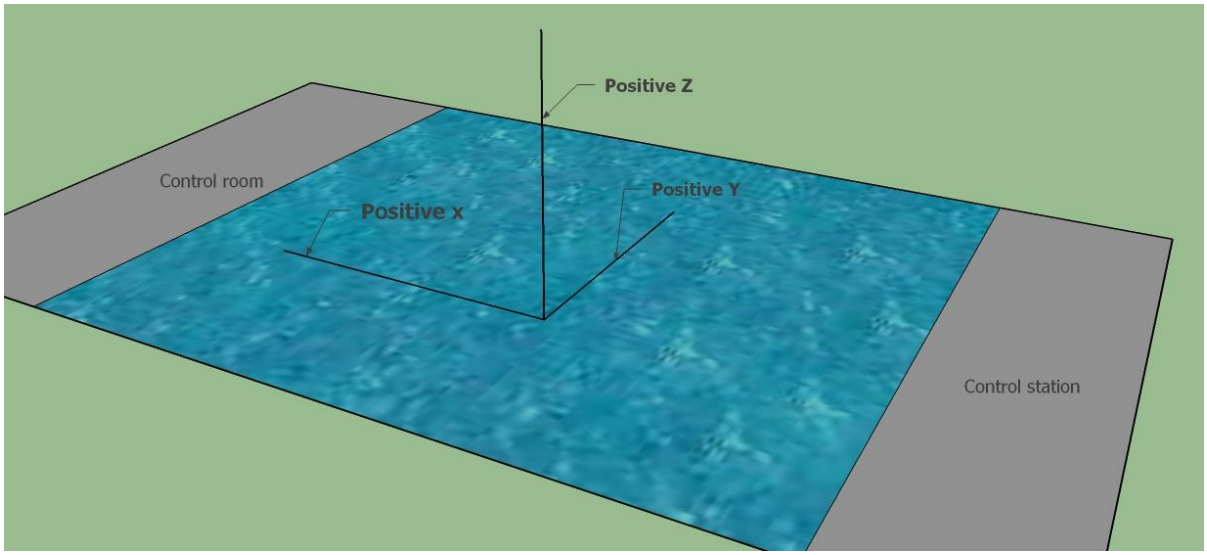

Figure 36: Laboratory coordinate system

The strain transducers, which measure forces, each have a local coordinate system. In order to keep track of the directions, the coordinate system was drawn onto the “ship side” frame. In this report, all results are given in the global coordinate system of the lab unless otherwise stated.

The Oqus cameras measure position, and gives time series in seconds, meters and degrees. The strain transducers give the force in newtons.

2.5 CALIBRATION AND VERIFICATION

2.5.1 WEIGHT AND WATERLINE

After assembling the platform, it was put into the water to check that the waterline was correct. The waterline was drawn onto each column by using a special-purpose measuring tool, so that this was completely straight. When the platform (with Oqus and connection system attached) was placed in water, it pitched very slightly. A nut taped onto the platform deck solved this.

The weight of the platform was measured to 11.48 kg. A digital scale was used, and several measurements performed, all of which produced the same result. This is very satisfying with respect to the calculated weight, which was 11.31 kg, keeping in mind that several layers of polyester and paint are difficult to calculate accurately.

After making sure that the weight and waterline requirements were satisfied, the keel-to-centre of gravity (KG) distance was measured. This was done by hanging the platform vertically in a hook-and-thread-system and use a level to check that the platform is suspended perpendicular to the thread. The results showed a KG 161 mm. This is below the calculated centre of gravity, which was 189.1 mm. This corresponds to a full scale deviation of 0.426 m. The reason why the centre of gravity is lower, is probably the lightness of Divinycell and the compensation of inserting brass disks into the bottom of the columns, resulting a much higher mass density in the bottom part of the platform.

This will impact the hydrodynamic performance of the platform. A longer distance $\overline{GM}$ (lower centre of gravity) implies that the Eigen period in roll becomes shorter, shown in equation (19).

$$T = \frac{2\pi k}{\sqrt{g\overline{GM}}} \quad (19)$$

This means the platform becomes more stable. This should be kept in mind when evaluating the results.

2.5.2 STRAIN TRANSDUCERS

The strain transducers need to be calibrated each time they are used. Chief engineer Torgeir Wahl helped us with this. The concept of calibrating the strain transducers is to apply known weights and measure the response. Applying several weights gives a regression matrix, which is then stored into the measurement programme on the computer, so that the results that show up on the screen are correct and calibrated. The complete calibration document including the measurements and graphs is attached in the electronic appendices.

The key aspects are shown here. A small overview of the transducers and units are shown in table 19 . The calibration equations (from the regression matrices) are shown in equations (20), for transducer 8158, and (21) for transducer 8196.

Table 19: Transducers overview

Transducer name:	8158	8196
Output unit	N	N
Input unit	mV/V	mV/V

$$\begin{aligned} Fx &= 243.9319 * Fx - 1.4812 * Fy - 6.8723 * Fz \\ Fy &= -39.7978 * Fx - 237.5822 * Fy + 37.8709 * Fz \\ Fz &= 9.6063 * Fx - 7.5303 * Fy + 1368.6451 * Fz \end{aligned} \quad (20)$$

$$Fx = 120.0201 * Fx - 3.2146 * Fy - 7.8849 * Fz$$
$$Fy = -2.4055 * Fx + 128.0802 * Fy + 0.5156 * Fz \quad (21)$$
$$Fz = 2.1841 * Fx + 46.1293 * Fy + 579.6695 * Fz$$

2.5.3 OQUS CAMERAS

The laboratory is equipped with a motion tracking system from Qualisys. The system consists of three Oqus cameras placed along the stationary wagon, as well as markers that are placed on the platform. The markers are attached to the platform by means of Velcro and some tape. The distance from the marker to the centre of gravity was measured and fed into the track manager, so that all motions are given in terms of the platform's centre of gravity.

To get measurements, the markers must be in view of all three cameras. One must therefore check carefully on the monitor and/or on the cameras themselves when placing the model into the water to make sure that the Oqus markers are within the reach of the cameras, and that there are no physical obstacles blocking the view. In addition, the laboratory is also fitted with a calibration "wand". The wand, which is a stick with an Oqus marker at the end, lets the user specify physically in which area the model will most likely be situated during the experiments. This gives better accuracy on the reading within this area.

The cameras record the position of the four markers with a frequency of 20 Hz and sends it to the Qualisys track manager software installed on a computer in the lab. The recordings are imported to the computer system continuously, so that the user may observe the recordings in real time.

2.6 DATA ACQUISITION

An overview of recorded data is shown in table 20. Translations and rotations are measured by using Oqus cameras. The wave height is measured by a wave probe. Two strain transducers record forces in x, y and z-directions.

Table 20: Acquired data overview

Coupled condition	Independent condition
Translations in x, y, z-direction	Translations in x, y, z-direction
Rotation about x, y, z-axis	Rotation about x, y, z-axis
Wave height	Wave height
Forces in x, y, z-direction, two transducers	

2.6.1 STRAIN TRANSDUCERS

The recommendation from Torgeir Wahl was to use simple three-component strain transducers to measure forces. Two strain transducers where placed between the platform and the ship. The strain transducers are connected directly to the computer in the lab, so that the recordings can be displayed together with the position measurements from the Oqus cameras.

2.6.2 WAVE PROBE

The wave height was measured by using a wave probe. The wave probe also has to be calibrated the same way as the transducers, and Torgeir Wahl helped with this as well. The probe was mounted on the movable wagon using clamps. The distance from the centre of gravity of the platform to the wave probe was measured and recorded for each configuration.

2.6.3 CONTROL CHECK AND ROUTINES

Before each run, the following points where checked:

- Check model orientation and position
- Check wave parameters in test programme
- Check that Qualisys is on and recording, all markers visible (green light flashing)
- Take zero-measurement for at least one minute
- Record time for run execution in test log
- Take pictures, start with run number
- When wavemaker stops, save measurement as “TESTNUMBERa”, if the test is repeated continue with “TESTNUMBERb” and so forth
- Review recordings, see if a re-run is necessary
- Write down any comments or observations in the test log

2.7 TEST CONDITIONS

2.7.1 ENVIRONMENTAL CONDITIONS

Both regular and irregular sea states will be used during the testing. The regular waves will have (full scale) wave heights from 0.5 m to 1.25 m, at intervals of approximately 0.15 m. To find the corresponding wave period, the water depth is assumed sufficiently large to use the deep water dispersion relation. Steepness is set to 0.04, so that the wave length may be calculated using equation (22), where h is the steepness.

$$T = \sqrt{\frac{H * g}{2\pi h}} \qquad (22)$$

The irregular waves will be specified using a JONSWAP wave spectrum. The spectrum has been explained previously in the theory part, see chapter 0. Only one irregular sea state will be tested, with parameters as shown in table 21. These were requested by Connect LNG, as they have chosen this as their design limit state based on own calculations.

Table 21: Irregular sea state parameters

H_S	1.2 m
T_P	5 s
γ	1.65

The maximum water depth in the laboratory of 1.5 meters is used in the experiment. This is deep enough to assume deep water conditions in the sense that the motion of the wave particles on the surface does not influence the particle at the sea bottom. Other environmental conditions like wind and current will not be tested in this experiment.

2.7.2 TEST ARRANGEMENT

In total, five different arrangements will be used in the experiments. For the independent, uncoupled condition, waves with headings 0 and 90 degrees will be investigated. In addition, uncoupled decay tests will be performed, to estimate uncoupled added mass, damping and Eigen periods. The independent condition test arrangement consists of the platform alone floating freely with only the simple mooring system described earlier to prevent too much drifting. See figure 32 for an illustration.

For the coupled condition, the platform will be tested in waves incident form 0, 315 and 90 degrees. In addition, decay tests will be carried out to find added mass and damping. The 315 degrees is equivalent to 45 degrees in the platform's local coordinate system, but will be referred to as 315 degrees, to be coherent with the SIMA notation. The coupled test arrangement consist of the platform as well as the connectors and the frame. This test arrangement simulates the operational condition of the LNG offloading system. The condition is illustrated in figure 33.

2.7.3 TEST PROGRAMME

A condensed version of the test programme is shown in table 22. The complete programme is attached in the electronic appendices. For simplicity, all the uncoupled conditions where run first, and the coupled conditions followed. This is simply because changing the direction of the wave was less time-consuming than changing from coupled to uncoupled, although some work is required to find the exact position of the platform.

Table 22: Condensed test programme

Waves	H/H_S [m]	T/T_P [s]	Direction	Condition
Regular	0.5-2.15	2.83-5.87	90	Uncoupled
Irregular	1.2	5	90	Uncoupled
Regular	0.5-2.15	2.83-5.87	0	Uncoupled
Irregular	1.2	5	0	Uncoupled
Decay test				Uncoupled
Regular	0.5-2.15	2.83-5.87	90	Coupled
Irregular	1.2	5	90	Coupled
Regular	0.5-2.15	2.83-5.87	315	Coupled
Irregular	1.2	5	315	Coupled
Regular	0.5-2.15	2.83-5.87	0	Coupled
Irregular	1.2	5	0	Coupled
Decay				Coupled

The sketch in figure 37 indicates the different directions of the waves and the orientation of the platform. The same is used for both uncoupled and coupled, regular and irregular. The strain transducers are also displayed in the figure. The first picture, to the left, is the wave heading 0 degrees. In the middle is 315 degrees, and the last picture (right) displays the 90 degree wave heading.

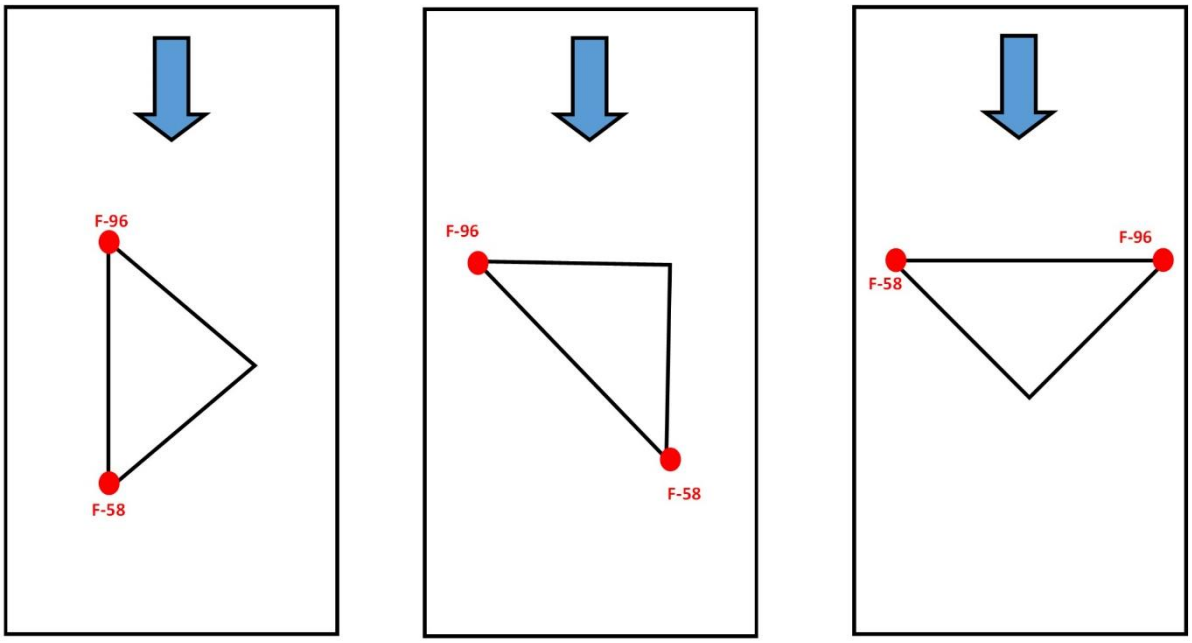

Figure 37: Illustration of wave headings and strain transducers.

2.7.4 Duration of tests

For regular wave testing, it is recommended to perform tests that are long enough so that after the test one can extract at least 10 consequent stationary wave oscillations. This means that the necessary time period for testing is ten periods plus some time at the beginning and end that one may discard to avoid transient effects in the results. Furthermore, the Oqus cameras can sometimes make wrong

measurements that result in so-called spikes in the recordings. These are completely unrealistic, like a heave movement of 200 meters. Because of the risk of such spikes, each test had a duration of 90 seconds to make sure ten good quality wave periods were available in the post-processing.

The irregular wave tests have a duration of a little more than 46-47 minutes. This is to obtain 45 minutes of stationary waves and again avoid any transient effects during build-up. A test duration of 45 minutes corresponds to a full scale duration of 3 hours, as will be explained in the subsequent sections.

3 DATA ANALYSIS AND POST-PROCESSING

All data post-processing is done in MATLAB. A ready-made MATLAB script written by HBM (Hottinger Baldwin Messtechnik), the company behind Catman, read the .bin-formatted result files is available from MARINTEK. This formed the basis of the post processing, and from the raw data different MATLAB scripts were produced to acquire the desired results.

3.1 SCALING

In order to get a correct picture of all motions and forces in full scale, the model must fulfil the following criteria [10]:

- Geometrical similarity
- Kinematic similarity
- Dynamic similarity

Geometrical similarity means that the model and the full scale structure has the same shape, and therefore also the same ratio between the different lengths. Another way of explaining geometrical similarity is that the scaling ratio should be constant, such that $\lambda = \frac{L_{model}}{L_{full}} = \frac{B_{model}}{B_{full}}$ and so on. It is important to keep in mind that this does not only apply to the structure, but also to the environment, wave basin and so on.

The requirement of geometrical similarity is in this experiment fulfilled to a certain extent. The dimension of the structure and the waves are scaled correctly, and the depth of the basin is deep enough to classify as deep water. However, the basin is too small to be considered “indefinite” in full scale. The model will experience reflected waves from the tank walls. Another concern is the surface roughness of the ship, which cannot be modelled to scale.

Kinematic similarity means that the model has similitude in velocity. This means that the fluid streamline image is the same around both model and full scale. This means that $\frac{u_{model}}{w_{model}} = \frac{u_{full}}{w_{full}}$ where u and w are the x- and z-components of fluid velocity.

Dynamic similarity implies that the force ratios between the model and full scale on all points in the system is constant. This includes (but is not limited to) the following force contributions [10] and requiring constant force ratio:

- Inertia forces
- Viscous forces

- Gravitational forces
- Pressure forces
- Elastic forces (in fluid)
- Surface forces

A different way of expressing dynamic similarity is using different scale numbers, like Froude's number, Reynold's number Mach's number and Weber's number. A model that is Froude scaled has the same ratio between inertia and gravity forces. When the Reynolds number is equal for model and full scale, the ratio between inertia and viscous forces is constant. A similitude in Mach's number signifies that the ratio between inertia and elastic forces are the same, while Weber's number is the ratio between inertia and surface tension.

It is not possible to scale all forces (or achieve similitude in all "numbers") in model testing. In each test the engineer must evaluate what force contributions are dominating and need to be prioritized in the choice of scaling. In this experiment, where wave (gravity) forces are dominating over viscous (drag) forces, Froude scaling is applied.

As mentioned previously, Froude number scaling implies that the ratio between inertia forces and gravity forces is constant. This relationship is shown in equation (23) [10].

$$\frac{F_i}{F_g} \propto \frac{\rho U^2 L^2}{\rho g L^3} = \frac{U^2}{gL} \Rightarrow F_N = \frac{U}{\sqrt{gL}} \quad (23)$$

Requiring that the Froude's number are equal gives the relationship as described by equation (24). Using the scale ratio $\lambda = \frac{L_{full}}{L_{model}}$ the relationships between the different parameters can be found as shown in equations (24)-(29).

$$F_N = \frac{U_{model}}{\sqrt{gL_{model}}} = \frac{U_{full}}{\sqrt{gL_{full}}} \quad (24)$$

Velocity:

$$U_{Full} = U_{model}\sqrt{\frac{L_{full}}{L_{model}}} = \sqrt{\lambda} \quad (25)$$

Mass:

$$M_{Full} = \frac{\rho_{Full}}{\rho_{Model}} \lambda^3 M_{model} \quad (26)$$

Force:

$$F_{Full} = \frac{\rho_{Full}}{\rho_{Model}} \lambda^3 F_{model} \quad (27)$$

Acceleration:

$$a_{Full} = a_{Model} \quad (28)$$

Time:

$$t_{Full} = \sqrt{\lambda} t_{Model} \quad (29)$$

Once the equations determining the relationships between model and full scale are known, scaling is a simple matter of inserting the known model values into the equations.

3.2 BIAS

For all the runs, translation measurements show some bias. The reason behind this may be mean drift forces and/or a fault in the measurements themselves. To find the correct extreme values, bias is removed by subtracting the mean value from the time series.

3.3 WAVE PROBE

The wave probe is clamped onto the adjustable wagon, some distance away from the platform. When calculating transfer functions, the wave elevation at the centre of gravity must be known. The placement of the wave probe was written down for each run, so that we may shift the wave to make up for this shift. The necessary shift is calculated by using taking the distance from the wave probe to the centre of gravity and dividing it by the phase velocity of the wave. The phase velocity is given in equation (30), where g is acceleration of gravity and ω is the wave frequency, again assuming deep water. Knowing the time shift, the wave elevation is adjusted accordingly.

$$V_P = \frac{g}{\omega} \quad (30)$$

3.4 FILTERS

Filters are used in post-processing to remove noise from the signal. These are measurements from lower or higher order frequencies than the wave frequency. An example in the coupled condition is that there seems to be some noise at around 5 Hz. A later quick check showed that the Eigen frequency of the frame was actually around 5 Hz, and is probably the reason behind this noise.

Different types of filters include low pass, high pass and band pass filters. The names indicate what kind of frequencies they delete. In this post-processing, a band pass filter seemed most suitable as there are noise of both high and low frequencies.

When choosing the cut-off limits of the filter, it is important to be careful to avoid so-called Nyquist phenomena, which result in erroneous recordings. This is avoided by choosing the high cut-off limit to lower than half the sampling frequency. In this case the maximum cut-off frequency should be 100 Hz.

There are many different types of filters to use. In marine applications, some common filters are Bessel, Butterworth and Chebyshev filters. Based on recommendations in Erik Lehn's lecture note "Tidsserier – Sampling, filtrering of analyse" (2009) a Butterworth filter was decided upon. The magnitude response for such a filter is shown in equation (31).

$$\frac{A_1}{A_0} = \sqrt{\frac{1}{1+f^8}} \tag{31}$$

To find the optimal order of the filter, the built-in MATLAB function "butter" was used. The function lets the user specify what parameters to use, and MATLAB calculates the minimum order of the filter. The maximum pass band ripple was set to 3 dB, and the stop band attenuation was set to 4 dB. A visualization of the magnitude and frequency response for a filter with cut-off limits 0.11677 and 0.2794 Hz is shown in figure 38.

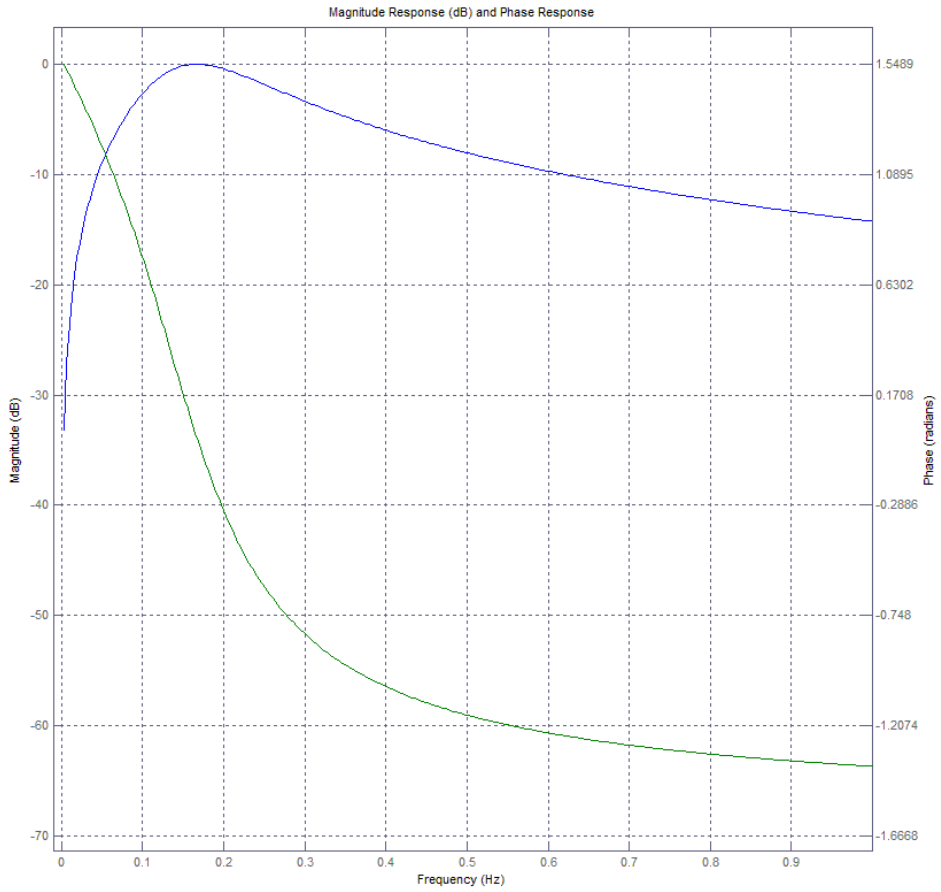

Figure 38: Example Butterworth filter

3.5 REGULAR TESTS

The regular wave tests are processed to find measurement statistics, and spectra for all channels, as well as transfer functions. The procedure is the same for coupled and uncoupled condition, the only difference being that coupled condition has six extra channels from the two three-component transducers. The measurements are adjusted for wave probe placement, bias and scaling as described previously, so that all time series are in full scale.

The best time periods are extracted from each run by visual inspection. At least ten subsequent wave periods are required for calculating statistics and transfer functions. This is done "manually" in MATLAB, by defining start and end times for each run. It is necessary to do this by hand, as there are both transient effects as well as spikes and other irregularities, so the best time periods can be anywhere along the time series. The extracted periods are plotted to make sure that the chosen time series are satisfactory.

Wave statistics are calculated by built-in MATLAB functions like min(), max() and std(). Values are stored to a result file for further post-processing and plotting in excel or MATLAB.

A Butterworth filter is applied to all channels. For the regular runs, a fixed pass band interval of wave frequency $\pm$ 25% is applied. The limits are calculated automatically using equations (32) and (33).

$$f_{lower} = \frac{0.75}{T} \quad (32)$$

$$f_{upper} = \frac{1.25}{T} \quad (33)$$

After filtering, the transfer function may be calculated.

Transfer functions, also known as Response Amplitude Operators (RAO) assume that there is a linear relationship between input and output, meaning that if the input signal (wave) is harmonic, the output (response) is also harmonic. In an ideal world, one could simply take the ratios of all the amplitudes. However, this is not possible as the amplitudes will vary slightly, and non-linearities may be present in the measurements. A more pragmatic method is to use Fourier analysis to find the frequency component with the largest contribution to the amplitude (the fundamental components) for input and output, and then find the ratio, as shown in equation (34).

$$RAO = \frac{A_{output}}{A_{input}} \quad (34)$$

In MATLAB, Fourier analysis is done by using the built-in MATLAB function “fft”, which takes the discrete Fourier transform of the signal. The fundamental components are found using “findpeaks”. The results for each run are stored in a matrix, so that they may be combined and presented as one transfer function for each condition.

3.6 IRREGULAR TESTS

As for the regular tests, time series from the irregular runs must be corrected for bias and a correction must be made for the wave probe placement. The procedure is the same as explained previously.

Furthermore, there are also some spikes in the irregular tests. In order to get measurements for a 3 hour duration, 45 minutes of continuous sampling is needed. It is therefore necessary to remove the spikes, to clean up the signal. This operation is executed after the correction for bias and wave probe shift, and after scaling the results.

To remove the spikes, a simple home-made MATLAB script is used. If the spikes were small, an option would be to use a moving average or median filter, but as the spikes are of the order 10 000 times as large as the correct measurements, this does not work. Instead, a two-step approach is used.

The first step is to remove the spikes. MATLAB searched through each time series, and sets all absolute values larger than a certain limit equal to the value of the previous measurement. The limit was set to two times the maximum value of a previously defined 500 second long spike-free time window. When a value above the set limit is found, the script stores the three last values before the spike occurs, searches for the next value below the limit and stores the next three values. Now a matrix with measurements at the time intervals before and after the spike is saved, and spline interpolation is used to synthesize measurements in the interval where the spike used to be. Lastly the spike values in the original signals are replaced by the new synthetic values. An example of such spike removal is shown in figure 39. It is observed that the synthesized values follow the general trend of the measurements. Moreover, the spike removal does not affect the rest of the signals in any way, and the method must be considered satisfactory.

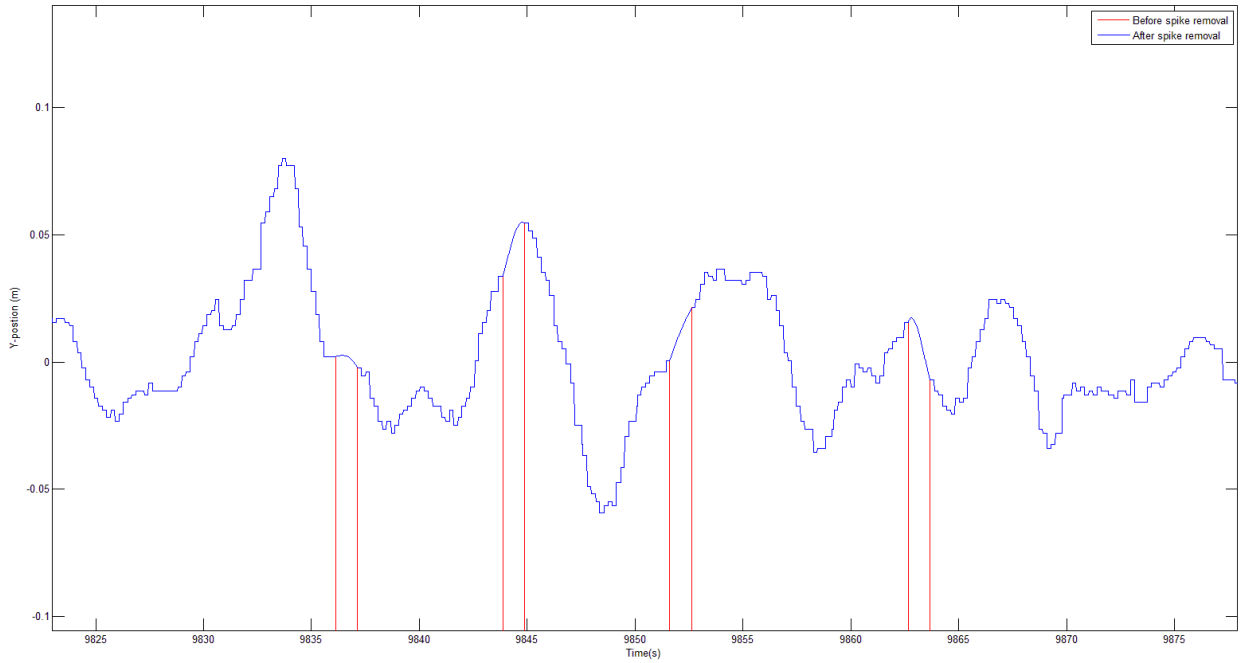

Figure 39: Spike removal

After the spikes are removed, a Butterworth filter is applied. The same method as for the regular waves was used, except that the pass-band was much broader. This is because the input signal is specified as a JONSWAP spectrum, and there will be many different frequency components present. Only the noise with very low frequencies and very high may be. The limit of the filter is fixed as fractions of the frequency, as shown in equations (35) and (36). Another possibility would be to use a high-pass filter, however, the band-pass filter seemed to give better results in terms of keeping the correct amplitudes in the wave frequency range, particularly at the peaks.

$$f_{lower} = \frac{0.4}{T} \quad (35)$$

$$f_{upper} = \frac{5}{T} \quad (36)$$

3.6.1 SPECTRAL ANALYSIS

From the irregular time series a lot of information can be extracted by performing a spectral analysis. This means that the time series are transformed from the time domain to the frequency domain. By using the built in Fourier transform routine, the frequencies with the largest contribution to response and the phase between waves and response can be found.

In addition, the *pwelch* function finds the power spectra of all time channels using Welch's method. The method splits the signal into segments, applies a filter to smooth the signal and then takes the discrete Fourier transform. The power spectrum is now the squared magnitude of this transform.

When the power spectra of input (S_{xx}) and output (S_{yy}) are known, transfer function H(ω) may be calculated from equation (37). The magnitude of $H(\omega)$ is plotted againt frequency to display the amplitude transfer function.

$$|H(\omega)|^2 = \frac{S_{yy}(\omega)}{S_{xx}(\omega)} \quad (37)$$

The phase shift between two signals gives information about the delay between input and output. If for example the input signal is a sinus wave with amplitude A_0 and frequency ω (see equation (38)) and the output signal is also a sinusoid with amplitude A_1, frequency ω and phase π (see equation (39)), the relative phase would be π.

$$A_0 \sin(\omega t) \quad (38)$$

$$A_1 \sin(\omega t + \pi) \quad (39)$$

In MATLAB, the relative phase between input and output can be calculated using fast Fourier transforms of each time series. By using the built-in MATLAB function "angle" and transforming the quantity to degrees, the relative phase is found by dividing one by the other. For simple visual inspection, the relative angle is plotted against frequency.

The coherence of two signals says something about how the relative phases changes with respect to each other, and how much they are likely to interfere. If the relative phase does not change much, then the coherence is high. There is a built in function in MATLAB that calculates the coherence,"mscohere". This is plotted against frequency.

In addition to the aforementioned plots, some interesting spectral parameters are calculated. The spectral moments are calculated from the power spectrum found earlier. The moments are defined by equation (40) where m_n is the nth moment.

$$m_n = \int_0^\infty f^n S(f) df \quad (40)$$

From the spectral moments parameters like significant value, standard deviation, average period of response and average zero-crossing period are calculated. In addition, some statistical values like average, minimum and maximum values are calculated and written to file.

3.6.2 EXTREME VALUE ANALYSIS

In order to find some statistical approximations for extreme values, some assumptions must be made. The first is to assume that the time history is stationary, homogeneous and ergodic. These are strong assumptions, but necessary if any statistical calculations are to be performed. Under these assumptions we assume that the waves are Gaussian distributed. When the instantaneous wave elevation follows the normal distribution, the wave amplitudes are Rayleigh distributed, see equation (41).

$$F(x) = 1 - exp\left\{-\frac{1}{2}\left(\frac{x-\mu_x}{\sigma_x}\right)^2\right\} \quad (41)$$

Where μ_x is the mean and σ_x is the standard deviation of the sampled signal x. Once the distribution is decided upon, it is possible to estimate the expected value of the largest maximum during three hours by equation (42) where f(x) is the probability density function, and $N_w = \frac{3*3600}{T_P}$ is the expected number of waves for a three hour sea state. The most probably largest max is found by deriving the probability function and find the value of x that gives zero change in probability, in other words the maximum, as shown in equation (43).

$$E[X_{LM}] = \int_0^\infty xf(x)dx = \sigma\left\{\sqrt{2\ln N_w} + \frac{0.5772}{\sqrt{2\ln N_w}}\right\} \quad (42)$$

$$\frac{d}{dx}f(x)|_{x=x_0} = 0 \rightarrow X_0 = \sigma\{\sqrt{2\ln N}\} \quad (43)$$

The Rayleigh distribution is well suited for linear responses has we have assumed this far. It should, however, be noted that the Rayleigh distribution excludes higher order contributions like drift forces and nonlinear drag, damping and restoring forces. The alternative would be to use the Weibull distribution, which better incorporates these second order effects [10].

3.7 DECAY TESTS

Decay tests are tests where the structure is excited once in one degree of freedom at a time, and the response is measured. From these time series it is possible to find information about added mass, damping and natural frequencies. In this experiment, decay tests were performed in coupled and

independent condition in heave, roll and pitch. Exciting the platform in only one degree of freedom at a time is very difficult, and some interpretation of the results is necessary.

As before, the results are scaled and bias is removed before the calculations start. First, the most suitable time periods is extracted. The first oscillation should be omitted, to avoid transient effects, and one should also avoid using the very last amplitudes due to the lack of accuracy [10]. The appropriate time series are defined for each run individually, to make sure that the accuracy is optimal. Within the chosen time window, the amplitudes are found using the built-in MATLAB function “findpeaks”. The function records both the time instant and the magnitude of each peak.

To estimate damping, natural period and added mass, the spring stiffness must be known. An estimate can be calculated for each degree of freedom according to known formulas shown in equations (44)-(46). V_D is displaced volume, and $\overline{GM}$ is the metacentric height in longitudinal and transverse directions.

$$C_{33} = \rho g A_{WL} \tag{44}$$

$$C_{44} = \rho g V_D \overline{GM}_T \tag{45}$$

$$C_{55} = \rho g V_D \overline{GM}_L \tag{46}$$

The damping is estimated by assuming that the damping can be split into two main contributions, linear and quadratic. The quadratic damping is linearised (see for example [11]) so that the equivalent damping is given by equation (47).

$$p_{EQ} = p_1 + \frac{8}{3\pi}\omega x_0 p_2 \tag{47}$$

Where x_0 is the amplitude.

Considering now the amplitudes of the decay tests, we define the logarithmic decrement between two succeeding amplitudes in equation (48).

$$\Lambda = \ln\left(\frac{x_i}{x_{i+1}}\right) \tag{48}$$

By assuming low damping ratio (less than 0.2), we can find the damping ratio ξ by equation (49) and the equivalent damping p_{eq} by equation (50).

$$\xi = \frac{\Lambda}{2\pi} \tag{49}$$

$$\mathrm{p}_{eq} = \frac{2C\xi}{\omega_0} \quad (50)$$

To find the damping contributions, we must first find the damped and undamped Eigen periods. The damped Eigen period is chosen as the first oscillation of the time window. The undamped Eigen period is then found by equation (51).

$$\mathrm{T}_0 = \frac{T_d}{\sqrt{1-\xi^2}} \quad (51)$$

Now to find the different damping contributions are found by plotting the mean amplitude between to succeeding peaks against the equivalent damping for each period. In MATLAB, the built in 'fit' and 'poly1' is used to fit a straight line to the data. These functions uses the least square method to find the linear regression line. The linear damping term is the damping at x=0 and the quadratic damping term is the gradient of the line.

Knowing the equivalent damping, the total mass of the platform is calculated using equation (52). The physical mass of the platform is known, and the added mass is now the difference between total and physical mass.

$$M_{tot} = \frac{p_{eq}}{2\omega_0\xi} \quad (52)$$

4 RESULTS

The model test resulted in a large amount of data and graphs. In the subsequent paragraphs, the most interesting and important observations are presented and commented. The tabulated results are attached in appendix B, while the spectral analysis plots for all channels are only included in the electronic appendices, as the number of plots is large.

Recall that all motions refer to the coordinate system of the platform and not the ship. The orientation and position of the platform as well as the position of the transducers, is shown in figure 40. The first figure (left) is 0-degrees wave heading, 315-degrees in shown in the middle, and the 90-degree condition is displayed in the rightmost drawing. The forces are displayed in terms of the transducer's coordinate system, and will be explained for each case.

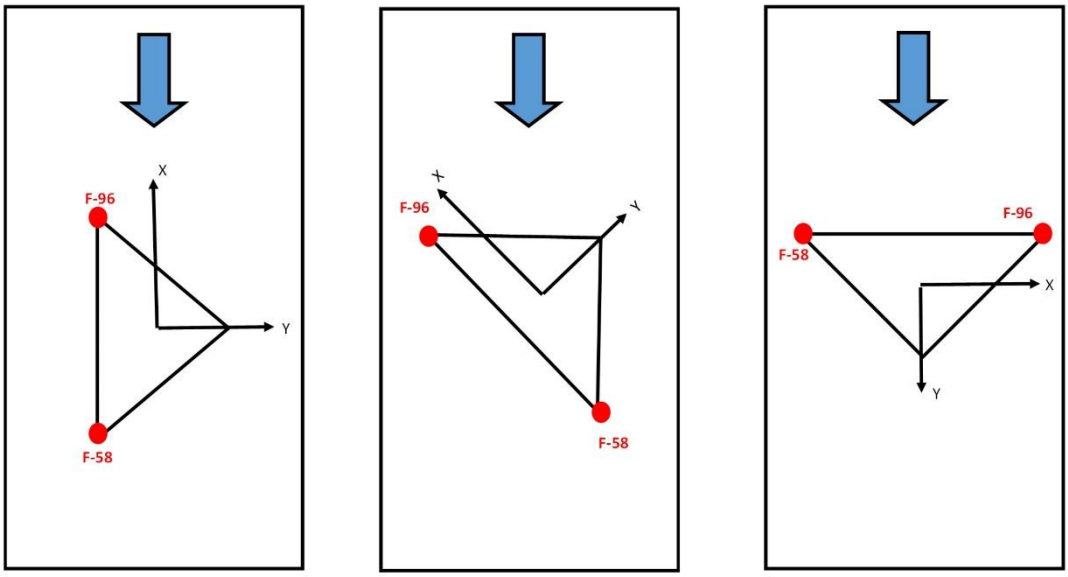

Figure 40: Overview of model test configurations

4.1 REGULAR RUNS

4.1.1 SETUP 1: UNCOUPLED CONDITION, WAVE HEADING 90 DEGREES.

Setup 1 is uncoupled and with a wave heading of 90 degrees. A picture of this configuration is shown in figure 41. The waves are incident from the left hand side of the picture, hitting the straight platform edge

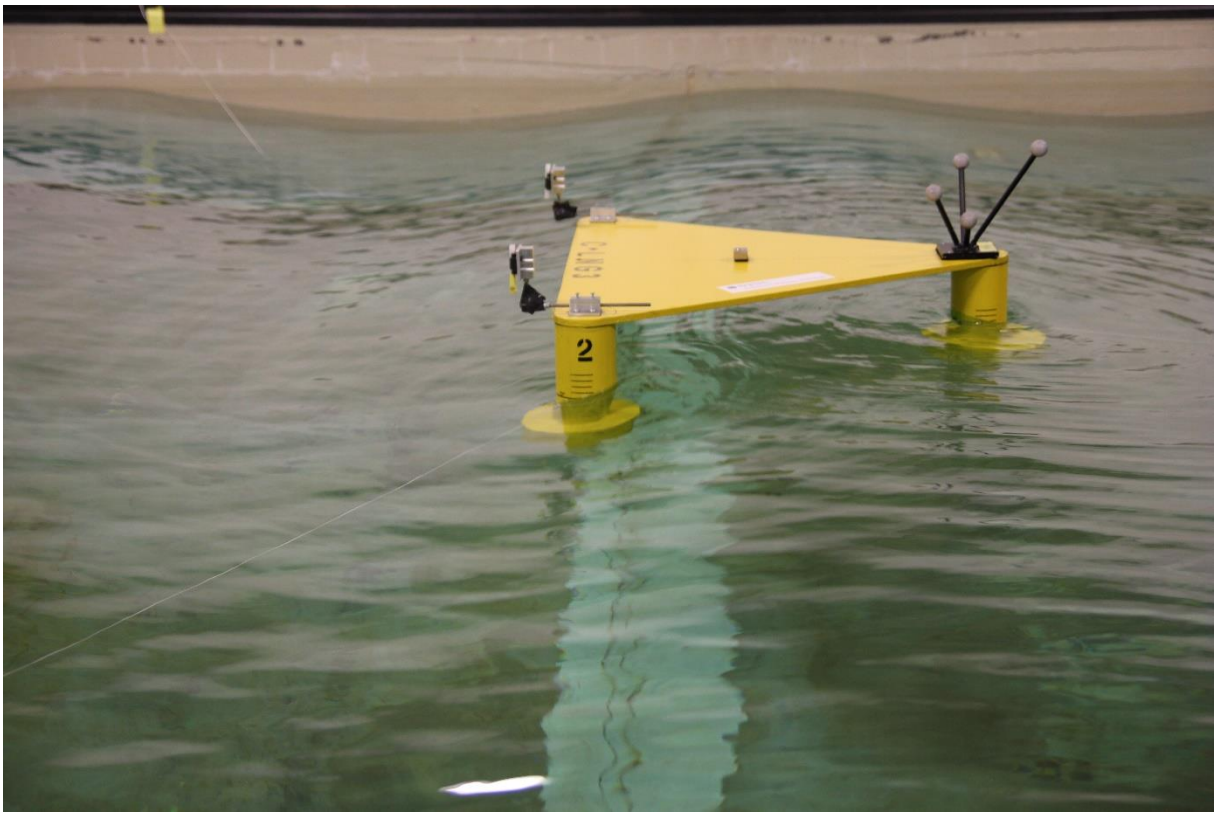

Figure 41: Model test setup 1

where the ship would have been in a coupled condition. The motion transfer function for the uncoupled condition, with a wave heading of 90 degrees is shown in figure 42. It is observed that the largest relative motions occur in roll, with amplification factors around 3.5 deg/m for wave periods in the interval 4-5 seconds. With waves incoming from a 90 degree angle, this is expected. In surge, heave and pitch there are small peaks around 5-5.5s, implying that a natural period may be located within this range. Sway, roll and yaw also has peaks in this interval, but in addition there is also a peak at 4 s for roll and sway, and at about 4 s for yaw, implying a second Eigen period. However, none of the peaks are much larger than the other responses, as one would expect at a natural frequency. It is therefore difficult to reach a conclusion based on these results alone. Furthermore, there are two peaks in the sway transfer function within a short period range. Neither this is of any real concern as the real platform will have an Eigen period in sway when uncoupled. The responses are generally small, with roll being the only degree of freedom with an amplification factor of more than one for any wave period, implying good sea keeping capabilities in a beam sea state. Table 23 shows some maximum values for this setup in full scale. The values are crest-to-trough (height) values, in other words, maximum amplitude minus

minimum amplitude. The values in the table reflect the transfer functions in the sense that roll is the degree of freedom with the definitely largest response, whereas there is some motion in surge, heave,

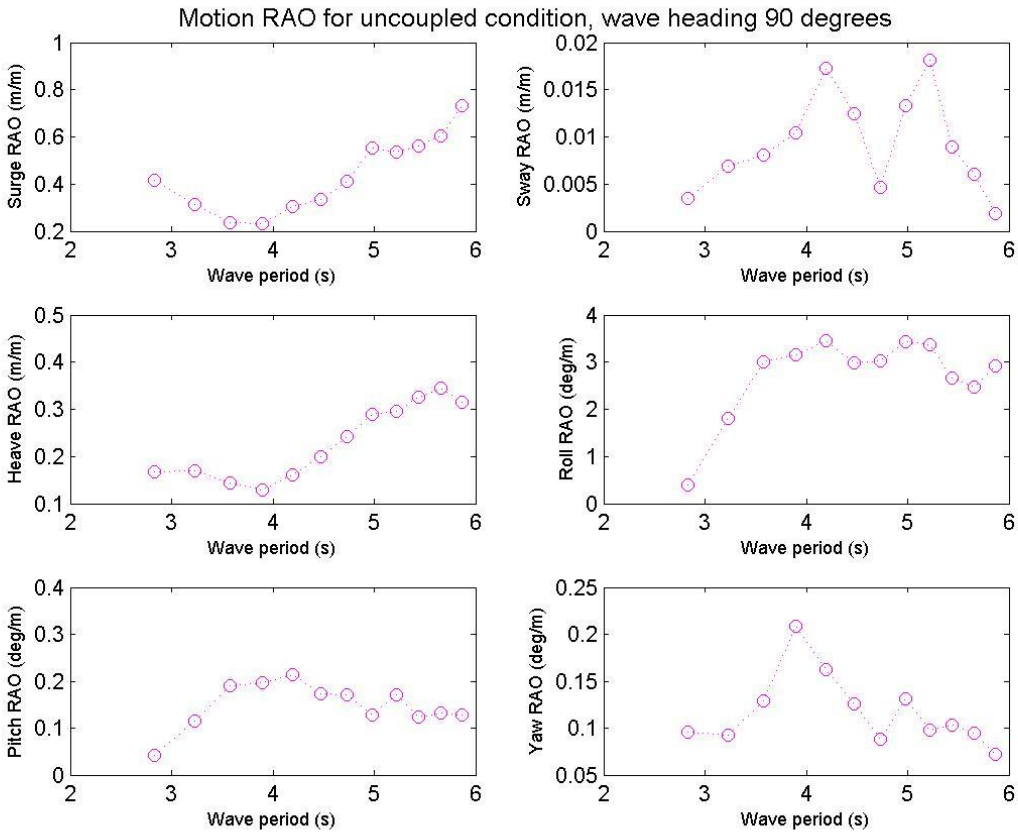

Figure 42: Motion transfer function, setup 1

pitch and yaw, but almost no motion in sway. The response in surge is quite large. This is, however, difficult to compare with a real situation, as the model was moored and the real platform will not be, hence there will be no Eigen period in this degree of freedom. Therefore, this has little practical consequences and is not concerning.

Table 23: Maximum statistics for setup 1

Max. Surge (m)	1.7235
Max. Sway (m)	0.111
Max. Heave (m)	0.675
Max. Roll (deg)	6.403
Max. Pitch (deg)	0.447
Max. Yaw (deg)	1.602

4.1.2 SETUP 2: UNCOUPLED CONDITION, WAVE HEADING 0 DEGREES

The second case runs has an independent platform, with wave heading 0 degrees. A picture illustrating the setup is shown in figure 43. The waves are, as in the previous condition, incident from the left hand

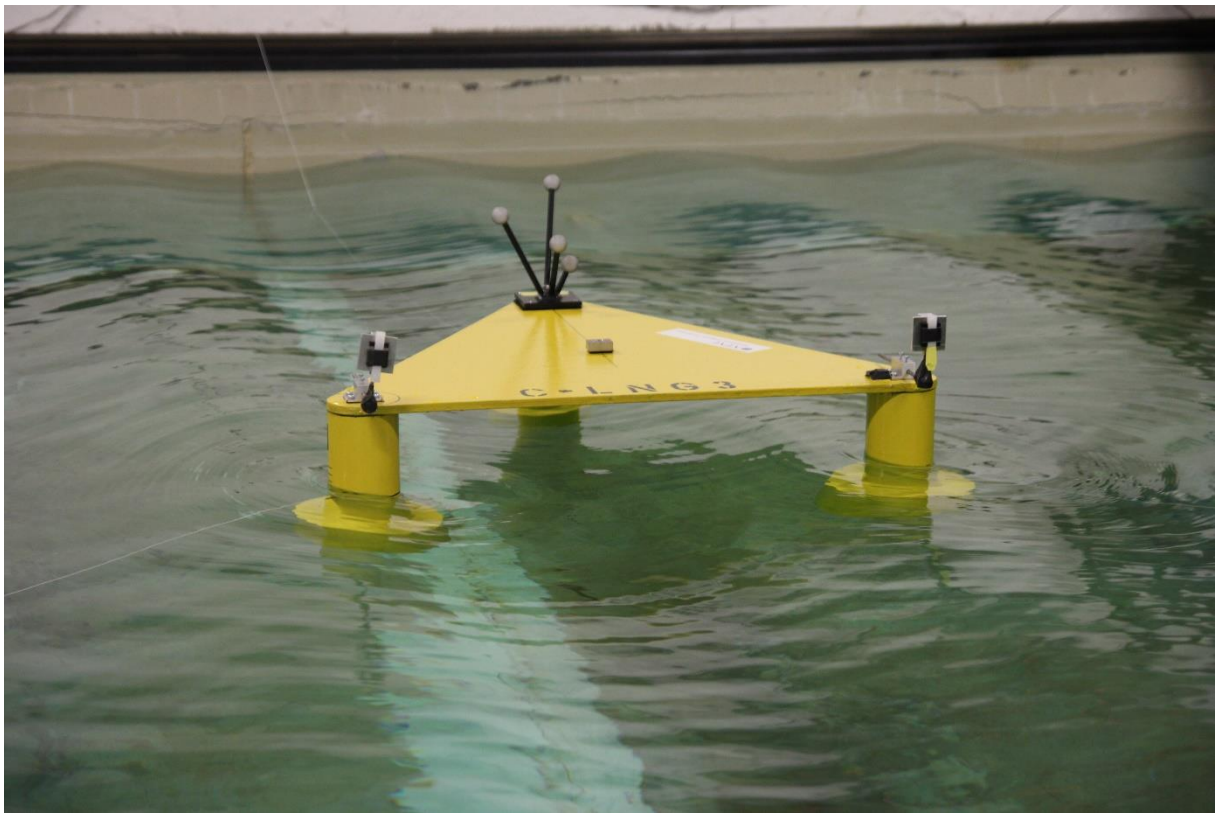

Figure 43: Setup 2

side of the picture, so that the left columns is hit first. The transfer functions for uncoupled condition, head sea, is shown in figure 44. The surge transfer function is very similar to that of the beam sea condition, as is the heave response. This is valid for both the magnitude of response, as well as which wave periods give larger responses. The heave response is as expected, as the wave heading does not influence the heave response on a symmetrical vessel, but surge should be larger for head sea than for beam sea. However, this might be influenced by the mooring system providing artificial restraint to the platform's movement, as well as the reflected waves from the tank walls providing excitation from different angles than zero. The peaks in the transfer functions are again found around 5 s, supporting the thesis that there might be Eigen periods in this area.

Sway response has increased, with the maximum being about three times as large for setup 2 as it was for setup 1. It is, however, still very small, with a maximum amplification factor of 0.06.

The roll motion has a large response, but smaller than the previous setup. This is only as expected, as there should be less roll motion in head sea than in beam sea, for a vessel that is symmetric about the x-axis. There are no peaks, but a rounded top around 3.5 seconds. It is difficult to say whether this is an

implication of a natural period or not, as the intervals between each tested period is too large. To see if there is a proper peak there, it would be necessary to check more periods at shorter intervals.

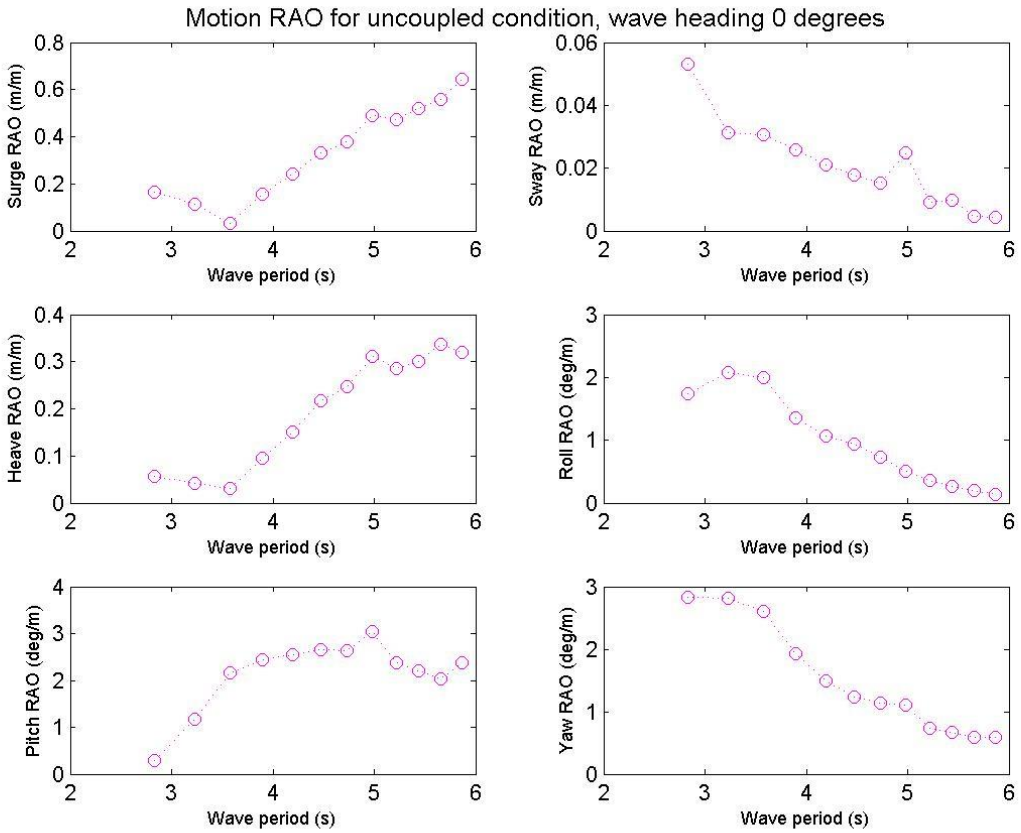

Figure 44: Motion transfer function, setup 2

Pitch motion is significantly larger in this setup, of the order of magnitude 10 times larger than beam sea. This is only to be expected in head sea. Also in this run there is a small peak at about 5 s.

The yaw response is large in this setup, and much larger than the previous setup. This might be one of the reasons why there is such a large roll response for this condition. Ideally, there should be only roll and no pitch in the 90 degree case, and vice versa, only pitch and no roll in a head sea condition. However, a yaw angle will lead to excitations in roll in addition to pitch. A connection can also be made to the first setup, where the yaw angles were small, so there was very little excitation in pitch. In this setup, however, there are large yaw angles, which amplification factors up to 3 deg/m, resulting in significant roll response that is, at its maximum, almost as large as the pitch response. The reasons behind this yaw/roll excitation effect, can have several possible causes. It is likely that it is a combination of the following that results gives the observed response:

- Asymmetry in the model resulting in a coupling of added mass, damping, stiffness and excitation terms. This will yield asymmetrical results.

- Reflections from the tank wall make waves of different incoming angles
- Initial placement of platform may not be perfect, so that the waves are not incident at exactly 0 degrees
- Asymmetries in the mooring system gives a yaw angle, which allows excitation in roll.

The largest responses found for this setup is shown in table 24. The sway motion is now much larger than surge, as is also evident from the transfer functions. Roll and yaw angles are much larger than pitch at over 5 degrees, but because of the yaw angle (and other reasons mentioned previously), there is also a pitch angle present. Again the heave motion is very small, with a maximum amplitude of 0.732 m.

Table 24: Maximum values, setup 2

Max. surge (m)	0.356
Max. sway (m)	1.700
Max. heave (m)	0.732
Max. Roll (deg)	5.354
Max. Pitch (deg)	1.353
Max. Yaw (deg)	5.508

4.1.3 SETUP 3: COUPLED CONDITION, WAVE HEADING 0 DEGREES

Setup 3 is the first of the coupled conditions, where the platform is connected to the frame representing the ship. The wave heading is again set to 0 degrees. The setup is displayed in figure 45. Note that the picture is taken from the opposite side of the basin (for better view of the connection system) so that the

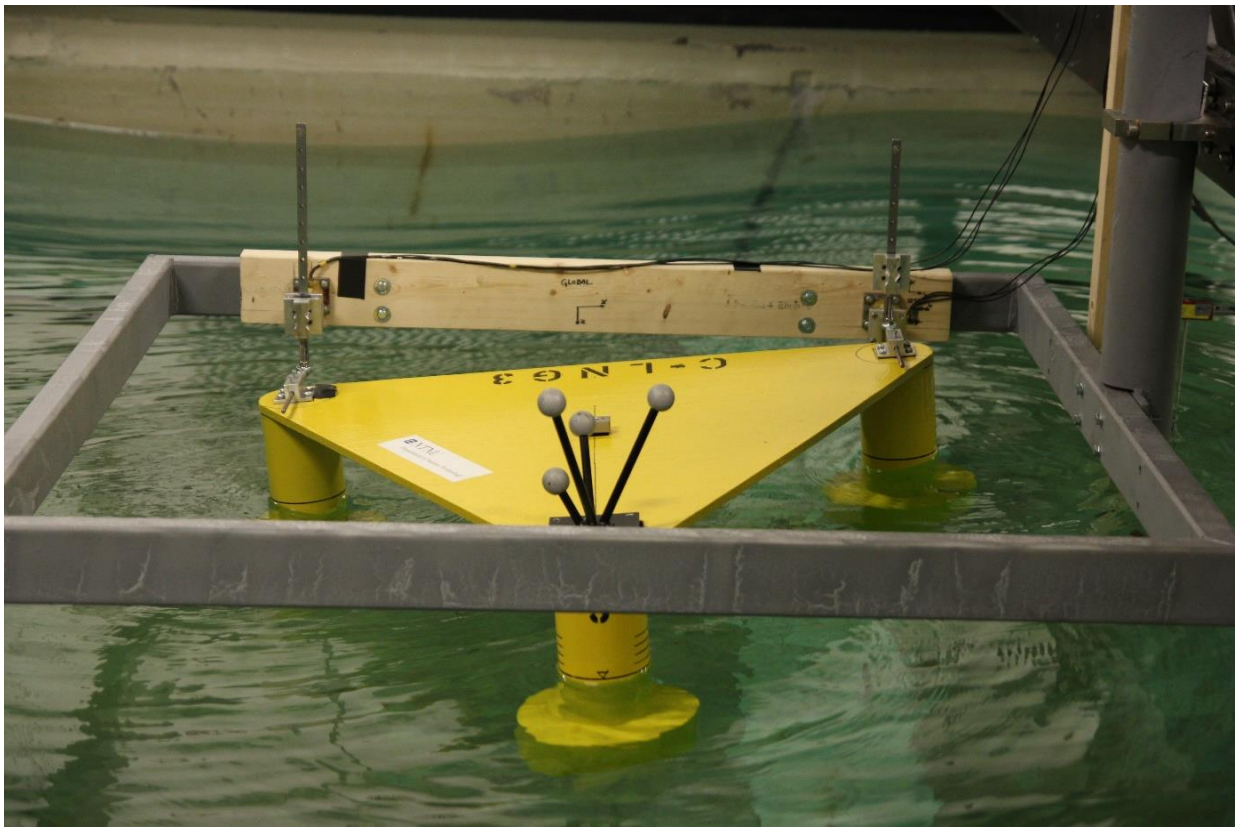

Figure 45: Model test setup 3

waves are now incident from the right hand side of the picture, hitting the right hand column first. The transducer on the right hand side of figure 45 is transducer 96, while the left hand side transducer is transducer 58. While considering the results, the reader should recall that the transfer functions describe the motions of the platform, not the ship. So for example, when the platform rolls, the ship that it is connected to, pitches, and so on. This is valid for all the coupled conditions.

The motion transfer functions for setup 5 is shown in figure 46.The surge and yaw transfer functions here are very small. Surge and yaw should be small, as the platform is restrained in these degrees of freedom. There will, of course, be some movements present due to both measurement inaccuracies and modelling errors, as is evident from the results. There is no indication of a natural period. This must be because the natural period is outside the frequency range of the waves, because when the motions are restrained by a mooring (or similar) system, a natural period will exist. Likewise, the sway movements are very small, almost non-existent, because of the constraints. However, there are two possible indicators of a natural period in the transfer function, one at about 3.5 s and one at about 5.25 s.

Heave motion is small in this condition, of the same order of magnitude as previous conditions. This is as expected as the waves are the same in coupled and uncoupled condition. Furthermore, it is an indicator of the connection system having low friction, so that the platform really is free to move in the z-direction.

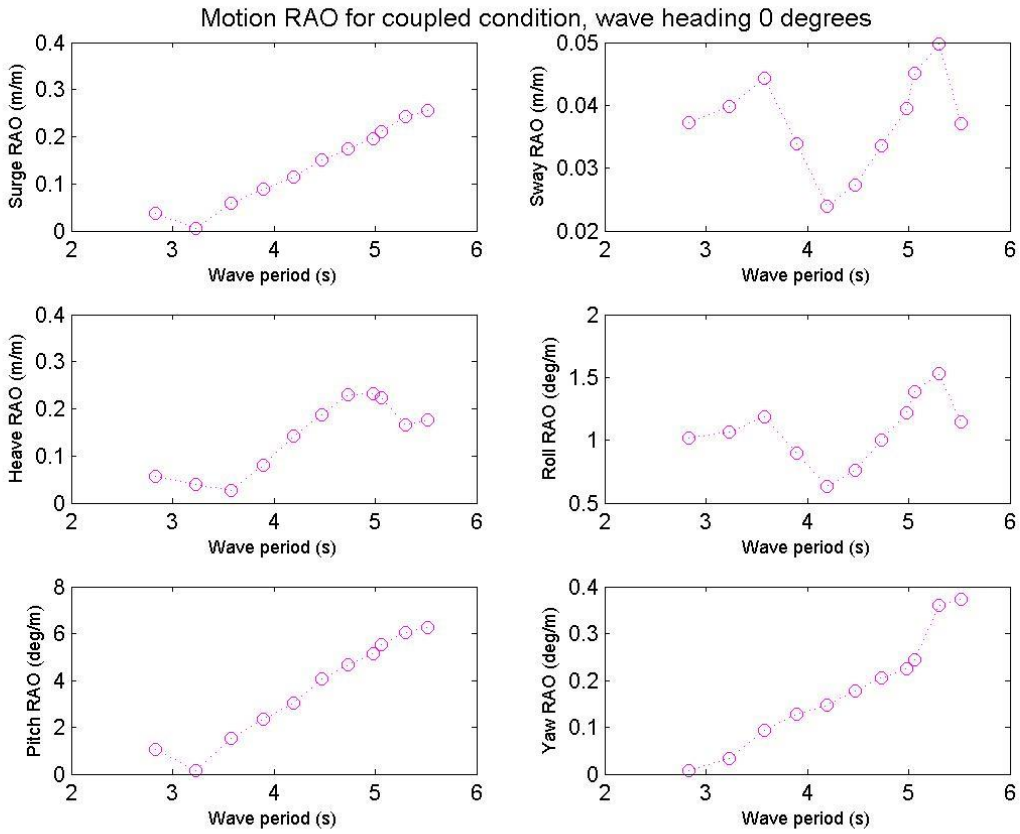

Figure 46: Motion transfer function, model test setup 3

Pitch motions are fairly large for these runs, with amplification factors exceeding 6 deg/m for the largest periods. This is more than what was seen in the 0 degree uncoupled condition. As the frame does not enter the water, there must be some other reason why the pitch angles are so much larger in the coupled than in the independent condition. One possibility is that the frame and/or the connections system acts as a spring, exciting the frame to increase the pitch motions. It is also possible that the would-be translations of the platform that the waves excites, are translated to pitch motions by the connection system.

The roll motion is significant for this setup, with amplification factors reaching approximately 1.5 deg/m. This is, however, only about half of the amplification for the same wave heading in the independent condition. Even though the connection system was designed to give the platform freedom to move in roll, there is clearly some restraint. Even though the ball joint has low friction, a limiting factor for the roll

movement could be the wagon-and-track system, providing some support and a “soft landing” when the platform heels, limiting the maximum response and dampening the movement. There is an indication of an Eigen period in roll at about 5.25 s, similar to the previous results.

The force transfer functions for the same setup are shown in figure 47. The forces in the x-direction (vertically) from both transducers follow each other quite closely, implicating that the force magnitudes are similar at the two transducers. This is as expected, because there are no accumulating moments or platform weight et cetera that could lead to larger forces at one of the vacuum pads. There is, however,

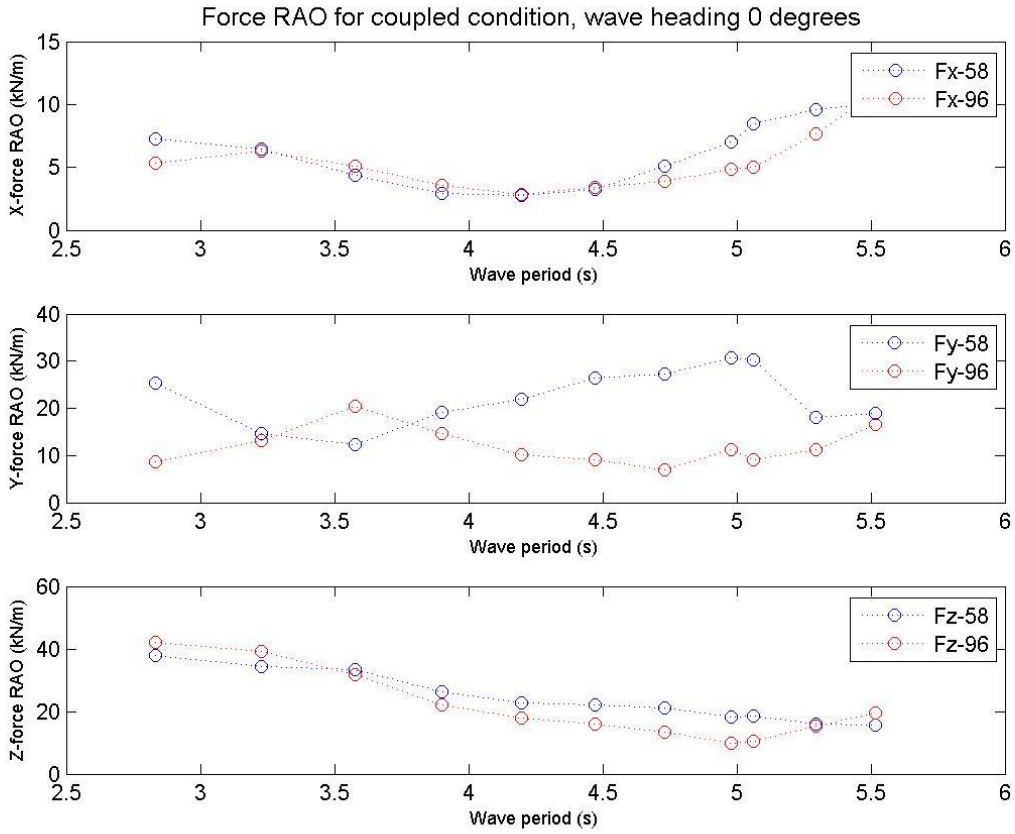

Figure 47: Force transfer function, setup 3

a significant amount of force in the x-direction. This should ideally be zero, but this is obviously not possible in a practical situation. One should, however, note that heave, roll and pitch motions may be underestimated. The vertical (x) force has larger values for large and small periods than for the middle range ones. It is speculated that this is connected with the friction coefficient of the wagon/track. At the largest periods, the platform is moving slowly, and if it comes to a standstill at a crest or trough, it must overcome the static friction before starting to move. This phenomenon was observed in the time series. As the wave periods decreases, the movement is continuous, and so the force decreases because the

platform no longer has to overcome the static friction. As the wave period decreases, the force increases again, almost linearly, as expected.

The lateral (y) force displays some unusual behaviour. It is observed that at long wave periods one is much larger than the other, while at the shortest wave periods, the order is reversed. The reason why they are not following each other as the two other force components do, might have its origin in the phase of the wave. For example, at the instant where the wave impacts the first column, where the first transducer is located, there might be a wave trough at the other column. For different wave periods there will be different phases, which leads to this reversal of the y-forces.

It is peculiar that the RAOs of the z-forces are of approximately the same order of magnitude as the y-forces when the waves are incoming from a 0 degree angle. Again, this might be a result of small inaccuracies in the setup leading to small sway motions which impacts the force in z-direction (alternating increasing and decreasing it on each side). In addition, waves reflected from the tank wall may push and pull the platform against/away from the ship side. The magnitudes increase for shorter periods, which is what one would expect. The two transducers give approximately the same values, and must be said to be equal, considering uncertainties involved.

The largest recorded values are shown in table 25. The maximum pitch is, as previously mentioned, very large, with almost 13 degrees. The maximum surge displacement is also larger than one might expect, whereas sway, roll and yaw are within the expected interval ranges, as is also evident from the transfer functions.

Table 25: Statistics for setup 3

Max. Surge (m)	0.57
Max. Sway (m)	0.15
Max. Heave (m)	0.43
Max. Roll (deg)	4.11
Max. Pitch (deg)	12.88
Max. Yaw (deg)	1.08
Max. Fx_58 (kN)	68.75
Max. Fy_58 (kN)	298.04
Max. Fz_58 (kN)	76.62
Max. Fx_96 (kN)	91.32
Max. Fy_96 (kN)	260.89
Max. Fz_96 (kN)	169.81

The forces in the vertical direction is small, as expected. The y-forces also show that the force distribution is approximately the same on the two columns, although they occur at different wave

periods, as shown in the transfer functions. The perpendicular forces however (z) show a large difference between the two transducers, with more than twice the magnitude on transducer 96. Further inspection of the values (see table b - 3) shows that the z-force values increases almost exponentially for the 96-transducer for the two last runs, as opposed to the 58-transducer as well as the rest of the runs for the 96-transducer, which increase linearly. There could be some higher order effect present causing this increase, or it could be artificial, as a result of measuring errors.

4.1.4 SETUP 4: COUPLED CONDITION, WAVE HEADING 315 DEGREES

An illustration of setup 4 is shown in figure 48. The platform is coupled to the frame and oriented such that the waves are incident of the platform at an angle of 315 degrees. The waves are again incoming from the right hand side of the picture, hitting the straight edge of the platform first and column 2 (number visible in the figure) last. The transducer at column 2 is transducer 58. The other transducer, at

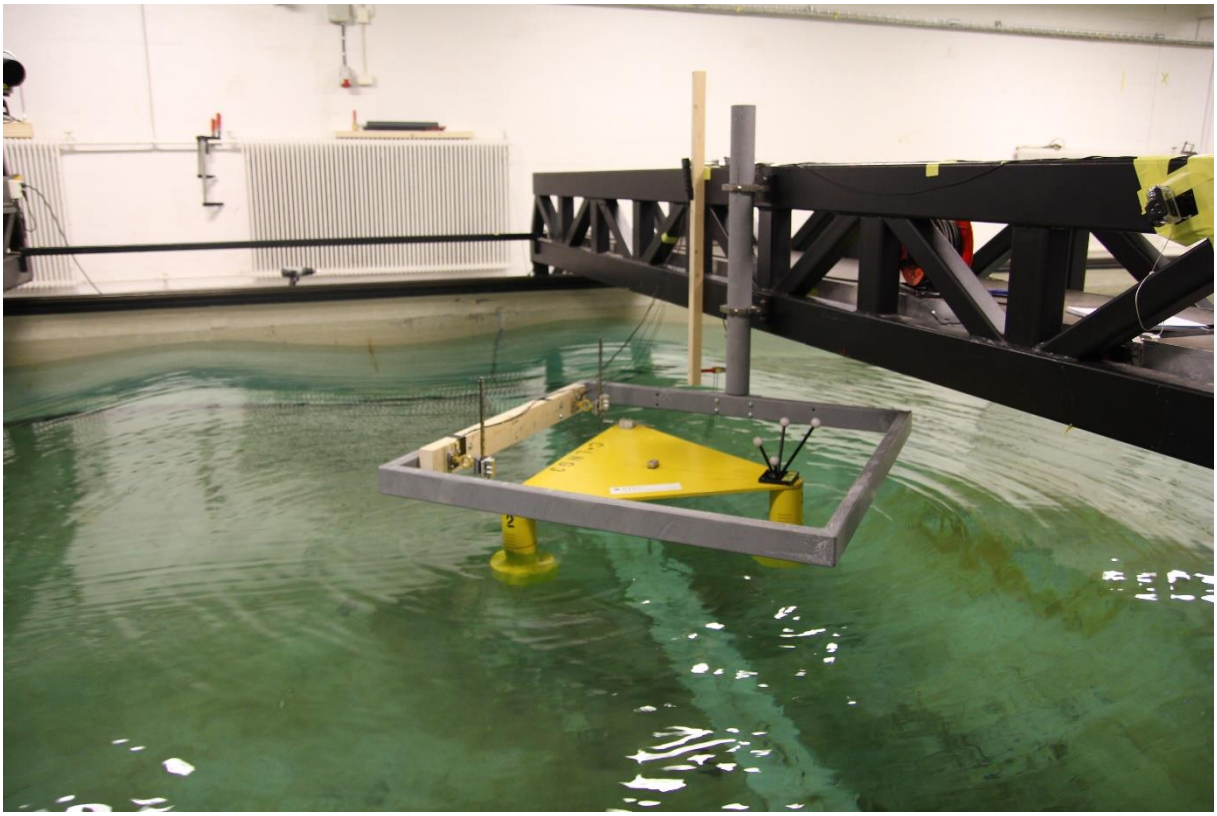

Figure 48: Model test setup 4

the far corner from the viewpoint in figure 48 is transducer 96. The setup is such that the waves are incident on the side of the platform on which it is attached to the ship. In reality, the ship will be in the water and sheltering the platform, but here only the platform is in the water. This is therefore an exaggerated scenario.

Figure 49 displays the motion transfer functions for the fourth setup, which is coupled condition with a wave heading of 315 degrees. The maximum recorded values for setup 4 in the model test is displayed in table 26.

Surge and yaw motions, and even more so sway, are small in this condition, for the same reasons as previously mentioned in the chapter concerning setup 4. The change in wave heading does not imply that these movements should change, and neither do they. Heave movements are in the same range of amplitudes as seen previously. This record shows two spikes, at about 4.5 s and 5 s. Also these measurements are quite similar to what was seen previously, as is only to be expected. The sway motions are also very small, and of the same order of magnitude as seen before. The wave heading does not affect how efficient the restraint is, seeing as the restraint is symmetric, and so the sway motion is approximately the same as for the other directions.

The transfer functions in roll and pitch are very similar for this run. Both have a small peak at around 4.5 s, and the amplification factors have maximums of around 4 deg/m. This is only as expected for quartering seas. There will be coupling between these two movements as this angle of incident waves,

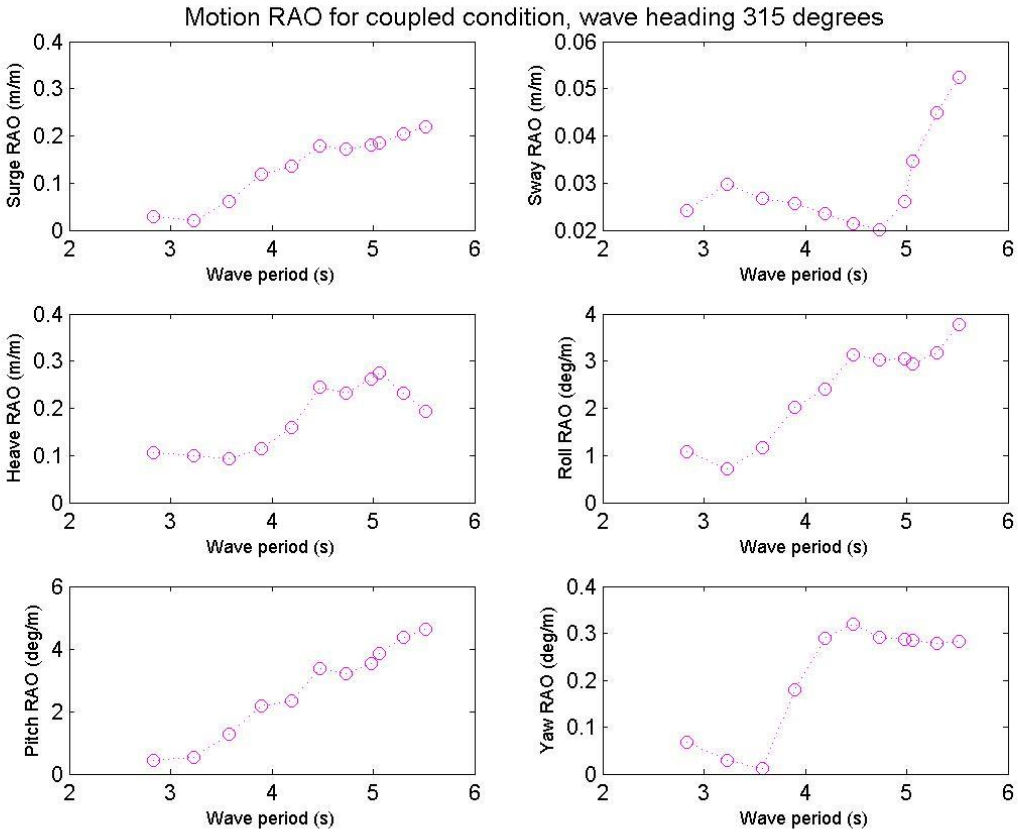

Figure 49: Motion transfer function, setup 4

as is also seen in the resulting transfer functions. The same result can be seen in table 26 displayed at the end of this section.

One peculiar observation is that surge is almost as large as heave is. As the platform is supposed to be (completely) restrained in surge and (completely) free in heave, there is clearly something off here. Considering the video recordings of the tests does not give any clear solution, as there is no surge motion of the platform itself that is visible to the naked eye. However, focusing on the Oqus markers reveals that the markers move in a circular fashion, indicating the recorded surge values are a result of significant coupled motion in roll and pitch. In the video, the markers seem to be moving in a fairly circular motion along the direction of wave propagation.

The force transfer functions for setup four are shown in figure 50. The vertical (x) forces follows each other quite closely, as before, except for a small reversal towards the shorter wave periods. This may be because of small differences in the friction coefficient in the connection system, in addition to measuring errors.

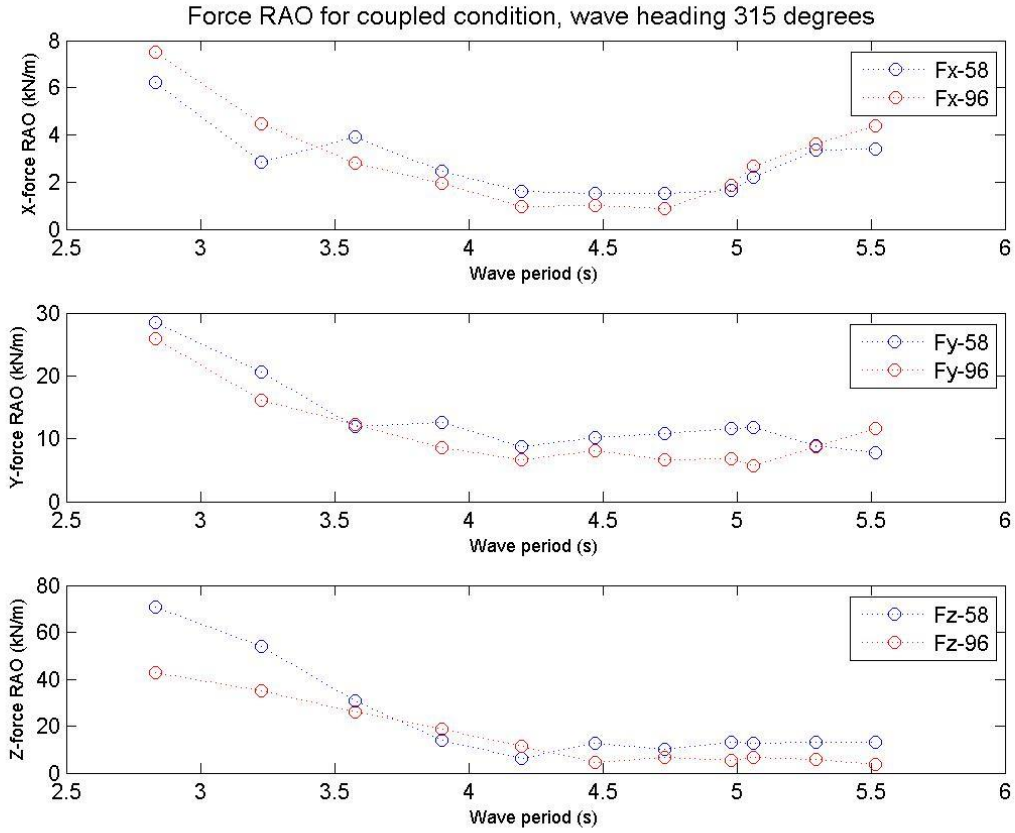

Figure 50: Force transfer function, setup 4

Furthermore, the same trend as in setup four is seen also here, that the force is larger for shorter and longer wave periods, while it is smaller for the middle range. The possible explanation is the same and

will therefore not be repeated. The y-force again shows the same trend as seen previously, which a slightly “opposite” behaviour of the two transducers. The difference is, however, this time much smaller.

The contact (z) forces show a strong correlation and a fairy linear decline as the time period increases. This is the same behaviour as seen previously, and it is expected that the general shape of the force transfer function does not change because of the change in wave heading.

Table 26: Statistics for setup 4

Max. Surge (m)	0.44
Max. Sway (m)	0.13
Max. Heave (m)	0.48
Max. Roll (deg)	8.06
Max. Pitch (deg)	9.64
Max. Yaw (deg)	0.54
Max. Fx_58 (kN)	31.48
Max. Fy_58 (kN)	132.07
Max. Fz_58 (kN)	45.86
Max. Fx_96 (kN)	38.02
Max. Fy_96 (kN)	135.70
Max. Fz_96 (kN)	80.87

4.1.5 SETUP 5: COUPLED CONDITION, WAVE HEADING 90 DEGREES

The fifth and final condition is coupled and with a wave heading of 90 degrees. The condition is shown in figure 51. This is the same orientation as used in setup 1, but because how the frame was attached to the wagon, the platform was situated partly beneath the wagon. In terms of visual inspection, this is not optimal, but the Oqus system works, as the markers are still clearly visible. The waves are now incoming from the left hand side of the figure, as in the first two setups, impacting the straight side with the connection system first. This case is also an exaggerated one, as in reality the ship side will shelter the platform. In this figure, transducer 58 is closest to the camera, while number 96 is furthest away.

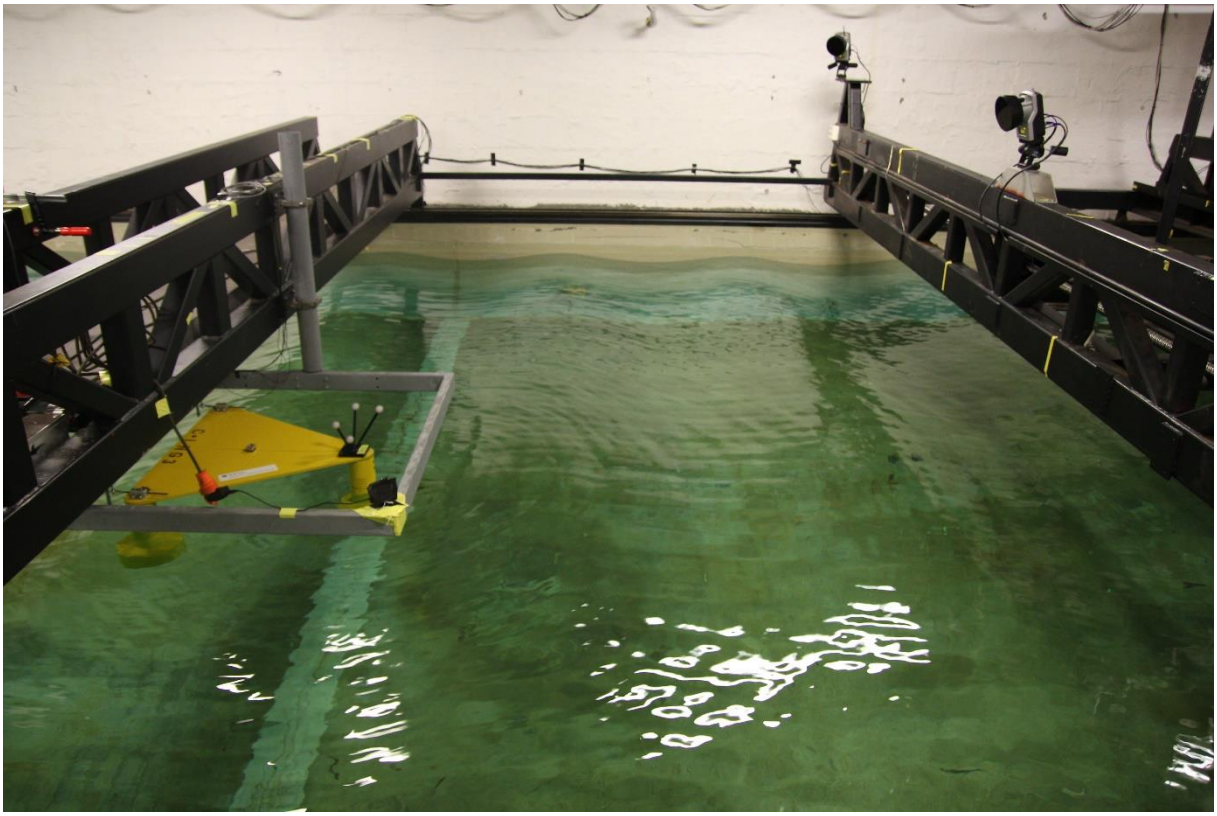

Figure 51: Model test setup 5

The motion transfer function for setup 5 is displayed in figure 52. Surge motions are very similar to the behaviour observed in the previous cases. There is a small dip in the transfer function at about 3.2 seconds, indicating some cancellation effects take place at this wave period. Otherwise the general trend is that the surge motion increases for increasing wave periods, as is only to be expected. Sway motions are even smaller for this case than the other runs. This is obvious, as the platform is not only restrained in sway, but the waves are coming from a 0 degree angle, meaning that the platform is not excited in sway.

Some sway measurements have been recorded (otherwise the transfer function would be only zeroes), but these are likely to be only small inaccuracies in measurements and/or some inefficiency in the restraint system. Considering the shape graph alone, it may seem that there are large fluctuations in the

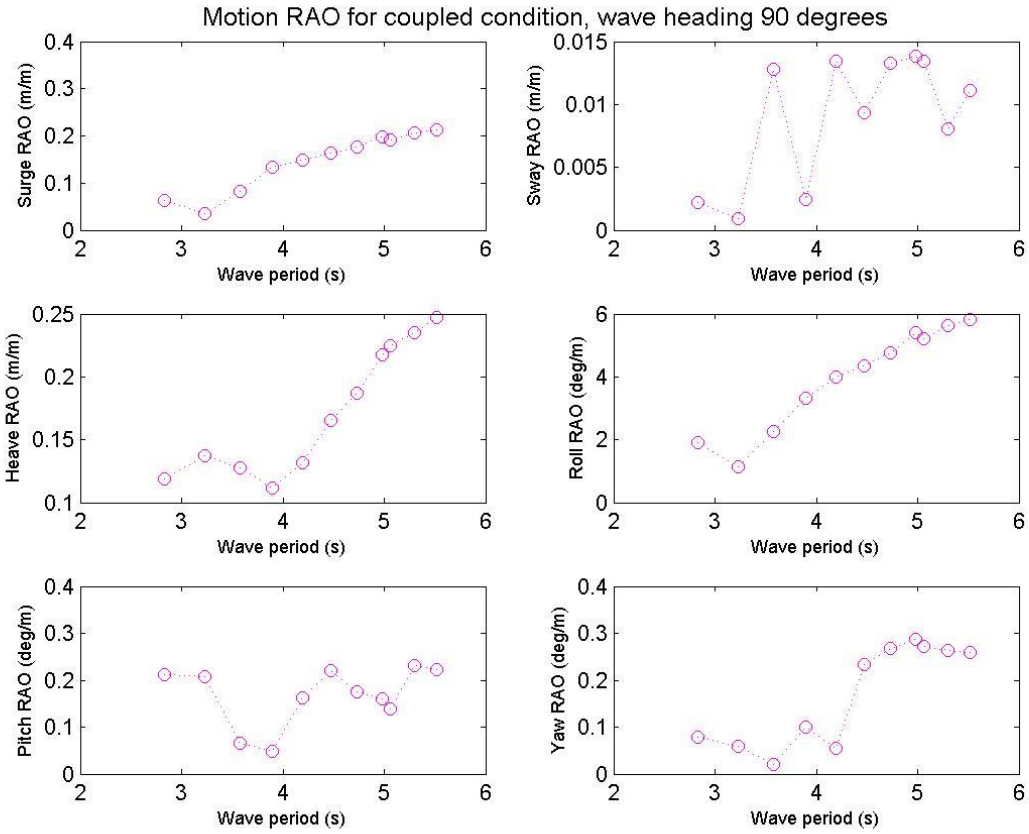

Figure 52: Motion transfer function, setup 5

sway response. However, considering the axes and the fact that the largest amplification factor is about 0.015, these differences might as well be statistical uncertainties as actual changes in the response of the system.

The vertical movements are similar to that of setup 3, with a maximum amplification factor of 0.25 and a dip at ~3.9 s. As mentioned for the uncoupled cases, this is to be expected as the wave heading does not affect the excitation in heave because of the symmetry in the platform geometry. The roll and pitch transfer motions are similar to those in case 3, except that the roles are reversed, and this is due to the 90 degree change in incoming wave angle. Roll is now by far the largest motion, with amplification factors ranging from approximately 1 deg/m at the dip up to 6 deg/m. Pitch, however, is small, with a maximum amplification factor of slightly above 0.2 deg/m. There are two apparent dips in the transfer function, where there are cancellation effects. These occur at wave periods of 3.5-4 s, as well as a small dip close to 5 s. The yaw transfer function shows that yaw angles are very small for the short wave periods, before they increase sharply from around 4.5 s.

The force transfer function is shown in figure 52. The vertical (x) force shows some of the same performance as seen earlier. However, in setup 5, the force declines steadily as the wave periods increase, whereas before the force would increase again towards the longest periods. Therefore this angle of incident bust be beneficial with respect to the friction in the track-and-wagon system. This is confirmed by the maximum values shown in table 27 at the end of this section, which shows a maximum vertical force of 5.06 and 9.06 kN, as opposed to values in the range of 31.48-91.32 kN. This could be

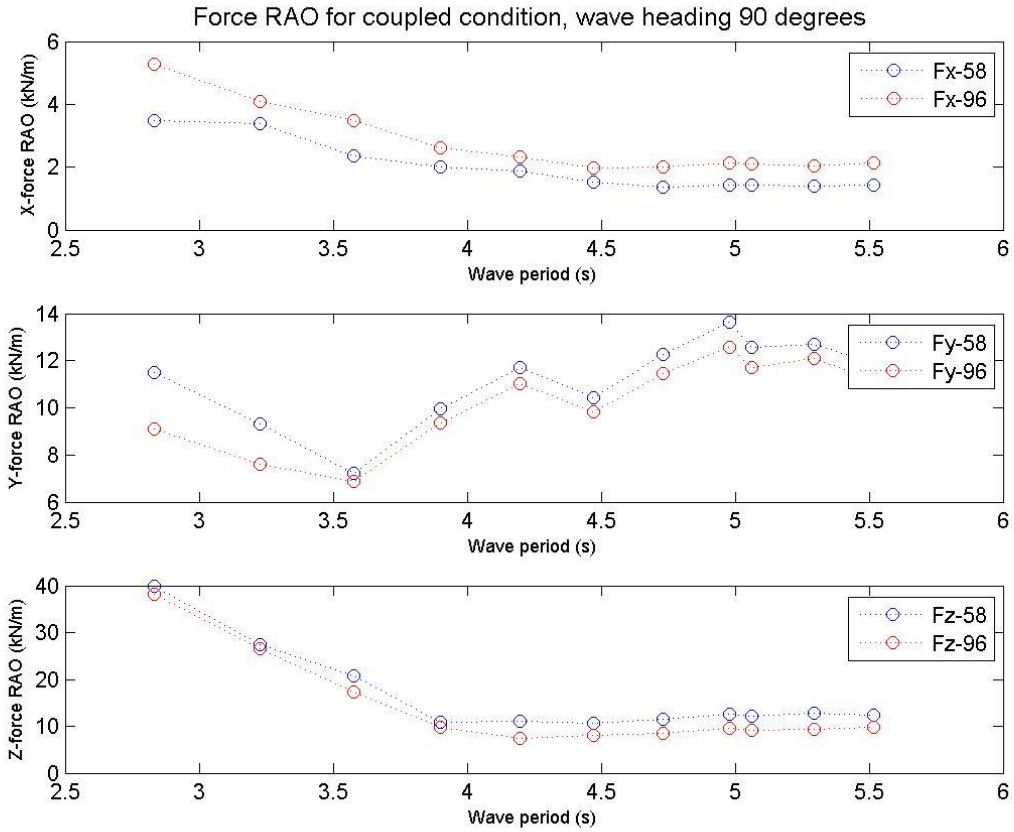

Figure 53: Force transfer function, setup 5

explained by the orientation of the platform in the sense that the platform is not “pushed” towards the ship by the waves as much as for the previous cases, so that the whole connection system is better aligned.

The parallel (y) force in this 90 degree wave heading run displays one feature that is quite different from the previous cases; in this setup the values from the two transducers follow each other closely and almost equidistantly, as the wave periods increase. In the other runs the y-forces from the two transducers alternated between being higher and lower than the other, whereas now the 58-transducer is constantly reports higher values than the 96-transducer. The explanation for this must be that the waves hit the columns beneath each transducer at the same time and with almost equal force. Thus the

only sources of differences are really modelling type errors and tank wall reflections. This behaviour is also reflected in table 27, displaying maximum values of 26.2 and 23.3 kN.

The force between the frame and the platform (the z-component) displays a large amplification factor for the shortest waves, and decreasing force as the wave period increases. The transfer function curve flattens out after the wave period has reached about 4 seconds. The magnitudes are all in all smaller for this run than for others, which is because the waves are now pushing the platform away from the frame/ship rather than against it. The contact force that appears is therefore the one experienced when the platform is on its way down from a wave crest to a wave trough. This is obviously much smaller than what the platform would experience if the waves were incoming from a 270 degree angle instead.

Table 27: Statistics model test setup 5

Max. Surge (m)	0.40
Max. Sway (m)	0.06
Max. Heave (m)	0.51
Max. Roll (deg)	11.04
Max. Pitch (deg)	0.69
Max. Yaw (deg)	0.48
Max. Fx_58 (kN)	5.06
Max. Fy_58 (kN)	26.20
Max. Fz_58 (kN)	29.92
Max. Fx_96 (kN)	9.06
Max. Fy_96 (kN)	23.30
Max. Fz_96 (kN)	30.33

4.2 IRREGULAR RUNS.

For the irregular runs, the following is calculated:

- Response spectrum
- Transfer function
- Relative phase
- Coherence
- Weibull extreme value plots
- Statistical values like spectral moments, expected value of largest max for a 3 hours period etc.

All of these are computed for all 6 channels for the uncoupled runs, and for all 12 channels for the coupled runs. The most interesting results will be presented in the subsequent sections.

4.2.1 MAXIMUM VALUES

The following tables display some extreme values from the irregular runs. Table 28 displays the largest recorded values during the run. The values show that the motions are generally smaller for the coupled condition than for the independent condition, which is only as expected. Another pattern that emerges in surge and sway, is that the displacements are within the same range for all directions in that condition. Heave is generally lower in the coupled conditions, which must be due to the friction in the connection system, which ideally should have been zero so that the heave values would have been approximately the same.

Table 28: Maximum measured values, irregular runs

	Uncoupled		Coupled		
Channel/Setup	0 degrees	90 degrees	0 degrees	315 degrees	90 degrees
Surge (m)	0.858	0.894	0.201	0.209	0.141
Sway (m)	0.078	0.070	0.046	0.096	0.022
Heave (m)	0.270	0.277	0.125	0.188	0.167
Roll (deg)	1.268	3.485	1.970	3.202	3.806
Pitch (deg)	3.252	0.173	5.412	3.916	0.168
Yaw (deg)	2.191	0.163	0.134	0.335	0.308
Fx-58 (kN)			22.2	7.7	2.6
Fy-58 (kN)			155.1	78.1	7.5
Fz-58 (kN)			26.3	33.0	18.1
Fx-96 (kN)			35.5	9.7	3.7
Fy-96 (kN)			21.6	18.8	13.2
Fz-96 (kN)			29.7	24.4	15.6

The records show that the rotations of the platform are more sensitive to changes in wave heading. Roll is small for the two 0 degrees cases, but large for 315 and 90 degrees, in both coupled and uncoupled condition. This indicates that roll depends more on the wave heading than on the presence of the ship. Pitch varies greatly with wave direction, with large motions in 0 degrees and smaller in 90 degrees, as expected. Yaw is generally small, with the only maximum value of any significance occurring in uncoupled, 0 degrees, where the yaw movement might just as well be due to the mooring system.

Forces are generally largest for the 0 degree case (with the exception of Fz-58, which is largest in 315 degrees) and smallest in the 90 degree case. The vertical (x) values are relatively small for all runs, which is the same as what was seen in the regular runs.

Fy-values are largest for wave heading 0 degrees and smallest for wave heading 90 degrees. Transducer 58 is also larger than 96. For the two first wave headings, the orientation of the platform is such that the waves hit the columns on which transducer 96 is placed first, and transducer 58 is placed further away from the wave probe (see figure 45, figure 48 and figure 51), which means that the transducer at 58 records not only the same wave forces as present on transducer 96 but also the moment that arises from the platform being bent and pushed by the waves. At 90 degrees wave heading, the “ship side” is perpendicular to the waves, so that the waves hit transducers 58 and 96 at the same time. There is a small difference in force between the two transducers (in all directions), but this must be due to inaccuracies and/or statistical deviation.

The Fz-forces, perpendicular to the ship side, are smaller than Fy for directions 0 and 90 degrees, but larger for 315 degrees. Considering the configurations, this is as expected. For the 315 degree case, the platform is “pushed” towards the ship side, resulting in large contact forces, whereas in the 0 degree case the platform side is parallel to the incoming waves so that y-forces (along the ship side) are largest. In the final configuration, the z forces are small because the platform is pushed away from the ship side rather than against it, which would be a more severe condition.

The largest force registered was 155.1 kN in the Y-direction. To put this into perspective, recall that the total weight of the platform in full scale is about 38 tonnes. The relative force that the platform exerts on the ship side is therefore small.

4.2.2 TRANSFER FUNCTIONS

Transfer functions were calculated for all channels, to allow the reader to investigate the behaviour of the platform in the frequency domain. As previously explained, the translational displacement of the platform is small for all the setups, so these are omitted in this report. The more interesting transfer functions are presented here, but the complete result is also attached in appendix B.

The wave spectrum recorded in the test is shown in figure 54. The spectra reveal that something has gone wrong in the first two setups, as the total energy in these sea states are much lower than the last three. The results from these two runs should therefore be considered as liberal estimates, as wave heights are smaller than anticipated. However, as the transfer functions provide relative figures, it is still possible to extract useful information in the form of trends and tendencies.

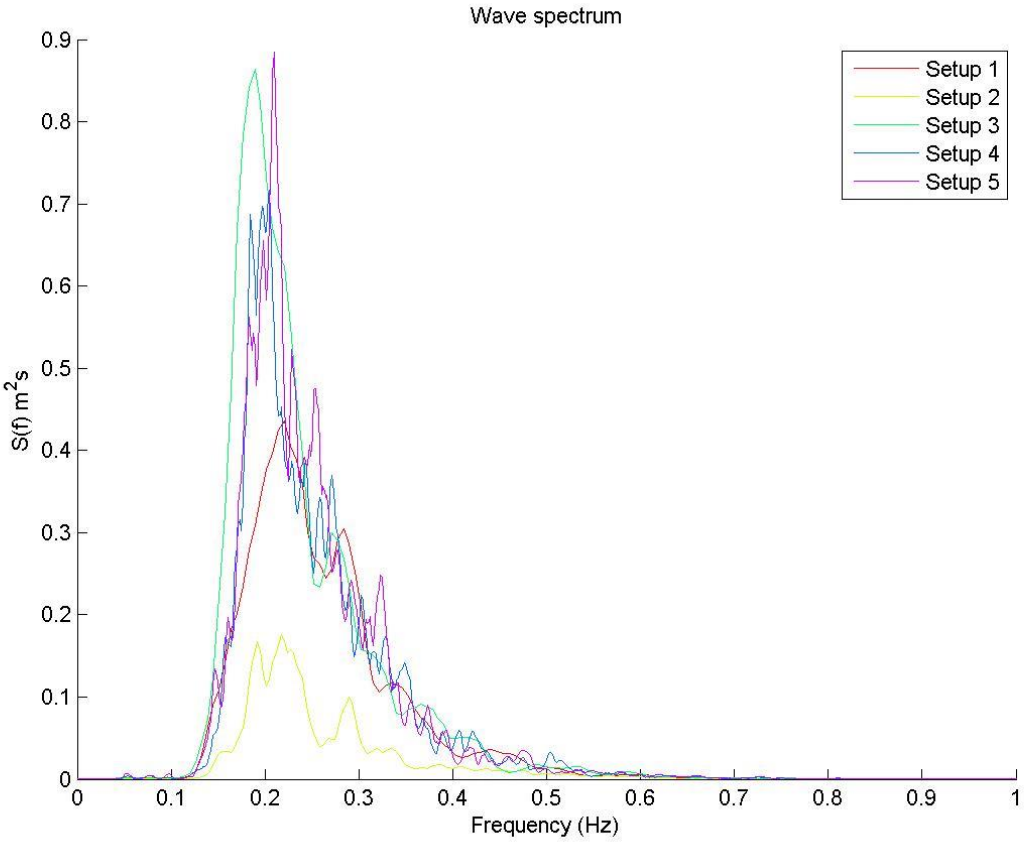

Figure 54: Wave spectra from irregular runs, model test

Figure 55 presents the roll transfer functions calculated from the irregular runs. There are some small peaks, around 0.15 Hz for setup 2 and 0.45 Hz for setup 3. However, the peaks are very small and might just as well be due to uncertainties. Setups 4 and 5 show very large amplification ratios around a frequency of 0.1 Hz. There are also some peaks in the frequency range 0-0.1 Hz for the first three setups. Considering the transfer function alone may lead the reader to think that there will be some serious responses around a wave frequency of 0.1. However, keeping in mind that the input wave

spectrum has a peak at 0.2 Hz and close to no energy in the 0-0.12 Hz range, the peaks in the low frequency range is of little consequence. In the range where the wave spectrum has a lot of energy (about 0.12-0.5 Hz) the transfer functions have small values.

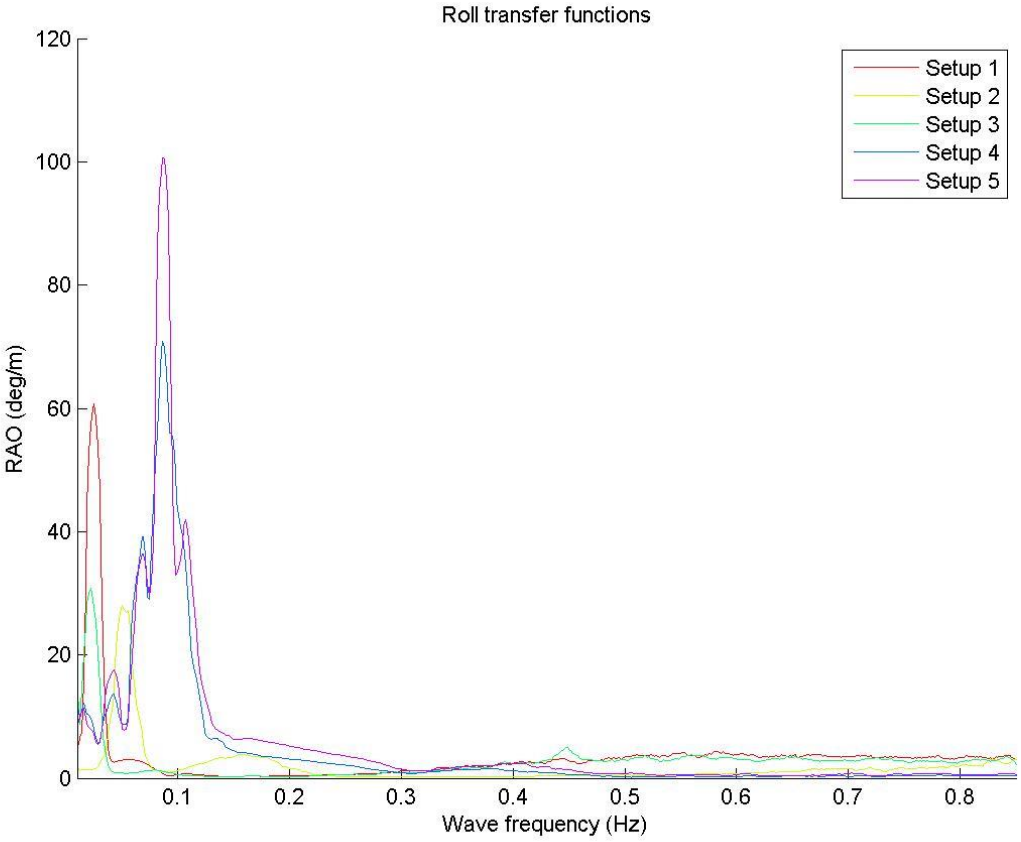

Figure 55: Roll transfer functions, irregular runs

The transfer functions in pitch are displayed in figure 56. They exhibit the same kind of behaviour as the roll transfer functions, with many peaks in the 0-0.1 Hz range, and very small values elsewhere. The values are almost zero for all setups except setup 1 and partly 3 in the wave frequency range. As with roll, there is therefore no risk of resonant motions in pitch in the tested conditions.

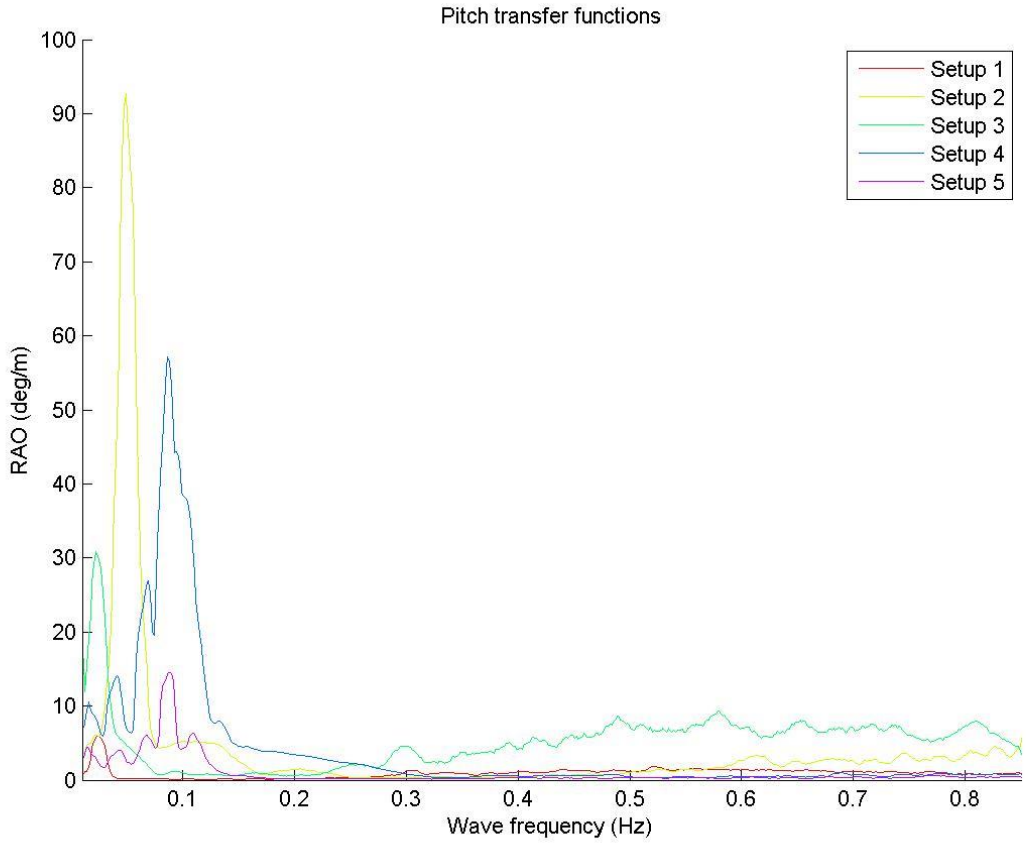

Figure 56: Pitch transfer functions for irregular runs

The y-force transfer functions are displayed in figure 57, and the z-force transfer functions are shown in figure 58. Forces from both transducers are included in the plots, with transducer 58 being the solid lines and 96 being the dashed lines. Similar trends are seen for both force components, with small peaks in the high frequency range, large peaks in the high frequency range, and relatively low response in the wave frequency range.

As seen also in the maximum values, it is setup 3 that has the largest forces in both y- and z-directions. The y-force is largest for transducer 58 most of the time, with some exceptions, most notably at about 0.44 Hz. This is in coherence with what was mentioned previously, that transducer 58 is placed furthest away from the wave maker in the laboratory, so that the weight of the platform adds to the forces of the waves. However, in the z-direction, the 96 transducer has the largest amplification factors for setup 3 in several frequency intervals. If the waves are propagating perfectly perpendicular to the z-direction, there is no reason why one should be larger than the other. The differences must therefore be due to experimental errors.

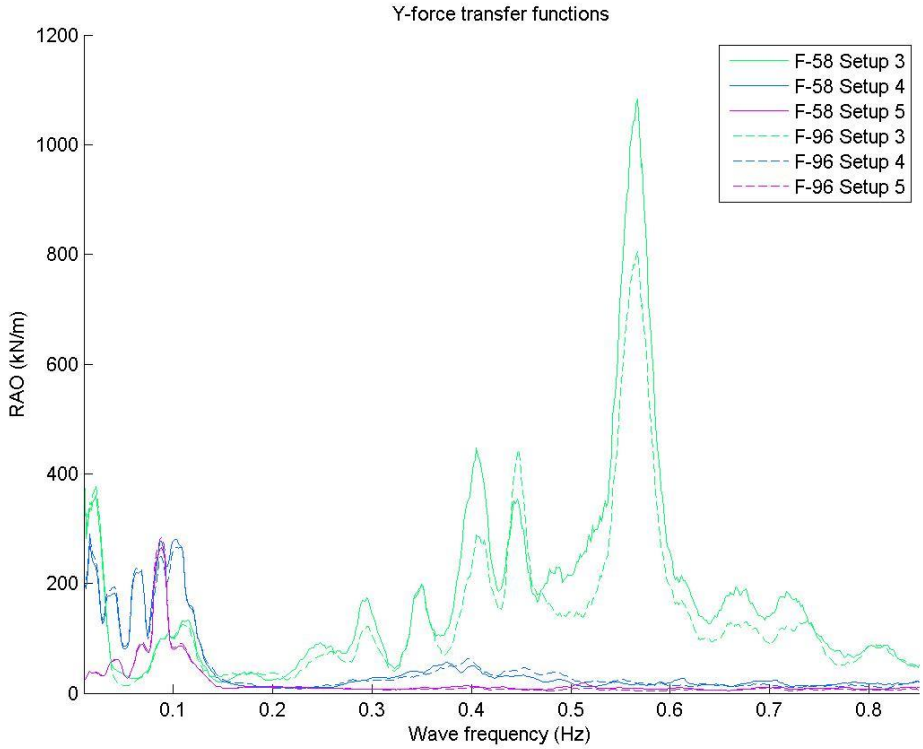

Figure 57: Y force transfer functions, irregular runs

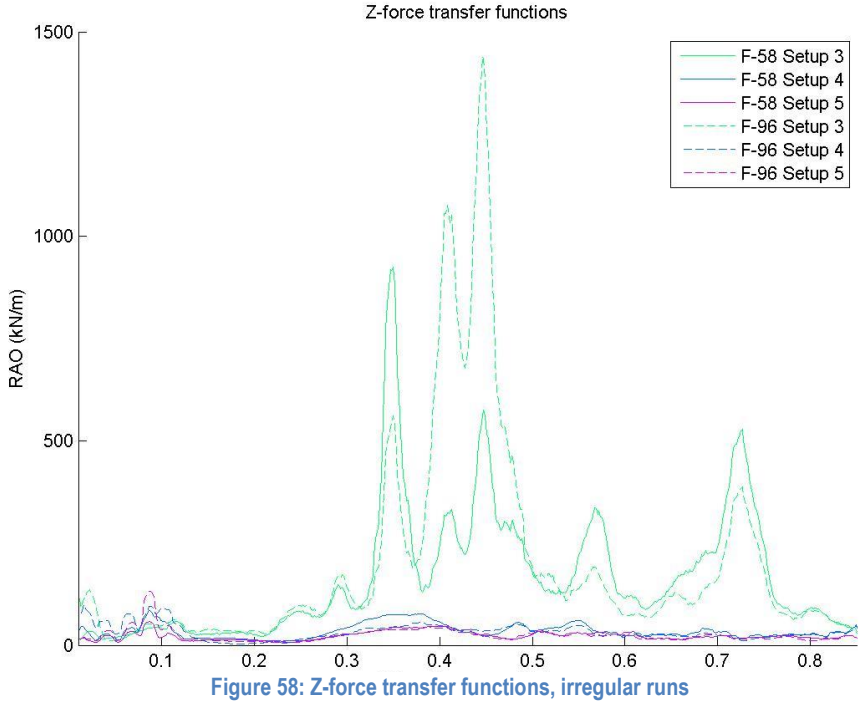

Figure 58: Z-force transfer functions, irregular runs

4.3 SPECIAL CASE – SETUP 6.

A few trial runs were carried out to investigate the effect of the flexible pipeline and a ship side on the platform. As has been mentioned previously, it was not possible to perform a model test including all these elements, mainly because of modelling challenges and the limited size of the laboratory basin. In order to get some sense of the impact of adding these extra elements, a few trials runs were performed at the very end. There was only time for one irregular run, so the 315-degree condition was chosen, as the immediate results indicated that this was the most vulnerable configuration. This condition, with the same sea state as seen previously, comprises setup 6.

A simple tension system represented the pipeline. The transducers measured the tension before each run, the result of this is shown in table 29. The pipeline representation was applied such that it is positioned perpendicularly with respect to the ship side, the same position the pipeline would have.

Table 29: Tension from pipeline representation

Transducer no.	Force in z-direction (kN)
58	-14.1
96	-14.2

The same results are for the ordinary irregular runs is presented below, while the results in their entirety is attached in appendix B. Table 30 displays the absolute maximum values and the expected values of maximum values of the different channels for this special case, as well as for setup 4. The values for setup 4 are the same as shown previously but are reprinted for easier comparison.

Table 30: Statistical values, special case run

Channel	Setup 6	Setup 4
Surge (m)	0.12	0.15
Sway (m)	0.06	0.03
Heave (m)	0.27	0.22
Roll (deg)	2.27	2.81
Pitch (deg)	3.12	2.60
Yaw (deg)	0.40	0.30
Fx-58 (kN)	7.3	3.7
Fy-58 (kN)	52.5	21.6
Fz-58 (kN)	30.3	31.8
Fx-96 (kN)	8.3	3.4
Fy-96 (kN)	47.4	21.4
Fz-96 (kN)	24.3	22.1

The motions of the platform does not seem to be influenced much by the added tension. The motion in surge and roll is slightly smaller in setup 6 than in setup 4, but the rest of the degrees of freedom are actually larger. One would expect that the pipeline provides an element of station keeping, damping the motions, but the results indicate that this is not the case. Another interesting feature is that the force in the z-direction does not decrease by the expected -14 kN provided by the “pipeline”, but actually increases by 1.5 kN for the 58 transducer. Furthermore, forces in both x and y directions increases, with more than a doubling of the magnitude in y-direction.

The transfer functions for roll and pitch motion is shown in figure 59. The transfer functions confirm what

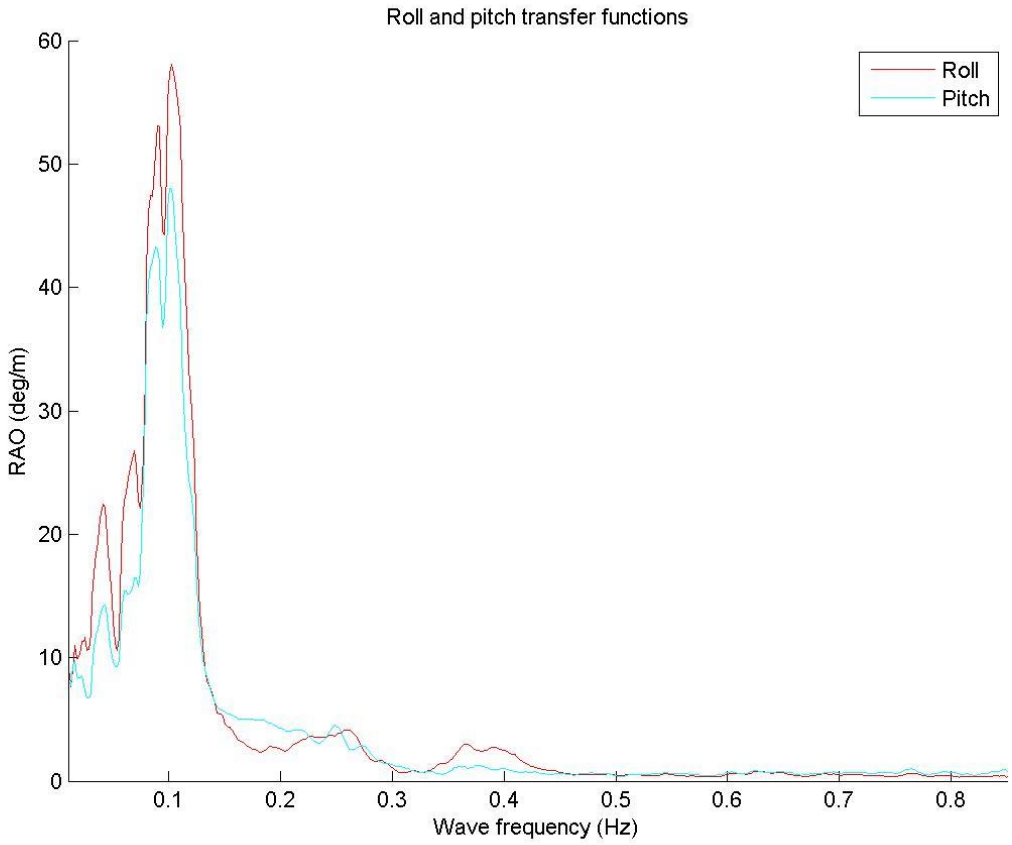

Figure 59: Roll and pitch transfer functions, setup 6

was seen in the other irregular runs, where the response amplitude operators are relatively small in the wave frequency range. The peaks in the relevant frequency range peak at about 5 deg/m. There is also a small peak around 0.36 Hz, especially in roll, that indicates and Eigen frequency.

One physical explanation of why the motions are larger for setup 6, is that the tension pulls on the platform so that its angle with the connection system is more favourable for movement. However, this should show up as smaller x-forces, which is not the case.

A possible cause for this unexpected behaviour is that the tension is not sufficiently large to properly represent the pipeline. This explains why the motions are not smaller for setup 6 than for setup 4, but it does not explain why the motions and forces are, in fact, larger. As the post processing, including the filtering, is identical for the two setups, the problem cannot lie there.

4.4 DECAY TESTS

The results from the decay tests are summarized in table 31. The time series for coupled heave motion in the decay test is shown in figure 60. The rest of the decay test time series are attached in appendix C.

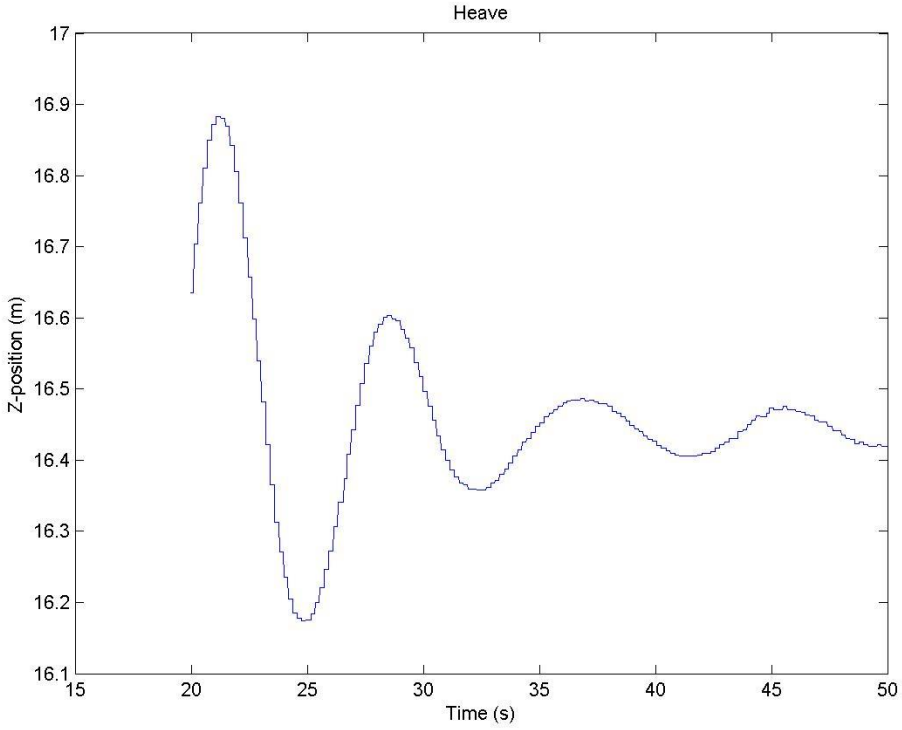

Figure 60: Coupled heave decay test

Table 31: Decay tests

Condition	Equivalent damping (kNs/m)	Added mass (t)	Damped Eigen period (s)	Undamped Eigen period (s)
Uncoupled Heave	17.3	49.4	7.55	8.08
Uncoupled pitch	225.2	1749.2	10.07	10.65
Uncoupled roll	197.6	1660.8	9.88	10.39
Coupled heave	23.6	49.6	7.36	8.09
Coupled pitch	1056.8	2148.2	8.13	8.28
Coupled roll	627.2	1773.8	9.00	10.73

For motion in heave, it is evident that the coupling of the platform and ship does not affect that platform's sea keeping abilities very much. Both damped Eigen period and undamped Eigen period are almost the same for the two conditions. The damping is, however, different, with an increase of almost 40% in the coupled condition compared to the independent condition. This due to the friction in the wagon/track system. In addition, the restraint provided in roll by the connection system may also help dampen the system in heave.

The added mass is also almost exactly the same for the two conditions, with a difference of only 0.2 t. As there is nothing in the connection system that could contribute to the added mass in heave, this difference must be a result of experimental errors.

The pitch Eigen periods are quite different in coupled and uncoupled, with a reduction of about 24-28% when the coupling is added to the system. This means that the connection system provides some kind of restraint that limits the pitch response, reducing the Eigen period. Considering the equation for the undamped period (see equation (51)), we may expect the undamped Eigen period to decrease when the relative damping decreases. This is not in coherence with the damping, which increases from 225.2 kNs/m in uncoupled to 1056.8 kNs/m in coupled condition. In an attempt to investigate this discrepancy, an alternative calculation on the damping was performed, omitting the two first cycles of the coupled pitch decay instead of just the first cycle, as the two first responses were large, before they decreased to very small (which is coherent with the values in table 31). This alternative calculation resulted in an equivalent damping of 54.7 kNs/m, which is a value that better suits the theory. At the same time, the damping should be larger when the connection system is introduced, because of the imperfections in the joint and wagon/track, which are not frictionless.

The added mass increases significantly from 1749.2 t in independent condition, to 2148.2 t in coupled condition. As added mass is mainly dependent on the geometry of the vehicle and not its restraint, the added mass should be similar. However, as the added mass is now calculated from the experiment (from the calculated spring stiffness and Eigen period), it is influenced by the measured values. The increase in added mass must therefore be accredited to the reduction in natural period.

It should also be noted that the calculation of the coupled pitch values has many possible errors and uncertainties. As is evident from the graph from which the calculations are made, it was very difficult to excite the platform in only pitch (and not heave/roll) and the measurements are uneven. There are also too few cycles to use in calculations, with 3-4 at best. The coupled pitch results can therefore not be considered very reliable.

The roll decay tests showed a slight increase in both damped and undamped natural period. The damped Eigen period increased by 0.12 seconds, whereas the undamped natural period increased by 0.34 seconds. This is similar to what was seen in pitch and heave, with a higher undamped than undamped natural period (obvious with respect to equation (51)). In addition, the damped Eigen period decreases while the undamped Eigen period increases in the transition from uncoupled to coupled condition, again as expected with respect to the relationship given in the aforementioned equation. The damping in roll increases by more than a threefold, which is evident from the graphs as well, where the response dies out quickly. The added mass differs by about 110 t, with the coupled condition having the largest added mass of the two. As with pitch, the calculations of the coupled roll values are subject to large uncertainties.

5 UNCERTAINTIES AND ERRORS

As for any model experiment, this model test is subject to different errors and uncertainties. The following paragraphs will cover the main contributions to errors in the results. Because of time limitations, we did not have the opportunity to run one condition many enough times to perform a proper statistical analysis of the results, estimating a confidence interval as well as precision and bias error. This would, however, require at least 10 (ideally 20) repetitions of just one run, and we did not this spare time. Therefore, a quantitative explanation of possible error sources will be given instead.

Model test errors can, roughly speaking, be divided into two main categories: systematic (bias) and random (precision) error. Systematic error are errors that are constant for all of the measurements. A simple example is a wrongly (or un-) calibrated wave probe. This will give the same error on all measurements. Precision errors are errors that are specific for each measurement, and has an element of randomness. Some or the precision might be due to statistical scatter, as is only expected when measuring values that have an aleatory nature. Random errors may also be unintended actions that affect the measurements. We noticed during the experiment, where if a person walked on the wagon in the laboratory while the strain transducers where recording, this would show up as noise.

5.1 SCALING ERRORS

As described in section 3.1, the chosen method of scaling influences the precision of the final results. One must choose what type of scaling to use, depending on what kind of forces one expects to govern in the experiment. In this experiment, Froude scaling was applied, ensuring similarity between inertia and gravity forces. The alternative, Reynolds scaling, would imply that the viscous forces were scaled correctly. As the parameters in this model test is Froude scaled, viscous effects are not modelled correctly. For correct viscous modelling, we would have: $Re_{full} = Re_{model}$. Instead, we have: $Re_{full} = Re_{model} * \lambda^{\frac{3}{2}} = Re_{model} * 58.1$. This is, in other words, a major source of error in dealing with wake distribution and drag forces. However, these phenomena are not the ones studied in this model test (except for perhaps the drag contribution to damping in the decay test), and that is why it is tolerated.

5.2 STRUCTURAL ERRORS

The model in itself is also a source of errors, in different ways. Firstly, some simplifications of the platform geometry were necessary to be able to create the model. Only the main particulars of the structure is included, and bellmouth/bend stiffener, and any other equipment on the deck is omitted. Another source of error is that the model might not be one hundred percent according to specification. The platform geometry is fairly simple and could be easily replicated, although the materials used are

different. This does not matter for the motions and sea keeping abilities, assuming that the centre of gravity and metacentric height are correct, but may influence how the forces travel through the platform and impacts the ship side.

Furthermore, the connection system is constructed in a completely different way than the real one, which uses vacuum pads. The friction in the wagon/track system and the ball joint has been mentioned already. The connection should be frictionless, and in addition, the geometry is not represented accurately in the test. For example, the vacuum pads will have a certain spatial extent, whereas the connection joints are very small by comparison. The joint in the model test was about 1 cm wide, which translates to 15 cm in full size whereas the vacuum pads are 2 m x 0.75 m. There are also in reality four vacuum pads, two at each side, as opposed to the two joints used in the model. The force distribution across the cross-section of the pads will be different than for the model connection system. However, as we are searching for the total connection force, our system must be deemed satisfying, although one should keep this difference in mind when assessing the results.

5.3 ENVIRONMENTAL MODELLING

Another source of errors is the modelling of the environment, in this case the waves and the sea. The waves are specified using period and wave height as parameters. The relationship between the wave height and period assumes deep water conditions, which means that the sea bottom does not “feel” the disturbance of the wave particles on the surface, in other words, the particle motion dies out before reaching sea bottom. We must therefore assume that this happens in the MC lab as well.

In the regular wave tests, the waves should be, as the name implies, regular. They are, however not all of the same height, due to random errors. Furthermore, when examining the waves during the tests, we did notice that the waves seemed to be asymmetrical for the largest wave heights (steeper on the right side than on the left), and that the wave troughs seemed more flat while the crests were more peaked. The regular waves, are, however not as regular as they should be.

Tank wall reflections is another important issue. The MC laboratory basin is 4.65 m wide, which means that diffracted and/or radiated waves from the platform will reach the tank walls and be reflected back, possibly interfering with the incoming waves and even the platform itself. For a rough worst-case estimate, consider the smallest wave period 0.73 s. This gives a group velocity of $V_g = \frac{gT}{4\pi} = 0.7$ m/s. With the platform in the middle of the basin, the time for a wave to reflect off the platform, and reach the tank wall is 3.32 s, or just above 4.5 wave periods. As 10 consecutive wave periods are needed to calculate transfer functions, and the first wave periods must be discarded to avoid transient effects in the transfer functions, it is obvious that reflected waves will influence the results.

In the irregular tests, the measured wave spectrum is used for calculations, and as the wave probe measure the wave heights and periods at the platform, this is not a source of error except for measuring errors by the wave probe as mentioned previously.

5.4 MEASUREMENTS AND CALCULATIONS

All measurements bring in some sort of uncertainty, because of the limited accuracy of the instrumentation devices. We used three different recording devices, so the accuracies of these three devices decide the accuracy of the results. The errors, as reported by MARINTEK are shown in table 32

Table 32: Accuracy of instrumentation

Device	Error (in model scale)
Oqus camera – translation	+-1.3 mm
Oqus camera - rotation	+- 0.1 degrees
Strain transducer	3%

To limit bias, all channels were zeroed out before each run. This improves the precision of the measurements. In addition comes the measurement accuracies shown in the table. The limitations of the instrumentation should be taken into account when considering the measurements. A 3 % error in the strain transducer means that a force measurement of 50 kN could lie somewhere between and 48.5 and 51.5 kN. Similarly, a heave motion recorded to be 0.5 m (full scale) may in reality lie within the range 0.48 to 0.52 m. This comes, of course, in addition to the previously mentioned modelling errors. It is clear that the accuracy of these experiments is not good enough to predict exact values. However, most of the errors are systematic errors, and so the results can give decent indicators of general trends, as well as the relative response of the platform in different setups.

PART 4: COMPARISON

1 REGULAR WAVES – VALIDATE INPUT RAO

One of the objectives of the model test is to validate the response amplitude operators that were calculated in WAMIT by Connect LNG. The main results are presented again on these pages, together with the calculated transfer functions for the two uncoupled conditions, 0 and 90 degrees wave heading.

1.1 WAVE HEADING 0 DEGREES

The calculated transfer functions from WAMIT are displayed in figure 61 , and the calculated transfer functions are shown in figure 62.

Surge RAO

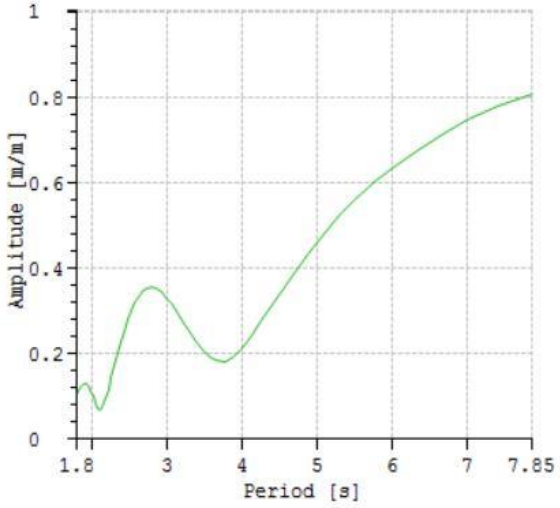

Sway RAO

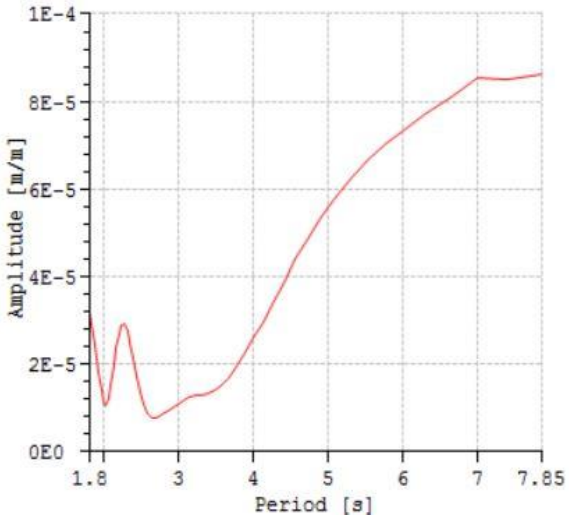

Heave RAO

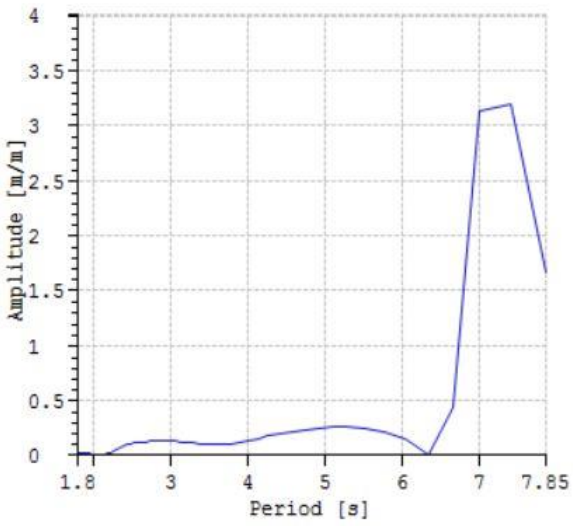

Roll RAO

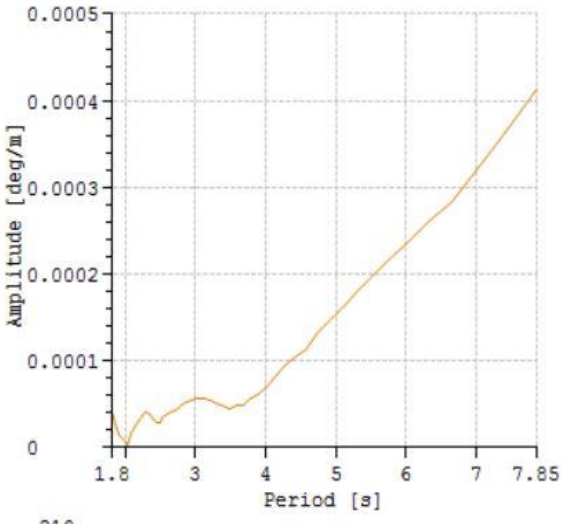

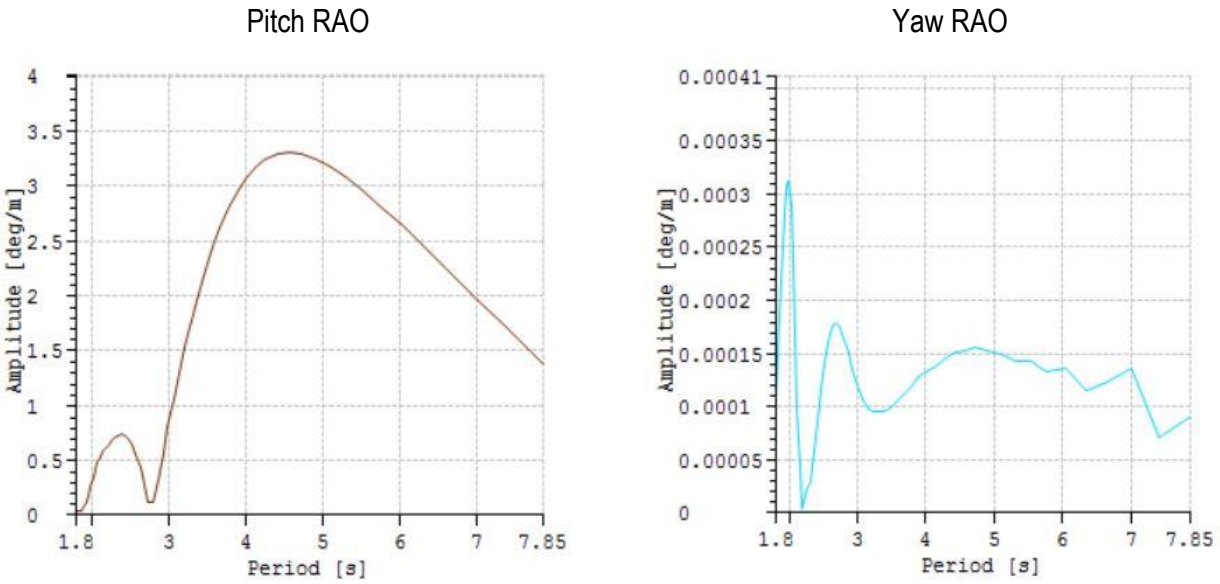

Figure 61: WAMIT transfer functions

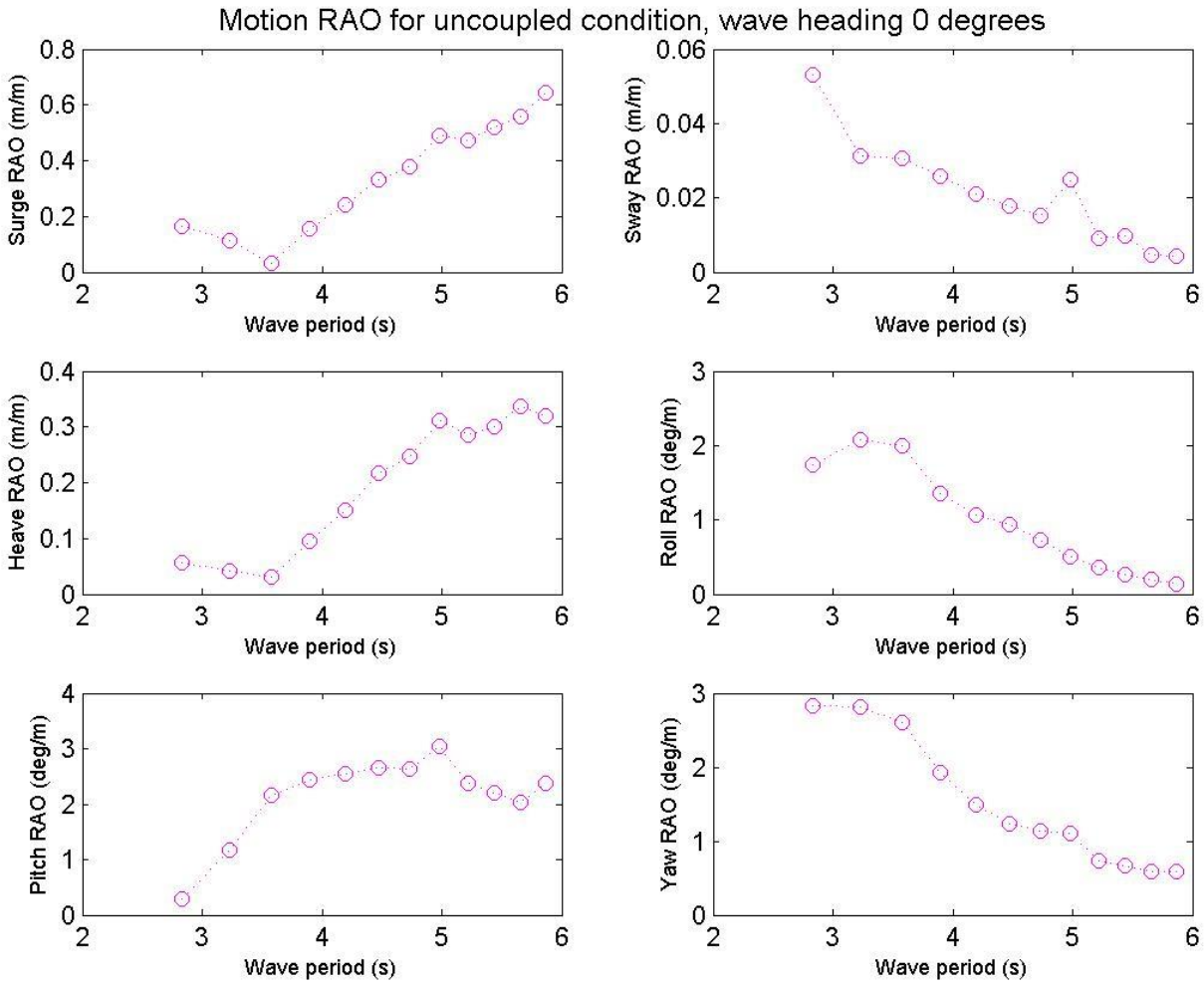

Figure 62: Motion transfer functions, model test

Comparing each transfer function from WAMIT with the corresponding calculated transfer function from the model test, it is evident that some are quite good, while others are not so good. In surge, the general trends are the same, as are the magnitudes. However, the cancellation that occurs at a wave period of 3.5 s in the model test transfer function is only a tip in the WAMIT transfer function, and it occurs at a wave period of 4 seconds. In sway, the general trend is completely opposite in the two transfer functions. However, the values are also not only wrong but also very small in WAMIT compared to the model test results. The same seems to happen for the roll and yaw transfer functions, where both trend and magnitudes are completely off.

The heave transfer functions are quite good, both in terms of general trends and in terms of magnitudes. It would be useful to have tested larger wave periods as well, but as has been mentioned before, time was limited. The pitch transfer function is also reasonable. An effect that is not clearly visible from the model test is the cancellation that occurs at about T=2.8 s, although the declining RAO of the model test implies that this effect is captured also in the model test.

From the transfer function plots it can be concluded that the surge, pitch and heave transfer functions are reasonably good, as the model test results do not contradict the WAMIT results. In sway, roll and yaw, there is obviously something wrong. The sources of errors in the model test, which have been discussed previously, are the most likely source of the discrepancy. Recall that the wave spectrum from wave heading 0 degrees (setup 2 in the irregular tests) was not correct, and therefore this comparison does not give reasonable evidence to reject the WAMIT results, although they cannot confirm them either.

1.2 WAVE HEADING 90 DEGREES

The second wave heading to compare is 90 degrees. The results from WAMIT are displayed in figure 63, and the corresponding transfer functions found in the model test are shown in figure 64. The waves are now propagating along the y-axis, resulting in significant sway motions and small surge motions. This is not what is shown in the model test results. Comparing the transfer functions with those from the first wave heading (0 degrees), it is clear that the amplitudes are of the same order of magnitudes. Next, studying the videos recorded during the model tests reveals that the platform seems to be moving in a circular fashion in the horizontal plane, which explains both why surge and sway motions are so similar in magnitude (like the calculated values from WAMIT, one should be large while the other is small when the waves are propagating exactly along the x/y-axis) and so different from the calculated values in WAMIT.

The heave transfer functions are more similar, and seems to be correct. Again the largest few wave periods are missing from the model test results. The roll transfer function from WAMIT is very similar to the pitch transfer function in the 0 degree wave heading. This is exactly as expected when the wave heading is changed by 90 degrees. A very similar change happens with the model test results. In other words, the trends are the same in both calculation methods. However, while the roll transfer functions are very similar in WAMIT and the model test, the pitch transfer functions are very different both in amplitude and in trends. The yaw transfer function show a similar trend to the one in WAMIT, but the amplitudes are not correct. This is, however, expected from observing the videos mentioned previously in this section.

It is difficult to draw a simple conclusion from these comparisons. Some of the transfer functions support the WAMIT calculations, like the heave transfer functions, which are very similar, providing physical evidence to the numerical calculations. At the same time, there are cases like the surge and sway transfer functions that are not in coherence with the WAMIT calculations at all. Based on the knowledge that WAMIT is a recognized software for transfer function calculations, in addition to the known uncertainties in the laboratory and the observed wave spectra, there is no reason to reject the calculations from WAMIT.

Surge RAO

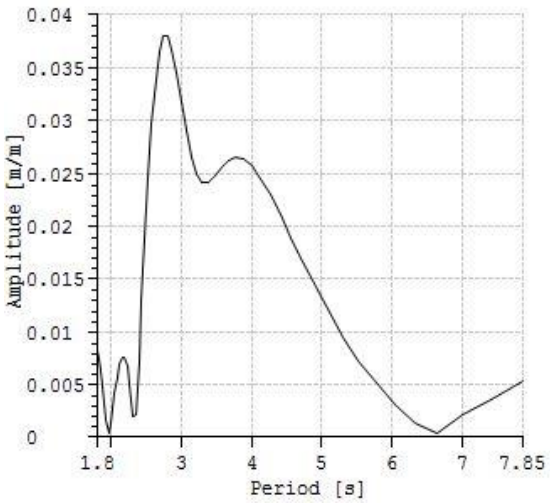

Sway RAO

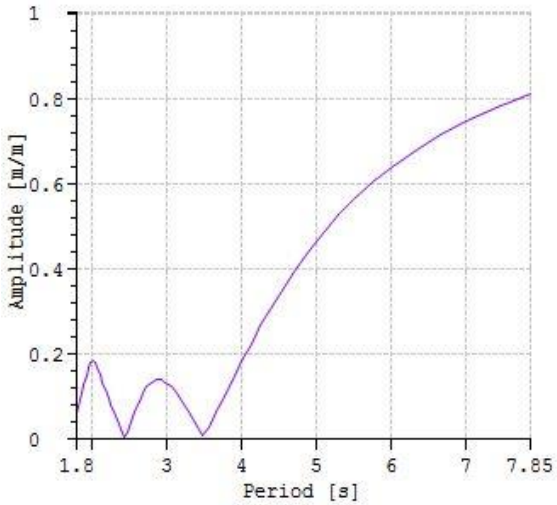

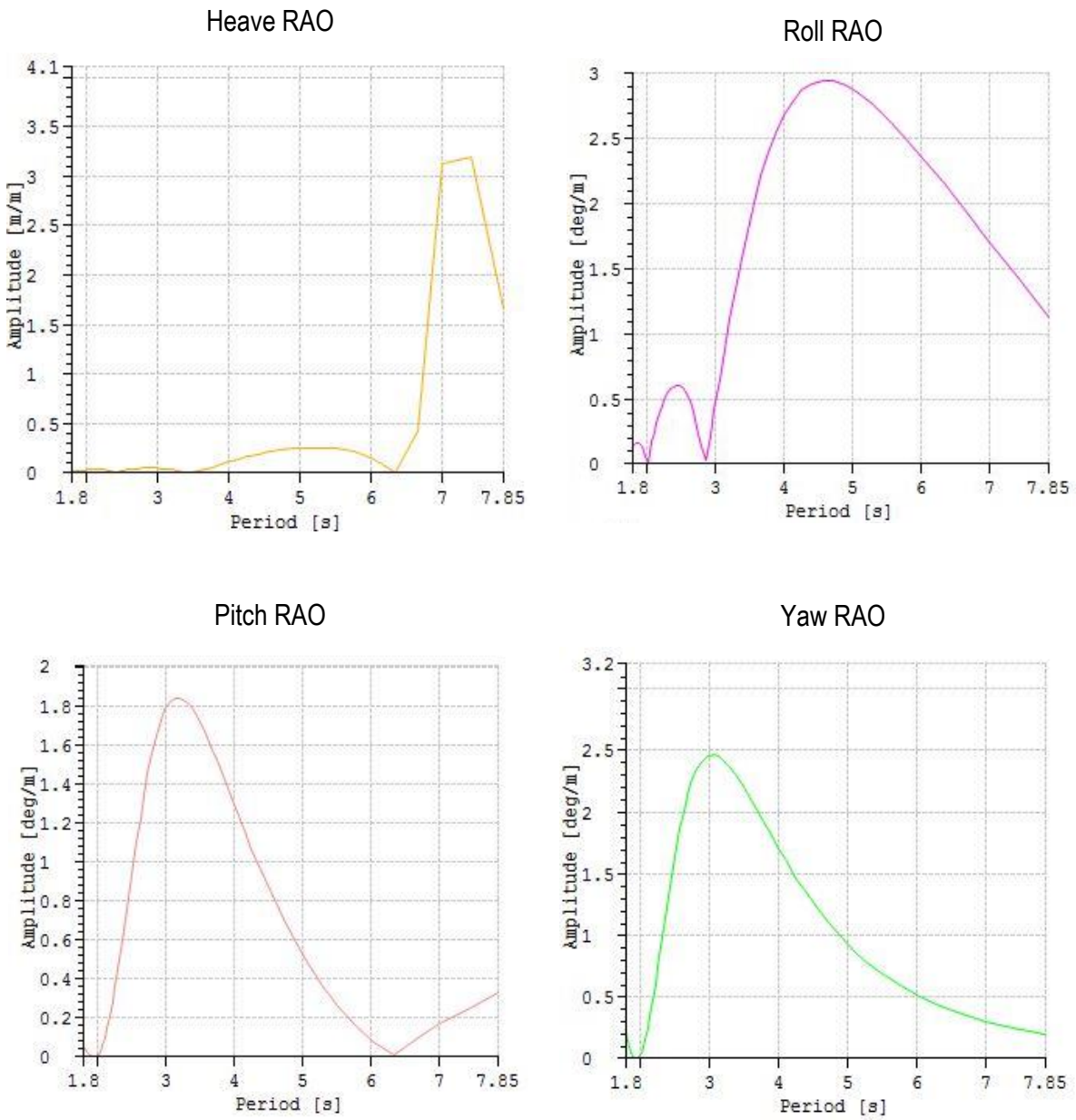

Figure 63: WAMIT transfer functions, wave heading 90 degrees

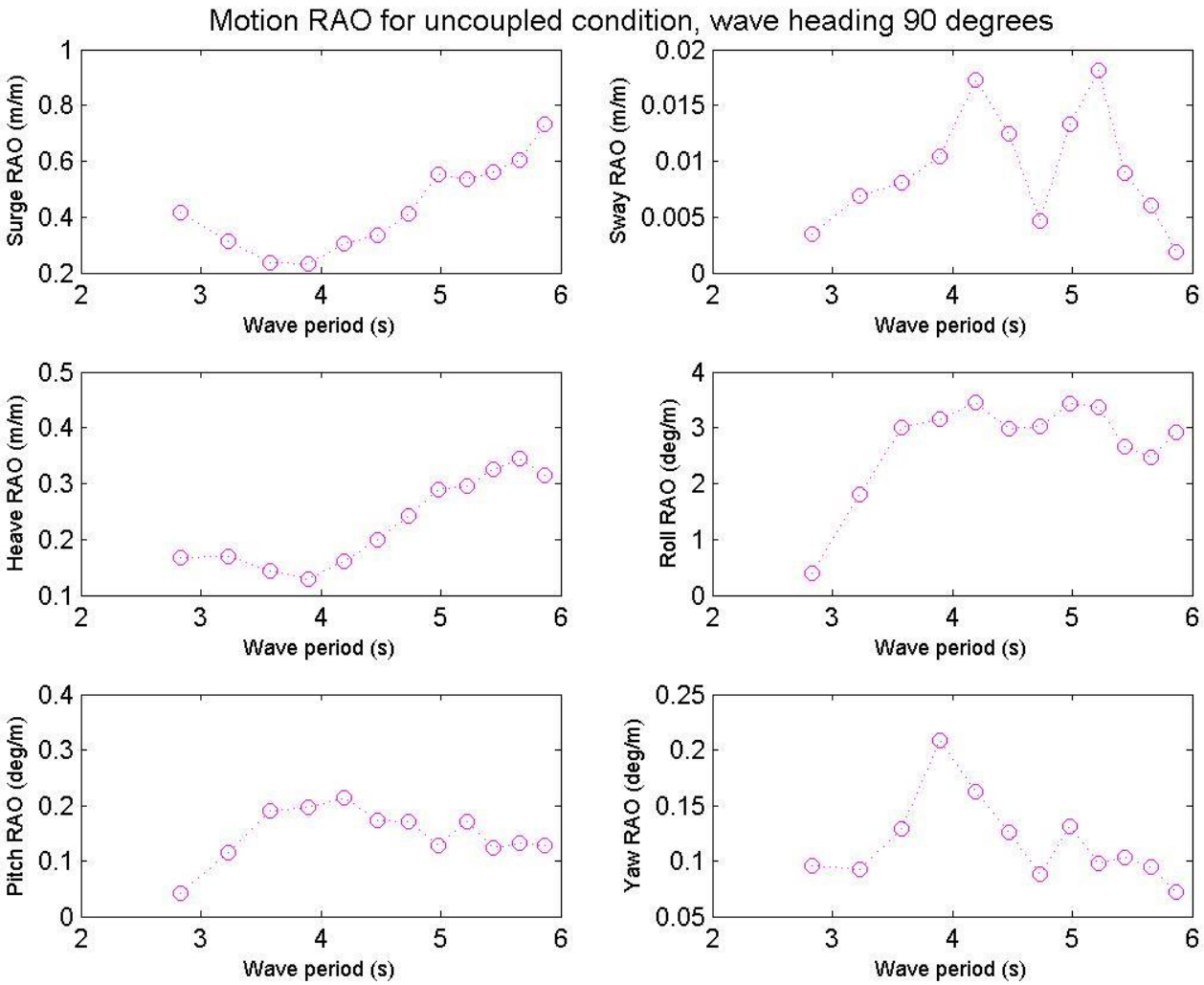

Figure 64: Motion transfer functions from model test, wave heading 90 degrees

2 DECAY TESTS

The decay tests were intended to validate the calculated added mass and damping. However, executing the decay tests in an efficient and accurate way proved very difficult, and the result was only 4-5 data points for each run. Studying the figures of equivalent damping plotted versus the mean amplitude between two peaks, it is clear that most of the tests are simply not good enough to compare with numerical values.

The best result with respected to goodness of fit, was the uncoupled heave condition, whose plot is displayed in figure 65. Its R^2 value is 0.86. The measured and calculated values of added mass and damping is displayed in table 33. As is evident from both the figure and the table, the decay tests were simply not accurate enough to produce satisfactory results.

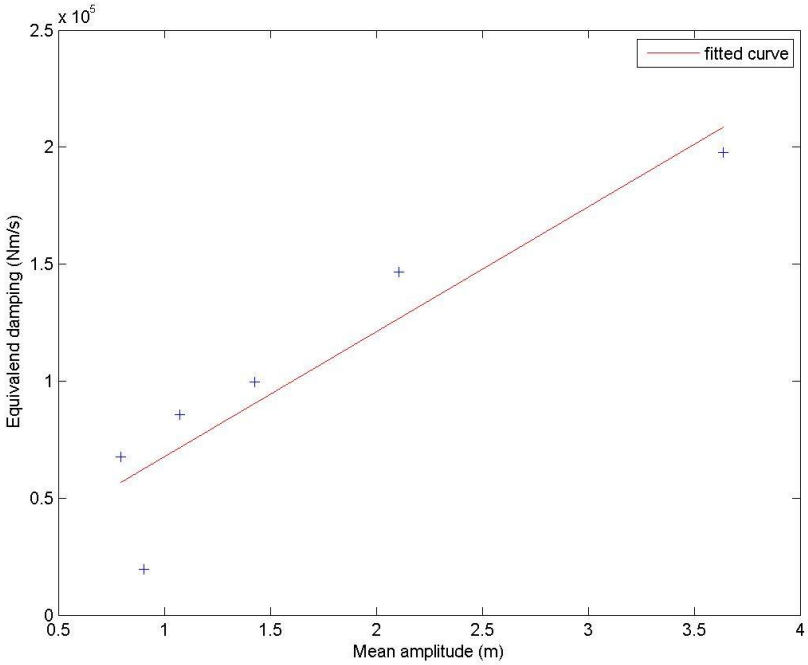

Figure 65: Fitted curve, decay test uncoupled heave

Table 33: Comparison of calculated and measured damping and added mass

Mode	Equivalent damping (kNm/s)		Added mass (t)	
	WAMIT	Model test	WAMIT	Model test
Uncoupled heave	0.06	17.3	30	49.4

This is disappointing, but not surprising as it was very difficult to excite the platform properly in only one degree of freedom, in addition to the fact that the damping is so large that there are very few oscillations to use. The combination of these two challenges makes the comparison of the numerically calculated and the measured values pointless.

3 IRREGULAR RUNS

3.1 UNCOUPLED CONDITION

For the uncoupled conditions, the 0 degree wave headings had the largest motions. The maximum values for the two methods for this run are displayed in table 34. The difference in results are significant. For two motions, heave and pitch, SIMA predicts larger displacements than the model test does. For the remaining degrees of freedom, the model test provides the most conservative values. How much they deviate from the SIMA estimates vary. For example, estimates for roll motion deviate by only 16%, while the surge values in the model test are as much as 4.6 times as large as the SIMA values. Judging from these values, the most severe degree of freedom is pitch, which is true for both methods. The other motions are significant, but not severe.

Table 34: Comparison of max.values for wave heading 0 degrees, uncoupled condition

	SIMA	Model test
Surge (m)	0.187	0.858
Sway (m)	0.072	0.119
Heave (m)	2.737	0.332
Roll (deg)	1.095	1.268
Pitch (deg)	5.216	3.252
Yaw (deg)	0.996	2.919

3.2 COUPLED CONDITION

The most severe of the coupled conditions was the case with a 90 degree wave heading. A comparison of the maximum recorded values for this condition in SIMA and in the model test is displayed in table 35. All directions are translated to SIMA notation so that they can be compared directly. The force contributions from the two transducers in the model test has been added together for simpler comparison with SIMA values. The extreme values for motions from both methods are likely and reasonable, but they are not the same in the two cases. As for the uncoupled condition, there is no clear pattern of how much more conservative one method is compared to the other, neither is there one method that is constantly more conservative than the other. As both methods provide results that are reasonable, it is difficult to tell which is more reliable.

All of the force components are much larger in SIMA than in the model test. The positive aspect is that there is a coherence in the relative size of the force components, with the y-force being by far the largest force and x- and z- force being of similar magnitude.

Table 35: Comparison of max. values for wave heading 90 degrees, coupled condition

	SIMA	Model test
X-force (kN)	201.3	57.7
Y-force (kN)	1042.7	176.7
Z-force (kN)	248.0	56.0
Surge (m)	0.230	0.175
Sway (m)	0.591	0.022
Heave (m)	0.196	0.301
Roll (deg)	5.124	4.983
Pitch (deg)	0.153	0.502
Yaw (deg)	4.006	0.308

3.3 FULL MODEL

The special case test run at the end of the model tests were intended to model the full model, including both pipeline, platform and ship side. This run was also simulated in SIMA, with a wave heading of 315 degrees. A comparison of the results is displayed in table 36.

Table 36: Full model comparison, SIMA vs. model test.

	SIMA	Model test
X-force (kN)	577.9	15.6
Y-force (kN)	383.4	99.9
Z-force (kN)	470.6	54.6
Surge (m)	0.388	0.116
Sway (m)	0.123	0.057
Heave (m)	0.406	0.274
Roll (deg)	3.778	2.271
Pitch (deg)	1.001	3.117
Yaw (deg)	3.082	0.397

Recall from section 4.3 where the model test results from the model with tension applied was compared with the coupled system without the tension that the addition of the pipeline did not influence the motions of the platform significantly. The motions and forces were all of the same order of magnitude. Therefore, it is not unexpected that the values differ. The motions seems to be within the same order of magnitude and may be justified as statistical randomness, however, the forces are completely different.

In both SIMA and in the model tests there are different limitations and sources of errors, which all have been discussed previously. One important source of the difference, in addition to those already mentioned, is that it was not possible to create a connection model in SIMA that represented the system used in the model test. It is therefore impossible to get exactly the same results.

3.4 WORST CASE SCENARIO FOR COMPLETE SYSTEM

In order to get a sense of a worst case scenario for the UBS system, the results from all runs of the full model are summarised in table 37. The values are all maximum values. The forces in the connection system are of the same order of magnitude for all wave directions in the computer simulations, with the 315 case being slightly more severe than the other two. The model test forces are, however, a lot smaller. The difference here is even larger than what was seen in the coupled condition. As for the motions, there are not a lot of large differences within the SIMA calculations, however, most are larger in SIMA than in the model test, with the exception being pitch motions.

Table 37: Summary of runs in SIMA, setup 3

	SIMA			Model test,
Channel/Wave heading	0 degrees	315 degrees	90 degrees	315 degrees
X-force (kN)	564.8	577.9	526.6	15.6
Y-force (kN)	347.4	383.4	364.9	99.9
Z-force (kN)	456.6	470.6	456.1	54.6
Surge (m)	0.386	0.388	0.195	0.116
Sway (m)	0.107	0.123	0.172	0.057
Heave (m)	0.267	0.406	0.548	0.274
Roll (deg)	2.524	3.778	4.540	2.271
Pitch (deg)	1.062	1.001	1.097	3.117
Yaw (deg)	3.280	3.082	1.455	0.397

To draw a conclusion regarding a worst case scenario, it is recommended to choose SIMA, as it proves more conservative than the model test in all channels except pitch. The forces are more severe in the 315 degree case, as are surge and sway. The conclusion is therefore that the 315 degree case is the most sensitive configuration for the UBS system, although the platform has such good sea keeping capabilities that this case is not considerably more risky than others.

PART 5: CONCLUSION

1 SUMMARY

This thesis has given an outline of the Universal Buoyancy System for LNG offloading for small scale ships. The system is designed for use in sheltered areas, with a sea depth of up to 10 meters. The design sea state is described by the JONSWAP spectrum with parameters H_s=1.2 m, T_P=5 s and peak parameter γ=1.65.

The behaviour of the system in this design sea state has been investigated by computer simulations in SIMA as well as by model tests in the Marine Cybernetics laboratory. In SIMA, three different configurations was tested; the platform alone, the platform connected to the ship side, and the complete system with pipeline, ship and platform. In the model test, input parameters to SIMA were validated by decay tests, and a model of the platform was tested in the same sea state in coupled and uncoupled condition. A trial case to include the pipeline in the model test was also attempted.

The results of the simulations in SIMA are summarized in table 38, where the maximum recorded value from each configuration n is shown. The largest value for each direction is highlighted. Although it is not unambiguously clear, there is a trend that the third configuration, the complete system, has the largest recordings for each of the wave headings. This confirms that the pipeline adds a net excitation to the system.

Table 38: Summary of SIMA simulations

	Wave heading 0 degrees			Wave heading 315 degrees		Wave heading 90 degrees		
	Platform	Platform and ship	Complete system	Platform and ship	Complete system	Platform	Platform and ship	Complete system
Surge (m)	0.187	0.077	**0.386**	0.150	**0.388**	**0.598**	0.230	0.195
Sway (m)	0.072	**0.198**	0.107	**0.394**	0.123	0.059	**0.591**	0.172
Heave (m)	**2.737**	0.241	0.267	0.233	**0.406**	0.002	0.196	**0.548**
Roll (deg)	1.095	1.730	**2.524**	3.435	**3.778**	2.808	**5.124**	4.540
Pitch (deg)	**5.216**	0.406	1.062	0.254	**1.001**	0.002	0.153	**1.097**
Yaw (deg)	0.996	**3.894**	3.280	3.950	3.082	0.000	**4.006**	1.455
X-force (kN)		209.4	**564.8**	214.7	**577.9**		201.3	**526.6**
Y-force (kN)		194.0	**347.4**	192.5	**383.4**		248.0	**364.9**
Z-force (kN)		**1428.9**	456.6	1211.2	470.6		**1042.7**	456.1

Moreover, the results show that a 315 degree wave heading is the most vulnerable direction for setup 3 both in terms of motions and forces. Note that the largest forces actually occur in setup 2, with a

maximum of 1418 kN in the Z-direction for wave heading 0 degrees and also 1211.2 kN in wave heading 315 degrees. Even though the motions are larger for setup 3 than for setup 2, the forces are actually smaller in the former.

In the model test, the transfer functions, added mass and damping values used in SIMA calculations were compared. The degree of compliance was varying; however, this may just as well be due to modelling errors as actual disagreement between the results from WAMIT and for model tests. The conclusion is therefore that while the model test cannot accurately confirm the WAMIT parameters, they do to some extent provide evidence for the results, and do not reject the values used in SIMA calculations.

Irregular runs were also performed in the model basin, to provide a basis for comparison with the SIMA simulations. A summary of the results is shown in table 39, where the largest motion for each direction is highlighted. The results show that the 0 degree wave heading is the worst case scenario considering all setups and wave directions, while for the coupled condition, 315 degrees is the most exposed case.

Table 39: Summary of model test results

	Wave heading 0 degrees		Wave heading 315 degrees	Wave heading 90 degrees	
	Setup 1	Setup 2	Setup 2	Setup 1	Setup 2
Surge (m)	**0.858**	0.201	0.209	**0.894**	0.175
Sway (m)	**0.119**	0.071	0.096	**0.085**	0.022
Heave (m)	**0.332**	0.247	0.247	**0.303**	0.301
Roll (deg)	1.268	**1.970**	4.823	3.485	**4.983**
Pitch (deg)	3.252	**5.412**	4.261	0.244	**0.502**
Yaw (deg)	**2.919**	0.372	0.335	**0.450**	0.308
X-force (kN)		11.1	7.1		6.0
Y-force (kN)		72.8	43.0		21.3
Z-force (kN)		55.4	53.9		39.6

A setup of the third configuration – the complete system – was also attempted to replicate in the model tests. A string with an applied tension of 14 kN was used to represent the pipeline. One only direction was tested, 315 degrees. The addition of this tension gave somewhat larger movements and forces.

Comparing the SIMA results with the model test results reveals some of the same tendencies as seen in the validation of SIMA parameters; that the results are not exactly the same (which they never will be, because of the inherent randomness of the problem), but most of the results are within the same order of magnitude. The test run with the tension applied confirmed the results from sima that the complete

system is more vulnerable to the sea than the platform and ship side alone, providing further evidence to the SIMA results.

2 RECOMMENDATIONS FOR FURTHER RESEARCH

The work with this thesis has revealed several areas that should be investigated further, which are summarised in the list below.

- Perform more model tests in a larger laboratory and shorter intervals between wave frequencies to confirm the transfer functions used in computer analysis.
- Model tests including a more complete system to further confirm SIMA analyses. The pipeline and the ship should be included in this test
- Due to the limitations of the laboratory, current effects were not included. Later research should include current, and different combinations or current and wave directions.
- The possibility of wind during operations should be considered, and if necessary, investigated in model tests and/or FEM analysis
- The motions seen in this thesis were all small. If further knowledge of the limit capacity of the platform and connection system is desired, more research is needed on this topic. Different limit states, such as ultimate limit state, fatigue limit state and accidental limit state should be researched.
- An investigation of other possible methods for modelling the connection system in SIMA, or alternatively a different FEM programme in order to validate the modelling of the connection system
- The focus in this thesis has been on the first order wave loads; second and higher order loads, especially mean drift and viscous forces, should be investigated.
- Include the bend stiffener necessary at the platform/pipeline connection in later analysis
- Research possible locations for use of the UBS system and establish a long-term joint probability density function to find long-term extreme responses

REFERENCES

[1] Kolwan, K. Narewski, M. *Latvian J. Chemistry.* Vol 4. 2012.

[2] Bech, Mogens. *North European LNG Infrastructure Project, Final Baseline Report*. Sweden, 2011.

[3] Jensen, Jacob. *LNG – towards a marine fuel*. Powerpoint presentation, Catalyst Strategy Consulting, Oslo. 2012.

[4] MARINTEK. *Riflex theory manual.* V4.0 Rev 0. Trondheim, 2012.

[5] MARINTEK. *SIMO theory manual.* V4.0 Rev 1. Trondheim, 2012.

[6] Faltinsen, Odd. *Sea loads on ships and offshore structures.* Cambridge: Cambridge University press, 1990.

[7] Magnusson, Stian. *Flexible riser for LNG offloading system*. Master thesis. NTNU, 2013.

[8] Langen, I. and R. Sigbjørnsson. *Dynamisk analyse av konstruksjoner*. Trondheim: Tapir, 1979.

[9] Achenbach, E. *J. Fluid Mech.* Vol 46, Part 2. 1971 Great Britain, 1971.

[10] Steen, Sverre. *Experimental Methods in Marine Hydrodynamics* Trondheim: Department of marine technology, 2012.

[11] Larsen, Carl Martin. *Drag forces in dynamic analysis.* Lecture note. Trondheim: Department of marine technology, 2005.

APPENDIX A: SIMA MODELLING RESULTS

Table A - 1: Statistical values SIMA run 1, platform only, wave heading 0 degrees

Channel/Motion	Surge	Sway	Heave	Roll	Pitch	Yaw
Moment m0:	0.00036	0.00013	0.303	0.013	0.747	0.046
Moment m1:	0.00003	0.00003	0.058	0.002	0.081	0.010
Moment m2:	0.00001	0.00001	0.012	0.001	0.015	0.003
Significant value:	0.076	0.045	2.201	0.456	3.458	0.856
Period T1:	11.037	4.595	5.200	5.333	9.260	4.456
Period T2:	7.905	4.486	5.099	4.417	7.018	4.265
Peak period:	64.243	28.477	16.428	64.243	57.105	16.428
Maximum value:	0.181	0.049	2.737	0.837	5.216	0.992
Minimum values	-0.187	-0.072	-2.397	-1.095	-5.110	-0.996
Standard deviation:	0.048	0.012	0.630	0.223	1.748	0.220
Expected value of largest maximum:	0.154	0.041	2.284	0.721	5.707	0.798
Most probably largest maximum:	0.153	0.041	2.270	0.715	5.660	0.793

Table A - 2: Statistical values SIMA run 2, platform only, wave heading 90 degrees

Channel/Motion	Surge	Sway	Heave	Roll	Pitch	Yaw
Moment m0:	0.01761	0.00019	0.00000	0.44248	0.00000	0.00000
Moment m1:	0.00353	0.00005	0.00000	0.09160	0.00000	0.00000
Moment m2:	0.00074	0.00001	0.00000	0.01982	0.00000	0.00000
Significant value:	0.53085	0.05523	0.00027	2.66077	0.00044	0.00006
Period T1:	4.984	3.971	6.537	4.831	11.963	3.251
Period T2:	4.890	3.839	5.866	4.725	9.459	2.973
Peak period:	16.428	16.085	70.084	16.428	55.922	16.428
Maximum value:	0.579	0.058	0.002	2.700	0.002	0.00007
Minimum values	-0.598	-0.059	-0.002	-2.808	-0.002	-0.00009
Standard deviation:	0.142	0.014	0.000	0.707	0.000	0.00002
Expected value of largest maximum:	0.516	0.051	0.001	2.561	0.001	0.00006
Most probably largest maximum:	0.513	0.051	0.001	2.546	0.001	0.00006

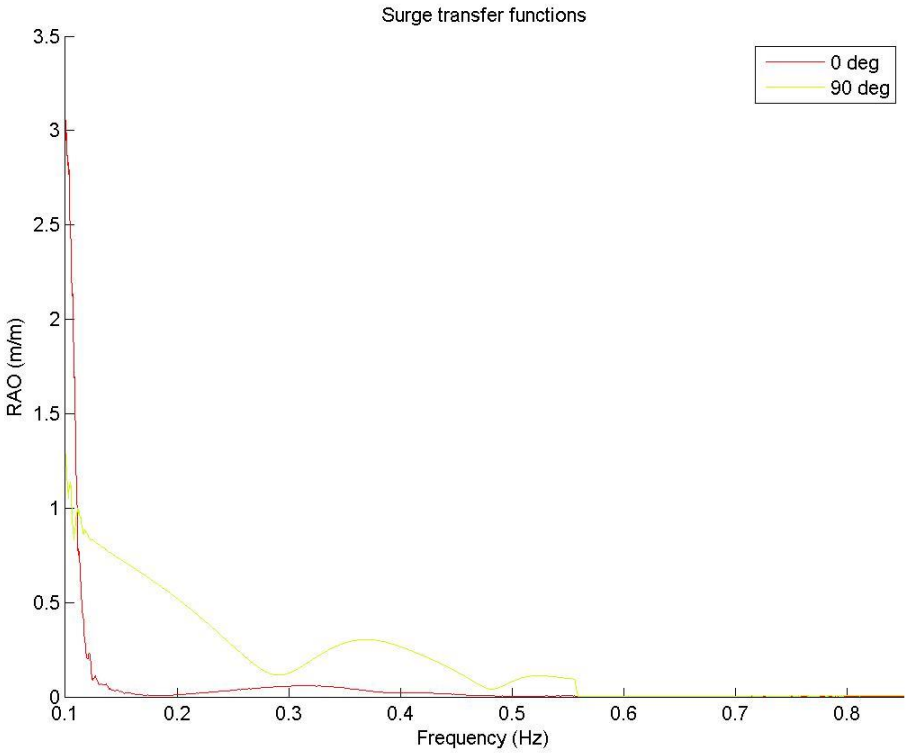

Figure A - 1: Surge transfer functions, SIMA runs 1 and 2: Uncoupled condition

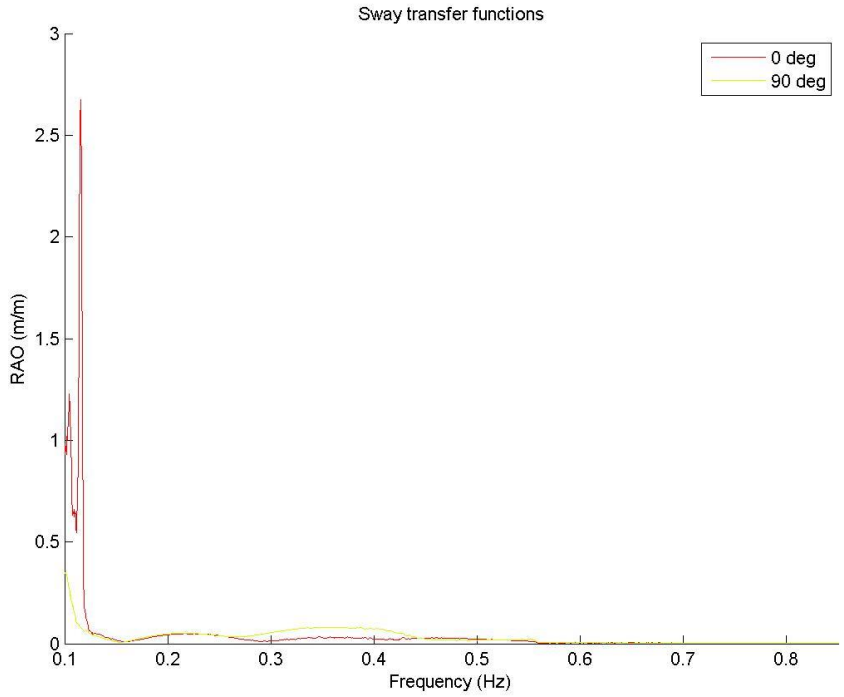

Figure A - 2: Sway transfer functions, SIMA runs 1 and 2: Uncoupled condition

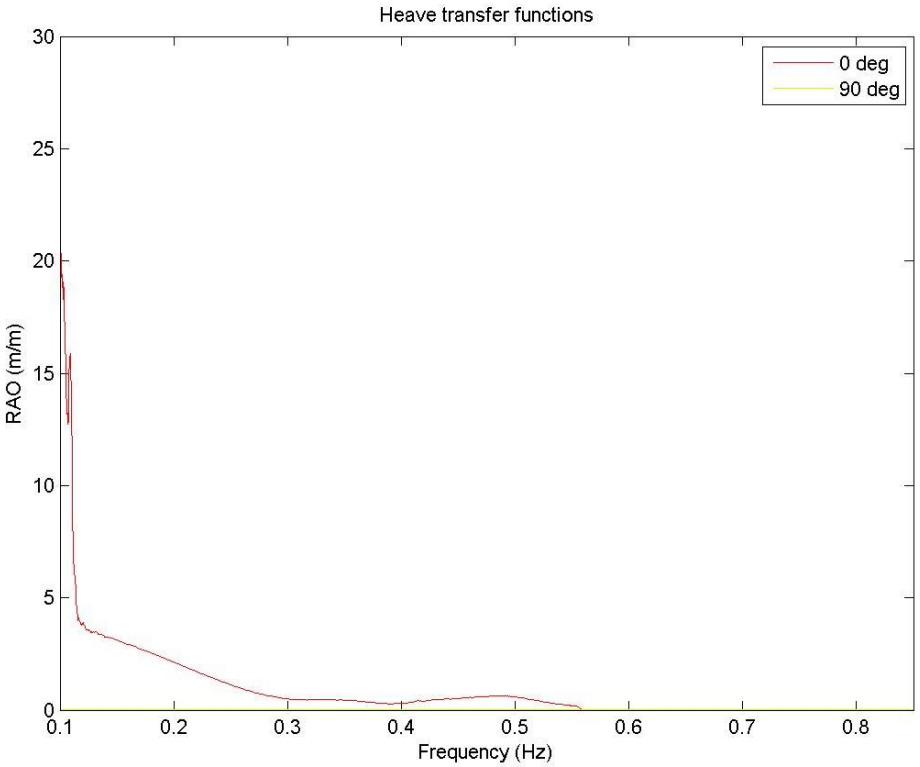

Figure A - 3: Heave transfer functions, SIMA runs 1 and 2: Uncoupled condition

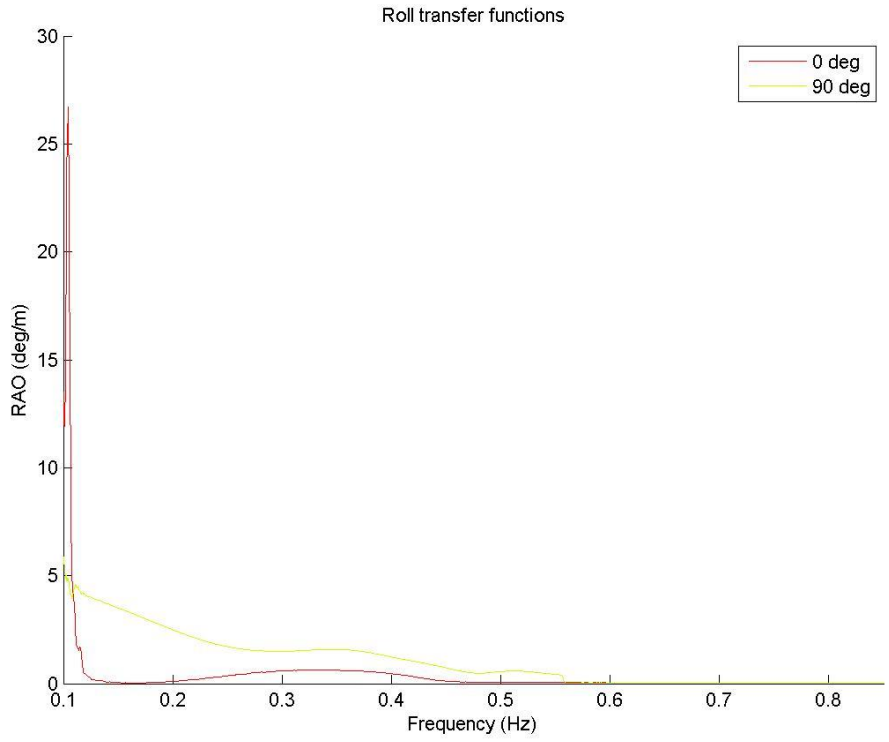

Figure A - 4: Roll transfer functions, SIMA runs 1 and 2: Uncoupled condition

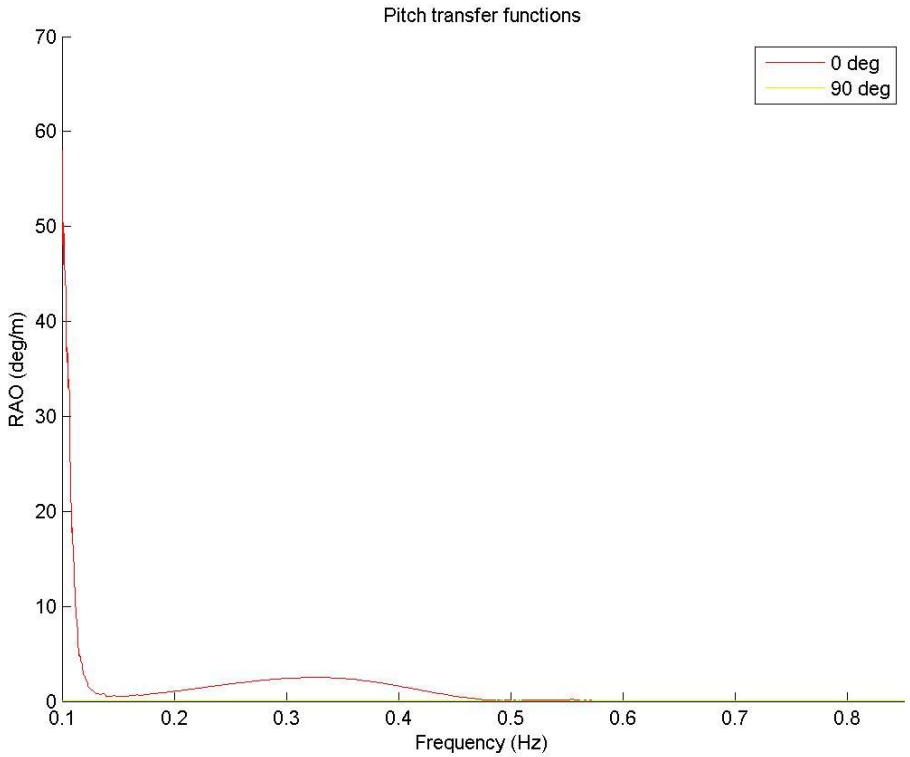

Figure A - 6: Pitch transfer functions, SIMA runs 1 and 2: Uncoupled condition

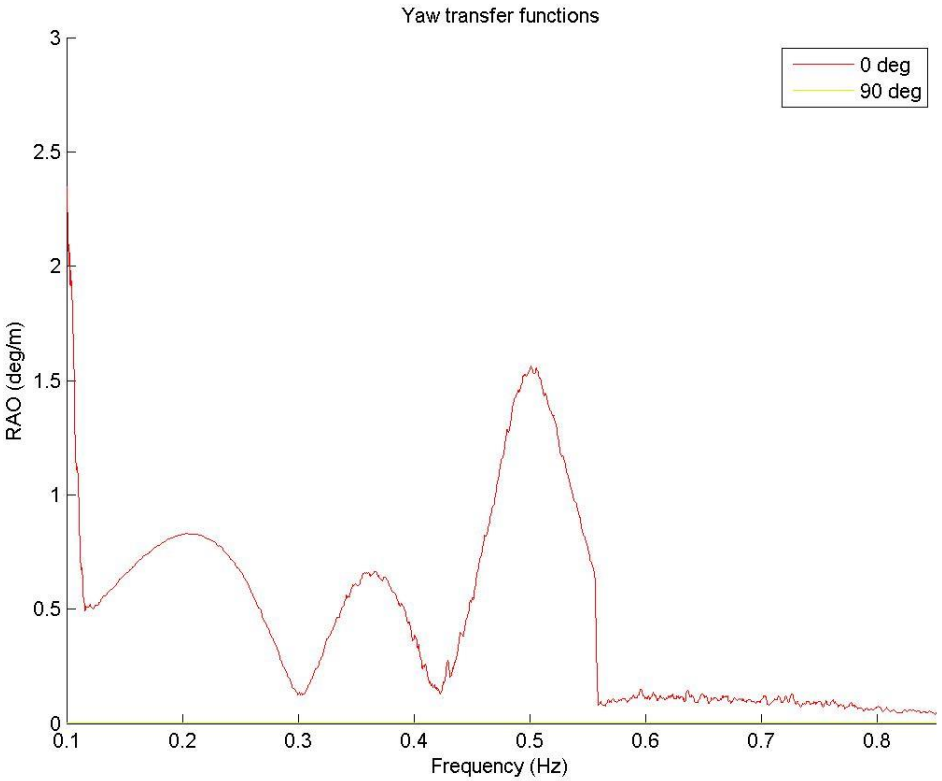

Figure A - 5: Yaw transfer functions, SIMA runs 1 and 2: Uncoupled condition

Table A - 3: Statistical values, SIMA run 3, coupled condition, wave heading 0 degrees

Channel/Motion	X-force	Y-force	Z-force	Surge	Sway	Heave	Roll	Pitch	Yaw
Moment m0:	2.2E+09	1.6E+09	4.0E+10	0.0003	0.0022	0.007	0.166	0.006	0.707
Moment m1:	1.4E+09	1.1E+09	2.7E+10	0.0001	0.0004	0.002	0.031	0.002	0.434
Moment m2:	1.5E+09	1.5E+09	3.4E+10	0.0000	0.0001	0.001	0.006	0.001	0.476
Significant value:	1.9E+05	1.6E+05	8.0E+05	0.067	0.188	0.343	1.629	0.317	3.363
Period T1:	1.64	1.44	1.50	4.909	5.362	3.016	5.366	3.644	1.630
Period T2:	1.22	1.04	1.08	4.347	5.172	2.374	5.157	3.065	1.219
Peak period:	12.65	15.46	17.72	23.874	23.874	16.425	23.874	16.082	12.651
Maximum value:	2.1E+05	1.9E+05	1.4E+06	0.057	0.193	0.241	1.697	0.336	3.894
Minimum values	-2.0E+05	-1.9E+05	-1.2E+06	-0.077	-0.198	-0.217	-1.730	-0.406	-3.746
Standard deviation:	5.8E+04	5.3E+04	2.6E+05	0.020	0.055	0.095	0.476	0.136	1.035
Expected value of largest maximum:	2.2E+05	1.9E+05	9.5E+05	0.069	0.193	0.344	1.676	0.493	3.826
Most probably largest maximum:	2.1E+05	1.9E+05	9.4E+05	0.069	0.192	0.341	1.665	0.490	3.804

Table A - 4: Statistical values, SIMA run 4, coupled condition, wave heading 315 degrees

Channel/Motion	X-force	Y-force	Z-force	Surge	Sway	Heave	Roll	Pitch	Yaw
Moment m0:	2.7E+09	1.8E+09	5.0E+10	0.001	0.007	0.008	0.550	0.002	0.875
Moment m1:	1.4E+09	1.1E+09	2.7E+10	0.0001	0.001	0.003	0.100	0.001	0.459
Moment m2:	1.4E+09	1.3E+09	3.0E+10	0.0000	0.0003	0.001	0.019	0.000	0.443
Significant value:	2.1E+05	1.7E+05	9.0E+05	0.113	0.344	0.366	2.966	0.179	3.742
Period T1:	1.91	1.65	1.85	5.406	5.474	3.115	5.498	2.604	1.908
Period T2:	1.40	1.18	1.29	5.024	5.317	2.536	5.337	2.230	1.405
Peak period:	19.58	21.54	16.40	25.632	16.425	16.082	16.425	9.837	19.585
Maximum value:	1.9E+05	1.9E+05	1.2E+06	0.116	0.394	0.233	3.399	0.254	3.686
Minimum values	-2.1E+05	-1.9E+05	-1.2E+06	-0.150	-0.393	-0.218	-3.435	-0.245	-3.950
Standard deviation:	6.4E+04	5.5E+04	2.9E+05	0.033	0.100	0.102	0.867	0.068	1.144
Expected value of largest maximum:	2.3E+05	2.0E+05	1.0E+06	0.117	0.364	0.369	3.143	0.256	4.090
Most probably largest maximum:	2.3E+05	2.0E+05	1.0E+06	0.116	0.361	0.367	3.124	0.255	4.064

Table A - 5: Statistical values SIMA run 5, coupled condition, wave heading 90 degrees

Channel/Motion	X-force	Y-force	Z-force	Surge	Sway	Heave	Roll	Pitch	Yaw
Moment m0:	7.0E+08	2.6E+09	1.2E+10	0.001	0.011	0.001	0.832	0.0002	0.250
Moment m1:	2.8E+08	9.2E+08	6.4E+09	0.0002	0.002	0.0002	0.152	0.0001	0.101
Moment m2:	2.3E+08	6.7E+08	7.8E+09	0.0000	0.0004	0.0001	0.029	0.0001	0.083
Significant value:	1.1E+05	2.1E+05	4.4E+05	0.140	0.421	0.093	3.649	0.050	2.000
Period T1:	2.49	2.87	1.87	5.432	5.509	2.767	5.492	1.992	2.485
Period T2:	1.75	1.98	1.24	5.195	5.389	2.149	5.362	1.612	1.740
Peak period:	19.87	16.35	21.54	16.861	16.861	20.399	16.861	17.985	19.873
Maximum value:	1.7E+05	2.5E+05	9.5E+05	0.163	0.591	0.196	5.001	0.149	3.277
Minimum values	-2.0E+05	-1.7E+05	-1.0E+06	-0.230	-0.575	-0.188	-5.124	-0.153	-4.006
Standard deviation:	3.5E+04	8.0E+04	1.6E+05	0.041	0.123	0.031	1.068	0.027	0.659
Expected value of largest maximum:	1.2E+05	2.9E+05	5.7E+05	0.149	0.445	0.112	3.862	0.096	2.352
Most probably largest maximum:	1.2E+05	2.9E+05	5.7E+05	0.149	0.442	0.111	3.838	0.095	2.337

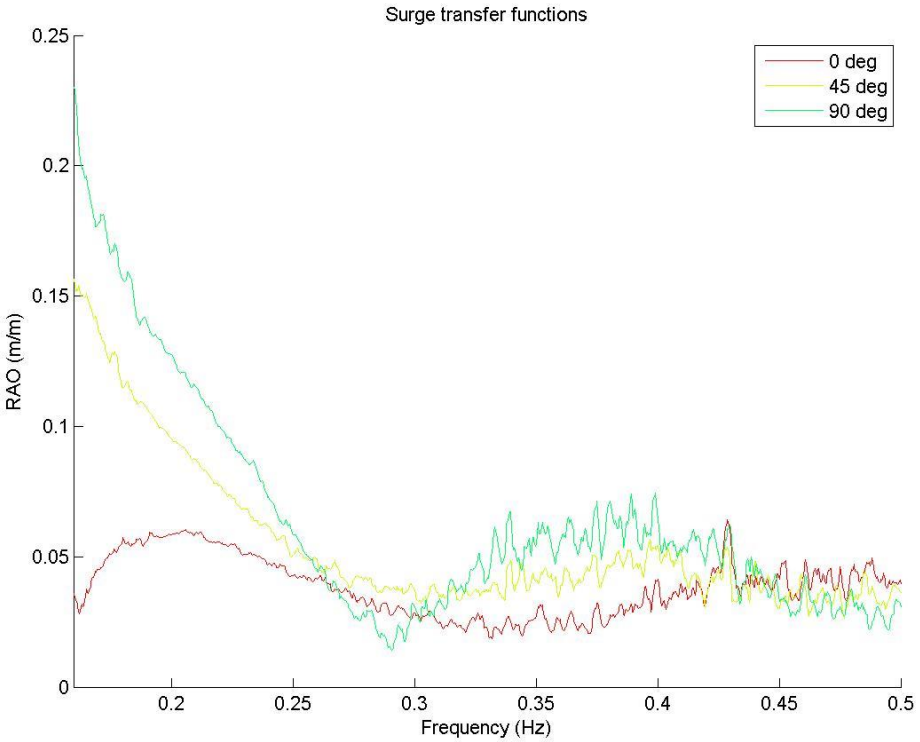

Figure A - 7: Surge transfer functions, SIMA runs 3-5, coupled condition

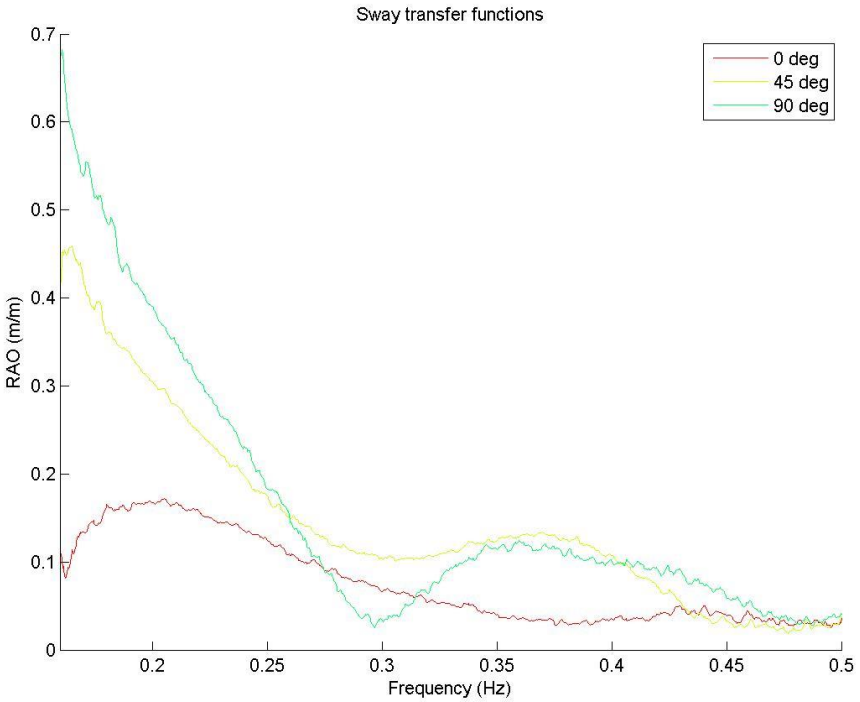

Figure A - 8: Sway transfer functions, SIMA runs 3-5, coupled condition

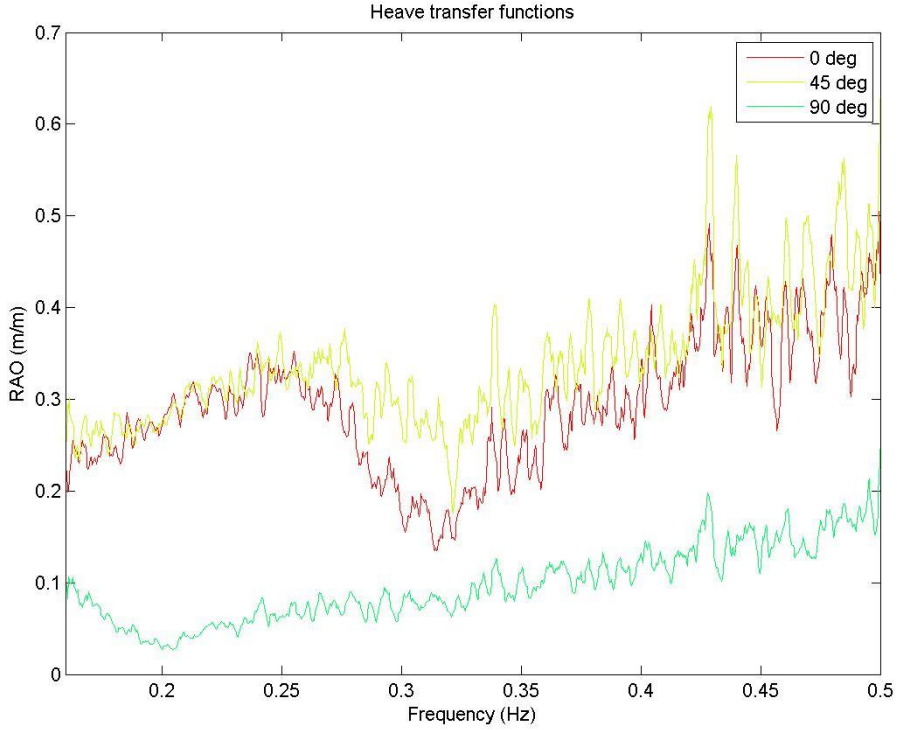

Figure A - 9: Heave transfer functions, SIMA runs 3-5, coupled condition

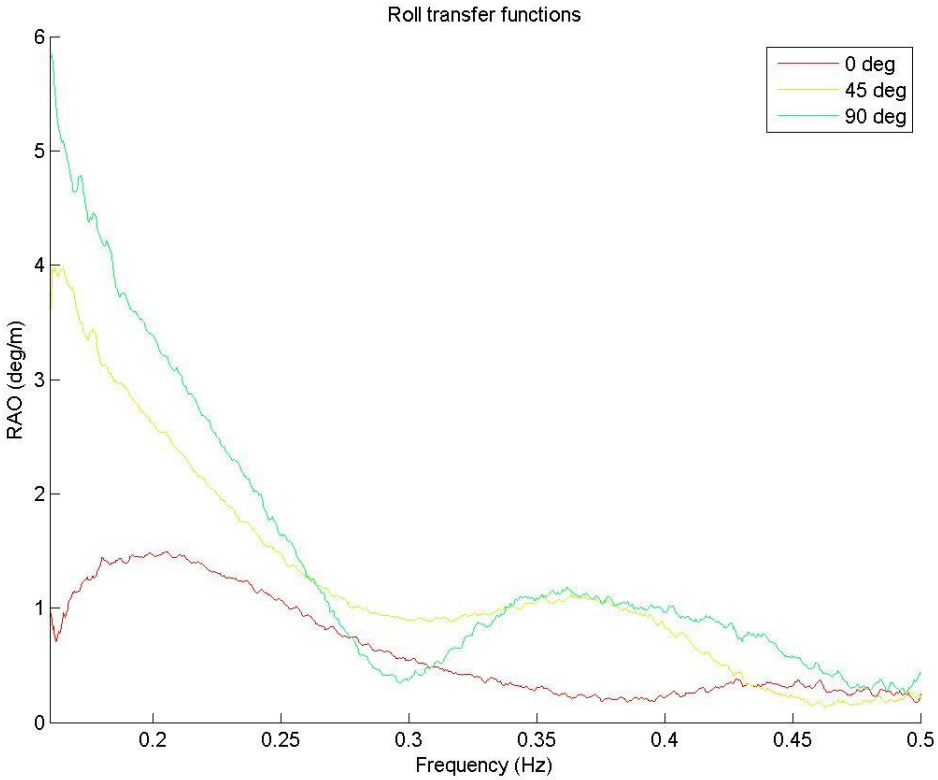

Figure A - 10: Roll transfer functions, SIMA runs 3-5, coupled condition

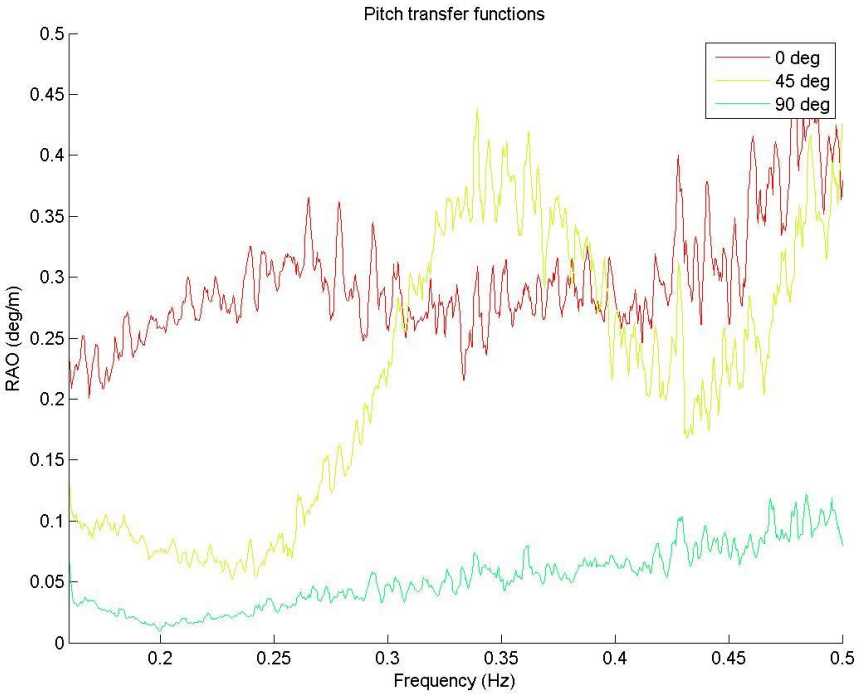

Figure A - 11: Pitch transfer functions, SIMA runs 3-5, coupled condition

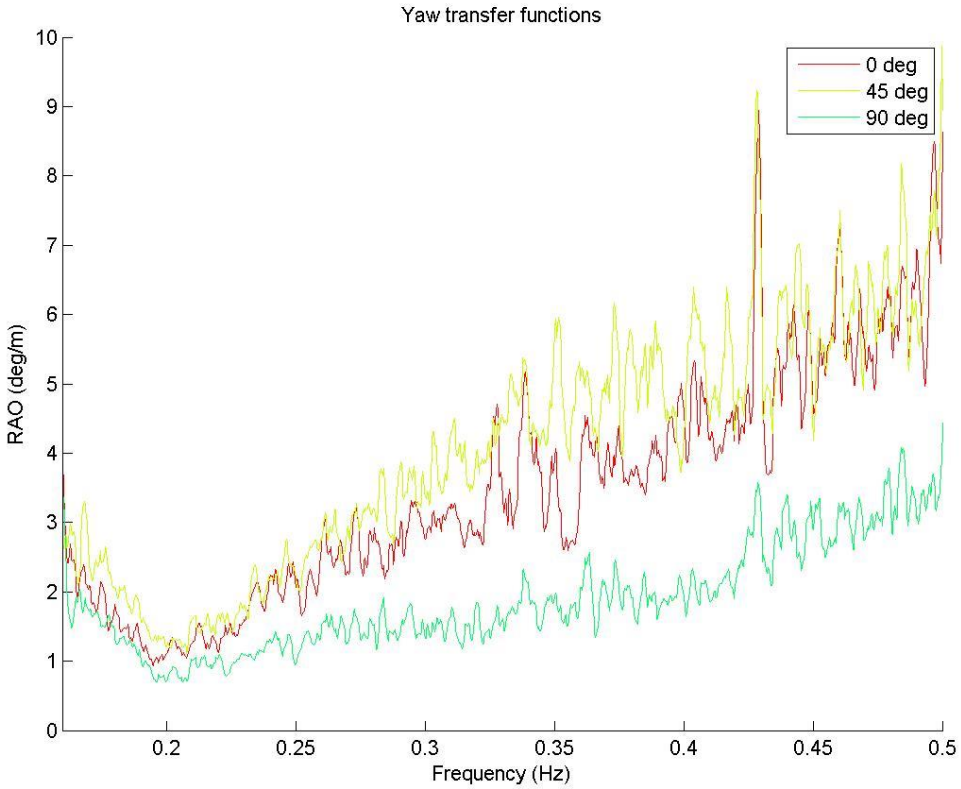

Figure A - 12: Yaw transfer functions, SIMA runs 3-5, coupled condition

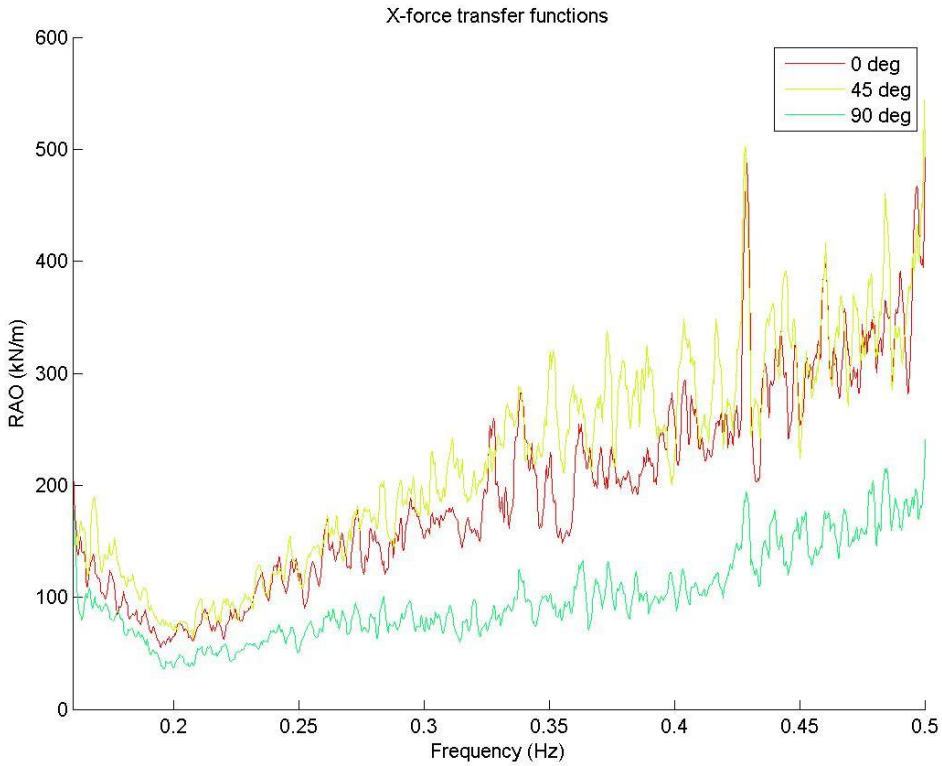

Figure A - 14: X-force transfer functions, SIMA runs 3-5, coupled condition

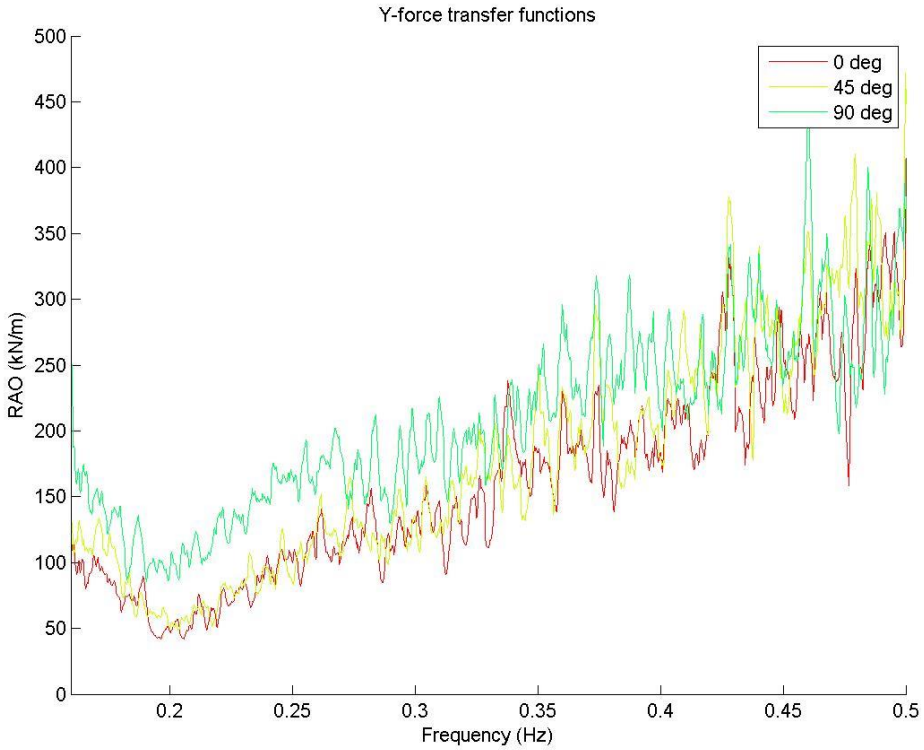

Figure A - 13: Y-force transfer functions, SIMA runs 3-5, coupled condition

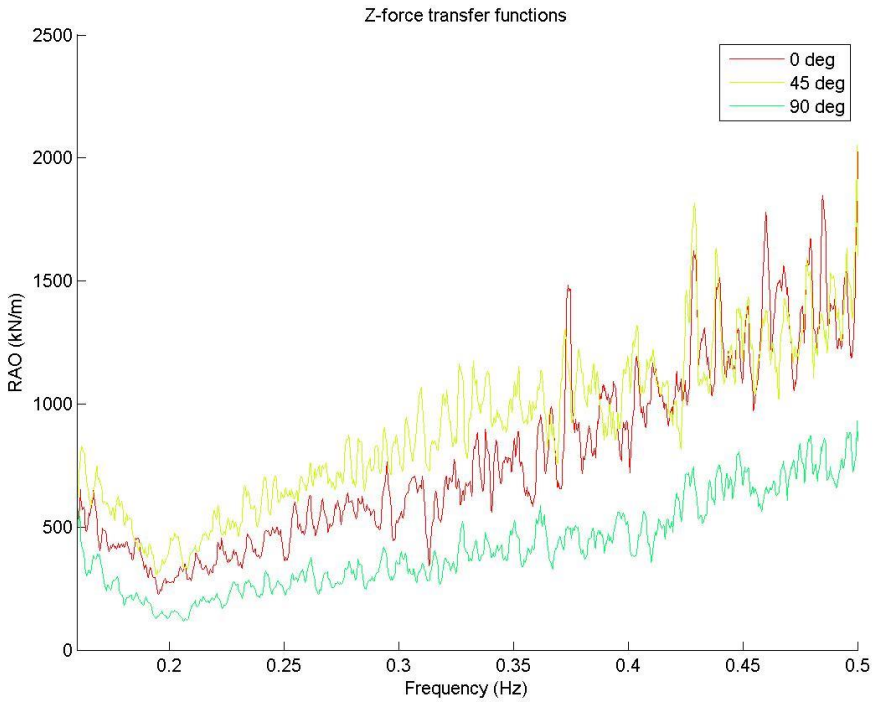

Figure A - 15: Z-force transfer functions, SIMA runs 3-5, coupled condition

Table A - 6: Statistical values SIMA run 6, total system, wave heading 0 degrees

Channel/Motion	X-force	Y-force	Z-force	Surge	Sway	Heave	Roll	Pitch	Yaw
Moment m0:	5.01E+09	1.11E+09	2.12E+09	0.0008	0.0003	0.0027	0.2084	0.0230	0.0315
Moment m1:	5.92E+09	8.79E+08	2.11E+09	0.0004	0.0001	0.0006	0.0520	0.0201	0.0192
Moment m2:	8.20E+09	1.10E+09	2.61E+09	0.0003	0.0000	0.0002	0.0203	0.0226	0.0193
Significant value:	2.83E+05	1.33E+05	1.84E+05	0.110	0.064	0.206	1.826	0.606	0.709
Period T1:	0.85	1.26	1.00355	2.064	3.572	4.357	4.011	1.145	1.638
Period T2:	0.78	1.01	0.901727	1.637	2.807	3.919	3.204	1.008	1.277
Peak period:	2.12	16.02	2.5435	15.126	15.126	15.126	15.147	15.147	14.937
Maximum value [N]:	5.36E+05	3.19E+05	4.83E+05	0.389	0.082	0.216	2.109	1.023	3.121
Minimum value [N]:	-5.62E+05	-3.00E+05	-4.66E+05	-0.389	-0.090	-0.232	-2.345	-1.111	-3.250
Standard deviation [N]:	1.66E+05	7.39E+04	9.51E+04	0.177	0.020	0.054	0.496	0.264	1.530
Expected value of largest maximum [N]:	6.87E+05	2.68E+05	3.90E+05	0.644	0.073	0.197	1.807	0.963	5.587
Most probably largest maximum [N]:	6.84E+05	2.67E+05	3.89E+05	0.640	0.073	0.196	1.796	0.957	5.553

Table A - 7: Statistical values SIMA run 7, total system, wave heading 315 degrees

Channel/Motion	X-force	Y-force	Z-force	Surge	Sway	Heave	Roll	Pitch	Yaw
Moment m0:	5.13E+09	1.46E+09	2.64E+09	0.0005	0.0011	0.0137	1.0085	0.0188	0.0294
Moment m1:	3.98E+09	1.00E+09	2.25E+09	0.0003	0.0003	0.0029	0.2145	0.0147	0.0131
Moment m2:	4.18E+09	1.22E+09	2.63E+09	0.0002	0.0001	0.0006	0.0530	0.0142	0.0091
Significant value:	2.87E+05	1.53E+05	2.05E+05	0.092	0.134	0.469	4.017	0.548	0.686
Period T1:	1.29	1.45	1.17	1.792	4.521	4.777	4.702	1.282	2.252
Period T2:	1.11	1.09	1.00	1.602	4.075	4.629	4.361	1.150	1.797
Peak period:	4.82	16.80	15.13	5.960	15.126	15.126	15.126	3.611	10.093
Maximum value [N]:	5.01E+05	3.30E+05	4.27E+05	0.173	0.120	0.461	4.140	0.964	1.331
Minimum value [N]:	-5.29E+05	-3.13E+05	-4.97E+05	-0.162	-0.175	-0.504	-4.251	-0.991	-1.501
Standard deviation [N]:	1.23E+05	8.30E+04	9.97E+04	0.042	0.035	0.121	1.044	0.209	0.345
Expected value of largest maximum [N]:	4.86E+05	3.00E+05	3.64E+05	0.162	0.128	0.441	3.809	0.841	1.296
Most probably largest maximum [N]:	4.83E+05	2.99E+05	3.62E+05	0.162	0.127	0.439	3.786	0.838	1.289

Table A - 8: Statistical values SIMA run 8, total system, wave heading 90 degrees

Channel/Motion	X-force	Y-force	Z-force	Surge	Sway	Heave	Roll	Pitch	Yaw
Moment m0:	5.13E+09	1.46E+09	2.64E+09	0.0005	0.0011	0.0137	1.0085	0.0188	0.0294
Moment m1:	3.98E+09	1.00E+09	2.25E+09	0.0003	0.0003	0.0029	0.2145	0.0147	0.0131
Moment m2:	4.18E+09	1.22E+09	2.63E+09	0.0002	0.0001	0.0006	0.0530	0.0142	0.0091
Significant value:	2.87E+05	1.53E+05	2.05E+05	0.092	0.134	0.469	4.017	0.548	0.686
Period T1:	1.29	1.45	1.17	1.792	4.521	4.777	4.702	1.282	2.252
Period T2:	1.11	1.09	1.00	1.602	4.075	4.629	4.361	1.150	1.797
Peak period:	4.82	16.80	15.13	5.960	15.126	15.126	15.126	3.611	10.093
Maximum value [N]:	5.01E+05	3.30E+05	4.27E+05	0.173	0.120	0.461	4.140	0.964	1.331
Minimum value [N]:	-5.29E+05	-3.13E+05	-4.97E+05	-0.162	-0.175	-0.504	-4.251	-0.991	-1.501
Standard deviation [N]:	1.23E+05	8.30E+04	9.97E+04	0.042	0.035	0.121	1.044	0.209	0.345
Expected value of largest maximum [N]:	4.86E+05	3.00E+05	3.64E+05	0.162	0.128	0.441	3.809	0.841	1.296
Most probably largest maximum [N]:	4.83E+05	2.99E+05	3.62E+05	0.162	0.127	0.439	3.786	0.838	1.289

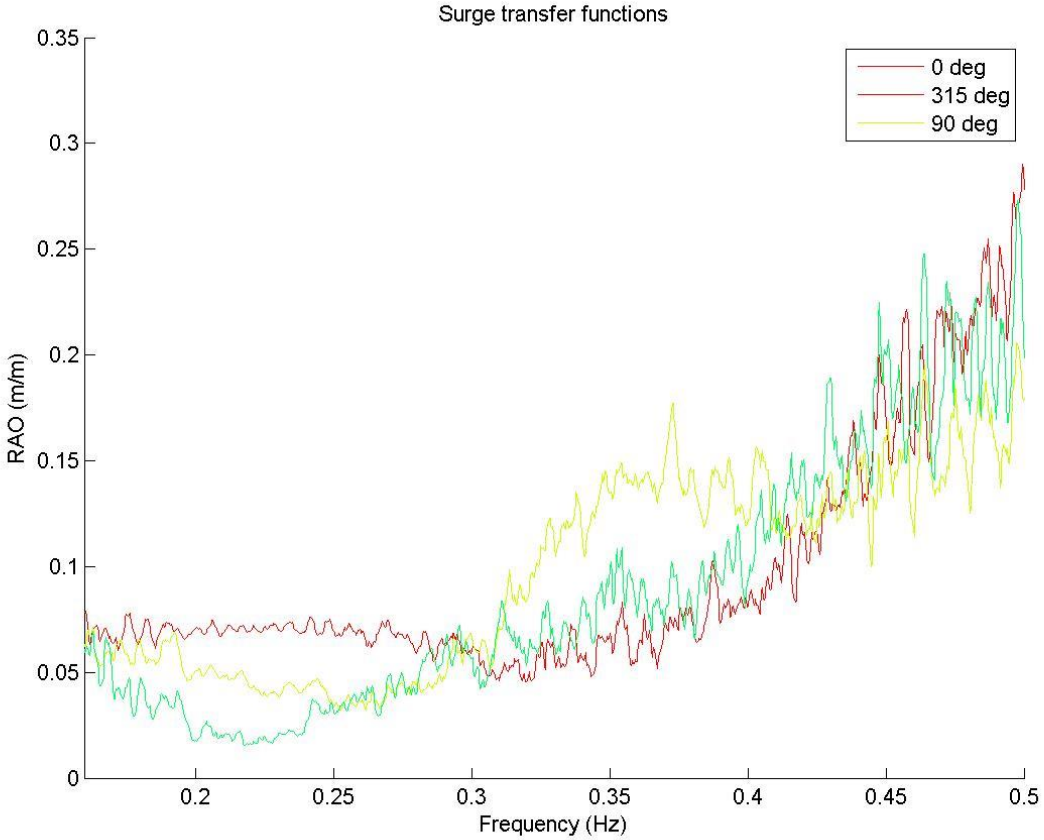

Figure A - 17: Surge transfer functions, SIMA, complete system

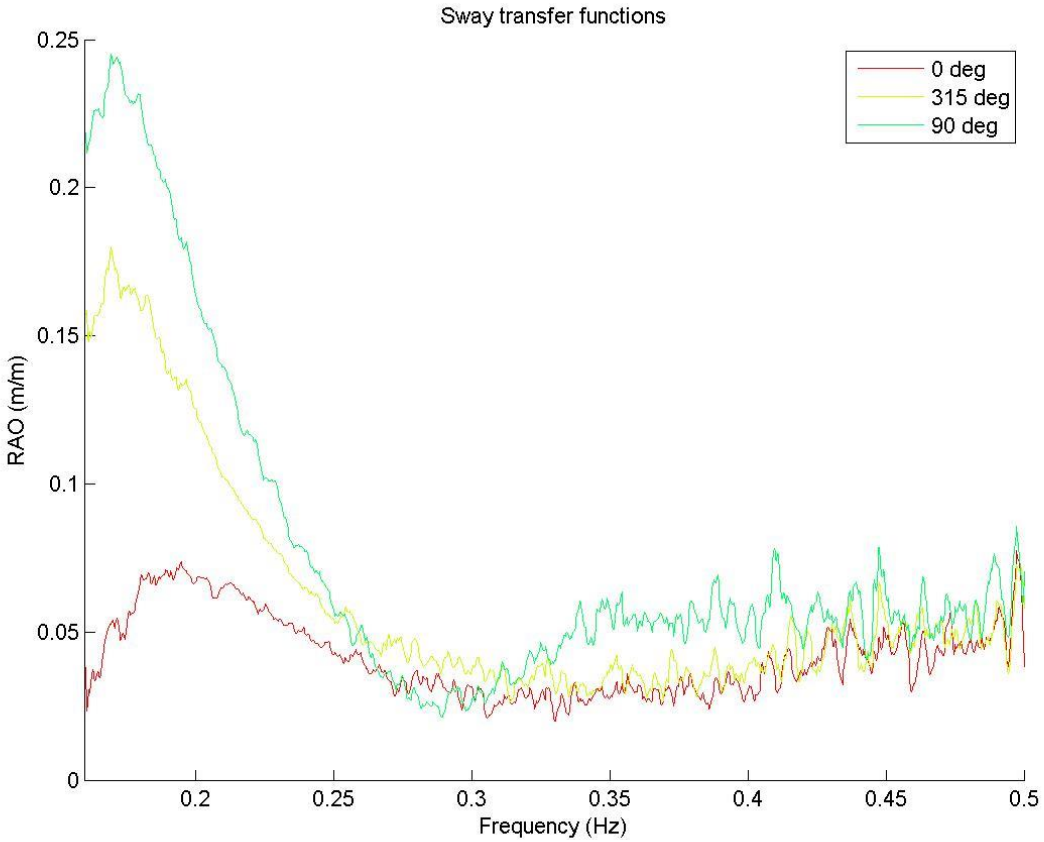

Figure A - 16: Sway transfer functions, SIMA, complete system

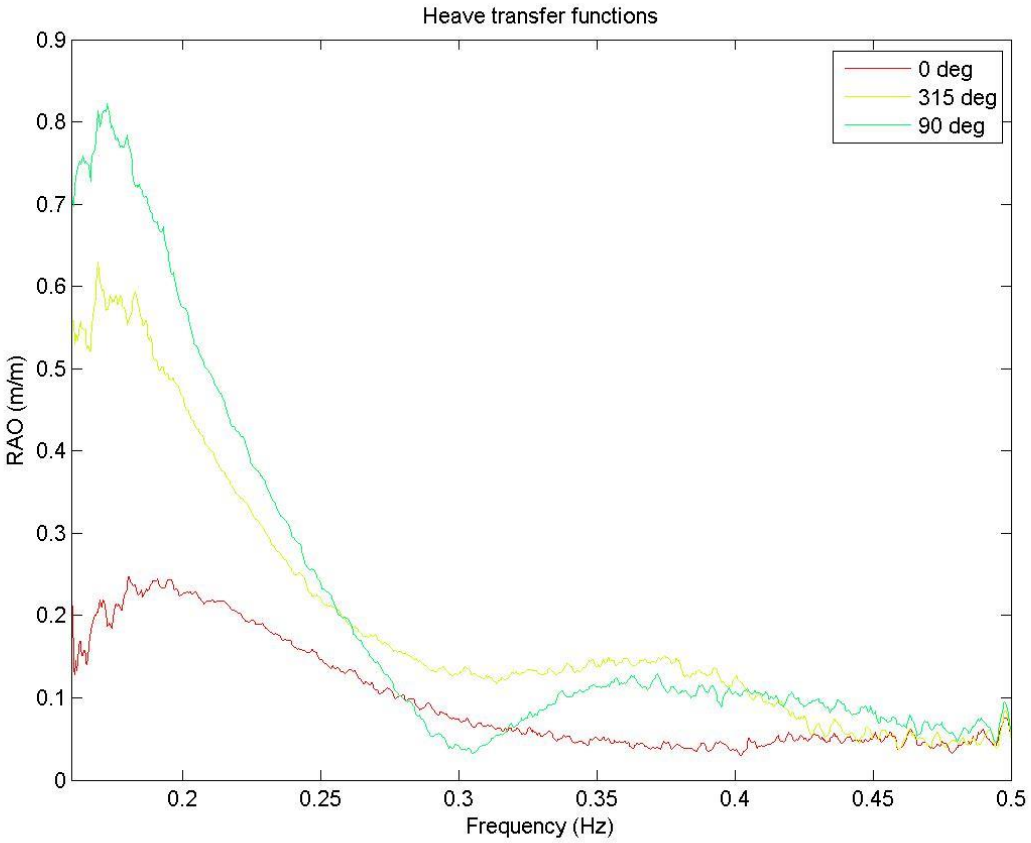

Figure A - 19: Heave transfer functions, SIMA, complete system

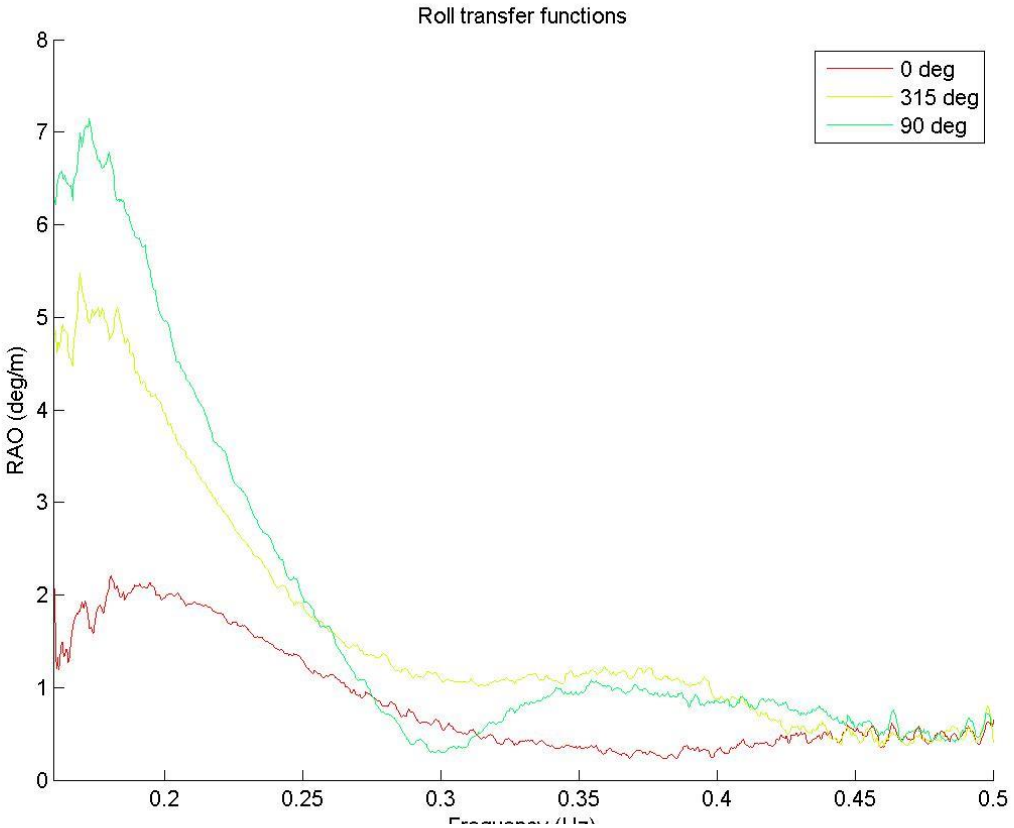

Figure A - 18: Roll transfer functions, SIMA, complete system

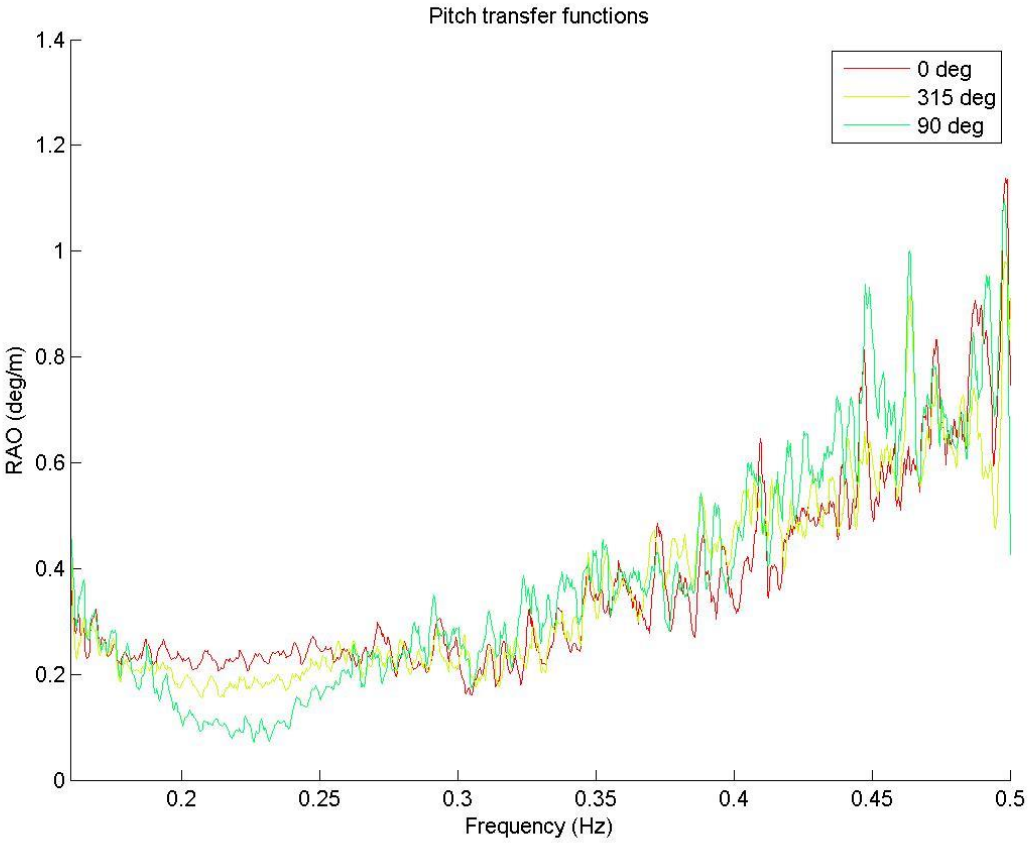

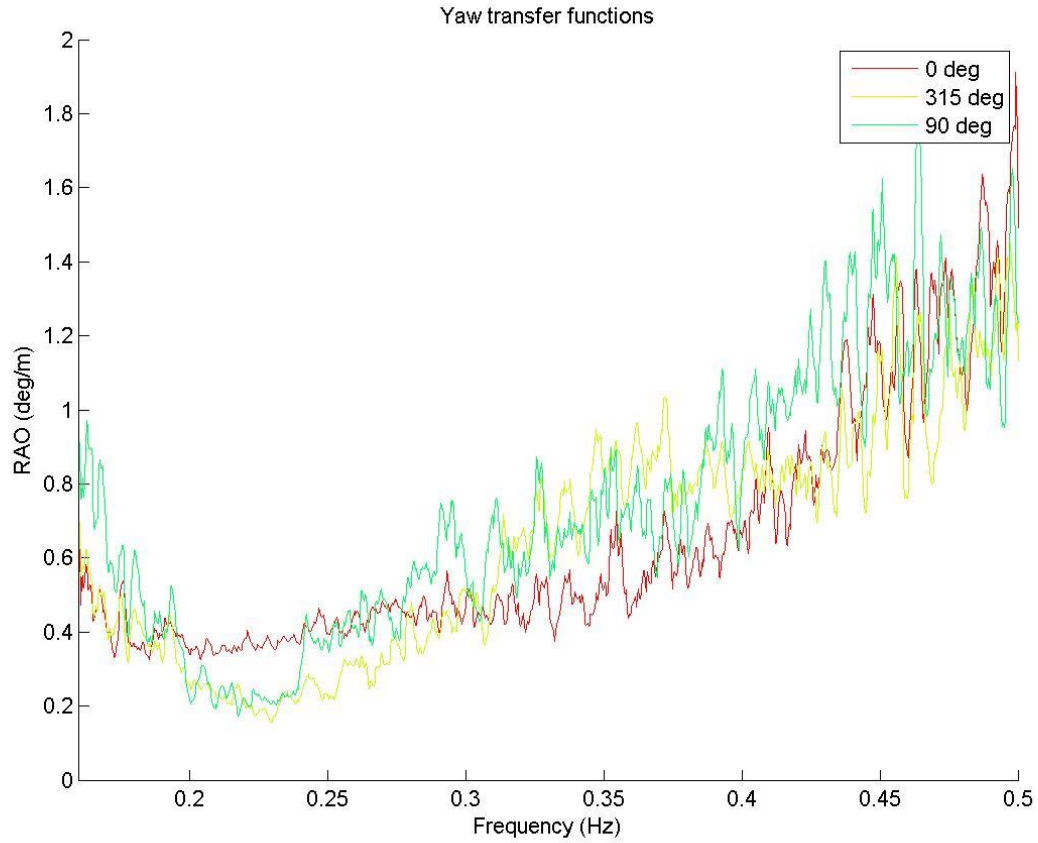

Figure A - 20: Yaw transfer functions, SIMA, complete system

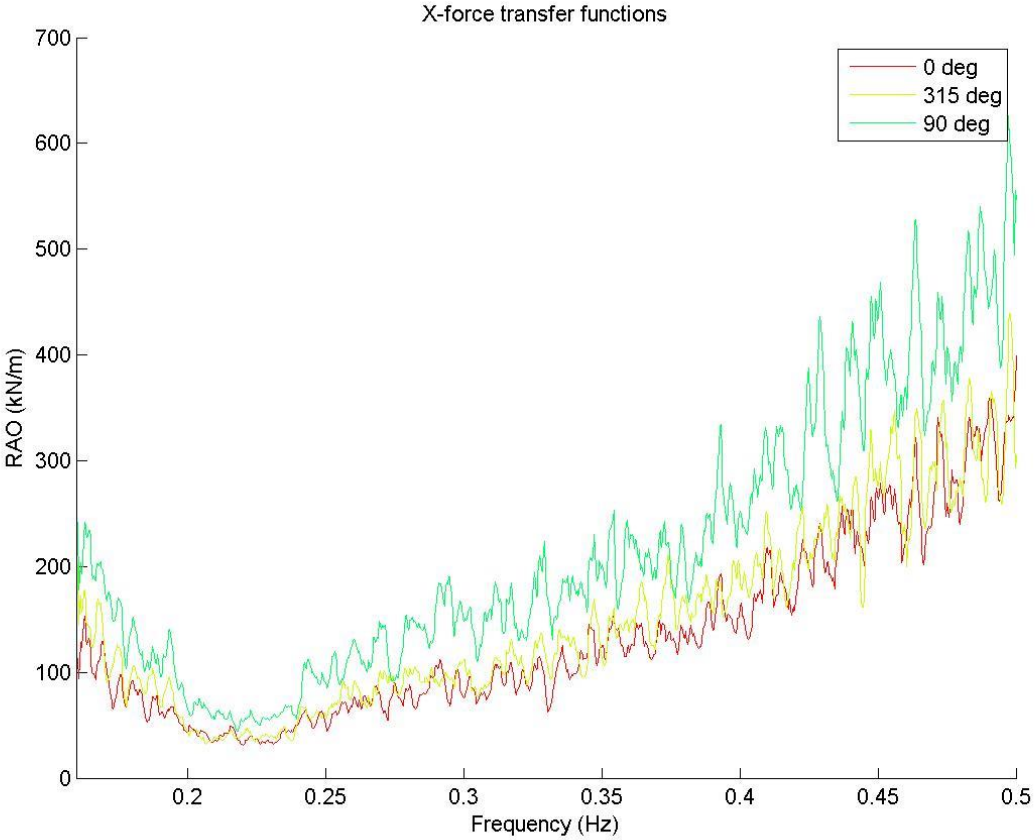

Figure A - 23: X-force transfer functions, SIMA, complete system

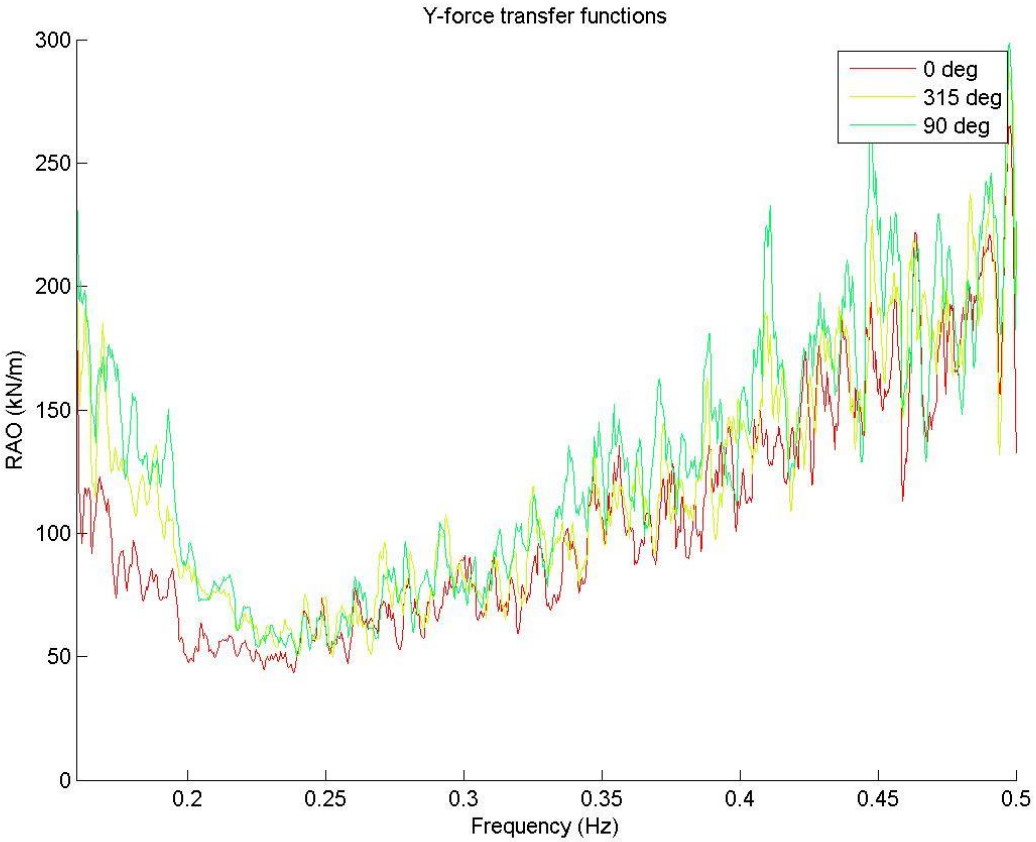

Figure A - 22: Y-force transfer functions, SIMA, complete system

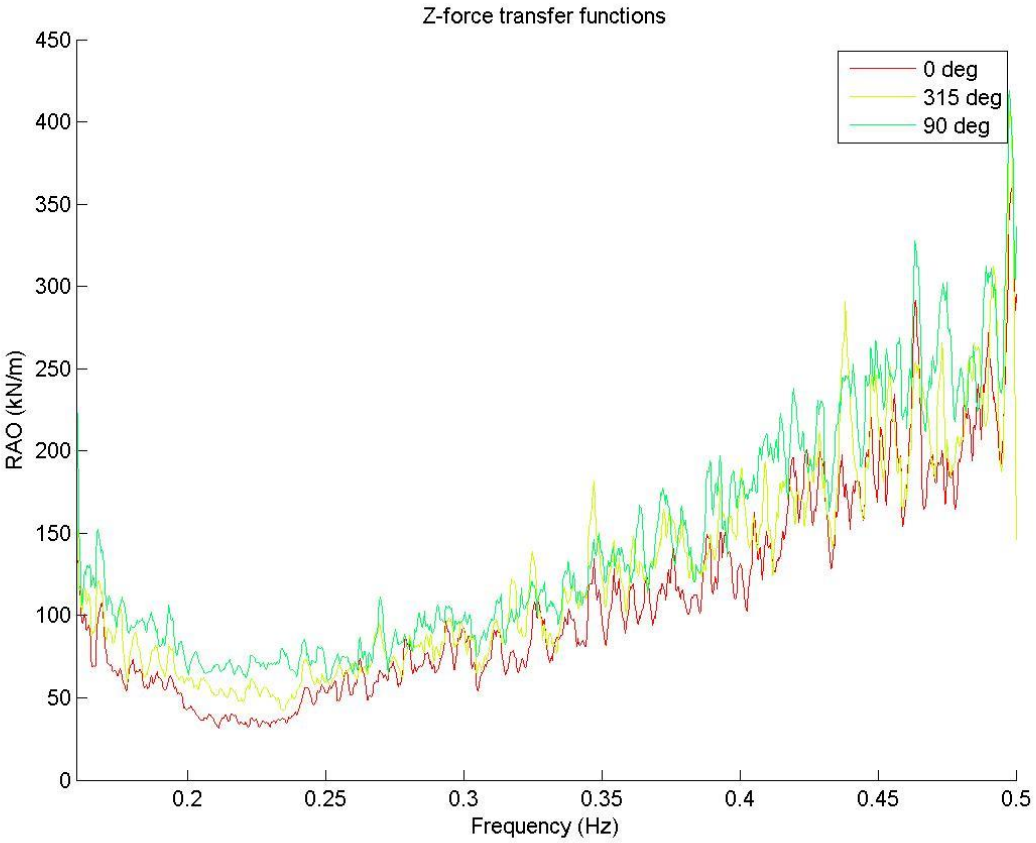

Figure A - 24: Z-force transfer functions, SIMA, complete system

APPENDIX B: MODEL TEST RESULTS, REGULAR AND IRREGULAR RUNS

Table B - 1: Statistical values, uncoupled regular runs, wave heading 90 degrees

Run	1000b	1001a	1002a	1003a	1004a	1005b	1006b	1007b	1008b	1009b	1010	1011a
Period (s)	2.83	3.23	3.58	3.9	4.2	4.47	4.73	4.98	5.22	5.44	5.66	5.87
Frequency (Hz)	0.35	0.31	0.28	0.26	0.24	0.22	0.21	0.20	0.19	0.18	0.18	0.17
Std. Surge (m)	0.077	0.127	0.123	0.127	0.130	0.173	0.219	0.277	0.275	0.349	0.393	0.513
Std. Sway (m)	0.009	0.013	0.007	0.013	0.010	0.012	0.022	0.013	0.013	0.022	0.015	0.016
Std. Heave (m)	0.029	0.035	0.035	0.038	0.052	0.085	0.112	0.132	0.146	0.196	0.217	0.218
Std. Roll (deg)	0.074	0.358	0.698	0.907	1.097	1.263	1.387	1.566	1.663	1.592	1.547	2.019
Std. Pitch (deg)	0.011	0.025	0.045	0.054	0.067	0.076	0.077	0.063	0.094	0.087	0.094	0.099
Std. Yaw (deg)	0.163	0.134	0.227	0.122	0.235	0.181	0.242	0.221	0.183	0.268	0.222	0.350
Max. Surge (m)	0.342	0.630	0.645	0.647	0.705	0.806	0.888	1.203	1.040	1.301	1.508	1.724
Max. Sway (m)	0.044	0.054	0.039	0.057	0.054	0.072	0.102	0.060	0.063	0.111	0.087	0.074
Max. Heave (m)	0.120	0.146	0.159	0.156	0.177	0.284	0.359	0.426	0.449	0.620	0.675	0.668
Max. Roll (deg)	0.366	1.151	2.138	2.710	3.288	3.816	4.174	4.742	5.006	5.063	4.970	6.403
Max. Pitch (deg)	0.065	0.117	0.212	0.231	0.334	0.295	0.316	0.283	0.427	0.413	0.447	0.439
Max. Yaw (deg)	0.608	0.548	0.946	0.742	1.085	0.943	1.179	1.039	0.857	1.381	1.120	1.602

Table B - 2: Statistical values, uncoupled regular runs, wave heading 0 degrees

Run	3000a	3001a	3002a	3003a	3004a	3005a	3006c	3007b	3008b	3009c	3010c	3011b
Period (s)	2.83	3.23	3.58	3.9	4.2	4.47	4.73	4.98	5.22	5.44	5.66	5.87
Frequency (Hz)	0.353	0.310	0.279	0.256	0.238	0.224	0.211	0.201	0.192	0.184	0.177	0.170
Std. Surge (m)	0.180	0.096	0.058	0.084	0.115	0.171	0.218	0.240	0.312	0.356	0.388	0.480
Std. Sway (m)	0.024	0.035	0.017	0.036	0.065	0.046	0.084	0.025	0.069	0.055	0.075	0.048
Std. Heave (m)	0.012	0.013	0.013	0.031	0.056	0.088	0.118	0.147	0.174	0.192	0.224	0.228
Std. Roll (deg)	0.314	0.430	0.456	0.417	0.378	0.399	0.371	0.240	0.225	0.194	0.165	0.156
Std. Pitch (deg)	0.117	0.244	0.496	0.756	0.915	1.072	1.290	1.443	1.432	1.418	1.358	1.717
Std. Yaw (deg)	1.072	0.896	0.891	0.662	1.150	1.258	0.930	0.591	0.612	1.290	0.699	0.924
Max. Surge (m)	0.108	0.138	0.075	0.150	0.221	0.162	0.356	0.105	0.264	0.252	0.306	0.198
Max. Sway (m)	0.783	0.450	0.276	0.383	0.525	0.788	1.028	0.887	1.274	1.433	1.430	1.700
Max. Heave (m)	0.062	0.083	0.086	0.134	0.218	0.299	0.386	0.444	0.539	0.602	0.689	0.732
Max. Roll (deg)	0.833	0.858	1.625	2.311	2.887	3.311	4.022	4.283	4.491	4.638	4.234	5.354
Max. Pitch (deg)	1.253	1.322	1.353	1.262	1.187	1.345	1.259	0.805	0.806	0.859	0.783	0.778
Max. Yaw (deg)	4.601	3.869	3.935	2.711	4.876	5.126	4.771	2.359	3.403	5.508	3.049	4.416

Table B - 3: Statistical values, coupled regular runs, wave heading 0 degrees

Run	4000b	4001b	4002b	4003b	4004b	4005d	4006a	4007a	4008a	4009a	4010a
Period (s)	2.83	3.23	3.58	3.9	4.2	4.47	4.73	4.98	5.06	5.29	5.52
Frequency (Hz)	0.353	0.310	0.279	0.256	0.238	0.224	0.211	0.201	0.198	0.189	0.181
Std. Surge (m)	0.009	0.003	0.017	0.032	0.047	0.067	0.085	0.106	0.119	0.150	0.172
Std. Sway (m)	0.008	0.010	0.013	0.012	0.011	0.012	0.017	0.022	0.026	0.031	0.027
Std. Heave (m)	0.015	0.013	0.012	0.030	0.059	0.084	0.112	0.125	0.126	0.101	0.112
Std. Roll (deg)	0.218	0.262	0.337	0.321	0.289	0.336	0.514	0.668	0.793	0.960	0.802
Std. Pitch (deg)	0.252	0.079	0.431	0.840	1.253	1.787	2.271	2.793	3.100	3.737	4.219
Std. Yaw (deg)	0.009	0.010	0.027	0.047	0.062	0.081	0.104	0.128	0.146	0.275	0.300
Std. Fx_58 (N)	1693.6	1843.0	1742.5	1504.2	1472.3	2138.5	3332.0	5295.1	6515.8	10397.5	12737.5
Std. Fy_58 (N)	5225.0	3655.5	3953.3	7389.0	10885.1	17276.5	24458.1	35551.2	41913.6	56667.4	70219.8
Std. Fz_58 (N)	7421.6	7925.2	9323.2	9468.0	9387.7	10055.9	10484.0	11449.1	11833.6	12340.7	14270.5
Std. Fx_96 (N)	2114.8	1908.2	1916.6	1477.0	1571.1	2323.1	3490.9	5294.6	6775.1	11404.0	16189.4
Std. Fy_96 (N)	2353.9	3147.7	5959.6	6214.5	8011.6	13509.1	21023.8	31811.5	38692.8	56048.4	70462.4
Std. Fz_96 (N)	8428.4	9064.3	8872.1	8458.4	7778.8	8828.0	9144.5	10447.4	13095.9	20604.6	27770.3
Max. Surge (m)	0.051	0.027	0.068	0.101	0.146	0.206	0.261	0.324	0.384	0.501	0.570
Max. Sway (m)	0.041	0.045	0.056	0.044	0.041	0.044	0.071	0.087	0.095	0.135	0.153
Max. Heave (m)	0.072	0.080	0.087	0.129	0.206	0.267	0.381	0.398	0.401	0.371	0.428
Max. Roll (deg)	1.114	1.162	1.459	1.089	1.083	1.215	2.092	2.624	2.873	3.938	4.112
Max. Pitch (deg)	1.342	0.666	1.665	2.682	3.833	5.375	6.841	8.463	9.705	11.411	12.881
Max. Yaw (deg)	0.086	0.059	0.115	0.164	0.218	0.260	0.340	0.425	0.520	1.055	1.079
Max. Fx_58 (N)	8428.5	11989.7	13218.7	9063.4	8427.0	11115.2	16260.4	25128.3	34224.9	57973.6	68752.0
Max. Fy_58 (N)	23497.3	16139.9	24093.7	32728.7	51718.3	71170.9	99470.4	142870.8	164469.8	221061.8	298041.0
Max. Fz_58 (N)	27618.0	27079.6	36876.4	34708.2	34419.0	38574.6	40660.2	53400.8	61458.6	67993.2	76617.7
Max. Fx_96 (N)	21165.2	15011.8	11225.6	8633.1	9453.9	14165.0	24915.9	36591.7	42740.4	68918.4	91322.3
Max. Fy_96 (N)	18779.8	13368.9	26959.7	28583.3	42471.6	55109.5	76546.4	114078.4	146933.1	201755.7	260888.7
Max. Fz_96 (N)	35576.4	32404.0	36257.5	37302.0	35423.0	39492.9	41509.5	48812.9	73683.3	115518.5	169812.0

Table B - 4: Statistical values, coupled regular runs, wave heading 315 degrees

Run	5000a	5001a	5002a	5003a	5004a	5005a	5006a	5007a	5008a	5009a	5010a
Period (s)	2.83	3.23	3.58	3.9	4.2	4.47	4.73	4.98	5.06	5.29	5.52
Frequency (Hz)	0.353	0.310	0.279	0.256	0.238	0.224	0.211	0.201	0.198	0.189	0.181
Std. Surge (m)	0.006	0.006	0.018	0.036	0.051	0.078	0.081	0.094	0.103	0.125	0.145
Std. Sway (m)	0.006	0.009	0.009	0.011	0.010	0.010	0.011	0.014	0.019	0.029	0.035
Std. Heave (m)	0.022	0.027	0.031	0.037	0.060	0.106	0.113	0.137	0.147	0.140	0.132
Std. Roll (deg)	0.229	0.223	0.359	0.630	0.879	1.363	1.426	1.597	1.659	1.931	2.489
Std. Pitch (deg)	0.127	0.177	0.381	0.673	0.879	1.455	1.506	1.845	2.137	2.714	3.042
Std. Yaw (deg)	0.017	0.014	0.012	0.086	0.124	0.148	0.148	0.158	0.165	0.180	0.193
Std. Fx_58 (N)	1612.7	999.3	1244.9	869.3	729.8	949.5	993.3	1447.8	2090.2	3896.3	5536.0
Std. Fy_58 (N)	5778.5	5347.2	3632.2	4247.2	4025.7	8225.3	9037.9	12561.6	16684.9	26497.7	31560.7
Std. Fz_58 (N)	14072.6	13659.5	9013.1	4366.8	3190.5	5921.3	4987.2	7658.2	7434.7	8247.2	9674.6
Std. Fx_96 (N)	1866.2	1708.2	1206.8	842.0	610.1	581.0	575.2	1205.2	1769.6	4345.7	6438.0
Std. Fy_96 (N)	5247.0	4121.2	3708.4	3590.1	4541.5	8705.4	9020.4	14230.3	17427.1	28369.2	36479.6
Std. Fz_96 (N)	8602.7	8997.4	7588.2	5828.5	4733.7	4481.9	4944.6	7129.7	7191.8	10076.4	14763.0
Max. Surge (m)	0.024	0.042	0.074	0.125	0.174	0.231	0.248	0.278	0.308	0.375	0.444
Max. Sway (m)	0.033	0.048	0.036	0.060	0.045	0.044	0.048	0.063	0.068	0.107	0.134
Max. Heave (m)	0.081	0.135	0.131	0.167	0.219	0.347	0.377	0.483	0.473	0.459	0.447
Max. Roll (deg)	0.921	1.224	1.513	2.307	2.825	4.210	4.698	5.093	5.008	6.105	8.063
Max. Pitch (deg)	0.709	0.865	1.455	2.448	3.296	4.546	4.748	6.004	6.645	8.395	9.636
Max. Yaw (deg)	0.092	0.087	0.072	0.324	0.362	0.427	0.407	0.428	0.460	0.492	0.541
Max. Fx_58 (N)	7257.5	6090.8	4526.0	4643.0	4698.9	4907.1	4841.6	8405.0	10519.1	20374.6	31482.4
Max. Fy_58 (N)	30093.6	19352.3	14886.5	23527.7	24118.2	39189.7	39534.8	63057.0	68613.3	104722.7	132074.7
Max. Fz_58 (N)	45863.5	45603.9	32058.5	20641.8	16811.2	23519.1	21371.3	31425.8	29792.3	35411.8	45014.3
Max. Fx_96 (N)	12563.7	11311.1	9648.9	13071.3	4485.6	4215.3	3424.1	8416.9	11884.7	26389.1	38023.3
Max. Fy_96 (N)	25808.4	14070.2	13829.7	19603.9	24001.7	37616.5	39228.1	58525.8	68839.6	104301.1	135700.1
Max. Fz_96 (N)	32876.6	30894.2	29160.2	24844.0	21415.8	21143.6	22496.9	37354.5	32353.0	46773.0	80867.0

Table B - 5: Statistical values, coupled regular runs, wave heading 90 degrees

Run	6000b	6001a	6002e	6003a	6004d	6005b	6006a	6007a	6008a	6009a	6010a
Period (s)	2.83	3.23	3.58	3.9	4.2	4.47	4.73	4.98	5.06	5.29	5.52
Frequency (Hz)	0.353	0.310	0.279	0.256	0.238	0.224	0.211	0.201	0.198	0.189	0.181
Std. Surge (m)	0.014	0.009	0.021	0.042	0.053	0.072	0.089	0.105	0.108	0.122	0.135
Std. Sway (m)	0.002	0.001	0.004	0.003	0.006	0.010	0.011	0.010	0.011	0.009	0.010
Std. Heave (m)	0.026	0.035	0.035	0.037	0.049	0.074	0.097	0.118	0.122	0.142	0.156
Std. Roll (deg)	0.405	0.293	0.597	1.048	1.414	1.922	2.396	2.858	2.940	3.320	3.696
Std. Pitch (deg)	0.061	0.063	0.043	0.033	0.061	0.104	0.105	0.101	0.100	0.140	0.161
Std. Yaw (deg)	0.023	0.023	0.017	0.038	0.028	0.127	0.151	0.164	0.166	0.167	0.173
Std. Fx_58 (N)	844.6	908.8	651.3	730.9	764.9	773.5	822.2	934.0	939.1	973.4	1067.9
Std. Fy_58 (N)	2460.1	2371.8	1984.7	3162.0	4185.0	4706.4	6208.9	7268.3	7141.7	7555.4	7627.0
Std. Fz_58 (N)	8365.4	6823.4	5475.3	3701.3	3951.3	4883.6	5872.3	6767.0	7050.0	7739.3	8186.6
Std. Fx_96 (N)	1266.4	1085.0	999.5	952.0	938.1	996.0	1152.6	1299.2	1302.2	1347.7	1470.6
Std. Fy_96 (N)	1969.1	1920.9	1878.2	2964.5	3890.6	4413.4	5796.9	6726.7	6600.3	7153.8	7139.5
Std. Fz_96 (N)	8003.5	6636.5	4561.4	3183.0	2842.4	3815.3	4371.1	5237.6	5442.2	5823.1	6749.2
Max. Surge (m)	0.048	0.050	0.080	0.131	0.162	0.212	0.263	0.314	0.314	0.365	0.401
Max. Sway (m)	0.009	0.009	0.020	0.018	0.024	0.044	0.042	0.044	0.042	0.048	0.059
Max. Heave (m)	0.104	0.113	0.147	0.164	0.177	0.263	0.339	0.378	0.384	0.441	0.513
Max. Roll (deg)	1.402	1.404	2.096	3.356	4.317	5.853	7.157	8.702	8.616	10.035	11.040
Max. Pitch (deg)	0.287	0.308	0.252	0.230	0.269	0.460	0.472	0.441	0.436	0.651	0.688
Max. Yaw (deg)	0.097	0.092	0.088	0.154	0.122	0.421	0.436	0.449	0.467	0.461	0.484
Max. Fx_58 (N)	3529.1	3153.2	2616.4	3404.2	2881.6	4211.1	3710.6	4377.7	4105.5	4700.9	5061.8
Max. Fy_58 (N)	10742.1	8572.0	8899.7	12497.7	14977.6	21050.7	20086.1	24441.9	23517.8	24961.3	26197.9
Max. Fz_58 (N)	28372.1	22266.7	20592.5	15402.1	15859.0	29398.2	22047.1	24837.5	26824.3	29024.6	29920.6
Max. Fx_96 (N)	9060.4	5074.2	6117.8	6581.6	5874.9	5020.0	5434.8	5684.5	6308.3	6937.3	7674.1
Max. Fy_96 (N)	8534.8	7562.9	8304.5	10543.3	13077.1	19105.2	18816.4	22046.1	21000.5	22885.0	23300.4
Max. Fz_96 (N)	25698.1	21955.1	16761.1	12783.7	13726.6	24551.2	17558.7	21431.0	23097.8	24647.3	30334.0

Table B - 6: Spectral analysis, coupled irregular runs, wave heading 90 degrees

Channel/Motion	Surge	Sway	Heave	Roll	Pitch	Yaw
Moment m0	1.15E-02	2.70E-05	4.37E-03	4.52E-03	0.603	1.94E-03
Moment m1	3.00E-03	1.20E-05	9.49E-04	1.20E-03	0.146	9.14E-04
Moment m2	8.15E-03	5.40E-05	2.27E-03	4.20E-03	0.397	4.02E-03
Significant value	0.430	0.021	0.264	0.269	3.106	0.176
Period T1	3.844	2.304	4.602	3.787	4.121	2.127
Period T2	1.190	0.709	1.386	1.038	1.232	0.695
Peak period	13.33	15.38	18.18	25.00	25.00	10.00
Maximum value	0.894	0.070	0.277	3.485	0.173	0.163
Minimum values	-0.651	-0.085	-0.303	-2.263	-0.244	-0.450
Mean value	0.171	0.013	-0.018	0.029	-0.004	-0.189
Standard deviation	0.107	0.005	0.066	0.067	0.776	0.044
Exp. largest max	0.396	0.019	0.238	0.236	2.723	0.166
Most prob. Largest max	0.393	0.019	0.236	0.234	2.705	0.165

Table B - 7: Spectral analysis, coupled irregular runs, wave heading 0 degrees

Name	Surge	Sway	Heave	Roll	Pitch	Yaw
Moment m0	0.0106	7.00E-05	4.29E-03	0.4765	0.1007	0.1771
Moment m1	0.0025	2.60E-05	8.92E-04	0.1141	0.0336	0.0666
Moment m2	0.0062	1.14E-04	2.03E-03	0.3072	0.1036	0.2141
Significant value	0.4117	0.0335	0.2620	2.7612	1.2696	1.6832
Period T1	4.2535	2.6637	4.8057	4.1768	2.9965	2.6583
Period T2	1.3089	0.7855	1.4543	1.2455	0.9863	0.9094
Peak period	13.3327	9.9996	18.1810	13.3327	9.9996	9.9996
Maximum value	0.8582	0.0777	0.2699	1.2684	3.2524	2.1914
Minimum values	-0.7003	-0.1188	-0.3316	-1.2296	-1.7906	-2.9186
Mean value	0.1419	-0.0227	-0.0146	0.0516	0.0809	-0.6213
Standard deviation	0.1029	0.0084	0.0655	0.6903	0.3174	0.4208
Exp. Value largest max	0.3789	0.0315	0.2355	2.5412	1.1929	1.5814
Most prob. Largest max	0.3767	0.0313	0.2341	2.5264	1.1863	1.5728

Table B - 8: Spectral analysis, coupled irregular runs, wave heading 0 degrees

Value/Channel	Surge	Sway	Heave	Roll	Pitch	Yaw
Moment m0	1.55E-03	1.14E-04	2.74E-03	1.131	0.089	2.50E-03
Moment m1	3.73E-04	3.30E-05	6.27E-04	0.271	0.024	7.27E-04
Moment m2	9.12E-04	1.22E-04	1.50E-03	0.654	0.084	2.40E-03
Significant value	0.158	0.043	0.209	4.255	1.190	2.00E-01
Period T1	4.1682	3.4686	4.3662	4.1824	3.6297	3.4402
Period T2	1.3052	0.9687	1.3520	1.3156	1.0266	1.0210
Peak period	19.999	42.855	19.999	19.999	42.855	19.999
Maximum value	0.2006	0.0457	0.1250	1.9703	5.4125	0.1341
Minimum values	-0.2014	-0.0713	-0.2470	-1.2907	-4.7385	-0.3721
Mean value	0.0059	-0.0018	-0.0385	0.0724	0.1850	-0.0024
Standard deviation	0.0394	0.0107	0.0523	1.0637	0.2976	0.0500
Exp. Value largest max	0.1407	0.0358	0.1869	3.7975	0.9972	0.1786
Most prob. Largest max	0.1398	0.0355	0.1857	3.7732	0.9895	0.1774

Value/Channel	Fx-58	Fy-58	Fz-58	Fx-96	Fy-96	Fz-96
Moment m0	2.66E+06	1.29E+08	5.83E+07	2.24E+06	7.38E+07	5.62E+07
Moment m1	1.72E+06	3.61E+07	1.93E+07	1.81E+06	2.39E+07	2.21E+07
Moment m2	4.25E+06	1.69E+07	1.70E+07	5.98E+06	1.24E+07	2.37E+07
Significant value	6.53E+03	4.54E+04	3.05E+04	5.98E+03	3.44E+04	3.00E+04
Period T1	1.5529	3.5690	3.0135	1.2332	3.0853	2.5500
Period T2	0.7913	2.7634	1.8506	0.6120	2.4442	1.5393
Peak period	19.999	19.999	14.999	19.999	9.999	14.285
Maximum value	2.22E+04	1.55E+05	2.63E+04	3.55E+04	2.16E+04	2.97E+04
Minimum values	-3.79E+04	-2.56E+04	-2.89E+04	-5.04E+04	-1.13E+05	-6.32E+04
Mean value	319.88	-1069.51	376.67	-3.41	1394.89	135.49
Standard deviation	1.63E+03	1.14E+04	7.63E+03	1.50E+03	8.59E+03	7.50E+03
Exp. Value largest max	5.83E+03	4.05E+04	2.79E+04	5.34E+03	3.23E+04	2.75E+04
Most prob. Largest max	5.79E+03	4.03E+04	2.77E+04	5.31E+03	3.21E+04	2.73E+04

Table B - 9: Spectral analysis, coupled irregular runs, wave heading 315 degrees

Value/Channel	Surge	Sway	Heave	Roll	Pitch	Yaw
Moment m0	1.64E-03	7.20E-05	3.69E-03	0.604435	0.518549	6.76E-03
Moment m1	4.01E-04	2.80E-05	8.66E-04	0.145557	0.12744	3.79E-03
Moment m2	1.03E-03	1.23E-04	2.12E-03	0.365224	0.331842	2.09E-02
Significant value	0.162	0.034	0.243	3.110	2.880	0.329
Period T1	4.105	2.594	4.263	4.153	4.069	1.783
Period T2	1.263	0.766	1.319	1.286	1.250	0.569
Peak period	16.949	17.241	16.949	16.949	16.949	16.949
Maximum value	0.209	0.096	0.188	3.202	3.916	0.335
Minimum values	-0.153	-0.093	-0.247	-4.823	-4.261	-0.152
Mean value	0.003	-0.001	-0.017	-0.024	0.044	0.015
Standard deviation	0.041	0.008	0.061	0.777	0.720	0.082
Exp. Value largest max	0.147	0.031	0.220	2.811	2.604	0.297
Most prob. Largest max	0.146	0.030	0.218	2.794	2.588	0.296

Value/Channel	Fx-58	Fy-58	Fz-58	Fx-96	Fy-96	Fz-96
Moment m0	1.03E+06	3.25E+07	7.07E+07	8.71E+05	3.12E+07	3.42E+07
Moment m1	7.40E+05	1.09E+07	2.66E+07	7.65E+05	1.01E+07	1.45E+07
Moment m2	2.28E+06	6.29E+06	1.93E+07	2.04E+06	4.99E+06	1.25E+07
Significant value	4.06E+03	2.28E+04	3.36E+04	3.73E+03	2.24E+04	2.34E+04
Period T1	1.394	2.974	2.660	1.138	3.101	2.357
Period T2	0.673	2.271	1.917	0.654	2.502	1.656
Peak period	16.949	9.009	9.009	14.286	7.874	9.009
Maximum value	7.72E+03	7.81E+04	3.30E+04	9.69E+03	1.88E+04	2.44E+04
Minimum values	-1.04E+04	-2.06E+04	-3.57E+04	-1.52E+04	-7.57E+04	-4.41E+04
Mean value	1.80E+02	3.08E+02	2.02E+02	-6.50E+01	-3.75E+02	-3.26E+02
Standard deviation	1.02E+03	5.70E+03	8.41E+03	9.33E+02	5.59E+03	5.85E+03
Exp. Value largest max	3.67E+03	2.16E+04	3.18E+04	3.42E+03	2.14E+04	2.21E+04
Most prob. Largest max	3.65E+03	2.15E+04	3.17E+04	3.40E+03	2.12E+04	2.20E+04

Table B - 10: Spectral analysis, coupled irregular runs, wave heading 90 degrees

Value/Channel	Surge	Sway	Heave	Roll	Pitch	Yaw
Moment m0	2.18E-03	4.20E-05	3.88E-03	5.92E-03	1.50E+00	5.87E-03
Moment m1	5.44E-04	4.20E-05	8.88E-04	2.39E-03	3.73E-01	3.71E-03
Moment m2	1.40E-03	2.73E-04	2.31E-03	1.15E-02	9.36E-01	2.13E-02
Significant value	0.187	0.026	0.249	0.308	4.906	0.306
Period T1	4.011	1.004	4.372	2.477	4.029	1.582
Period T2	1.248	0.392	1.297	0.718	1.268	0.525
Peak period	15.267	16.949	21.978	20.000	15.267	15.267
Maximum value	0.141	0.022	0.167	3.806	0.168	0.308
Minimum values	-0.175	-0.020	-0.301	-4.983	-0.502	-0.152
Mean value	0.004	-0.007	-0.055	0.134	-0.172	0.004
Standard deviation	0.047	0.006	0.062	0.077	1.227	0.077
Exp. Value largest max	0.170	0.023	0.221	0.275	4.470	0.279
Most prob. Largest max	0.169	0.023	0.219	0.273	4.444	0.277

Value/Channel	Fx-58	Fy-58	Fz-58	Fx-96	Fy-96	Fz-96
Moment m0	4.86E+05	9.35E+06	3.06E+07	8.56E+05	7.83E+06	2.50E+07
Moment m1	3.29E+05	2.73E+06	1.16E+07	5.38E+05	2.02E+06	9.94E+06
Moment m2	1.16E+06	2.43E+06	1.21E+07	1.64E+06	1.70E+06	1.08E+07
Significant value	2.79E+03	1.22E+04	2.21E+04	3.70E+03	1.12E+04	2.00E+04
Period T1	1.474	3.422	2.628	1.590	3.878	2.518
Period T2	0.647	1.960	1.589	0.722	2.149	1.520
Peak period	13.699	15.267	9.804	15.151	15.267	9.804
Maximum value	2.62E+03	7.51E+03	1.81E+04	3.69E+03	1.32E+04	1.56E+04
Minimum values	-2.25E+03	-1.45E+04	-1.71E+04	-5.48E+03	-7.82E+03	-1.55E+04
Mean value	2.72E+02	-2.43E+02	2.70E+02	4.96E+01	2.42E+02	-2.81E+01
Standard deviation	6.97E+02	3.06E+03	5.53E+03	9.25E+02	2.80E+03	5.00E+03
Exp. Value largest max	2.56E+03	1.11E+04	2.08E+04	3.37E+03	1.02E+04	1.88E+04
Most prob. Largest max	2.55E+03	1.11E+04	2.07E+04	3.35E+03	1.01E+04	1.87E+04

Table B - 11: Spectral analysis, irregular runs, total system, wave heading 315 degrees

Value/Channel	Surge	Sway	Heave	Roll	Pitch	Yaw
Moment m0	1.87E-03	4.41E-04	7.43E-03	7.66E-01	1.12E+00	4.75E-03
Moment m1	3.79E-04	9.30E-05	1.44E-03	1.56E-01	2.24E-01	1.28E-03
Moment m2	8.30E-05	2.20E-05	2.97E-04	3.56E-02	4.75E-02	5.35E-04
Significant value	0.173	0.084	0.345	3.500	4.237	0.276
Period T1	4.941	4.719	5.157	4.906	5.017	3.705
Period T2	4.749	4.437	5.004	4.634	4.860	2.980
Peak period	13.178	10.559	14.407	10.494	13.178	14.407
Maximum value	0.115	0.046	0.179	1.853	2.655	0.397
Minimum values	-0.116	-0.057	-0.274	-2.271	-3.117	-0.100
Mean value	0.003	-0.001	-0.050	0.049	0.036	0.021
Standard deviation	0.046	0.021	0.088	0.819	1.134	0.099
Exp. Value largest max	0.169	0.080	0.323	3.068	4.179	0.362
Most prob. Largest max	0.168	0.079	0.321	3.051	4.155	0.359

Value/Channel	Fx_58	Fy_58	Fz_58	Fx_96	Fy_96	Fz_96
Moment m0	2.37E+06	8.16E+07	8.69E+07	2.23E+06	7.74E+07	4.67E+07
Moment m1	7.79E+05	2.52E+07	2.98E+07	7.56E+05	2.54E+07	1.72E+07
Moment m2	3.87E+05	9.08E+06	1.21E+07	3.86E+05	9.54E+06	7.59E+06
Significant value	6.15E+03	3.61E+04	3.73E+04	5.97E+03	3.52E+04	2.73E+04
Period T1	3.039	3.238	2.917	2.952	3.047	2.722
Period T2	2.474	2.997	2.682	2.406	2.850	2.481
Peak period	13.178	8.213	7.328	13.178	6.615	7.556
Maximum value	7.27E+03	5.25E+04	1.94E+04	5.36E+03	2.07E+04	1.77E+04
Minimum values	-7.34E+03	-2.12E+04	-3.03E+04	-8.28E+03	-4.74E+04	-2.43E+04
Mean value	1.44E+03	9.16E+02	-4.12E+03	-1.34E+00	9.62E+01	-6.06E+02
Standard deviation	1.86E+03	1.12E+04	8.73E+03	1.55E+03	1.01E+04	6.37E+03
Exp. Value largest max	6.84E+03	4.28E+04	3.35E+04	5.72E+03	3.91E+04	2.44E+04
Most prob. Largest max	6.80E+03	4.25E+04	3.34E+04	5.69E+03	3.89E+04	2.43E+04

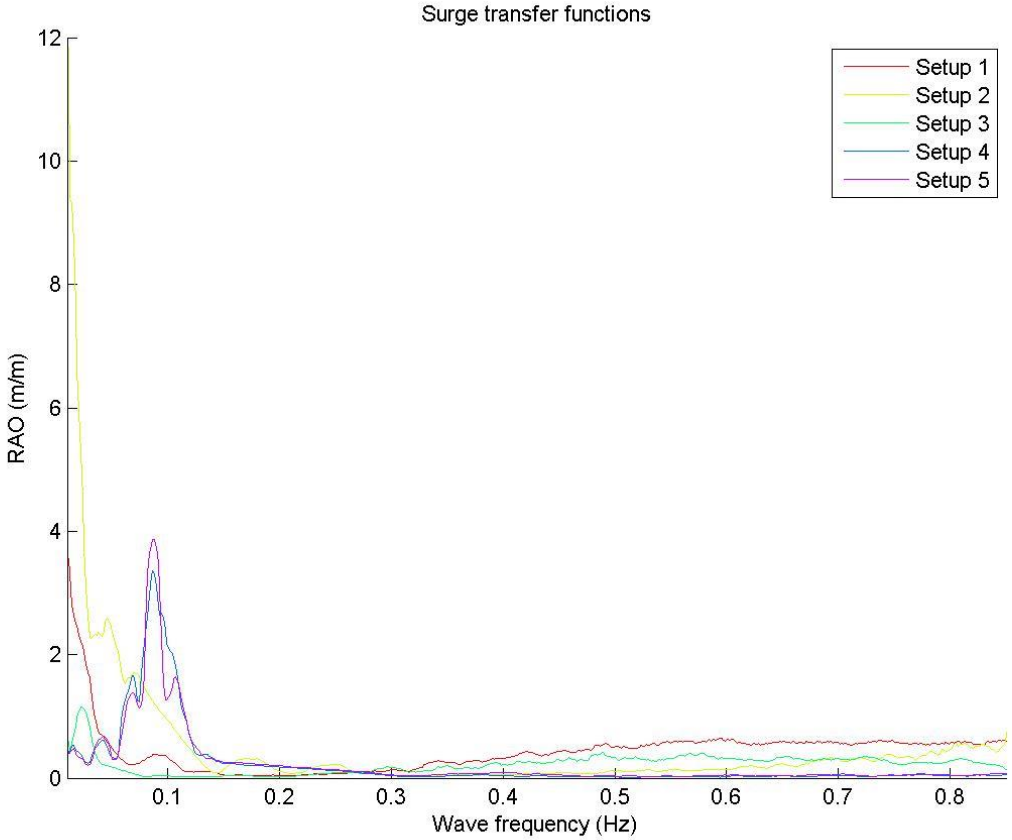

Figure B - 1: Surge transfer functions, irregular model test runs

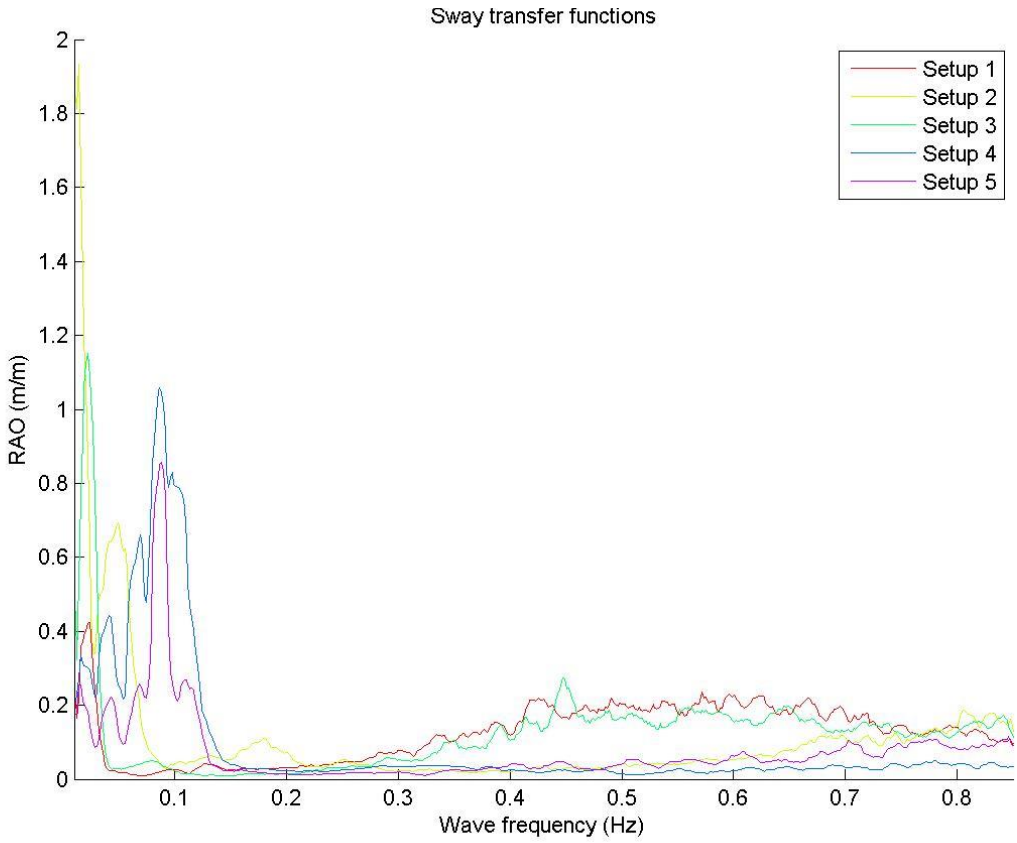

Figure B - 2: Sway transfer functions, irregular model test runs

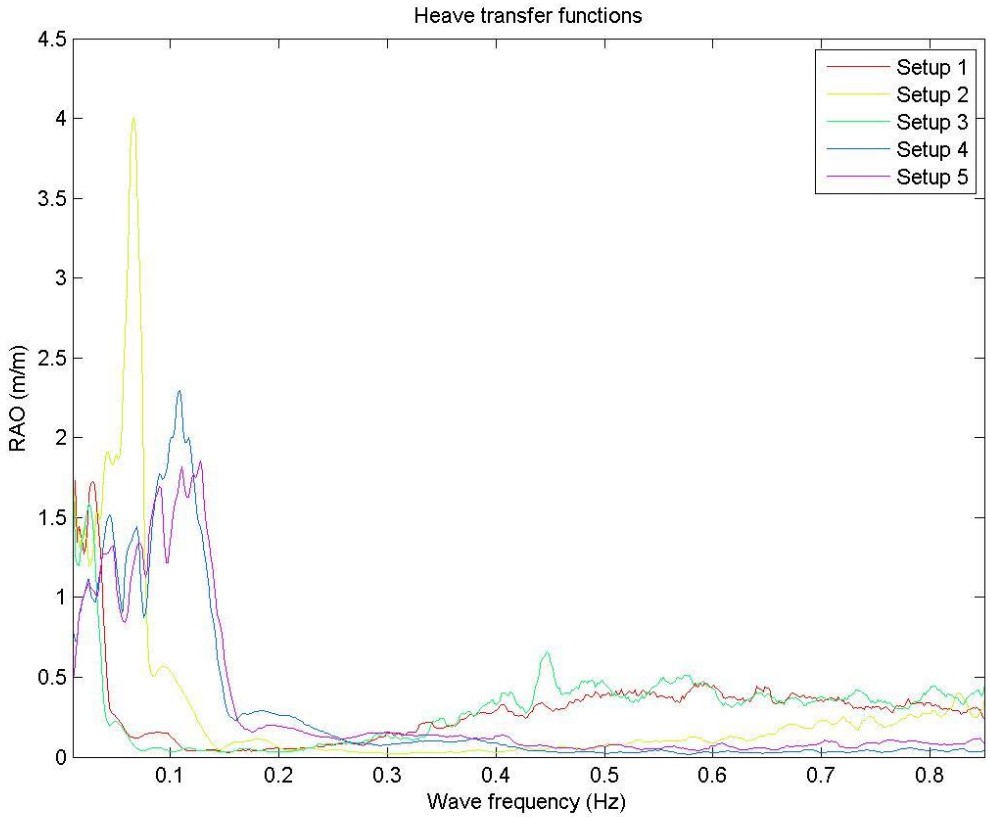

Figure B - 4: Heave transfer functions, irregular model test runs

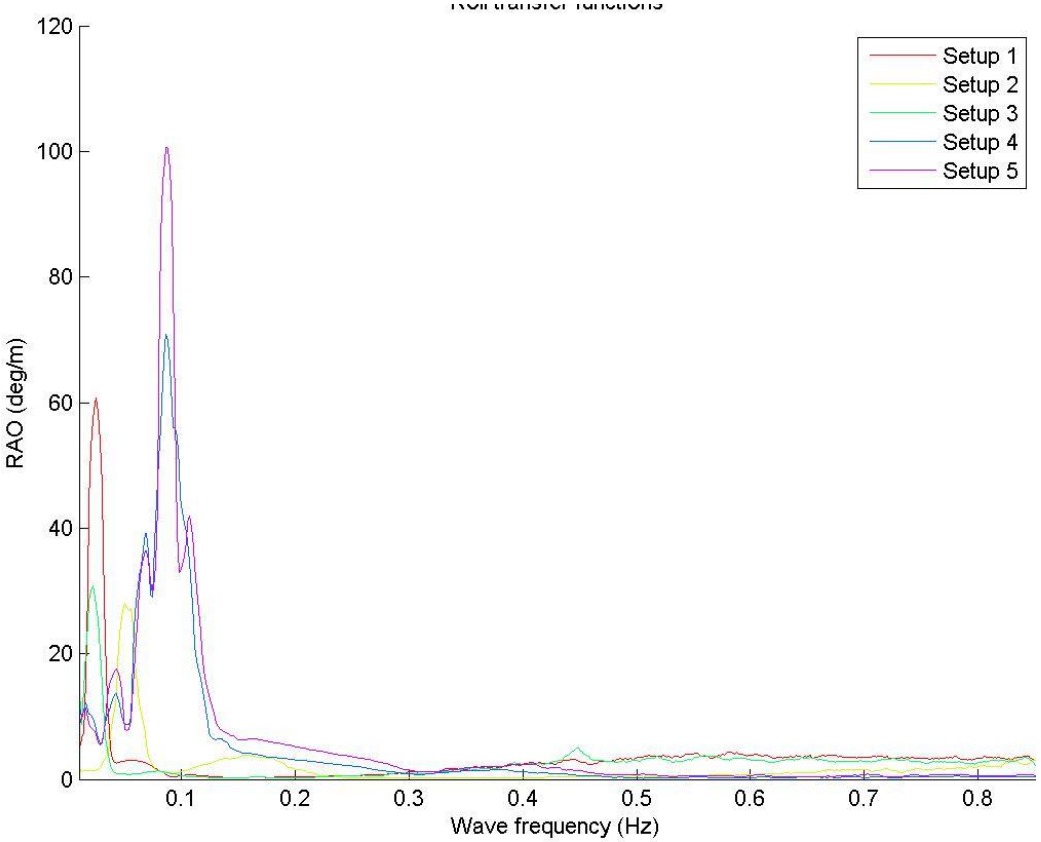

Figure B - 5: Roll transfer functions, irregular model test runs

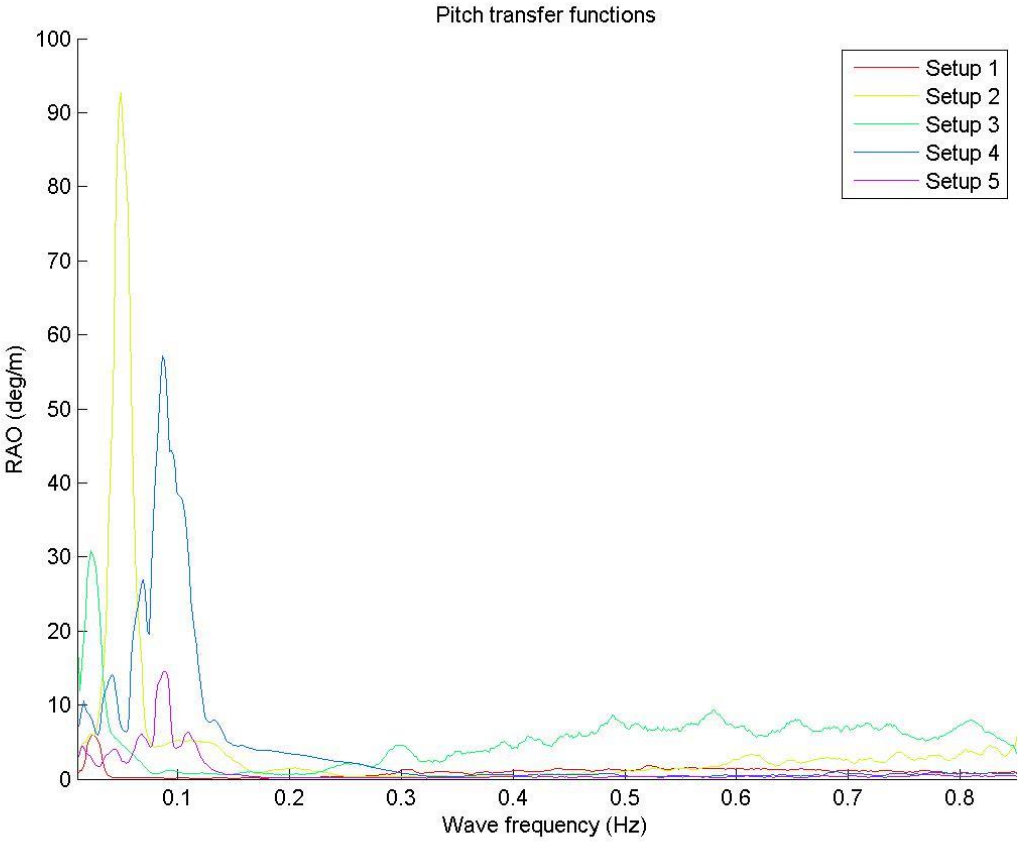

Figure B - 7: Pitch transfer functions, irregular model test runs

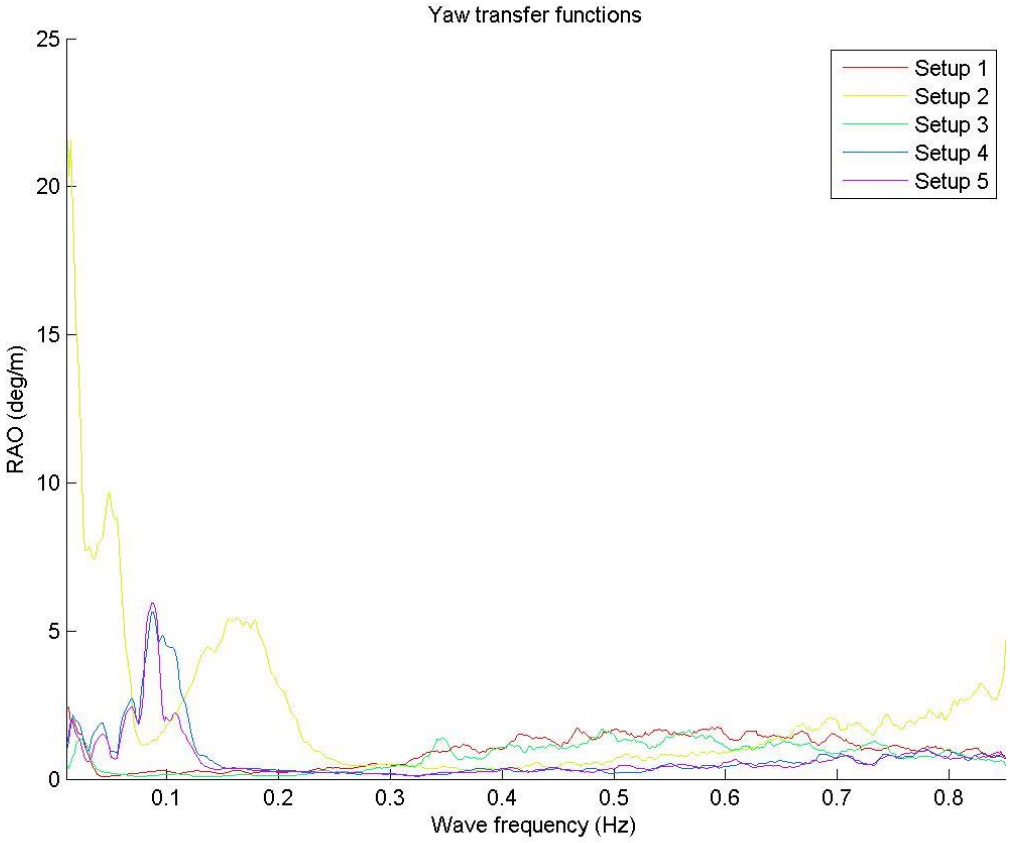

Figure B - 6: Yaw transfer functions, irregular model test runs

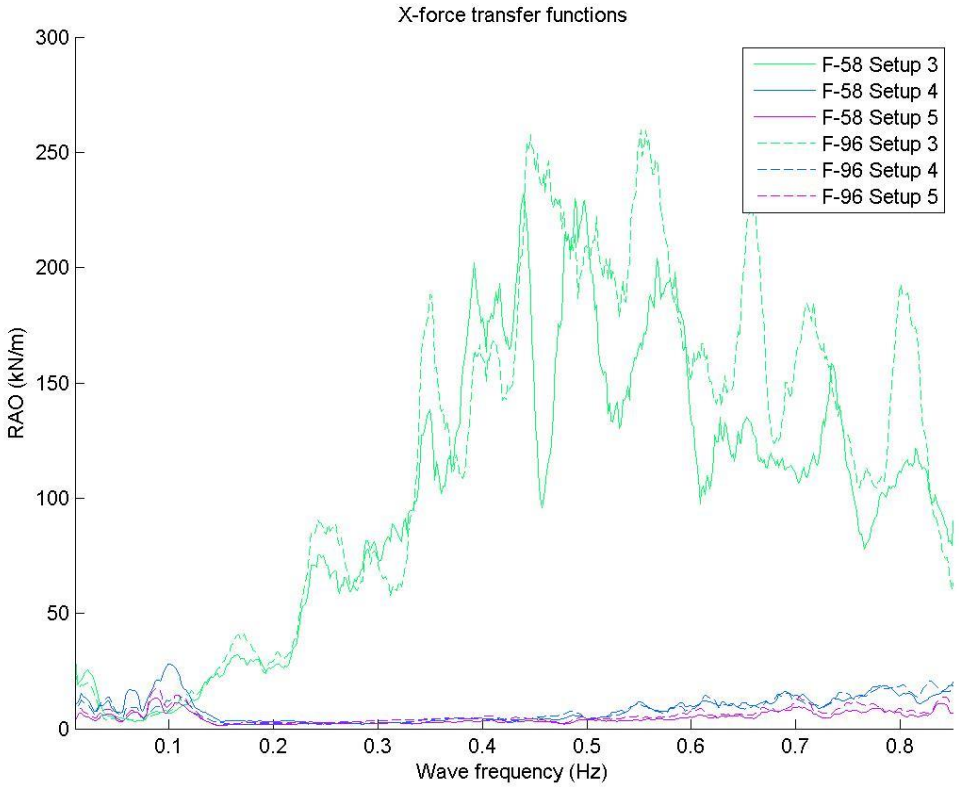

Figure B - 8: X-force transfer functions, irregular model test runs

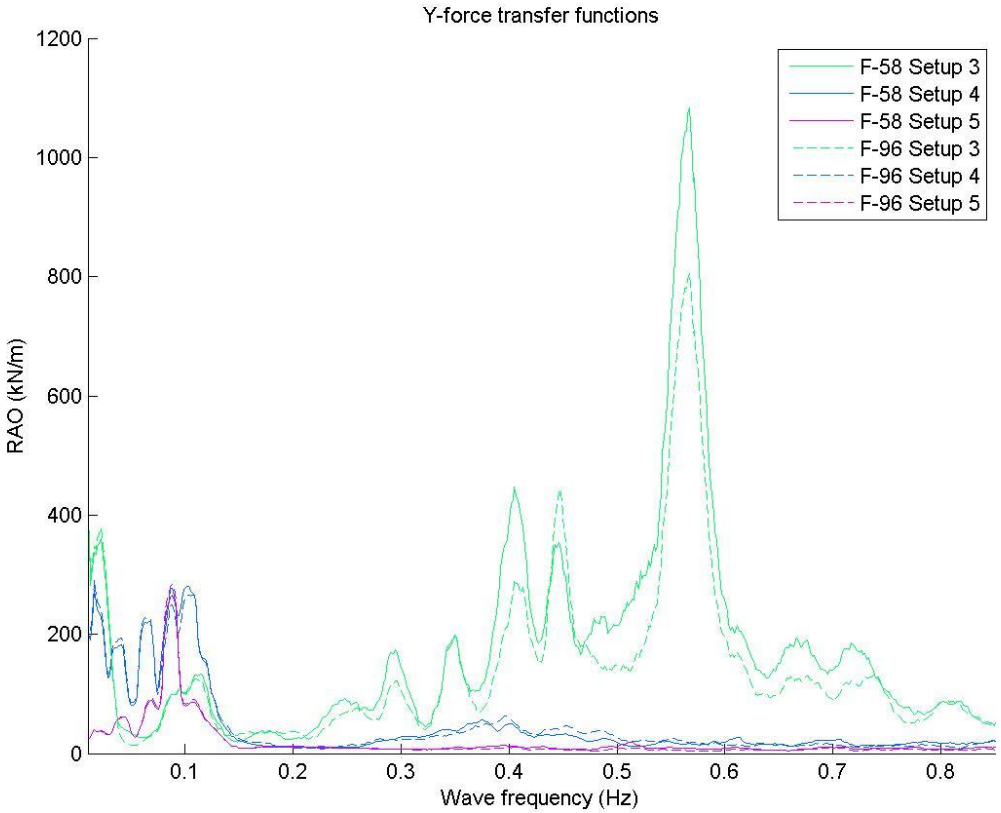

Figure B - 9: Y-force transfer functions, irregular model test runs

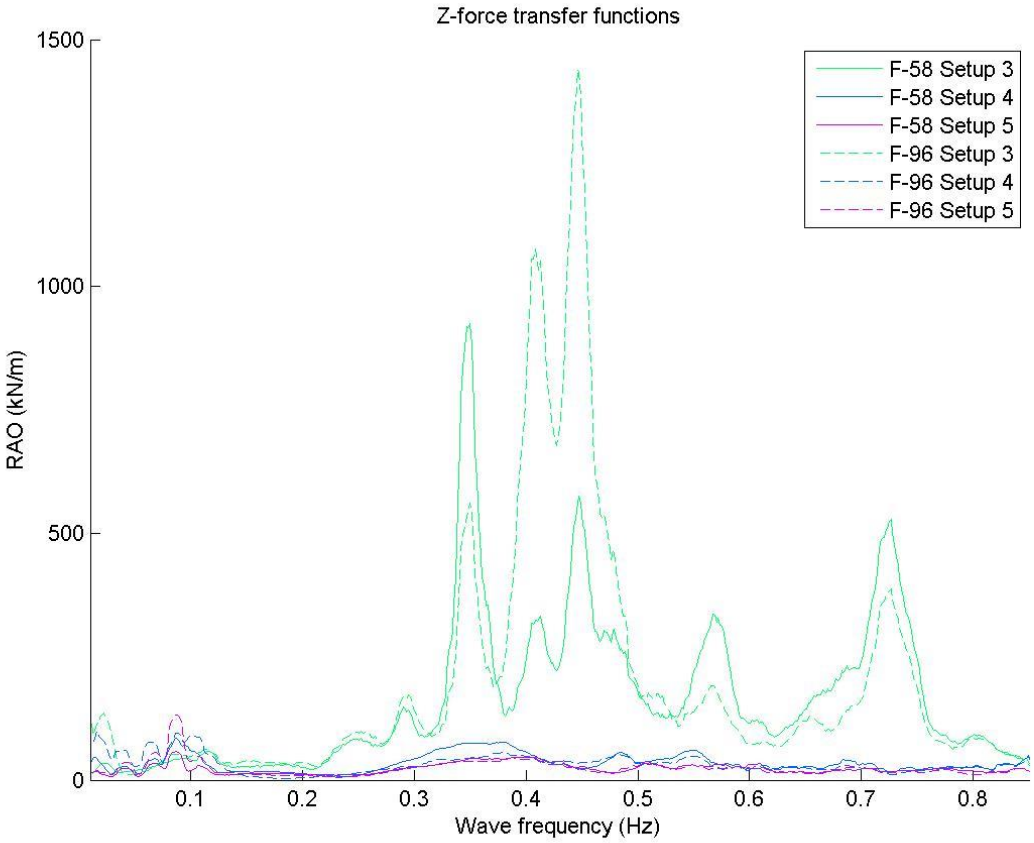

Figure B - 10: Z-force transfer functions, irregular model test runs

APPENDIX C: DECAY TEST TIME SERIES

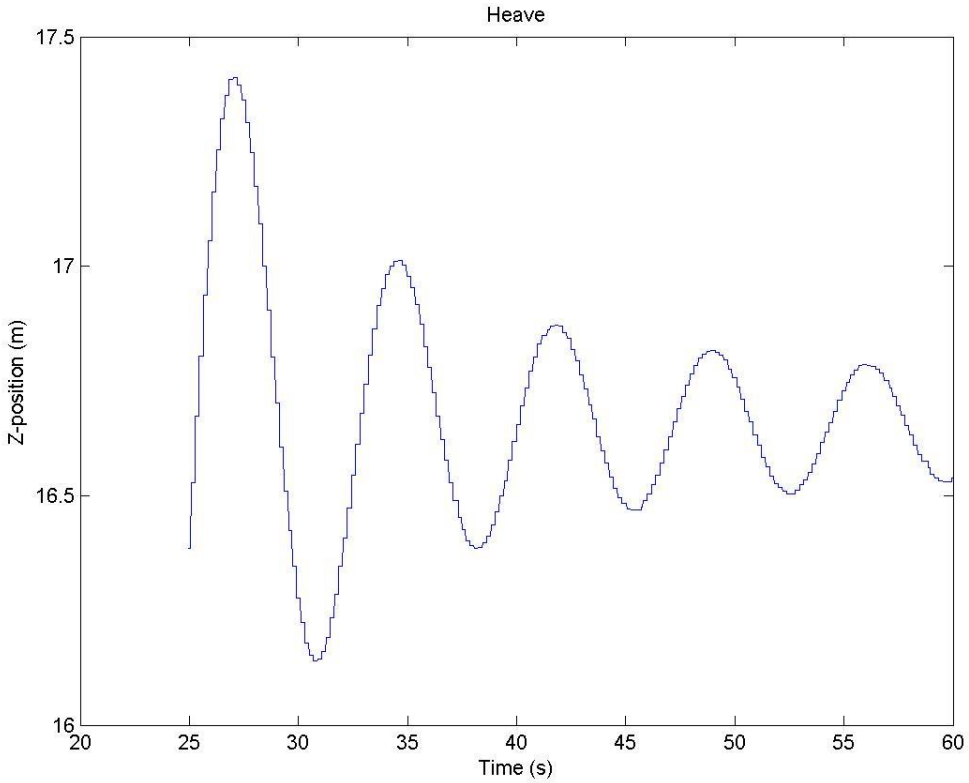

Figure C - 1: Decay test, uncoupled condition, heave

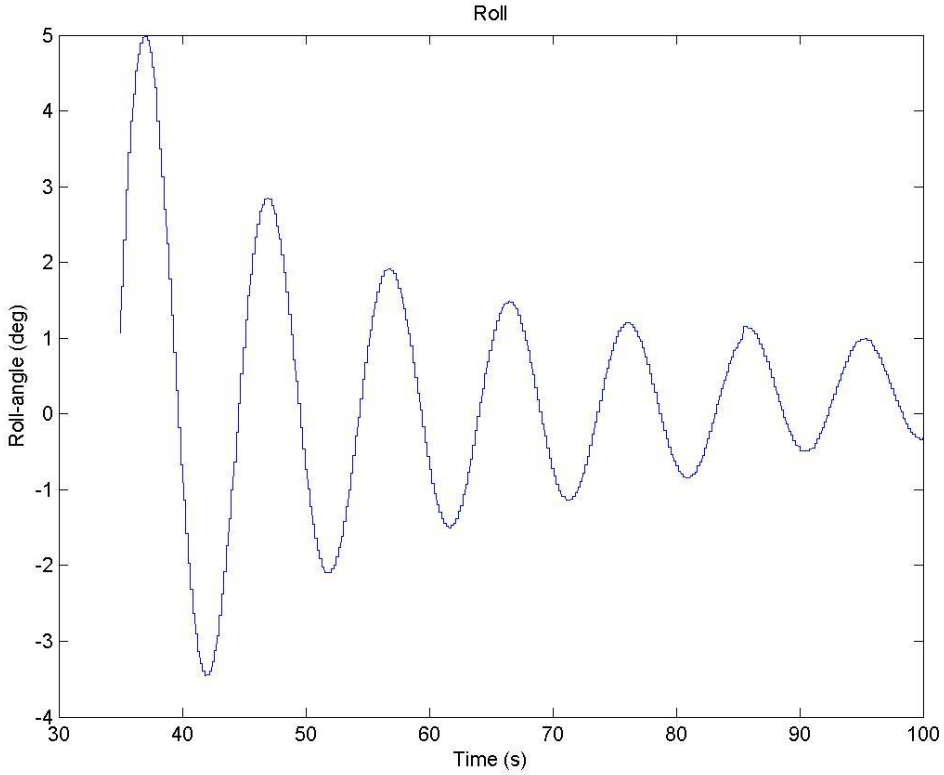

Figure C - 2: Decay test, uncoupled condition, roll

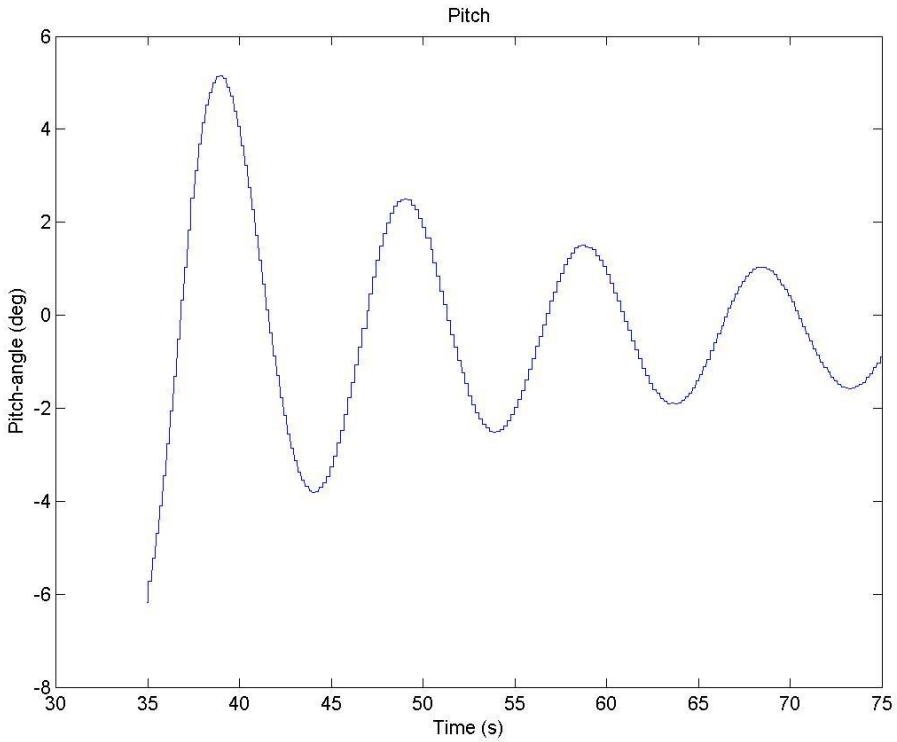

Figure C - 3: Decay test, uncoupled condition, pitch

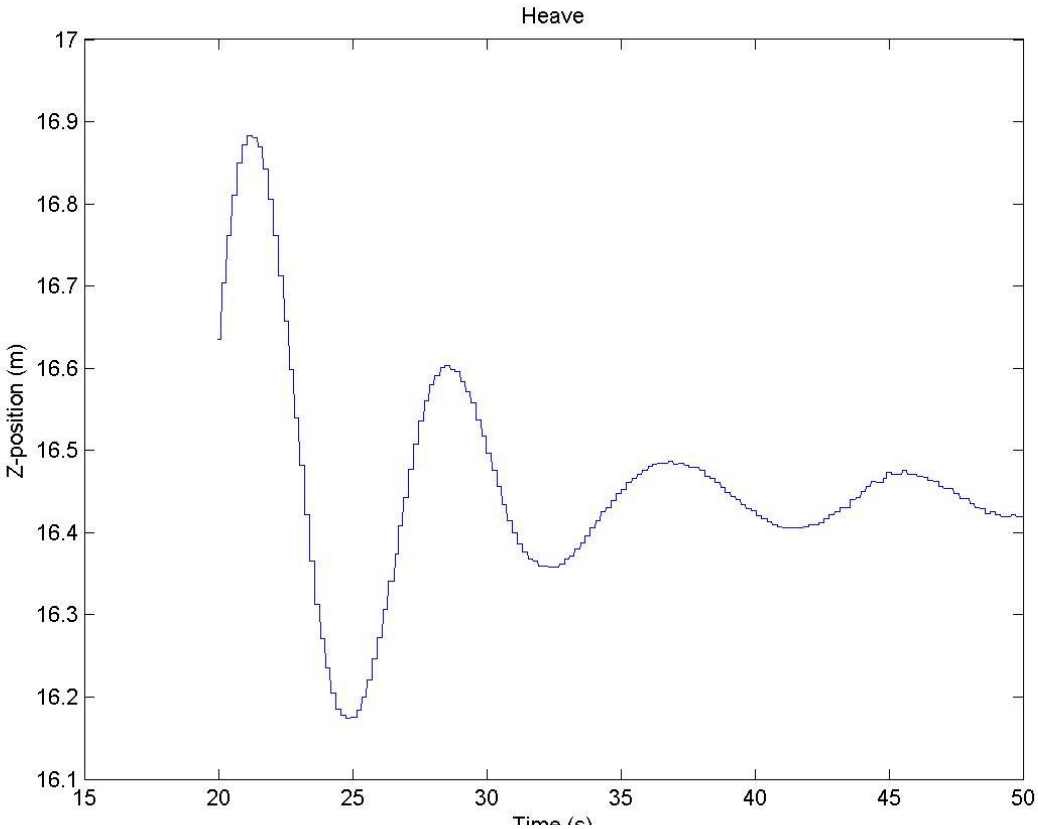

Figure C - 4: Decay test, coupled condition, heave

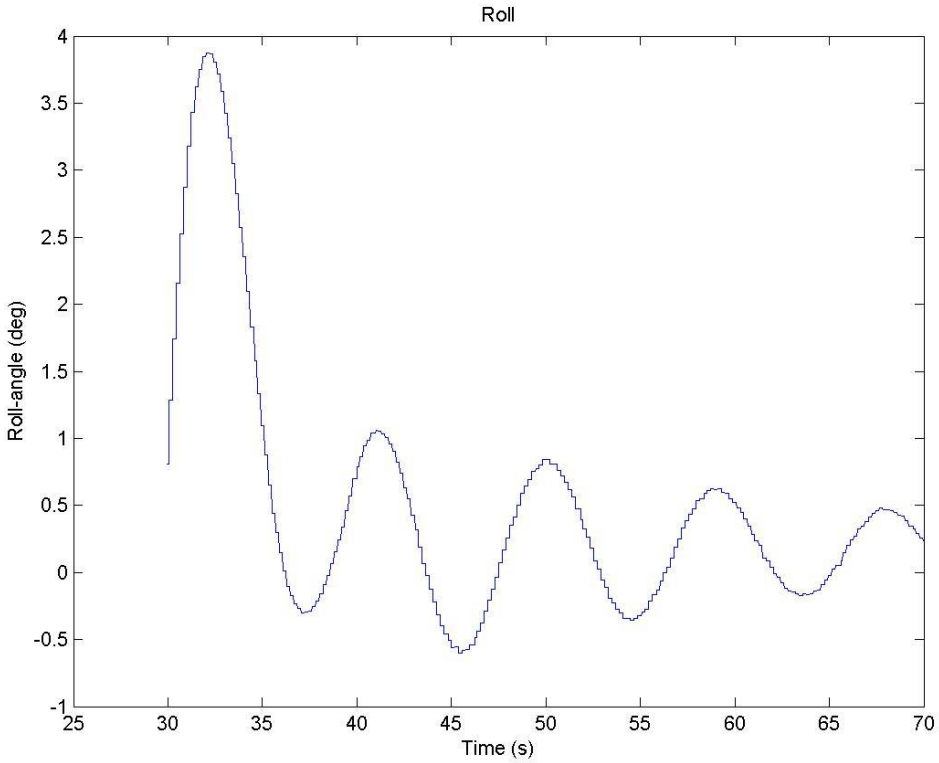

Figure C - 5: Decay test, coupled condition, roll

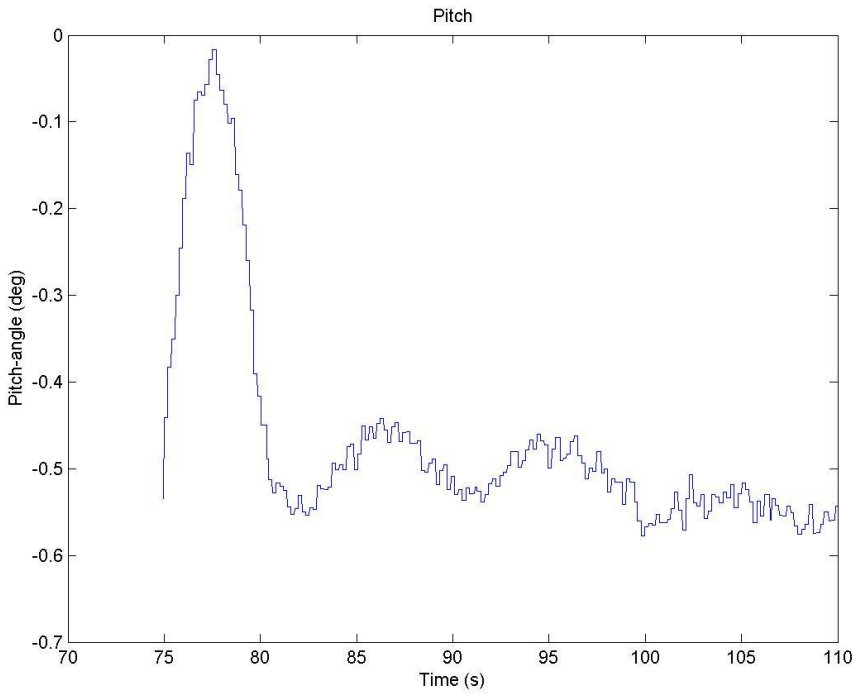

Figure C - 6: Decay test, coupled condition, pitch